AD_____

Award Number: DAMD17-01-C-0065

TITLE: Rapid Detection of Cellular Response to Biological Agents

PRINCIPAL INVESTIGATOR: Bryan R. Williams, Ph.D.

CONTRACTING ORGANIZATION: Cleveland Clinic Foundation
Cleveland, Ohio 44195

REPORT DATE: February 2005

TYPE OF REPORT: Final

PREPARED FOR: U.S. Army Medical Research and Materiel Command
Fort Detrick, Maryland 21702-5012

REPORT DOCUMENTATION PAGE

Form Approved
OMB No. 074-0188

1. AGENCY USE ONLY (Leave blank)	2. REPORT DATE	3. REPORT TYPE AND DATES COVERED
	February 2005	Final (1 Oct 2001 - 30 Sep 2004)

4. TITLE AND SUBTITLE
Rapid Detection of Cellular Response to Biological Agents

5. FUNDING NUMBERS
DAMD17-01-C-0065

6. AUTHOR(S)
Bryan G. Williams, Ph.D.

7. PERFORMING ORGANIZATION NAME(S) AND ADDRESS(ES)
Cleveland Clinic Foundation
Cleveland, Ohio 44195

E-Mail: Williab@ccf.org

8. PERFORMING ORGANIZATION REPORT NUMBER

9. SPONSORING / MONITORING AGENCY NAME(S) AND ADDRESS(ES)
U.S. Army Medical Research and Materiel Command
Fort Detrick, Maryland 21702-5012

10. SPONSORING / MONITORING AGENCY REPORT NUMBER

11. SUPPLEMENTARY NOTES

12a. DISTRIBUTION / AVAILABILITY STATEMENT
Approved for Public Release; Distribution Unlimited

12b. DISTRIBUTION CODE

13. ABSTRACT (Maximum 200 Words)

Our program objective is to develop simple and rapid methods for detecting, at a cellular level, individual responses to environmental stresses elaborated by exposure to infectious agents such as bacteria and viruses. Our methods are based on transcript profiling and post-translational modification of proteins involved in signal transduction. Our hypothesis is that human cells respond to infectious insults to a genetically predetermined extent by stimulating the expression of sets of genes and activating signaling pathways that provide a specific signature for a given agent. We propose that this response will determine the outcome of the infection. We will test this hypothesis by developing custom cDNA and protein arrays designed to detect cellular responses to infectious agents. These will be tested using RNA and protein isolated from tissues sources most likely to be exposed. Our long term goal is to develop rapid quantitative detection devices to measure exposure and response to biological warfare, bioterrorism or emerging agents enabling appropriate triaging and medical intervention to save lives and to avoid unnecessary treatments. We have made significant progress towards this goal during the funded period of 1 Oct 01-28 Feb 05. We have used our custom cDNA microarrays to characterize the responses of mouse and human cells, *in vitro* and *in vivo*, to a variety of pathogens and shown that transcriptional profiles can indeed serve to differentiate between different types of infections. We have also made progress in the development of single chain antibodies for use in protein arrays to detect activation of signaling pathways impacted by biological agents. Moreover, in the course of these studies, we have made a number of discoveries regarding the involvement of specific pathogen and host factors in the mechanism and regulation of these signaling pathways.

14. SUBJECT TERMS
Viruses, bacteria, transcripts, proteins, signal transduction, microarrays

15. NUMBER OF PAGES
135

16. PRICE CODE

17. SECURITY CLASSIFICATION OF REPORT	18. SECURITY CLASSIFICATION OF THIS PAGE	19. SECURITY CLASSIFICATION OF ABSTRACT	20. LIMITATION OF ABSTRACT
Unclassified	Unclassified	Unclassified	Unlimited

Table of Contents

Introduction

There has been recent recognition of an increased risk posed by the use of weapons of biological warfare and bioterrorism. By enhancing our ability to respond by rapidly identifying exposed populations and through the triaging of high-risk individuals, we can overcome both deliberate and naturally occurring pathogen releases. Restricting distribution to exposed and susceptible individuals can also alleviate shortfalls in therapeutic products (when they exist). The rapid testing methods we propose here have as their long-term objective the detection and identification of individuals who have been exposed to any one of a number of biological agents and who are at the greatest risk of succumbing from this exposure. We hypothesize that specific gene and protein expression patterns exist for cells exposed to particular viruses and bacteria and that these "signatures" can be used as diagnostic tools. To test this we have been establishing gene expression and protein modification signatures of cells exposed to different important viruses and bacteria that serve as surrogates for highly pathogenic agents. The foundation of this work has been the assembly and production of microarrays of large numbers of sequence-verified human and mouse cDNA probes. For pathogens in which cell culture models exist, RNA is isolated from virus- and bacteria-infected cells. In addition, we have been obtaining RNA from vaccinated humans, infected primary human cells and mouse models. RNA isolated from mammalian cells is converted to dye-labeled complementary DNA or RNA and the labeled nucleic acids are used to probe cDNA microarrays representing selected human genes implicated in host responses to infection. Viral- and bacterial-specific signature profiles are obtained in this way. Once specific signatures have been established that can discriminate amongst infectious agents, a composite virus- and bacteria-induced gene microarray could be envisaged that would be a prototype for eventual development of a product to be used in the field for rapid detection of biological agent exposure ("lab on a chip" concept). Finally, we have worked to assess the feasibility and practicality of using large-scale sampling of airway epithelium to test for biological agent exposure. The proposed work will result in technology capable of determining if individuals have been exposed to a life-threatening virus or bacteria and will identify the particular infectious agent by virtue of the signature transcripts or protein modifications induced in the cells. Furthermore, signal transduction pathways activated by infection of human cells by pathogenic bacterial and viral agents are being identified and single chain antibodies targeting specific signaling components are being generated. In addition to improving our understanding of the molecular mechanisms involved in the pathogenesis of these agents, this work may reveal new therapeutic targets.

Personnel supported by this grant:

Bryan R.G. Williams	Principle Investigator
Robert H. Silverman	Project Director
Joseph A. DiDonato	Project Director
Serpil C. Erzurum	Project Director
Suzy Comhair	Research Associate
Ying Xiang	Research Associate
(replaced by Jay Paranjape)	
Mathias Frevel	Research Fellow
(replaced by Jeanna Guenther)	
Nilardri Kar	Research Fellow
Thomas Tallant	Research Fellow

Body

Hypothesis

Our hypothesis is that human cells respond to infectious insults to a genetically predetermined extent by stimulating the expression of sets of genes and activating signaling pathways that provide a specific signature for a given agent. We will ask the question whether different agents implicated in bioterriorism and biological warefare or as emerging infectious entities induce specific cellular RNAs in infected human cells. This will be achieved by screening RNA from infected cells using probes selected from those for more than 60,000 human genes that we have in our collection. We will also identify components of signaling pathways activated in human cells by these agents. This will be done using biochemical assays with components specific to distinct signaling pathways. The specific transcripts identified and represented by cDNA and antibodies to relevent signaling components will be assembled as microarrays and used in simulated experiments with human respiratory epithelial cells to test the feasibility of developing rapid screening methods for exposed populations.

D3. Technical Objectives: Assembly and testing of prototype sentinel cDNA and protein microarrays for detecting signatures of biological agents.

D3A. Generation of agent-specific gene expression profiles for a select group of virological and bacterial agents involved in bioterrorism.

Because of restrictions placed on access to and transport of select groups of biological agents, our work has focused on surrogate agents as outlined in our annual progress reports. In particular, we have concentrated on viruses that infect the respiratory tract. The viruses selected include Vaccinia Virus, a surrogate for small pox, and Influenza and Parainfluenza Viruses, because of their importance for public health and as potential agents of bioterrorism. These agents are approved for use in our BSL certified laboratories and can be modeled in mice. Importantly, during the course of this work, immunization programs with vaccinia were implemented and offered the opportunity to obtain specimens from vaccinated individuals that were used to test our arrays and expand the numbers of genes identified as potential sentinels.

1) Vaccinia Virus.

a. Gene expression changes in Vaccinia Virus-infected mice.

Studies were performed using the poxvirus, vaccinia virus (WR strain, a gift from R. Condit, University of Florida), as a surrogate smallpox virus. C57 BL6 mice were infected intranasally with vaccinia virus and brain RNA was extracted at 3 days post-infection. Expression levels of over 15 thousand genes were measured relative to levels in brain RNA from uninfected control animals using a cDNA microarray that we constructed from the National Institute of Aging 15K mouse cDNA probe collection (Tanaka *et.al.*, 2000).

In a typical experiment, a total of 92 genes exhibited a 3 fold or greater level of induction in infected brain whilst 9 genes were repressed 2 or more fold. This data was described in detail in our December 2002 progress report. Included in the upregulated class are Hsp86 and 15 mitochondrial genes. Only 35 genes were induced to a level above 5 fold. In addition to Hsp86, this set of highly upregulated genes encodes a number of proteins not previously linked with disease, such as the carbonic anhydrase related polypeptide (>30 fold induced) and erythroid differentiation regulator (12 fold induced). These genes could represent specific markers of vaccinia infection, and of other poxvirus infections.

It is imperative that inherent differences between different suppliers (JAX vs Taconic), sex, age and weight of the mice be carefully evaluated to minimize these variables in the pathogenesis models. We have carefully examined the effects of sex and weight of commercially available mice in Vaccinia Virus (VV) lung (intratracheal) infections. Parameters of disease including changes in body temperature, weight and respiration, other clinical symptoms and lethality have been mapped as a function of VV dose administered. Initially, significant weight-dependent differences in susceptibility of same-age mice were noted. However, we have shown that any inherent weight dependent responses seen between the sexes can be negated with feeding alternative diets resulting in a sex independent weight average at the time of VV infection. More importantly, we have determined that when animals are of similar weight, no differences in response to the virus between males and females are observed.

Currently we have RNaseL, PKR, and RNaseL/PKR knockout and wild type mice breeding colonies producing mice for VV infection experiments. The breeding colony wild type mice have demonstrated no difference in susceptibility to VV infection or course of disease seen in the commercially available mice. However, some of these engineered mice strains were derived on B6 mice from JAX labs and others from Taconic B6 mice. To examine the extent in which background of the mice being bred would affect susceptibility to VV infection, two commercial suppliers of wild type mice have been examined and, fortunately, no differences in the course or susceptibility to VV have been observed.

We have now established conditions that allow us to perform meaningful experiments with minimum or irrelevant variables. As an extension of the susceptibility studies in these mouse strains microarray-based gene expression analyses are also currently underway. Preliminary results from the microarray studies performed on lung tissue taken at death have shown results similar to those seen in microarray analyses of poxvirus infected tissue culture cells. A survey of time points of 5 and 9 days post VV infection show no significant differences to that of the control animals which would be expected of wild type virus that is known to control the host immune response efficiently.

b. Gene expression changes in humans exposed to Vaccinia Virus through vaccination.

Vaccinia as a vaccine agent provides approximately 95% cross-reactive protection against clinical disease from variola (smallpox). Yet, as a live virus vaccine, vaccinia can multiply in susceptible hosts, resulting in clinical disease or, rarely, death. Vaccinia retains its significant efficacy in preventing smallpox even when given 3-4 days post-exposure (Breman and Henderson, 2002). Unfortunately, vaccinia is also the most toxic vaccine routinely used during the last century with significant side effects that can be local (98%), systemic (20-30%), or occassionally lethal (1/million). (Bartlett, 2003). These rates of known side effects are among normal hosts. Particular concern exists with effective immunosuppressive treatments and solid organ and bone marrow transplantation which results in a larger cohort of persons at increased risk for frequency and severity of side effects. Some areas of cryptic immunodeficiency may also be identifiable through screening. While certain individuals may progress to severe disease because of HIV status (approximately one-third of the estimated 900,000 people in the United States with HIV infection are unaware of their status) immunosuppressive medication or pregnancy, more specific reasons for why certain individuals progress to severe disease are unknown. Of additional serious concern is that twelve of the sixty-eight deaths reported the 1960s occurred in unvaccinated persons exposed to recently

vaccinated friends or family members (Sepkowitz, 2003). Since our work in mice identified a number of vaccinia–induced genes that could serve as sentinels of infection we took advantage of a vaccination program in the health care setting established nationwide as part of the biodefense efforts to measure responses of healthy volunteers using our interferon, dsRNA and stress activated human gene array. As described in our December 2002 progress report, this microarray (termed IAD) comprises approximately 850 known human interferon stimulated genes (ISGs), 1500 human genes containing adenylate-uridylate-rich elements (AREs) and 300 human genes responsive to treatment with the viral analogue dsRNA.

Participants were in one of three groups: A: Pre and 24 hour post testing (n=8); B: Pre and 24 hour testing, with additional samples at 2, 5, 7, and 14 days post vaccination (n=4); or C: Testing at the time of a serious adverse event after vaccination (n=1, generalized vaccinia). Participants served as their own control, except for Group C where enrollment occurred only after onset of the adverse event. Isolated and amplified whole blood RNA was subjected to cDNA microarray testing.

The comparison of pre-vaccination and 1 day post-vaccination samples revealed that the transcriptional response was highly variable between different patients. As shown in our February 2004 progress report, 71 genes exhibited a minimum of 1.8-fold up-regulation at 24 hours post-vaccination, but these varied among individuals. We conclude from these preliminary studies that immune activation can be detected in whole blood RNA following live orthopox virus infection using gene expression arrays and that these early immune signatures for orthopox virus infection may assist with identification, containment and treatment decisions. Importantly, significant differences in gene expression profiles were noted in an individual suffering an adverse event indicating the utility of the arrays in following the outcome of vaccination.

c. Gene expression changes in primary and transformed human cell lines infected with Vaccinia Virus.

We also studied gene expression profiles in human lung cell lines and primary cells infected with vaccina virus (VV, Western Reserve (WR) strain, a gift from R. Condit, Gainesville, FL). Conditions for virus growth, infection, and plaque titration were as described (Condit et al., 1983). Both BEAS2B and BET1A cells, human bronchial epithelial cell lines transformed by adenovirus12-SV40 virus and SV40 T-antigen respectively (Reddel, et al. 1988), and primary human airway epithelial cells (HAEC), 399 and 585, were studied. Primary HAEC were grown on collagen-coated dishes in specialized serum-free media (Clonetics). As described in section D3L-M 1. ("Clinical Samples") below, Dr. Erzurum has shown that cell cultures of HAEC lead to pure epithelial monolayer cultures. Cells were infected with vaccinia virus at a multiplicity of infection (MOI) of 10 plaque forming units (pfu) per cell in phosphate buffered saline (PBS). After 30 min, the cells were washed once with PBS and complete medium containing serum was added. Separate cultures of virus-infected cells were processed for either virus recovery or total RNA isolation a 4, 8, 24 and 48 hours post-infection. Total RNA was isolated using Trizol reagent (Invitrogen). Viral yields were determined by plaque assays on BSC40 monkey kidney cells. Virus was harvested by freeze-thawing infected cells three times and sonicating for 1 min. Virus replicated to higher titers in the cell lines than in the primary cells (**Figure 1**). Virus growth in the four cell types (from the highest to the lowest titers) was Beas2B>Bet1A>585>399.

RNA isolated from the cells was processed and analyzed on our custom-made IAD

(ISG/AU-rich/DsRNA) cDNA microarray. There were similarities in the VV-induced genes between the two cell lines and between the two primary cell types. However, there were remarkable differences between the primary cells and the cell lines, pointing to the value of using primary human cells for obtaining viral-response mRNA profiles. The two most highly upregulated genes in the cell lines were histone (2bI) and heat shock protein (HSP70B'). These genes are known VV inducible genes, thus validating our findings (Brum et al., 2003). Virus-induced gene expression was observed to peak between 8 hr and 24 hr post-infection in all of the cell types. These finding demonstrate that cell lines may be inappropriate model systems for extrapolating to humans and highlight the importance of using primary, freshly isolated cells.

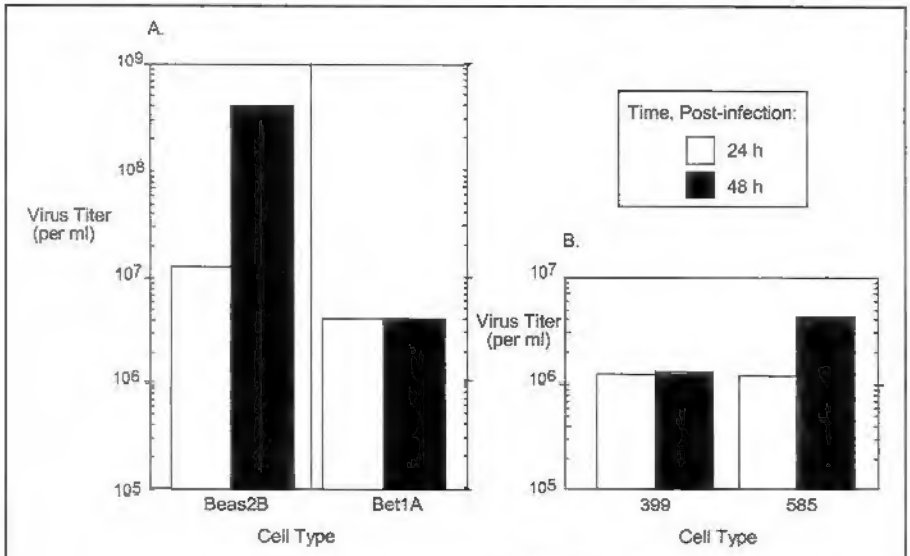

Figure 1. VV yields from (A) human lung epithelial cell linesBeas2B and Bet1A and (B) primary human lung epithelial cells.

Interestingly, ribosomal protein genes were the most highly VV-downregulated genes in the two cell lines. Indeed, the genes for ribosomal proteins S4, S6 S10, S14, S16, S23, S24, S27a, S28 and L18 are among the most highly downregulated genes. Again, there were significant differences between the cell lines and the primary cells, although ribosomal protein gene S24 was the second most highly downregulated gene in the primary cells. These data could describe a novel mechanism for viral shut-off of host protein synthesis and suggest that a VV-induced pathway can selectively degrade ribosomal protein mRNAs.

In the case of vaccinia virus infection of HAEC, the group of genes showing changes in expression was different from that identified for influenza infection of HAEC (see below for discussion of Influenza experiment). Lists of genes induced by these viruses in HAEC and their induction levels and kinetics were included in our February 2004 progress report. These results suggest that, by using gene arrays, it may be possible to discriminate among common respiratory tract infections such as influenza and parainfluenza and orthopox where the early clinical symptoms are similar. Indeed, as discussed below (section D3L-M 2.), statistical analysis of our gene profiling data has revealed a set of 25 genes whose expression is sufficient to discriminate between different viral infections. **Thus, the major hypothesis of our grant proposal, that unique gene expression signatures may allow detection of particular infectious agents, is supported by this data.**

2) Influenza Virus

HAEC were grown to approximately 85-90% confluence in 100 mm dishes. We infected cells with Influenza A/Japan/305/57, subtype H2N2 (Advanced Biotechnologies, Columbia, MD) which was grown in Madin-Darby canine kidney (MDCK) cells, and suspended in serum-free MEM with Earle's Salts. The virus stock contained $10^{6.25}$ TCID50 (50% of tissue culture infectious dose) per ml. Cells were infected with Influenza A2 Japan virus using 0.2 viral particles/cell for an estimated $8x10^6$ cells/plate. Infection of cells was performed using sterile techniques in the BSL2 virus facility in the tissue culture hood. All plastics, disposables and biohazard wastes were disposed of using bleach and then placed appropriately in biohazard waste bags and boxes. The virus was added to each plate, then plates were transferred to a 37° C incubator. After 1 hour the media and virus was removed from the plates and replaced with 10 ml of fresh media. The cells were returned to the incubator until harvest according to the time course scheduled for each experiment. In addition, control uninfected cells were also harvested at each time point as control for microarray analyses involving competitive hybridization. RNA was prepared using phenol/chloroform purification and extraction methods. RNA concentrations and quantities were determined for each of the samples, which were then confirmed on agarose gels. Four influenza experiments have been completed using cells extracted from 4 different human donor lungs. Total RNA extracted from plates was 11± 4 ug/$1x10^6$ cells. RNA was of good quality with no degradation as evaluated by gel electrophoresis. RNA was converted to labeled cDNA and hybridized to the IAD microarry. Evaluation of microarray results was performed using Genespring software. A list of genes showing significant changes in expression at any time point following influenza infection in each of the four samples was presented in our February 2004 progress report. In addition, we showed the extent and kinetics of induction for each of these genes. Interestingly, distinct waves of differential gene expression were observed at 1, 8 and 24 hours post-infection, each involving largely non-overlapping sets of genes. This work is being prepared for publication.

3) Ebola virus.

We performed experiments aimed at determining changes in gene expression profiles elicited by several different species of Ebola virus in human cells. For these experiments we used derivatives of human HT1080 fibrosarcoma cells that are either normal or mutated for Jak1 kinase which is required for an interferon (IFN)-mediated antiviral response. The IFN responsiveness of the different cell lines was characterize by performing gene expression array experiments. In addition, the same cell lines were sent to USAMRIID laboratory in Ft. Detrick, Maryland for Ebola virus experiments (performed by Dr. Jason Paragas). The cell lines were infected with Reston, Sudan and Zaire species of Ebola virus and analyzed for the ability of the virus to replicate.

The characteristics of the various Jak mutant cell lines and their susceptibility to Ebola virus was presented in our December 2002 progress report. Our results showed that cells harboring the truncated Jak1ΔB have enhanced ability to replicate the Reston and Zaire species of Ebola virus. In contrast, four other cell lines have a reduced ability to replicate Ebola virus. These data suggest that there may be a genetic component to individual susceptibility to Ebola virus.

4) Vesicular Stomatitis Virus and Encephalomyocarditis Virus

We also used Vesicular Stomatitis Virus (VSV), a rhabdovirus, and Encephalomyocarditis Virus (EMCV), a picornavirus, as surrogates for pathogenic viruses such as the Rabies virus and Poliovirus, respectively. RNA profiles were determined for human Hey1b ovarian carcinoma cells, in which the interferon antiviral response was regulated with siRNA. As reported in the Journal of Virology, our findings suggest a general antiviral effect for the interferon-induced protein, phospholipid scramblase 1 (PLSCR1) that appears related to marked enhancement of the cellular response to IFN (Dong et al., 2004). Specifically, we compared mRNA profiles in untreated and IFN-β treated cells using the IAD array (**Figure 2**). Triplicate cultures of Hey1B vector control, mismatch siRNA or PLSCR1 siRNA clones were treated with IFN-β at 6 h and the RNA isolated from identically-treated cultures was combined for microarray analysis. The experiment was independently performed twice (i.e., experiments "A" and "B", were both from RNA pools of triplicate, identically-treated cultures). In addition, several of the ISGs were present at multiple positions on the array (indicated by multiple rows for the same gene in **Figure 2**). Twenty-four genes were more highly induced by IFN-β in the control cells expressing mismatched siRNA than in the cells expressing siRNA specific to PLSCR1. Twenty-one of these genes are previously identified ISGs. Three genes are newly identified ISGs from these experiments, and are also AU-rich genes (hypothetical protein expressed in osteoblasts, TEB4, and transcription factor AP-2 gamma). ISG54, present at three locations on the array, was one of the most highly elevated ISGs associated with PLSCR1 expression. The average IFN-induction of ISG54 was about 5-fold greater in the control siRNA

Figure 2. PLSCR1 enhances expression of a set of IFN stimulated genes as determined in DNA microarrays. Hey1B cells expressing siRNA mismatch or siRNA to PLSCR1 were incubated with or without IFN-β (1,000 U/ml) for 8 h. Gene array results are from RNA samples isolated from triplicate cultures of IFN treated or control cells. Numbers represent the fold increase in RNA levels after IFN treatment in two replicate experiments, A and B.

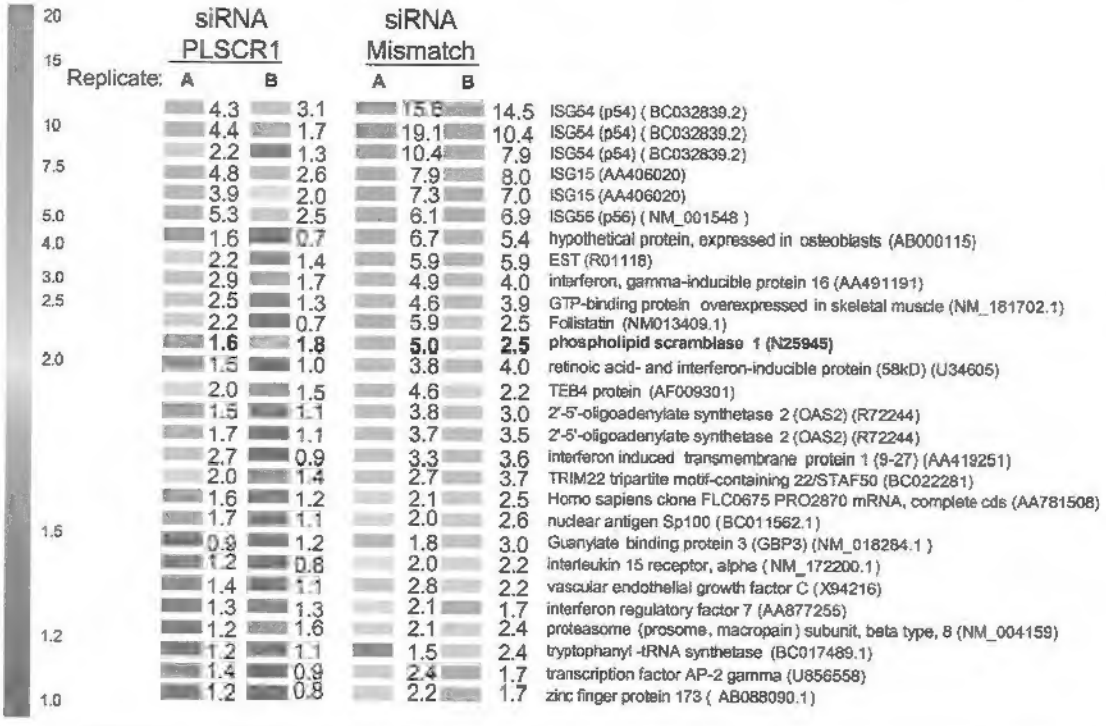

cells than in the PLSCR1 siRNA cells. The remaining 23 ISGs were induced 1.7- to >5-fold greater by IFN in the control siRNA cells than in the PLSCR1 siRNA-expressing cells. Our results suggest a contribution of PLSCR1, a known ISG, to the IFN-stimulated expression of a limited subset of ISGs. However, because siRNA ablation of PLSCR1 was incomplete, the values obtained may underestimate the contribution of PLSCR1 to IFN stimulated gene expression. A decreased IFN-induction of PLSCR1 itself was observed in the PLSCR1 siRNA cells. PLSCR1 siRNA did not significantly affect expression of any of the 85 "housekeeping" genes serving as controls on the microarray (data not shown). To confirm the gene array results, immunoblot measurement of several IFN-induced proteins was performed (Dong et al., 2004). Deficient IFN-mediated induction of PLSCR1, p56, and ISG15 were observed and there was a small effect on Stat1 levels while PKR and RNase L amounts were essentially unaffected. The siRNAs by themselves did not induce ISG expression as determined by both gene microarrays and western blot assays (**Figure 2** and data not shown). Furthermore, PLSCR1 greatly inhibited replication of both VSV and ECMV.

D3B-G. Assembly and manufacture of sequence-verified cDNA arrays containing interferon stimulated genes (ISGs), control genes and genes identified as induced by infectious agents; probe preparation, hybridization, scanning and data analysis.

These tasks have been central to the majority of the work undertaken as part of this grant and are described throughout this report as well as in our previous annual progress reports (dated December 2002 and February 2004) and the appended publications.

D3H-J. ***Protein arrays*** **and** ***Construction and arraying of single chain antibodies to cell signaling components and bacterial/viral agents*** **and** ***Preparation of synthetic peptides that are the activated forms of key signaling molecules, non-activated forms, heart and liver enzymes, and virulence factors of pathogenic bacteria and viruses and immunization of chickens.***

Our goals were to develop single chain antibodies against activated signaling molecules, sensors of cellular damage, certain pathogenic markers, and cellular proteins increased in expression after bacterial or viral exposure. These antibodies were to be arrayed on slides to form a protein array that would be used to monitor levels of signature bodily proteins obtained from field operatives. The resulting profiles would be compared to known signaling/abundance profiles of model bacterial or virus-infected cells to determine what agent(s) the field operatives had been exposed to. These data would be compared with microarray-derived gene expression data to accurately assess exposure, weigh treatment options and predict outcome.

Initially we planned on using peptides to immunize chickens and make immune libraries from their splenic cDNAs and use antibody-specific primers and overlap PCR to construct a library of single chain (scFV) antibodies as phagemids. Our initial attempts to derive high affinity (as determined by ELISA signals >0.75) with a small number of peptides (phospho-IKK, phospho-IκB, and IKKgamma) were not successful in generating scFv's that met this criteria. Due to this fact and the availability of a large (>10E11) library of human scFv's that were provided by Cambridge Antibody Technologies Inc. (CaT) [Cambridge, UK], we decided to utilize this library to screen peptides corresponding to many of the proteins listed in Figure 1 of the original proposal (proteins encoded by genes that are induced by EMCV infection of interferon-treated cells). The human antibody repertoire is estimated to contain ~10E9 various

antibody possibilities, therefore we expected to be able to isolate high affinity single chain antibodies specific to our peptide targets using this library. Another benefit would be that with such a large library, there would be no need to construct numerous immune libraries from various immunized animals. The time frame covering this period was the entire 1st year.

We found that selections using peptides, especially phospho-specific peptides was not yielding high-quality ELISA-positive results. Sentinel scFv's (phospo-IκB and phospho-p38) that showed limited success by ELISA (~0.5-0.3) were tried in immunoprecipitation experiments using proteins from activated mammalian cell extracts without success. Initial attempts to increase the affinity of these antibodies by ribosome display were unsuccessful and this strategy was abandoned. Midway through the second year we took the strategy of panning the CaT scFV library on His-tagged or GST-fusion proteins of our list of proteins of interest. In order to perform this task we had to PCR amplify desired coding regions corresponding to the proteins from cDNAs that we either generated from cellular RNA or obtained from other investigators who already had the gene-specific cDNA in vector form. We initially used GST and green fluorescent protein (GFP) as targets to test the system. We had very good success at obtaining a large number of scFv's that gave strong ELISA signals (>0.75). We found that performing the typical 4-5 rounds of selection resulted in a very limited set of diverse scFv's to the target (typically 1-3) and that we would likely stand a much better chance of identifying a larger set of diverse binders by screening the selected scFv's after only 2 rounds of selection. Due to the low numbers of positive binders at the initial stage of panning (typically 0.1-0.5%) many clones (thousands) needed to be analyzed. We utilized a colony picking and arraying robot purchased by an NIH-awarded equipment grant to Dr. DiDonato. This allowed mass pickings and arraying of thousands of clones for each selection target. The entire set of phage clones were replica plated and grown in culture to induce production of single chain antibodies that were then tested by ELISA using specific and irrelevant target proteins. The automated ELISA plate washer was absolutely required to perform the task of screening these large numbers of samples. Developing the system to this point covered year two. With this success, we began to pursue this strategy with many of our targets at the beginning of year three in earnest. Because of the increased time involved in preparing the antigenic targets we had to narrow our list of targets from those listed in Table 1 of the original proposal and concentrate on only a few of the targets in each category (chromatin & transcription factors, metabolic enzyme markers, proinflammatory cytokines and chemokines, protein kinases, pathogens and toxins, growth factors & receptors and apoptosis-related factors). At this point too, we were aware from our signaling studies that analysis of signaling pathways activated in response to bacterial or viral infection of lung and intestinal epithelial cells was not very discriminatory among either different bacterial infections or among viral infections per se, and that the major difference between the viral and bacterial infection was the interferon response early from viral infection and ER stress in viral responses later during infection. Therefore, we decided to add a subset of interferon-stimulated genes to our target list that also are known to play an essential role in innate host responses, namely the Toll-like receptors (TLRs) and their signaling adapter proteins (MyD88, Mal, TRIF and TRAM).

In an attempt to offset our initial screening setbacks during the final half of the project period we began selecting multiple targets simultaneously. We found that we could select up to four antigenic targets simultaneously in the 1st round of selection and then select each target separately in round 2 and then pick approximately 2,000 clones from the second round of selection and perform ELISA assays using specific and non-specific proteins. This adjustment allowed us to generate scFv's with many strong ELISA signals against a number of proteins listed in the **Table above.**

Table: Selected scFv's that are strong ELISA positive

Growth factor receptors & receptors	Chromatin and transcription factors
Toll-like receptors 2, 4, 5* ,7* & 8* MyD88*, Mal*, TRIF*, TRAM	c-jun, ATF, RelA*, p50*, IRF9 (p48), STAT3
Apoptosis-related factors	**Metabolic enzyme markers**
Bcl-2	alkaline phosphatase, bilirubin, albumin, creatine kinase , catalase
Protien kinases	**Proinflammatory cytokines, chemokines, enzymes & cell damage markers**
IKKalpha*, IKKbeta*, IKKgamma*, PKR, p38 JNK1, MEK1	TNFalpha, IL-1alpha, IL-1beta, IL-6, IL-8
Pathogens & toxins	* denotes verified by immunoprecipitation
Flagellin*, HPIV-3 N protein, anthracis lethal factor & anthracis protective antigen (PA)	

The strongest ELISA positive scFv's were selected (typically 20-30) and used in immunoprecipitation experiments to verify that the single chain antibody could recognize the whole protein. This extra verification was extremely time consuming and labor intensive but we felt it was extremely important since we found that a number of very strong ELISA positive scFv's failed to immunoprecipitate their target protein. This increased selection pressure has slowed our scFv developmental pipeline during this final year; however, we are confident that the antibodies that we have generated will be extremely useful. **Figure 3** illustrates our ability to generate scFv's that can efficiently immunoprecipitate a number of target proteins.

It is important that at least two different immunoprecipitation positive antibodies be generated for each target, one for capture and the other for detection. As we have discovered many strong ELISA-positive scFv's do not always immunoprecipitate the target protein or do so very inefficiently. We have tested a number of target antigens by immunoprecipitation as denoted in the Table above. We plan on screening the remaining strong ELISA-positve scFv's for their ability to immunoprecipitate their target antigens for use in constructing a prototypical scFv antibody array. What has become apparent over the time of this project is that monitoring of the signaling pathways that are activated may be important but due to their transitory nature, the only tangible or lasting impression of them is at the gene expression level (both mRNA and protein levels). Therefore, looking back in hindsight, a protein array that would be built to reflect detection of proteins shown to have its expressions altered significantly, as determined by gene-chip analysis, along with cell damage and pathogen protein/substance markers would be ideal. However, there was no way to know or suspect this apriori.

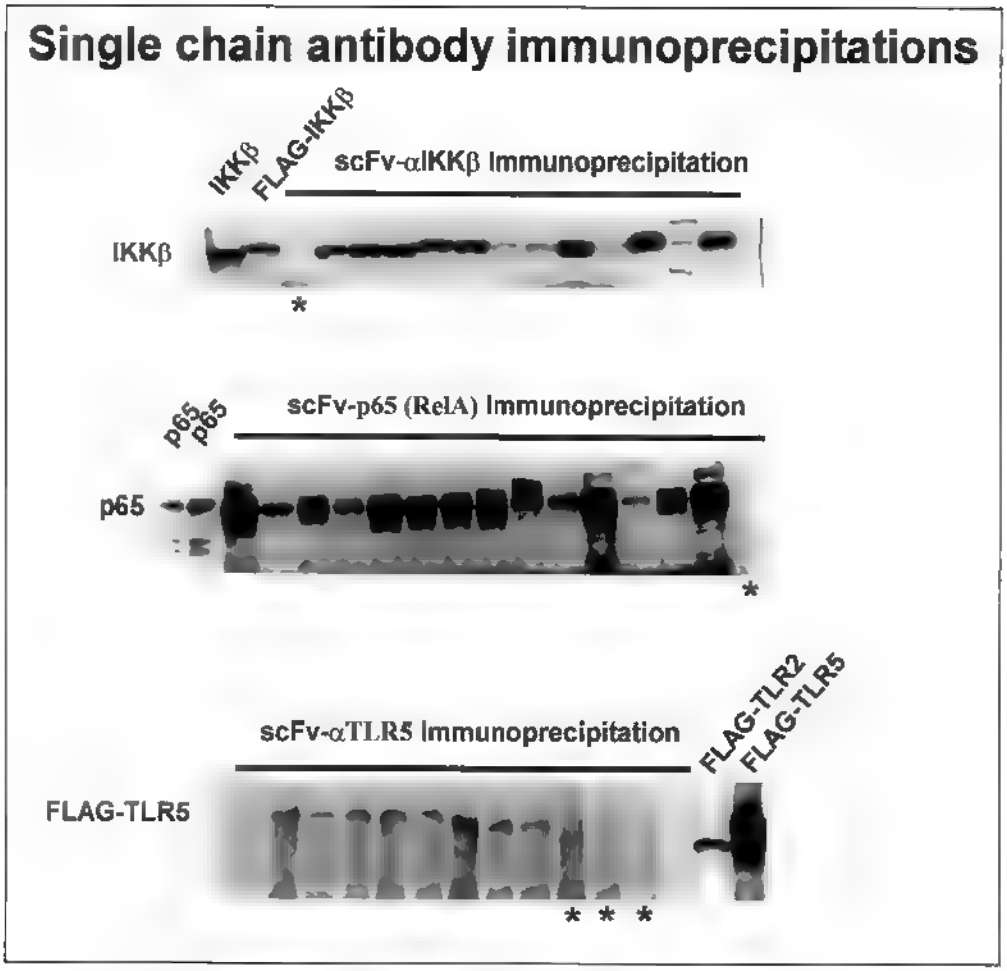

Figure 3. Single chain antibodies as indicated were used to immunoprecipitate either exogenously expressed FLAG-tagged IKKbeta (baculovirus infected cell extract) or endogenous p65 or stably expressed FLAG-tagged TLR5. Input specific proteins were at levels five-teimes greater than observed in the marker lanes for FLAG-IKKbeta, FLAG-TLR5 and p65. Lanes marked with asterisks denote scFv's that were used as negative controls.

D3K: ***Molecular signaling pathway characterization of model stimuli***

1. Flagellin is a major regulator of inflammatory responses during bacterial infection

Our studies in signal transduction have focused on cataloging cellular responses to bacterial and viral infection. Of chief note is our discovery that the bacterial protein flagellin is that major regulator of the proinflammatory gene response and signal transduction cascade activator as described in our recent paper (Tallant et al., 2004) and seen in **Figures 4 and 5** below. This finding is of particularly keen interest since flagellin potentially can be used as a potent biological weapon simply by adding a cell-permeating peptide sequence (~13 amino acids) allowing it to pass into and through epithelial barrier cells which the natural flagellin protein does not normally do. This modified protein could be made in vast quantities at an

extremely low cost, is easily purified to almost homogeneity and is heat stable allowing it to be administered either in food or water or aerosolized, it is also quite stable in the environment and therefore could be considered a potent "poor man's" biological weapon and its use as such must be considered as a viable threat so the more detailed information we have about its effect on cells, the more effective our responses to neutralize its activity will be.

In **Figure 4**, wildtype (WT) or flagellin-minus strains (134) of *Salmonella typhimurium* were used to infect intestinal epithelial cells and whole cell extracts were prepared at the inidicated times after infection and analysed for NF-κB DNA binding activity by electrophoretic mobility shift assay (EMSA) and JNK, p38, ERK and IKK kinase activity were determined by immunoprecipitation (IP) kinase assays for IKK and JNK with their specific substrates as indicated or by immunoblot analysis with phospho-p38 or phospho-ERK antibodies as indicated.

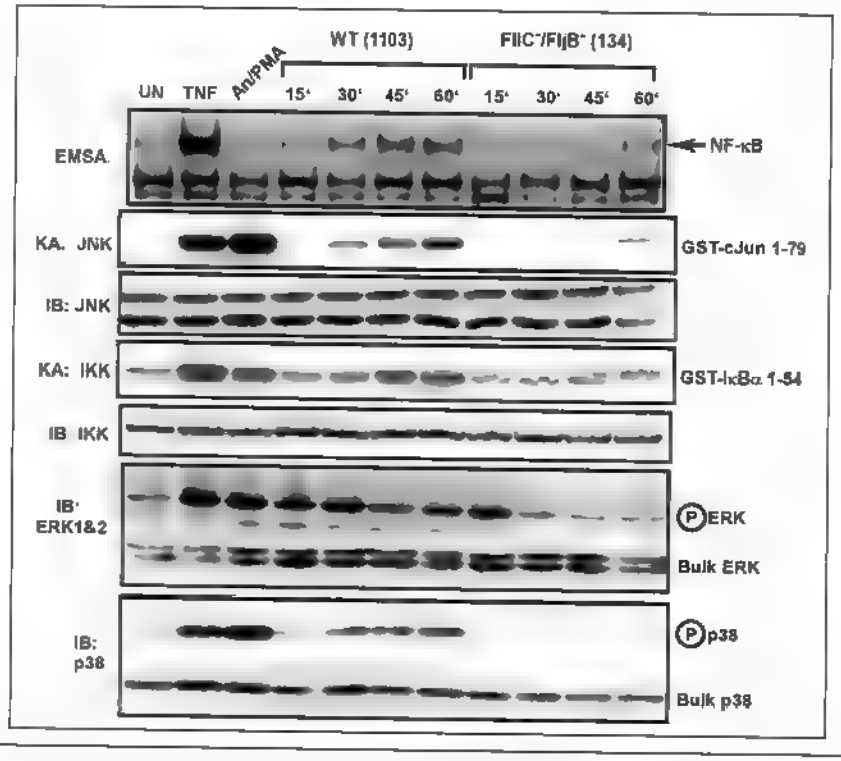

Figure 4. DNA binding and kinase activity in Salmonella infected intestinal epithelial cells.

Purified flagellin (1ug ml) stimulated NF-κB DNA binding activity and the same signaling pathways (panel A & B) as those activated by wild type bacterial infection (as seen in **Figure 5** below), demonstrating that flagellin is one, if not the major, driving force of proinflammatory signaling during bacterial infection. Similar results were obtained with *yersinia enterolytica* infections.

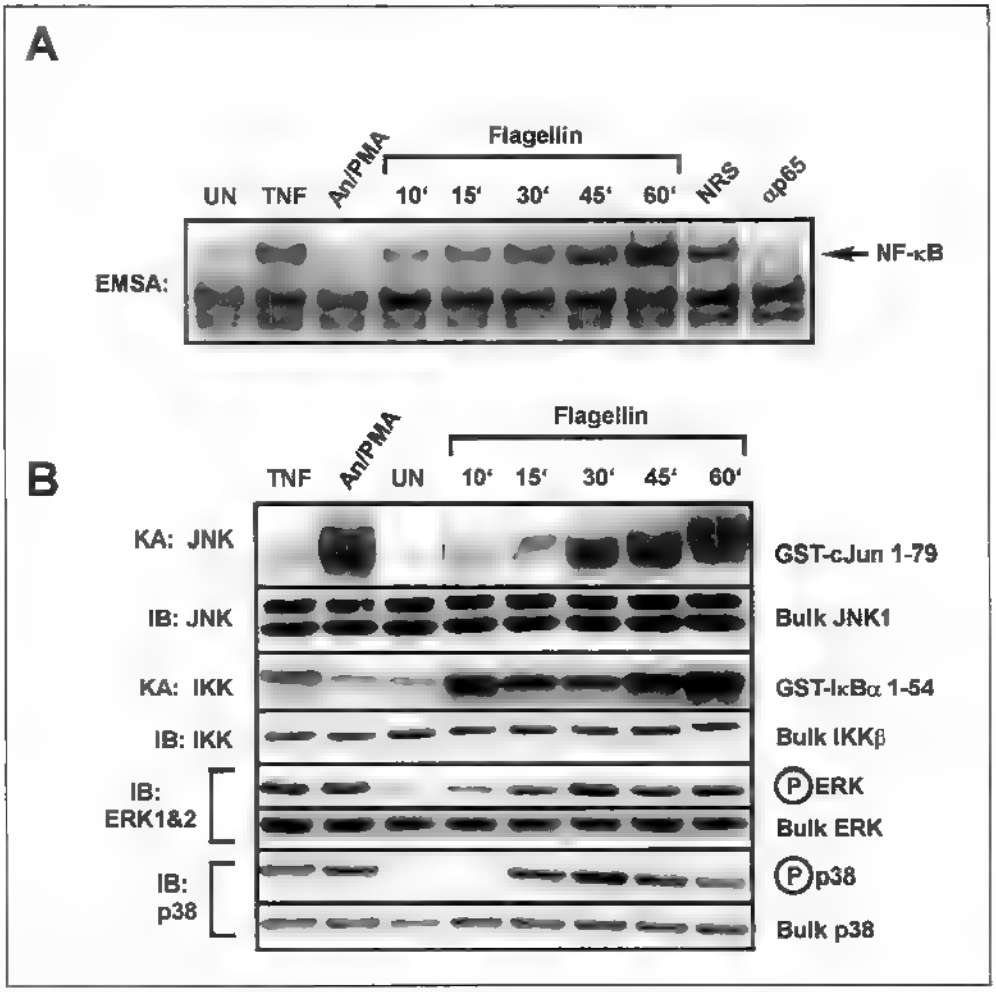

Figure 5. Signaling induced by treatment of intestinal epithelial cells with purified Flagellin.

2. Identification of Flagellin as a novel radioprotectant.

In the course of our signaling studies using flagellin, we have uncovered a novel and surprising characteristic of flagellin. We have, in collaboration with Dr. Andrei Gudkov's laboratory here at CCF, discovered that flagellin and a number of its smaller derivatives (created in the DiDonato laboratory) have the capability of providing extraordinary radioprotective effects. Flagellin and its derivatives can completely protect mice from hematopoetic and gastrointestinal (GI) syndrome death in mice irradiated with up to 13Gy of gamma-radiation. The protection is consistent with flagellin's ability to activate NF-κB. A flagellin derivative (CBLB501) is currently being developed as a radioprotectant drug by Cleveland Biolabs (Cleveland, OH) and is the focal point of a number of anti-bioterrorism grants. The survival graphs shown below illustrate the unusual, highly significant protective effect of flagellin on mice exposed to gamma radiation. All animal work was performed by our collaborators, Dr. Gudkov and CBL.

2a. Optimal radioprotective dose of Flagellin (CBLB501). Whole body irradiation of mice with 15 Gy gamma radiation leads to death within 8 days from GI syndrome providing a conventional model of radiation induced damage of GI tract. Accordingly, high doses of 15 Gy was chosen so that the primary cause of death in mice is GI syndrome. Two flagellin doses (2.0 μg/mouse and 5 μg/mouse) were chosen on the basis of its potency to induce efficiently NF-κB - dependent production of IL-8 and IL-1β in vivo. C56BL6 mice (6 week old males, 10 animals per group) were given intravenous injection of two doses 2.0 μg/mouse (0.08 mg/kg) or 5 μg/mouse (0.2 mg/kg) of CBLB501 four hours before 15 Gy gamma-irradiation and mouse survival was monitored daily (**Figure 6**). Vehicle-treated animals, as expected, died within 8 days. Flagellin, however, significantly delayed mouse death in dose-dependent manner. This study led us to choose the higher dosage of 5 μg/mouse (0.2 mg/kg) for subsequent experiments. This dose, while providing good radioprotection, is five times lower than the dose demonstrating moderate toxicity (1 mg/kg) and 50 times lower than lethal dose (10 mg/kg).

Figure 6. Dose dependent radioprotective effect of Flagellin.

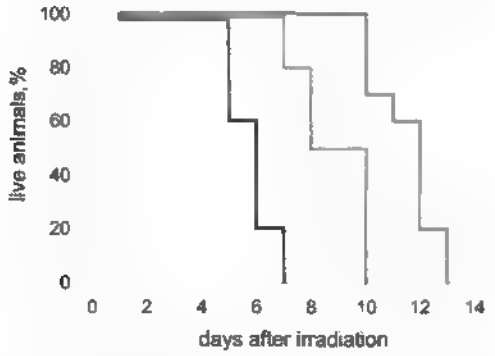

2b. Optimal pharmacodynamics (time of the administration) of Flagellin. We had estimated the dependence of the radioprotective activity of flagellin on the time of treatment by injecting mice at several time points relative to the moment of gamma-irradiation. Experiments were done essentially as explained above, using intraperitoneal injection of 5 μg/mouse (0.2 mg/kg) of flagellin or, for control mice, 5 μg/mouse (0.2 mg/kg) of bacterial RNA polymerase. The experiments described below were performed on NIH-Swiss mouse strain. The results show that flagellin provides 90% survival if injected at 1 or 2 hours before irradiation with 13 Gy (**Figure 7**). Only the -1 hour graph is shown for clarity, however, both time points (-1, and -2 hour) provided similar degree and dynamics of survival. Flagellin injected 2 minutes before or 1 hour after irradiation had no protective effect against 13 Gy induced death (data not shown). Also, flagellin did not provide protection when injected 24 hours prior to 13 Gy irradiation.

Interestingly, administration of flagellin 24 hours before 10 Gy gamma-irradiation provided 100% protection. While 13 Gy irradiation in mice primarily induces death from GI syndrome, 10 Gy-induced death is mostly mediated by hematopoietic syndrome. Accordingly, such long-term protection from 10 Gy irradiation may be mediated by enhanced proliferation or survival of hematopoietic stem cells induced by flagellin and/or long-living secondary cytokines.

In conclusion, we have shown that Flagellin currently provides the best protection of any known natural product to gamma radiation, especially since it is protective against death by gastrointestinal syndrome.

Figure 7. Effect of flagellin (CBLB501) injected intraperitoneally at indicated times before irradiation on mouse sensitivity to 13 Gy and 10 Gy of total body gamma radiation.

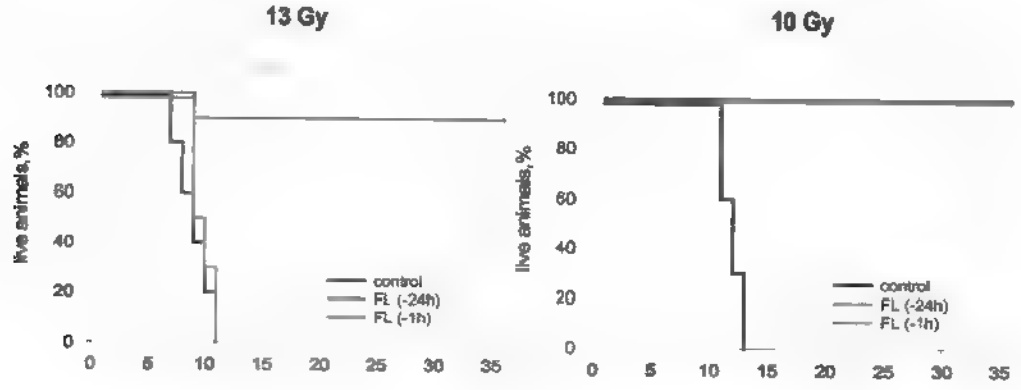

3. Discovery of a novel NF-κB-dependent antiviral response that does not involve interferon.

One of the goals of this project has been to identify the molecular signaling pathways activated by bacterial and viral pathogens and their products in a number of relevant cell types including lung epithelial, intestinal epithelial, oral epithelial cells and macrophages. We have identified the major stress-activated pathways in lung epithelial cells and in intestinal epithelial cells (Bose et al., 2003). We have used the lung-tropic viruses Respiratory Syncitial Virus (RSV) and Human Parainfluenza Virus (HPIV-3), the bacterial pathogen Salmonella typhimurium and the bacterial protein flagellin to stimulate responses in tissue culture cells. As a by-product of these studies, we have found that flagellin is the main proinflammatory mediator in both intestinal epithelial cells (as described above) and also in lung epithelial cells (Tallant et al., 2004). Additionally, and perhaps even more importantly, we have uncovered a novel anti-viral innate host response that requires activation of the NF-κB transcription factor and expression of one of its unknown target genes. This unknown gene(s) can turn a mildly cytopathic virus (HPIV-3) into an extremely virulent one similar to RSV. Also, triggered expression of this NF-κB target gene

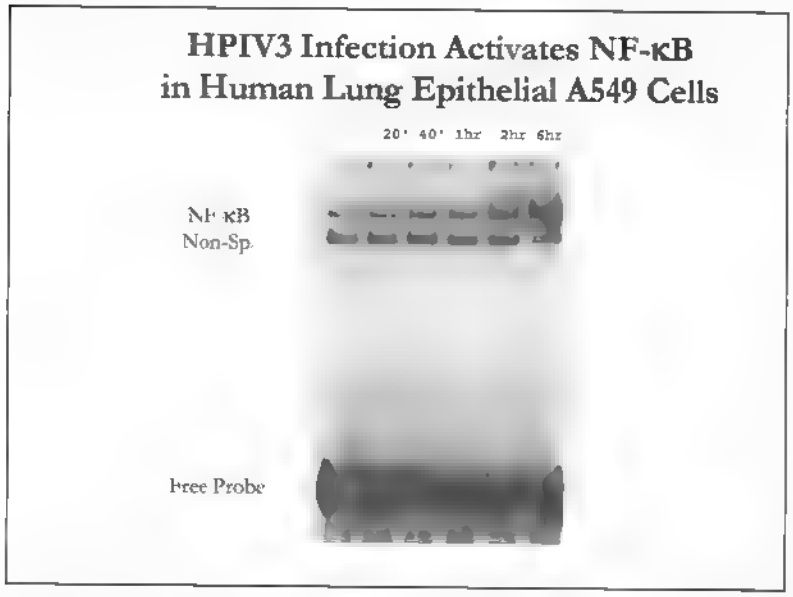

Figure 8. HPIV3 infection activates NF-κB HPIV3 was used to infect A549 cells at an m.o.i. of 0.5 and whole cell extracts were prepared at the indicated times after infection. EMSA assays were performed with 25ug of cell extract and an NF-κB –specific radiolabeled probe.

by a number of means prior to RSV or influenza A severely limits the infectiveness of these and other negative strand RNA viruses. These results are have been published (Bose et al., 2003). These findings are significant in that they identify a mechanism by which a mildly cytopathic virus can be turned into a virulent one without genetic manipulation. As importantly, these results also point to the existence of a factor(s) that can negate the effects of virulent negative strand RNA viruses and could have broad-spectrum protective effects among a number of current Category A biologicals. Further study of these two aspects of our work are beyond the scope of this project and are being investigated in the DiDonato laboratory and other CCF laboratories using other funding.

We have preliminarily identified the envelope glycoprotein HN of HPIV-3 as the viral protein recognized by one of the Toll-like receptors (TLRs) in the host cell. We have also found that the NF-κB activation and anti-viral activity work through the TLR adapter protein MyD88 (**Figure 9**). The identity of the TLR that recognizes this protein is putatively TLR7 (**Figures 10 and 11**). We have also found that TLRs 6, 7 & 8 play an important role in activating the anti-viral state triggered by HPIV-3 infection. We are not certain yet whether TLRs 6, 7 and 8 form heterodimeric partnerships that can recognize this protein, although particular combinations of the dominant-negative alleles when expressed in A549 cells inhibit NF-κB activation (**Figure 10**). In addition, TLR7 expressed exogenously in 293HEK cells which do not activate NF-κB in response to HPIV-3 viral infection and are known to lack TLRs except for TLRs 1, 5 and 6, restores responsiveness to HPIV-3 as measured by NF-κB activation (**Figure 11**). These results further imply a role for TLR7 (and perhaps TLR6) in responding to HPIV-3 viral proteins and infection. We are currently trying to finish these analyses and are in the initial phases of writing a manuscript addressing these findings.

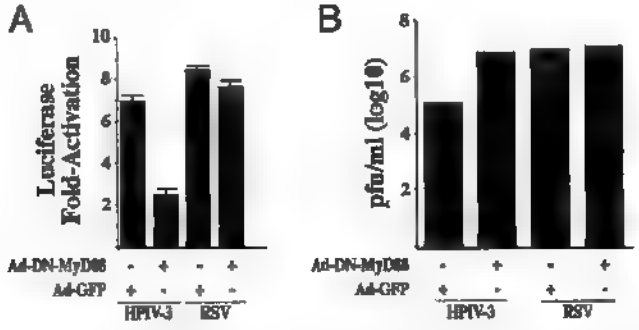

Figure 9. HPIV3 infection activates NF-κB and requires MyD88. HPIV3 was used to infect A549 cells that were transfected with an NF-kB reporter gene (IL-8 luciferase) at an m.o.i. of 0.5 and cell extracts were prepared 12h after infection and analysed for luciferase activity in (A). B. A549 cells infected previously with either GFP or DN-MyD88 expressing adenovirus (m.o.i. 50) were infected 36h post infection at an m.o.i. of 0.1 with either HPIV-3 or RSV virus. Viral supernatants were serially diluted and plaque assays performed on CV-1 cells and the results plotted.

Figure 10. TLR7DN expression blocks HPIV3 –mediated NF-κB activation. HPIV3 was used to infect A549 cells (m.o.i. of 0.5) that had previously been infected with self-inactivating lentiviruses expressing either GFP, DN TLRs 1-5, or TLRs 6-9 or the listed combinations of DN-TLRS. The cells in the top panel were stimulated with either nothing, HPIV-3 or IL-1 (10ng/ml) and whole cell extracts were prepared 90min after infection or 45min after IL-1 stimulation. EMSA assays were performed with 25ug of cell extract and an NF-κB –specific radiolabeled probe.

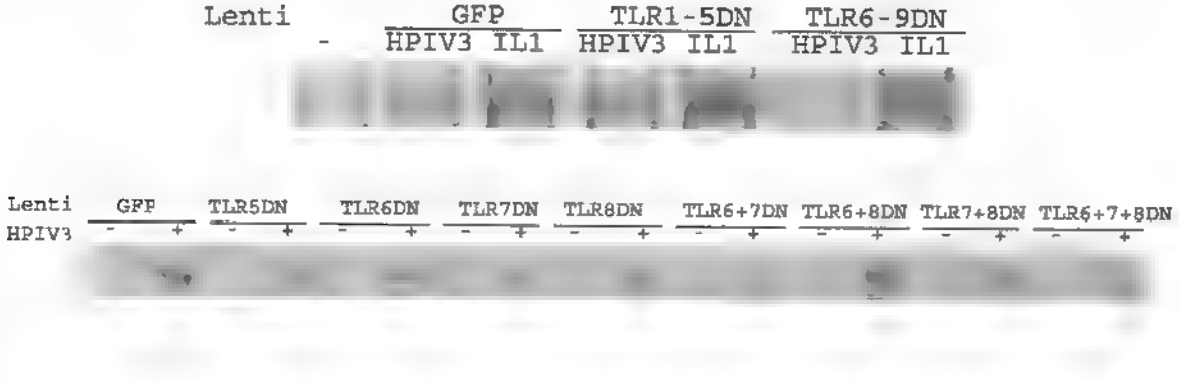

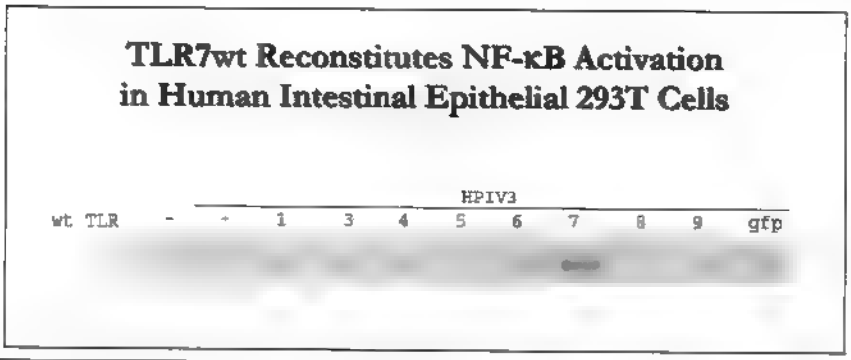

Figure 11. HPIV3 infection activates NF-κB in response to TLR7 expression. HPIV3 (an m.o.i. of 0.5) was used to infect 293HEK cells that were transiently transfected with mammalian expression vectors encoding wildtype TLRs 1-9 as indicated along with GFP as a negative control. Whole cell extracts were prepared 90 min after infection. EMSA assays were performed with 25ug of cell extract and an NF-κB–specific radiolabeled probe.

4. PKR as a target for therapy of virulent orthopoxvirus infections

Protein kinase R (PKR) is an interferon (IFN) regulated dsRNA-activated host defense enzyme essential in higher vertebrates to effectively suppress the spread of different viruses (Williams 1999; Williams 2001). PKR is a key regulator of immune responses through its effects on both gene transcription and protein synthesis. For example, upon activation by viral dsRNA, PKR phosphorylates the translation initiation factor, eIF2α, leading to inhibition of mRNA translation. PKR also responds to viral and bacterial inflammatory stimuli by

phosphorylating transcription regulators, including the inhibitor of NF-κB, IκB, and the transcription factors IRF-1, Stat3 and ATF2 (Williams 1999).

Preclinical studies demonstrate that PKR is a potentially important drug target. Although PKR is a key anti-viral protein in the interferon host defense system, becomes activated during viral infection and is required for efficient suppression of the replication of a variety of viruses, PKR has also been implicated in cellular stress responses and signaling pathways regulating inflammation. Therefore, controlling PKR activity may be a viable strategy to treat a number of chronic inflammatory conditions as well as the inflammatory side effects associated with the pathogenesis of infection with select agents such as Anthrax and Pox viruses. PKR has recently been implicated in neurodegenerative diseases including Alzheimer's and Huntington disease (Peel et al. 2001; Chang et al. 2002a, 2002b; Onuki et al. 2004), expanding the potentially important targets for PKR therapeutic approaches. Most relevant to this grant is our recent discovery that PKR plays a key role in modulating NF-κB transcription factors activated by Poxvirus infection.

Currently, the molecular mechanisms contributing to the virulence of variola virus and monkeypox virus are largely unknown. Genomic analyses of variola virus, monkeypox virus and other members of the orthopoxvirus genus have not revealed any variola or monkeypox virus specific genes that can account for the virulence of these viruses. Indeed, these virulent viruses lack many immunomodulatory genes present in the genomes of less virulent orthopoxviruses. One explanation for the virulence of these viruses is that rather than expressing unique virulence factors, these viruses act type-specifically to induce host responses that become destructive to or lethal to the host, instead of protecting the host. In this model, the virulent viruses may possess greater abilities to induce such host responses than avirulent viruses, or they may lack the ability to suppress such responses, or they may possess both properties. Consistent with such a model, victims of variola virus (even in the absence of bacterial infection) typically exhibit symptoms of toxemia that could result from deregulated cytokine production, similar to that induced by many bacterial infections.

Transcription of many of the genes induced during bacterial or viral infections is under the control of the NF-κB family of transcription factors (reviewed in Karin and Ben-Neriah 2000; Karin et al. 2004; Williams 1999). Examples of immune response genes under the control of NF-κB include those encoding cytokines, chemokines, cell adhesion molecules, acute phase response proteins and other genes important to the immune response, such as TAP-1, MHC class I, IL-2R, IκB, iNOS, cyclooxygenase-2, and cIAPs. Our collaborator, Dr. David Pickup, has shown that orthopoxviruses act in a type-specific manner to either induce or inhibit NF-κB activation (Oie and Pickup 2001). Accordingly, we hypothesize that viral activation may contribute to poxvirus pathogenesis. Our rationale is that variola virus pathogenesis resembles that of bacterial toxemia, and NF-κB activation has been implicated as a major contributory factor in establishment of this state (Koplan and Foster 1979; Barnes and Karin 1997; Neish et al. 2000). To test this hypothesis, in collaboration with Drs. Inger Damon and Joe Esposito (at the CDC) Dr. Pickup has begun to examine the potential of monkeypox virus to affect NF-κB signaling. Preliminary results (**Figure 12**) are consistent with this hypothesis. A highly virulent strain of monkeypox virus (MPV-V79-I-005) induces IκBα degradation in the absence of external stimuli, whereas cowpox virus does not, and the avirulent MPV Copenhagen is intermediate in effect between the other two viruses.

Figure 12. Virulent Monkeypox Virus Induces Turnover of IκBα.

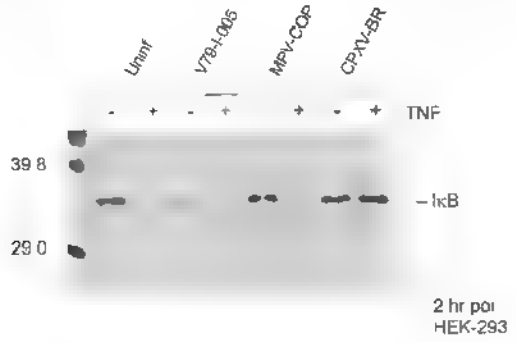

Recently, in collaboration with Dr. Pickup, we have demonstrated that vaccinia virus (strain MVA)-mediated activation of NF-κB is dependent upon host PKR (**Figures 13 and 14,** manuscript in preparation). We hypothesize that a major contributory factor in monkeypox virus infection is deregulated cytokine production generated by viral induction of PKR-mediated activation of NF-κB-regulated gene expression.

Figure 13. MVA-induced degradation of IκB is impaired in PKR-/- cells.

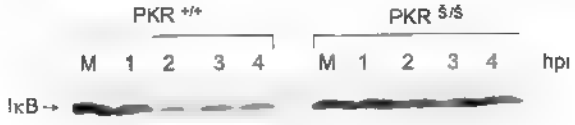

Figure 14. MVA-induced degradation of IκB is restored in PKR-/- cells expressing human PKR.

Therefore, in contrast to the generally accepted notion of PKR as an anti-viral protein, we have shown that PKR is essential for the ability of Poxviruses to activate NF-κB. Thus, an inhibitor of PKR could be used to reduce the inflammatory response associated with Poxvirus infection as well as limit the symptoms associated with Anthrax infection.

Based upon existing experimental evidence and our understanding of the physiological activity of PKR, our hypothesis is that highly selective PKR inhibitors will have high potential for use in clinical applications against potential agents of bioterrorism such as Poxvirus and *Bacillus anthracis*. In the future, it should be possible to use a high throughput screening (HTS)

method based on fluorescence polarization (FP) to identify PKR inhibitors within libraries of chemical compounds.

Our data is significant in that it suggests that new classes of therapeutics could be developed targeting host proteins such as PKR, or components of the NF-κB signaling pathway, as a means of abrogating or reducing the pathogenic effects of variola or monkeypox virus infections. Therapeutics of this type would not be directly antiviral, but they could be expected to reduce the morbidity and mortality associated with these infections. Such supportive therapy might enable patients to resist the infection, in the same way that most patients tolerate and clear less virulent viruses. In addition, such therapies could be given as adjuvant therapies in conjunction with antiviral drugs designed to block viral replication. Currently, with the exception of the fairly toxic drug, cidofovir, neither form of therapy is available.

5. Analysis of interferon- and double stranded RNA-regulated signaling pathways impacted by Sendai virus infection.

Many cellular genes, encoding proteins of diverse functions, are transcriptionally induced during viral infections. Because host-virus co-evolution has tolerated this host response to virus infection, it is thought to be conducive to maintaining proper viral homeostasis at the cellular and organismal levels. Many virally induced proteins have direct or indirect anti-viral effects. They may inhibit protein synthesis in infected cells, impair viral assembly, initiate the innate immune response, or prime the adaptive immune response. Diverse components of the infecting virus or viral intermediates, produced during replication, can be the responsible agents that trigger the signaling pathways leading to cellular gene induction. Depending on the specific virus, viral envelope proteins, viral ribonucleoproteins, or viral single-stranded (ss) or double-stranded (ds) RNAs have been shown to be the critical inducer. Among these, dsRNA has been historically viewed as the most important agent because it is often produced in virus-infected cells; and synthetic dsRNA, when added to cells, can induce transcription of some of the same cellular genes that are induced by virus infection. A major transducer of signaling, activated by exogenously added dsRNA or intracellular viral dsRNA is a member of the Toll-like receptor (TLR) family, TLR3.

One set of common genes induced by many viruses and dsRNA encode type I interferons (IFNs). These secreted cytokines have strong anti-viral effects. Surprisingly, many dsRNA-induced and virally induced cellular genes are also induced by IFNs, thus creating a positive feedback loop that reinforces induction of the same genes in infected cells.

To pursue our interest in identifying the signaling pathways responsible for inducing specific sets of cellular genes upon virus infection, we focused our attention, in this study, on human genes that are induced early after SeV infection. We were interested in characterizing the repertoires of genes induced by SeV infection by classifying them into groups that are induced by IFNs, dsRNA, or other viral products. For identifying SeV-induced genes, we used the "IAD" cDNA microarray that was customized for this purpose. This array contains a subset of sequence verified cDNA clones from the Research Genetics 40K clone representing 1) 950 genes containing adenylate/uridylate rich elements and 18 genes potentially involved in AU-directed mRNA decay as previously described (Frevel et al., 2003), 2) 855 interferon stimulated genes representing an expansion of a previously described clone set (de Veer et al., 2001), 288 genes responsive to the viral analog poly (I).poly(C), representing an expansion of the clone set described by Geiss et al. (Geiss et al., 2001) and 85 housekeeping genes. Using this approach,

we previously identified many genes whose transcription is induced by IFNs (de Veer et al., 2001) or dsRNA (Geiss et al., 2001). In addition to many virally induced genes, dsRNA- and IFN-inducible genes were represented in the microarray used here. We had used mutant cell lines, which could not respond to IFN or dsRNA, for delineating the signaling pathways activated by those inducers. We took advantage of some of those mutant cell lines to assess the relative contributions of the IFN- and the dsRNA-signaling pathways in gene induction by SeV. Other mutant cell lines were used to investigate the relative contributions of NFκB and IRF-3, the major transcription factors activated by SeV infection, to cellular gene induction. The relevant characteristics of the cell lines used in this study are listed in the **Table below**.

Our study revealed that among the genes that are induced immediately after SeV infection, only a few were dependent on IFN signaling and none were dependent on dsRNA signaling through TLR3. As expected, one class of genes required NFκB, whereas another class required IRF-3 for induction in SeV-infected cells. Surprisingly, viral induction of a subset of NFκB-dependent genes was negatively regulated by IRF-3, thus revealing a new aspect of cross-talk between the two transcription factors.

Cell Line	*Lineage*	*Altered protein*	*Effected pathway*
HEK293	N/A	none	TLR3 non-responsive
293/TLR3	HEK293	TLR3 expression	TLR3 responsive
2fTGH	HT1080	none	w t
2F-SR	2fTGH	IκB dominant negative	NFκB signaling
U4C	2fTGH	Jak1 null	IFN signaling
P2.1	U4C	*decreased* IRF-3 expression, X?	IRF-3 signaling
U4C.2	U4C	*Increased* IRF-3 expression	
1080.10	HT1080		

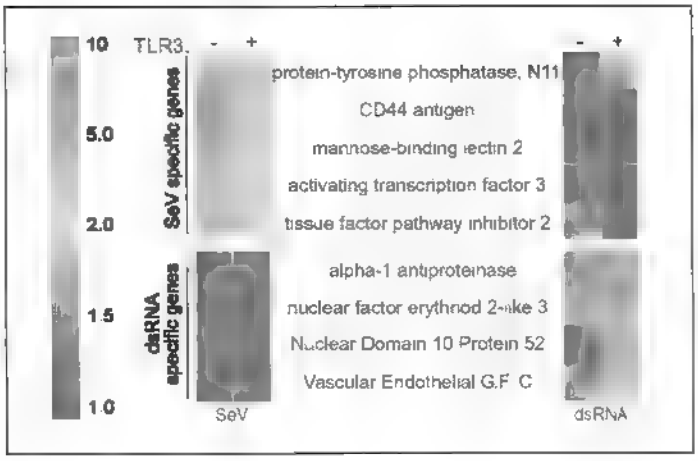

Figure 15. Differential induction of genes by SeV and dsRNA. Select genes differentially regulated by SeV and dsRNA in cells both without (-, 293) and with (+, 293/TLR3) TLR3. The tiles show the fold-increase in mRNA expression for specific genes in SeV- (left column) or dsRNA-treated (right column) cells relative to untreated cells as a function of color. Green indicates that expression was unchanged by treatment with SeV or ds RNA. Yellow→Red coloring shows that expression was induced to increasing degrees.

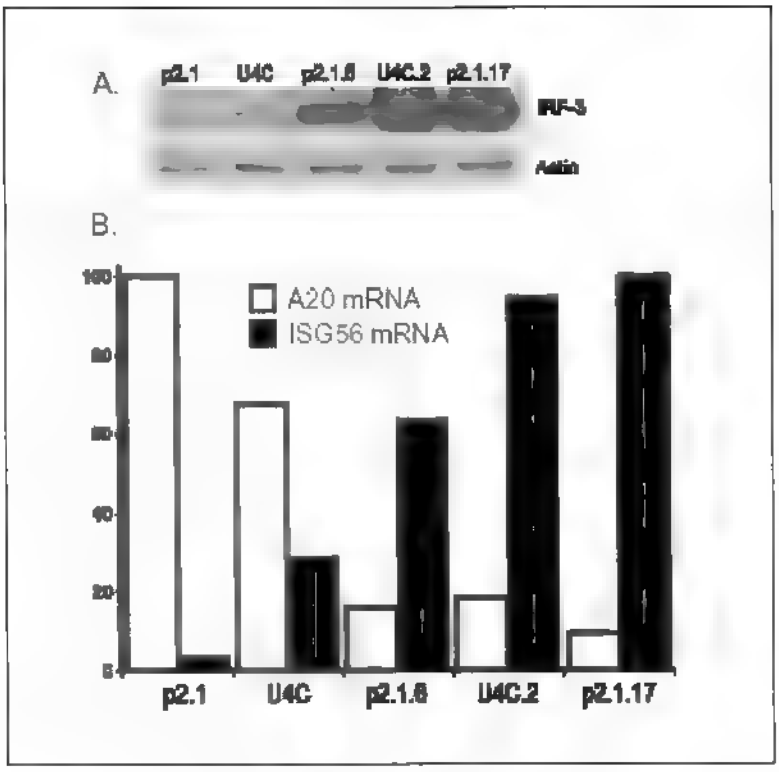

Figure 16. Modulation of A20 and ISG56 mRNA expression by cellular levels of IRF-3. Cell lines, derived from U4C and p2.1 cells, expressing different levels of IRF-3 protein were infected with SeV and analyzed for their expression of A20 and ISG56. (A) Western blot showing the relative levels of IRF-3 expression in the different cell lines relative to actin. (B) Percent maximum fold-induction of A20 (white) and ISG56 (black) in cells six hours after infection, normalized to actin expression as determined by RPA.

One of the most interesting and surprising observations of this study was that increased levels of IRF-3 negatively affected induction of some genes following SeV infection. Using the A20 gene as the sentinel for this group of genes, we demonstrated that, unlike the ISG56 gene, induction of A20 mRNA was inversely related to the level of IRF-3 (**Figure 16**). As described in more detail in the appended manuscript (Elco et al., 2005), this phenomenon was not restricted to the U4C cells and its derivatives; the same trend was also observed in wild type HT1080 cells over-expressing IRF-3. It is not clear how IRF-3 affects A20 gene induction by SeV. The promoter of this gene contains κB sites, but no ISRE and, as expected, its induction required NFκB, but not IRF-3. Thus, probably the observed negative effect of IRF-3 is expected at some level of the NFκB-signaling pathway, not at the A20 promoter level. Further investigation should reveal cross-talk between the two major virus-activated signaling pathways.

What are the possible physiological implications of the above phenomenon? SeV and other viruses cause active and rapid degradation of IRF-3 in infected cells (Lin et al., 1998). Consequently, the degree of induction of genes, such as A20, can be temporally regulated in the infected cells. Moreover, the level of IRF-3 expression varies greatly among different cell types and different tissues (data not shown). From the observations reported here one can predict that the profiles of gene induction, and hence the outcome of virus infection, will also vary greatly among different host cells. To speculate about the possible cellular functions of the genes that are negatively regulated by IRF-3, it is interesting to note that several such as A20, CIAP1 and CIAP2, have anti-apoptotic functions. The encoded proteins may protect the infected cells from the actions of the pro-apoptotic proteins that are also induced with virus infection. It has been reported that apoptosis of virus-infected cells is mediated by IRF-3 (Heylbroeck et al., 2000). Our results suggest that this function of IRF-3 may be mediated not only by inducing pro-apoptotic genes, but also by suppressing the induction of anti-apoptotic genes.

D3L-M. ***Feasibility of large scale screening of airway epithelium exposed to biological agents*** **and** ***Human Clinical Samples***

1. Clinical Samples.

We have completed a proof of principle experiment to identify potential sentinel transcripts activated by the presence of viral pathogens infecting Human Airway Epithelial Cells (HAEC). In general, exposures to biological agents in bioterrorism in humans occur first by the aerosol route with inhalation into the respiratory system. However, the feasibility of using these types of samples for large-scale detection of exposures is unknown. Our goals for this funding period included identification of early biomarkers of toxin exposure in human cells with the ultimate objective being the design of remediation techniques to remove toxins that contribute to diseases. In this context, our objectives were to:

(1) Provide sterile lung epithelial cells for evaluation of feasibility of use of primary cells in experiments.

(2) Expand and maintain primary lung cell cultures for use in *in vitro* studies of toxin or infectious agent exposure.

Specifically, these tasks allow access to human clinical samples allowing the direct study of the effects of toxins on primary human cells and tissues. We are using a lung sample repository that has been maintained in the Cleveland Clinic Lung Biology laboratory over the previous 8 years. Nontrackable sample numbers, which are not linked to the donor, are used as unique nontraceable identifiers. This task has been successful during this interim period in establishing the lung epithelial cells in culture, confirming epithelial phenotype, lack of infectious contaminants, and providing epithelial cell RNA in sufficient quantity for microarray experiments using *in vitro* exposure of primary cells to Influenza (see Zheng S et al., 2003 appended).

Human airway epithelial cells (HAEC) are grown on collagen-coated dishes, in specialized serum-free media (Clonetics). We have shown that cell cultures of HAEC lead to pure epithelial monolayer cultures. The epithelial nature of cultured HAEC was confirmed by morphology and positive reactions to anti-cytokeratins, which are epithelial cell specific. We characterize cells in culture as epithelial using anti-cytokeratin stains [(AE1/3 (Biogenex), 34BE12 (Dako)] while we have excluded contamination by mesenchymal cells, macrophage, lymphocyte cells by absence of staining for vimentin (Neomarkers), CD68 and CD3 (Dako). Non-transformed HAEC are limited to ±25 population doublings, a culture span of about 1-month and a maximum of 4 to 5 passages. All cells were mycoplasma tested and confirmed negative before use in experiments. These cultures of HAEC were used to determine gene expression changes elicited by either Influenza or Vaccinia infection (see sections D3A 1. and 2. above).

2. Discriminating among different viruses infecting lung epithelial cells using transcript profiling.

The finding that influenza- and vaccinia virus-infected HAEC gave very different gene expression profiles (see sections D3A 1. and 2. above) encouraged us to use the IAD array to identify a vaccinia virus-specifc gene expression signature using data from vaccinia virus-,

influenza virus- and parainfluenza virus-infected HAEC. As shown in our February 2004 progress report, a list of 25 genes was derived with Genespring 6.0 software using the class prediction function in which you can ask for the minimum number of genes that permit 100% success in assigning viral identity to a set of gene expression profiles from viral infection experiments. A set of profiles representing 19 different hybridizations including both biological and technical replicates of vaccinia, influenza and parainfluenza virus-infected HAEC were used. The data for those 25 genes are sufficient to correctly assign viral identity to each profile. This data supports the major hypothesis of our grant proposal, that unique gene expression signatures will allow detection and discrimination of specific infectious agents.

3. Impaired innate host defense causes susceptibility to respiratory virus infections in Cystic Fibrosis.

The application of the IAD array has allowed us to identify host factors in patients with cystic fibrosis (CF) that promote increased virus replication and cytokine production thus providing a mechanism for understanding the severity of viral disease in CF. NO produced by NOS2, following its induction by inflammatory cytokines acts as a major effector in host defense against viruses and bacteria. The expression of NOS2 in healthy airway epithelial cells has been demonstrated at both the protein and mRNA level *in vivo*. CF airway epithelial cells are more susceptible to viral and bacterial infection because of defective innate host defense mechanisms of NOS2 expression and STAT1 activation. We hypothesized that the IFN-γ signaling pathway that leads to NOS2 gene induction in CF airway epithelial cells is defective. In contrast to NOS2, the major histocompatibility complex class 2 (MHCII) gene, an IFN-γ regulated delayed-responsive gene, is similarly induced in CF and non-CF airway epithelial cells (NL), suggesting a NOS2 specific defect in the IFN-γ signaling pathway. STAT1 and activator protein 1 (AP-1), both required for NOS2 gene expression, interact normally in CF cells. Protein inhibitor of activated STAT1 (PIAS1) is not increased in CF cells. Interferon-γ induces NOS2 expression in airway epithelial cells through an autocrine mechanism involving synthesis and secretion of IFN-γ-inducible mediator(s), which activates STAT1. Here, CF cells secrete IFN-γ inducible factor(s) which stimulate NOS2 expression in NL cells, but not in CF cells. In contrast, IFN-γ inducible factor(s) similarly inhibit virus in CF and NL cells. Thus, autocrine activation of NOS2 is defective in CF cells, but IFN-γ induction of antiviral host defense is intact. The results of this work have been published (Zheng S. et al., 2003 and 2004, appended).

NO donors or NOS2 over-expression provides protection from virus infection in CF, suggesting that NO is sufficient for antiviral host defense in the human airway and is a potential strategy for antiviral therapy in CF children. The fact that heterozygous alleles are common in the caucausian population gives cause for concern that these individuals may be at higher risk for viral agents of bioterrorism than the normal population. NO donors may be useful as antivirals in this instance. Furthermore, extension of CF children's life expectancy occurred with the introduction of antibiotics, but also through vaccination against virus. For example, vaccination against measles was one of the earliest interventions that led to improved survival in the 1960's. Prior to vaccination, CF children who contracted measles, a virus like HPIV3 in the paramyxovirus family, had progressive decline in their general condition, worsening of pulmonary infections and early death. These clinical observations taken together with the identification of enhanced virus susceptibility of CF airway cells suggest that therapies aimed at

improving antiviral host defense may further delay the onset of bacterial colonization and extend the life of CF individuals.

Key research accomplishments

1. Successfully used arrays constructed and tested during the previous granting period to analyze gene expression patterns in RNA extracted from whole blood from subjects undergoing orthopox vaccination against smallpox.

2. Established that infection of HAEC by different viruses results in virus-specific gene expression profiles.

3. Established a gene expression profile that can distinguish orthopox infection from commonly occurring respiratory infections.

4. Demonstrated that the activity of the Jak1 kinase impacts replication of Ebola virus.

5. Showed that genes encoding ribosomal proteins are significantly and coordinately downregulated upon Vaccinia Virus infection of lung cell lines.

6. Used siRNA-mediated gene ablation together with gene expression analysis to determine that Phospholipid Scramblase is required for induction of a discrete subset of interferon stimulated genes and for limiting replication of VSV and EMCV.

7. Demonstrated our ability to select single chain antibodies that efficiently immunoprecipitate cellular proteins of interest.

8. Demonstrated that Flagellin is a major regulator of inflammatory responses in intestinal epithelial cells, acting through a pathway involving TLR5 and NFκB.

9. Identified the bacterial protein Flagellin as a novel radioprotectant.

10. Discovered a novel NF-κB-dependent anti-viral response that determines virus virulence.

11. Showed that impaired NOS2 signaling in the airway epithelium of Cystic Fibrosis patients increases their susceptibility to respiratory virus infections.

12. Demonstrated that Vaccinia Virus-mediated activation of NF-κB is dependent upon the double stranded RNA activated kinase PKR.

13. Identified roles for IFN, NF-κB and IRF-3, but not TLR3, in Sendai virus-mediated gene induction. We also found that viral induction of a subset of NFκB-dependent genes was negatively regulated by IRF-3, thus revealing a new aspect of cross-talk between the two transcription factors

Reportable outcomes

Publications resulting from this grant award:

1. Zheng S, De BP, Choudhary S, Comhair SA, Goggans T, Slee R, **Williams BR**, Pilewski J, Haque SJ, **Erzurum SC** (2003). Impaired innate host defense causes susceptibility to respiratory virus infections in cystic fibrosis. Immunity; 18(5):619-30.

2. Bose S, Kar N, Maitra R, **DiDonato JA**, Banerjee AK (2003). Temporal activation of NF-kappaB regulates an interferon-independent innate antiviral response against cytoplasmic RNA viruses. Proc Natl Acad Sci U S A; 100:10890-10895.

3. Dong B, Zhou Q, Zhao J, Zhou A, Harty RN, Bose S, Banerjee A, Guenther J, Slee R, **Williams BRG**, Wiedmer T, Sims PJ and **Silverman RH** (2004). Phospholipid Scramblase 1 (PLSCR1) Potentiates The Antiviral Activity of Interferon. J. Virol; 78: 8983-93.

4. Tallant T, Deb A, Kar N, Lupica J, Takeuchi O, deVeer M and **DiDonato JA** (2004). Flagellin acting via TLR5 is the major activator of NF-κB and the proinflammatory gene program in intestinal epithelial cells. BMC Microbiology; 4:33-45.

5. Zheng, S, Xu W, Bose S, Banerjee A, Haque SJ, **Erzurum SC** (2004). Impaired Nitric Oxide Synthase (NOS) 2 signaling pathway in cystic fibrosis airway epithelium. Am J Physiol Lung Cell Mol Physiol; 287:L374-L381.

6. Elco CP, Guenther JM, **Williams BRG**, Sen GC (2005, in press). Analysis of genes induced by Sendai virus infection of mutant cell lines reveals essential roles of IRF-3, NFκB, and interferon, but not TLR3. Scheduled for publication in: J. Virol; April 2005, Vol 79 No. 7.

Conclusions

A custom array specifically designed to detect changes in cellular gene expression resulting from infection by viruses of bacteria has been tested in a live orthopox virus vaccination study. While individual variations were quite marked, adverse events could be detected as a change in profile. This study established that RNA can be extracted from small (2-5ml) quantities of whole blood and exposure to a smallpox surrogate detected using our IAD array. Furthermore, the utility of the array in detecting early adverse events in small samples of whole blood was demonstrated. While we noted that there are cell line specific responses in gene expression profiles to infection with the same virus, the infection of primary airway epithelial isolated from different individuals infected with the same virus gave very similar results suggesting that the individual variation seen in RNA isolated from whole blood was not a major factor in primary airway epithelial cells. A gene expression profile has been established that yielded 25 genes that successfully discriminated orthopox virus infection from other common respiratory viruses. Accordingly we have succeeded in one of our major objectives, which was to define sentinel markers of infection with specific agents. In addition we have made progress in the

development of antibody reagents to study cellular signaling pathways utilized or impacted by viral or bacterial pathogens. Our goal remains to use these antibodies to construct a prototype protein array. The combined use of cDNA microarrays and protein arrays promises to provide a rapid and accurate diagnostic tool to identify and manage exposure to pathogenic biological agents. In addition, our work has resulted in a number of unanticipated discoveries that have revealed new areas for further study. These include the identification of potential therapeutics such as flagellin, potential targets such as PKR and novel signaling pathways. Thus the funding provided by this grant has led to a number of advances in our understanding of the impact of viral and bacterial agents on host cells. This knowledge provides a foundation that will contribute to the development of diagnostic and therapeutic tools to deal with the ever-increasing threat of biological agents to human health.

References

Breman JG, Henderson DA. Diagnosis and management of smallpox. N Engl J Med. 2002 Apr 25; 346(17):1300-8.

Bartlett JG. Smallpox vaccination and HIV infection. Hopkins HIV Rep. 2003 Jan;15(1):1-3

Sepkowitz KA. How contagious is vaccinia? N Engl J Med. 2003 Jan 30;348(5):439-46.

Zheng S, De BP, Choudhary S, Comhair SA, Goggans T, Slee R, Williams BR, Pilewski J, Haque SJ, Erzurum SC.(2003) Impaired innate host defense causes susceptibility to respiratory virus infections in cystic fibrosis.Immunity;18(5):619-30.

Condit RC, Motyczka A, Spizz G. Characterization, and physical mapping of temperature-sensitive mutants of vaccinia virus.Virology. 1983 Jul 30;128(2):429-43.

Reddel RR, Ke Y, Gerwin BI, McMenamin MG, Lechner JF, Su RT, Brash DE, Park JB, Rhim JS, Harris CC. Transformation of human bronchial epithelial cells by infection with SV40 or adenovirus-12 SV40 hybrid virus, or transfection via strontium phosphate coprecipitation with a plasmid containing SV40 early region genes. Cancer Res. 1988 Apr 1;48(7):1904-9

Brum L.M., et al., *Virology* 315:322-34, 2003

Dong B, Zhou Q, Zhao J, Zhou A, Harty RN, Bose S, Banerjee A, Guenther J, Slee R, Williams BRG, Wiedmer T, Sims PJ and Silverman RH (2004). Phospholipid Scramblase 1 (PLSCR1) Potentiates The Antiviral Activity of Interferon. J. Virol; 78: 8983-93.

Bose S, Kar N, Maitra R, DiDonato JA, Banerjee AK (2003). Temporal activation of NF-kappaB regulates an interferon-independent innate antiviral response against cytoplasmic RNA viruses. Proc Natl Acad Sci U S A; 100:10890-10895.

Tallant T, Deb A, Kar N, Lupica J, Takeuchi O, deVeer M and DiDonato JA (2004). Flagellin acting via TLR5 is the major activator of NF-κB and the proinflammaorty gene program in intestinal epithelial cells. BMC Microbiology; 4:33-45.

Barnes, P.J. and M. Karin (1997). "Nuclear factor-kappaB: a pivotal transcription factor in chronic inflammatory diseases." *N Engl J Med* 336(15): 1066-71.

Chang, R. C., K. C. Suen, C. H. Ma, W. Elyaman, H. K. Ng and J. Hugon (2002a). "Involvement of double-stranded RNA-dependent protein kinase and phosphorylation of eukaryotic initiation factor-2alpha in neuronal degeneration." *J Neurochem* 83(5): 1215-25.

Chang, R. C., A. K. Wong, H.K. Ng and J. Hugon (2002)."Phosphorylation of eukaryotic initiation factor-2alpha (eIF2alpha) is associated with neuronal degeneration in Alzheimer's disease." *Neuroreport* 13(18):24232.

Karin, M. and Y. Ben-Neriah (2000). "Phosphorylation meets ubiquitination: the control of NF-[kappa]B activity." *Annu Rev Immunol* 18: 621-63.

Karin, M., Y. Yamamoto, and Q.M. Wang (2004). "The IKK NF-kappa B system: a treasure trove for drug development." *Nat Rev Drug Discov* 3(1): 17-26.

Koplan, J.P. and S.O. Foster (1979). "Smallpox: clinical types, causes of death, and treatment." *J Infect Dis* 140(3): 440-1.

Neish, A.S., et al. (2000). "Prokaryotic regulation of epithelial responses by inhibition of IkappaB-alpha ubiquitination." Science 289(5484): 1560-3.

Oie, K.L. and D.J. Pickup (2001). "Cowpox virus and other members of the orthopoxvirus genus interfere with the regulation of NF-kappaB activation." *Virology* 288(1): 175-87.

Onuki, R., Y. Bando, E. Suyama, T. Katayama, H. Kawasaki, T. Baba, M. Tohyama and K. Taira (2004). "An RNA-dependent protein kinase is involved in tunicamycin-induced apoptosis and Alzheimer's disease." *Embo J* 23(4): 959-968.

Peel, A. L., R. V. Rao, B. A. Cottrell, M. R. Hayden, L. M. Ellerby and D. E. Bredesen (2001). "Double-stranded RNA-dependent protein kinase, PKR, binds preferentially to Huntington's disease (HD) transcripts and is activated in HD tissue." *Hum Mol Genet* 10(15): 1531-8.

Williams, B. R. (1999). "PKR; a sentinel kinase for cellular stress." *Oncogene* 18(45): 6112-20.

Williams, B. R. G. (2001). Signal integration via PKR, Science's STKE. 2001.

de Veer, M.J., et al., Functional classification of interferon-stimulated genes identified using microarrays. J Leukoc Biol, 2001. **69**(6): p. 912-20.

Geiss, G., et al., A comprehensive view of regulation of gene expression by double-stranded RNA-mediated cell signaling. J Biol Chem, 2001. **276**(32): p. 30178-82.

Frevel, M.A., et al., p38 Mitogen-activated protein kinase-dependent and - independent signaling of mRNA stability of AU-rich element-containing transcripts. Mol Cell Biol, 2003. **23**(2): p. 425-36.

Heylbroeck, C., et al., The IRF-3 transcription factor mediates Sendai virusinduced apoptosis. J Virol, 2000. **74**(8): p. 3781-92.

Lin, R., et al., Virus-dependent phosphorylation of the IRF-3 transcription factor regulates nuclear translocation, transactivation potential, and proteasomemediated degradation. Mol Cell Biol, 1998. **18**(5): p. 2986-96.

Appendices

1. Zheng S, De BP, Choudhary S, Comhair SA, Goggans T, Slee R, **Williams BR**, Pilewski J, Haque SJ, **Erzurum SC** (2003). Impaired innate host defense causes susceptibility to respiratory virus infections in cystic fibrosis. Immunity; 18(5):619-30.

2. Bose S, Kar N, Maitra R, **DiDonato JA**, Banerjee AK (2003). Temporal activation of NF-kappaB regulates an interferon-independent innate antiviral response against cytoplasmic RNA viruses. Proc Natl Acad Sci U S A; 100:10890-10895.

3. Dong B, Zhou Q, Zhao J, Zhou A, Harty RN, Bose S, Banerjee A, Guenther J, Slee R, **Williams BRG**, Wiedmer T, Sims PJ and **Silverman RH** (2004). Phospholipid Scramblase 1 (PLSCR1) Potentiates The Antiviral Activity of Interferon. J. Virol; 78: 8983-93.

4. Tallant T, Deb A, Kar N, Lupica J, Takeuchi O, deVeer M and **DiDonato JA** (2004). Flagellin acting via TLR5 is the major activator of NF-κB and the proinflammatory gene program in intestinal epithelial cells. BMC Microbiology; 4:33-45.

5. Zheng S, Xu W, Bose S, Banerjee A, Haque SJ, **Erzurum SC** (2004). Impaired Nitric Oxide Synthase (NOS) 2 signaling pathway in cystic fibrosis airway epithelium. Am J Physiol Lung Cell Mol Physiol; 287:L374-L381.

6. Elco CP, Guenther JM, **Williams BRG**, Sen GC (2005, in press). Analysis of genes induced by Sendai virus infection of mutant cell lines reveals essential roles of IRF-3, NFκB, and interferon, but not TLR3. Scheduled for publication in: J. Virol; April 2005, Vol 79 No. 7.

Immunity, Vol. 18, 619–630, May, 2003, Copyright ©2003 by Cell Press

Impaired Innate Host Defense Causes Susceptibility to Respiratory Virus Infections in Cystic Fibrosis

Shuo Zheng,[1,2] Bishnu P. De,[3,5] Suresh Choudhary,[2] Suzy A.A. Comhair,[1,2] Tannishia Goggans,[1,2] Roger Slee,[2] Bryan R.G. Williams,[2] Joseph Pilewski,[4] S. Jaharul Haque,[1,2] and Serpil C. Erzurum[1,2,*]
[1]Department of Pulmonary and Critical Care Medicine
[2]Department of Cancer Biology
[3]Department of Virology
Lerner Research Institute
Cleveland Clinic Foundation
Cleveland, Ohio 44195
[4]Departments of Medicine, and Cell Biology and Physiology
University of Pittsburgh
Pittsburgh, Pennsylvania 15261

Summary

Viral infection is the primary cause of respiratory morbidity in cystic fibrosis (CF) infants. Here, we identify that host factors allow increased virus replication and cytokine production, providing a mechanism for understanding the severity of virus disease in CF. Increased virus is due to lack of nitric oxide synthase 2 (NOS2) and 2′, 5′ oligoadenylate synthetase (OAS) 1 induction in response to virus or IFN-γ. This can be attributed to impairment of activation of signal transducer and activator of transcription (STAT)1, a fundamental component to antiviral defense. NO donor or NOS2 overexpression provides protection from virus infection in CF, suggesting that NO is sufficient for antiviral host defense in the human airway and is one strategy for antiviral therapy in CF children.

Introduction

Cystic fibrosis (CF) is the most common lethal genetic disorder among Caucasians, affecting an estimated 30,000 persons in the US (Cystic Fibrosis Foundation, 2000). The gene responsible for CF (Kerem et al., 1989; Riordan et al., 1989; Rommens et al., 1989) produces the cystic fibrosis transmembrane conductance regulator (CFTR), a polypeptide of 1480 amino acids with molecular mass of 168 kDa, and function of a cAMP-dependent Cl^- channel (Anderson et al., 1991; Sheppard and Welsh, 1999). CF is characterized by chronic lung infections with bacteria, mostly *Pseudomonas aeruginosa*, intense neutrophil-dominated airway inflammation, and progressive lung disease, which is the major cause of morbidity and mortality. Bacterial colonization of CF lung is usually established in the first decade of life (Rosenfeld and Ramsey, 1992). Little is known about the factors associated with initial colonization in CF lung, but viral infections predispose CF lung to bacterial colonization. Although chronic bacterial infection occurs in older CF children, 39% of CF children in the first year of life are hospitalized with respiratory compromise related to respiratory virus infection. Furthermore, individuals hospitalized with respiratory symptoms during infancy are six times more likely to acquire *Pseudomonas aeruginosa* during early childhood (Armstrong et al., 1998). Studies show a relationship between viral respiratory tract infection with respiratory syncytial virus, parainfluenza virus, and influenza virus and pulmonary exacerbation and disease progression in CF children (Hiatt et al., 1999; Hordvik et al., 1989; Petersen et al., 1981; Wang et al., 1984). Although CF patients have no higher incidence of viral infection, severity of viral infection is amplified.

The innate antiviral response of human cells involves distinct cellular programs (Iordanov et al., 2001). In the presence of dsRNA, a common viral intermediate, 2′, 5′ oligoadenylate synthetase (2′, 5′ OAS), and dsRNA-dependent protein kinase (PKR) promote inhibition of host cell protein synthesis by activating RNase L to degrade viral and cellular RNA and by phosphorylating the α subunit of translation initiation factor, eIF2, to block its recycling from an inactive form, respectively. This prevents viral replication, eventually leading to the self-elimination of the infected cell via apoptosis. This program is probably most efficient for viral infections that are initiated by a small number of infected cells at a local site of virus entry. A second program is the production of antiviral interferons (IFN) by mucosal cells and serves the purpose of preparing adjacent naive cells for resistence to viral invasion. This program requires survival of infected cells and expression of antiapoptotic genes through activation of nuclear factor-κB (NF-κB) transcription factor. NF-κB and interferon regulatory factors (IRF) 3 and 7 are required for production of type 1 interferons (Grandvaux et al., 2002). Subsequently, IFN induces antiviral pathways including PKR, 2′, 5′ OAS/RNase L system, and Mx proteins (Samuel, 1991; Stark et al., 1998) Mx proteins are IFN-inducible, high-abundance GTPases which interfere with viral replication, impairing the growth of negative-strand RNA viruses at the level of viral transcription and other steps (Stark et al., 1998). dsRNA or IFN-γ are also potent activators of nitric oxide synthase 2 (NOS2)- and nitric oxide (NO)-dependent antiviral pathways. High-level NO synthesis results in a large variety of reactive products, which can inhibit viral replication by modifying a number of target molecules essential for replication (Biron, 1999). STAT1, a member of a family of proteins that transduce signals from cell surface receptors to the nucleus and activate transcription by binding directly to regulatory DNA elements, is essential for host antiviral defense. IFN-α and IFN-γ lead to phosphorylation of STAT1 and binding to unique elements in a number of IFN-stimulated genes (ISGs), activating transcription (Haque and Williams, 1998). Although many antiviral genes are induced or activated in direct response to viral dsRNA, fundamental components of antiviral defense are activation of PKR, 2′, 5′ OAS, and NOS2 via the IFN/STAT1 pathways. In support of this, STAT1-deficient mice, which display

*Correspondence: erzurus@ccf.org
[5]Present address: Belfer Gene Therapy Core Facility, Weill Medical College of Cornell University, New York, NY 10021.

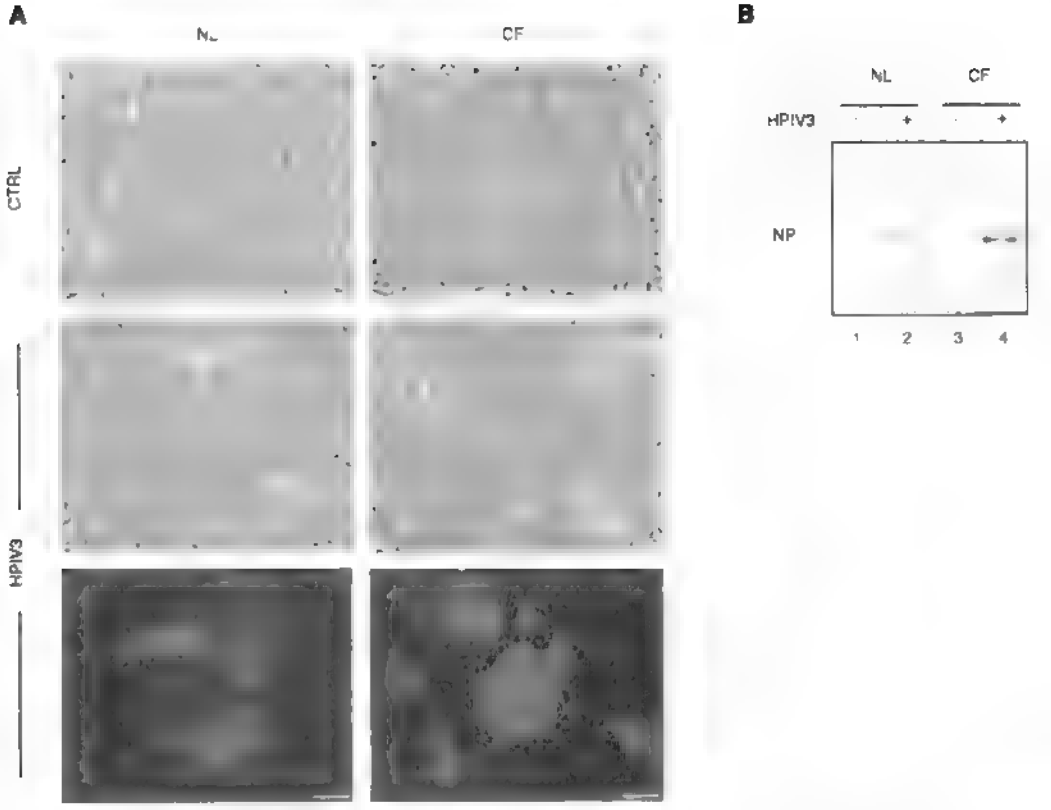

Figure 1. Increased HPIV3 Replication in CF Cells

(A) Phase contrast picture of NL and CF cells, uninfected (upper panels) or 24 hr after HPIV3 infection (middle panels) and immunofluorescence staining for HPIV3 NP 24 hr postinfection (lower panels) ($n = 3$). Bars, 100 μm.

(B) Equal amounts (20 μg) of ^{35}S-methionine-labeled new protein synthesized in NL and CF cells were immunoprecipitated by HPIV3 anti-RNP antibody and loaded in each lane ($n = 3$).

a complete lack of responsiveness to IFN, are highly sensitive to infection by virus (Durbin et al., 1996; Meraz et al., 1996).

In this context, we hypothesized that CF airway epithelial cells may be less effective in eliminating viral infection due to an impairment of the antiviral host defense mechanisms in CF lung. Here, we show that CF airway epithelial cells allow increased replication of parainfluenza virus and an increased production of proinflammatory cytokines. Investigation of the innate and interferon (IFN)-mediated antiviral pathways reveals that the antiviral pathway of nitric oxide synthesis is absent in CF. Furthermore, upregulation of 2′, 5′ OAS1 does not occur in CF cells in response to IFN or dsRNA. This can be attributed to impaired STAT1 activation, which may be a central mechanism responsible for the deficiencies in CF antiviral host defense.

Results

Increased Viral Replication in CF

CF and normal (NL) human airway epithelial cells (HAEC) were infected with human parainfluenza virus 3 (HPIV3) (0.1 moi) and syncytia (cell-cell fusion) formation evaluated (Figure 1A). Cell-cell fusion was increased in CF cells compared to NL 24 hr after infection (middle panel). Immunofluoresent staining for HPIV3 N-protein (NP) revealed greater size and number of syncytia containing virus in CF cells (lower panel). To confirm that the NP present in the cell lysate was from viral replication and not from added virus, new protein synthesized was evaluated by ^{35}S-methionine incorporation followed by SDS polyacrylamide gel electrophoresis of cell lysates immunoprecipitated with anti-RNP antibody which recognizes HPIV3 NP. NP was detected at ~2-fold higher level in CF than NL (Figure 1B).

IFN Pretreatment Protects CF Cells from Virus

First identified because of their ability to interfere with virus replication, IFNs are fundamental in host antiviral defense (Biron, 1999; Briscoe et al., 1996; Durbin et al., 1996; Grandvaux et al., 2002; Isaacs et al., 1957; Karaghiosoff et al., 2000; Karupiah et al., 1993; Samuel, 1991; Stark et al., 1998). To investigate IFN antiviral effects in CF, CF cells were pretreated with 1000 U/ml IFN-α, IFN-γ, or no cytokine for 24 hr, and then infected with HPIV3 (0.1 moi). Syncytia formation was prevalent in untreated CF cells (Figure 2A, upper-right panel), but pretreatment with IFN-α or IFN-γ prevented viral syncytia formation (Figure 2A, lower panels). Evaluation of HPIV3 N-mRNA expression revealed that more virus N-mRNA was formed in infected CF than in NL cells,

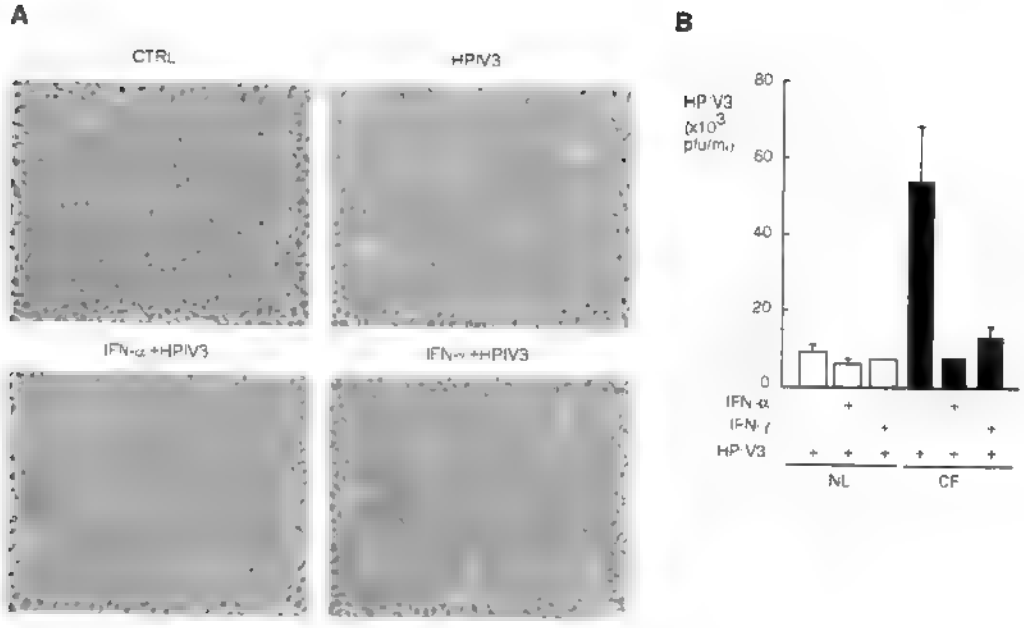

Figure 2. IFN Pretreatment Protects CF Cells from HPIV3 Infection

(A) Phase contrast pictures of CF cells, untreated (upper-left panel), infected with HPIV3 (upper-right panel), or pretreated with IFN-α (lower-left panel) or IFN-γ (lower-right panel) 24 hr before HPIV3 infection (n = 2). Bars, 100 μm.

(B) Infectious viral particles in media overlying cells untreated or pretreated with IFN-α (1000 U/ml) or IFN-γ (1000 U/ml) measured by plaque assay [plaque forming units (pfu)/ml × 10^2] after HPIV3 infection (0.1 moi). Infectious viral particles are higher titer in media overlying CF cells (n = 5) than NL (n = 3) [p = 0.015].

and IFN-α or IFN-γ pretreatment significantly reduced the N-mRNA in both NL and CF cells (data not shown). Media overlying cells were evaluated for infectious HPIV3 particles by plaque assay. CF produced ~6-fold more infectious HPIV3 as compared to NL (CF: 53 ± 15, range 30~70, n = 5; NL: 8 ± 2, range 6~10, n = 3 [$\times 10^3$ pfu/ml]). IFN-α and IFN-γ pretreatment reduced virus in CF to NL levels (Figure 2B). Innate antiviral pathways in NL cells appeared effective in eliminating viral replication, but IFN pretreatment reduced viral load by ~1.5-fold. IFN-α and IFN-γ pretreatment reduced virus in CF by 7- and 5-fold, respectively ($p < 0.05$, student's t test).

Increased viral replication may result in an increase in proinflammatory cytokine production and contribute to severity of virus infection in vivo (Matsukura et al., 1996; Zhu et al., 1996). Thus, cytokine production by cells was evaluated. Supernatant from CF cells 24 hr after HPIV3 infection had higher IL-6 and IL-8 compared to NL, although baseline levels were similar [(baseline: IL-6 pg/ml, CF 13 ± 1, NL 12 ± 2; IL-8 pg/ml, CF 195 ± 87, NL 164 ± 30; n = 3, $p > 0.05$ CF versus NL), (24 hr postinfection: IL-6 pg/ml, CF 2568 ± 1996, NL 208 ± 62; IL-8 pg/ml, CF 11920 ± 8606, NL 2822 ± 245, n = 3, $p < 0.05$, 24 hr comparison, CF versus NL, Mann-Whitney test)].

Expression of Antiviral Proteins in CF

CF and NL cells infected with HPIV3 (0.1 moi) or treated with IFN-α for 24 hr expressed MxA. IFN-α induced higher MxA compared to HPIV3, while IFN-γ did not induce MxA (Figure 3A). MxA was produced at later times after HPIV3 infection as compared to IFN-α stimulation (data not shown). IFN-α is synthesized by lung epithelial cells after viral infection (Gao et al., 1999), and virus-induced MxA expression is likely a consequence of IFN-α (Pavlovic et al., 1992; Ronni et al., 1997). Similar levels of IFN-α were produced by CF and NL in response to virus, reaching peak levels in media overlying cells by 6 hr postinfection (data not shown).

Western analyses for IRF-1, PKR, RNase L, and 2′, 5′ OAS1 were performed with cell lysates collected at 4, 16, and 24 hr after stimulation with virus mimic, dsRNA, or IFN-γ. PKR and IRF-1 were induced by IFN-γ and polyIC in both NL and CF. RNase L did not change before or after stimulation but was present in both cell types. Although NL cells increased 2′, 5′ OAS1 after stimulation, CF cells failed to upregulate expression of 2′, 5′ OAS1 (Figure 3B). Viral induction of NOS2 in CF and NL was assessed 24 hr after HPIV3 infection (0, 0.2, 0.4, 1.0 moi). NL showed a dose-dependent induction of NOS2 by HPIV3, but CF had no detectable NOS2. Expression of MxA confirmed the presence of viral infection (Figure 3C). Reverse transcription of RNA and polymerase chain reaction of cDNA (RT-PCR) analysis of NOS2 mRNA in CF and NL confirmed lack of NOS2 induction in CF in response to HPIV3 (data not shown).

Early in virus infection, host defenses including NOS2 may be induced by dsRNA through PKR signaling pathways, independent of IFN-γ, in NL cells (Uetani et al., 2000). However, by 24 hr after infection, large amounts of IFN-γ are produced which lead to activation of numerous downstream target genes. Specifically, IFN-γ is a

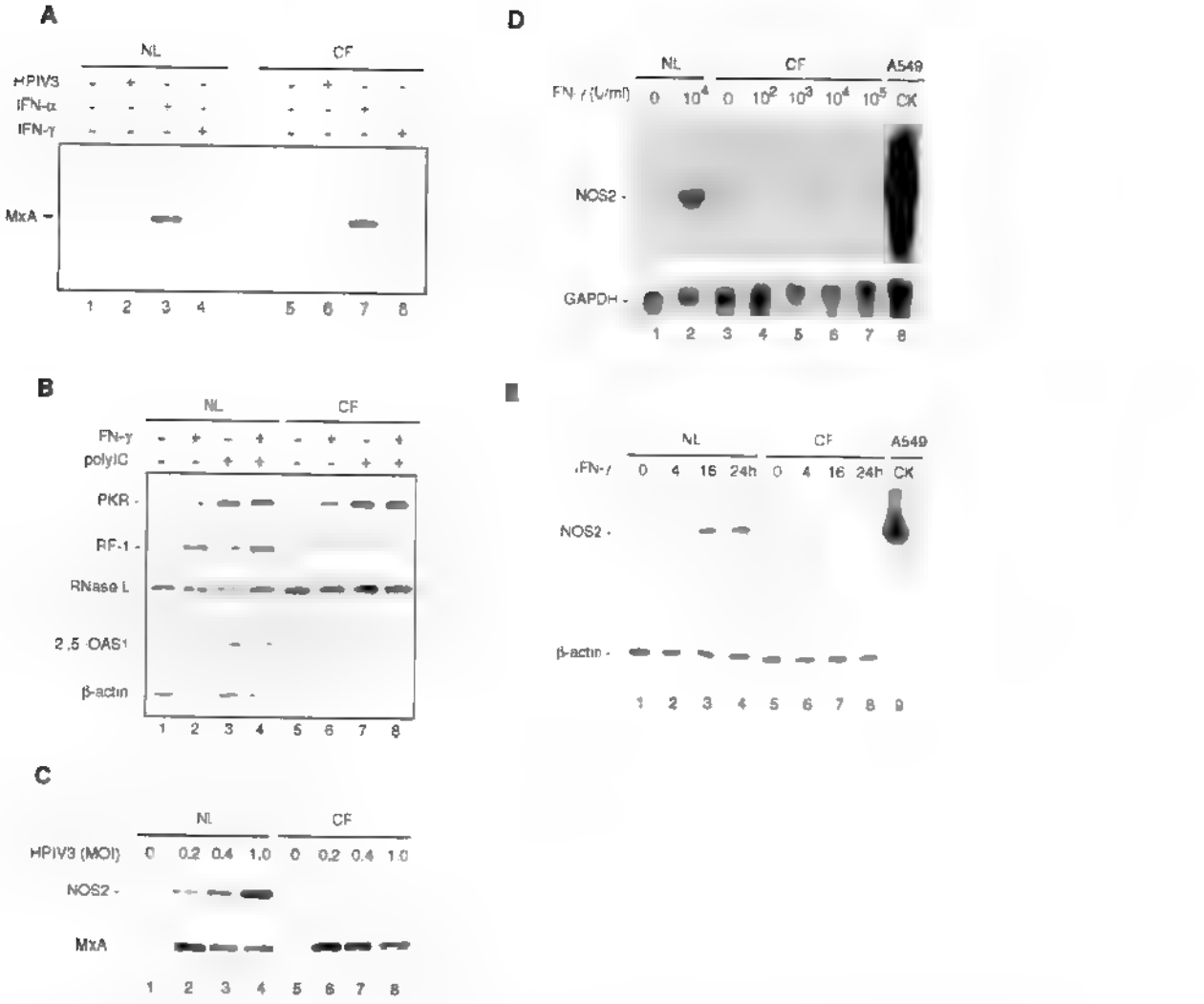

Figure 3. Impaired Antiviral Pathways in CF Cells

(A) Western analysis of MxA in CF and NL cells, untreated, infected with HPIV3 (0.1 moi), or stimulated by IFN-α (1000 U/ml) or IFN-γ (1000 U/ml) for 24 hr (n = 2).

(B) Western analysis of PKR, IRF-1, RNase L, and 2', 5 - OAS1 in CF and NL cells, untreated, or treated with IFN-γ (1000 U/ml), polyIC (100 ng/ml), or by mixture of IFN-γ and polyIC (n = 3).

(C) Western analysis for NOS2 and MxA in NL and CF cells, uninfected and infected with HPIV3 (n = 2).

(D) Northern analysis for NOS2 in total RNA (4 μg/lane) from CF or NL cells 24 hr after IFN-γ stimulation. Total RNA (5 μg/lane) from A549 cells 8 hr after stimulation with 10^3 U/ml IFN-γ, 0.5 ng/ml IL-1β, and 10 ng/ml TNF-α (cytokine mixture, CK) was used as positive control (n = 2).

(E) Western analysis of NOS2 protein in cell lysate (50 μg total protein/lane) from NL or CF cells 24 hr after IFN-γ stimulation (n 3).

potent inducer of NOS2 gene expression in normal human airway cells (Guo et al., 1997; Uetani et al., 2000). Here, Northern analysis of NOS2 expression revealed that NL cells expressed NOS2 mRNA upon IFN-γ exposure, while CF cells did not (Figure 3D). Western analysis of proteins extracted at different time points after IFN-γ stimulation showed that NL produced NOS2 protein as early as 16 hr, while CF had no detectable NOS2 (Figure 3E). We also tested induction of NOS2 by polyIC, and combinations of cytokines (IFN-γ, IL-1β, TNF-α) in replicate experiments (n = 3). NOS2 was not induced in CF cells by any combination of stimuli (data not shown).

Similar IFN Response in CF and NL Cells

Based upon findings of defective induction of two antiviral pathways, we expanded evaluation of the IFN response in CF. We compared gene expression profiles in CF and NL at baseline (Figure 4A) and 8 hr after IFN (Figures 4B and 4C) by a custom-constructed ISG/AU/dsRNA cDNA microarray, which contains 2921 genes specific for viral and IFN responses. IFN responses were similar between CF and NL with only 0.9% and 0.5% difference in IFN-α- and IFN-γ-induced changes in gene expression (correlation of CF to NL response: IFN-α R^2 0.931; IFN-γ R^2 = 0.940). IFN-α induced 81 genes and

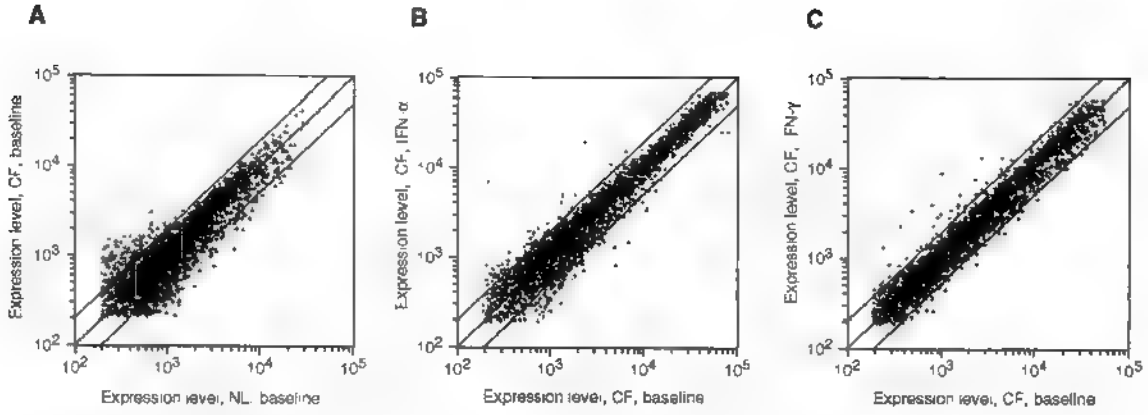

Figure 4. Gene Expression Profile of CF and NL Cells

(A) Baseline gene expression of CF cells compared to NL. (B) Gene expression 8 hr after IFN-α or (C) IFN-γ treatment in CF cells.

repressed 68 genes; IFN-γ induced 27 genes and repressed 33 genes. This similarity of CF response to NL accounts for the effectiveness of IFN pretreatment in inhibiting virus replication in CF cells. On the other hand, a baseline comparison between CF and NL evaluated by ISG/AU/dsRNA microarray identified 226 differentially expressed genes. In CF cells, 136 genes (4.6% of total genes) were 2-fold upregulated, and 90 genes (3% of total genes) were 2-fold downregulated as compared to NL. This baseline difference was confirmed by transcriptosome analysis on Affymetrix HG-U133A GeneChips. Table 1 highlights the genes that are different (≥1.2-fold change) and relevant to IFN, antiviral effects, and/or NOS2 induction. Notable findings include decreased JAK1, a receptor-associated kinase essential for IFN signaling, and increased IRF2, a competitive inhibitor of IRF-1. Both genes are key to antiviral defense and specifically to NOS2 induction (Briscoe et al., 1996; Kamijo et al., 1994; Nelson et al., 1993). The 2′, 5′ OAS1 was also lower in CF at baseline, confirming the Western blot analysis (Figure 3B).

Transcription Factors in CF

Further experiments were performed to investigate the mechanism of deficiency of antiviral host defense in CF, and specifically the reduced NOS2 expression in CF. To evaluate signal transduction proteins IRF-1 and NF-κB, which are important to the host antiviral response including NOS2 induction, we treated CF and NL with IFN-γ (10^3 U/ml), tumor necrosis factor-α (TNF-α) (10 ng/ml), or synthetic dsRNA (polyIC) (100 ng/ml) as a mimic of virus infection, then the transcription factor activation

Table 1. Gene Expression in CF Cells Relative to NL at Baseline

UniGene	Gene Description	Ratio CF/NL	Genebank
Cytokine-Related Genes			
Hs.93913	IL-6: interleukin 6	3.1	NM_000600
Hs.624	IL-8: interleukin 8	2.22	NM_000584
Hs.1722	IL-1 α: interleukin 1 α	3.13	M15329
Hs.285115	IL-13 receptor, α 1	1.42	U81380
Hs.25954	IL-13 receptor, α 2	2.26	NM_000640
Hs.196384	PTHS2: prostaglandin-endoperoxide synthase 2	2.59	NM_000963
Hs.372783	SOD 2: superoxide dismutase 2, mitochondrial	2.79	X15132
Hs.211600	TNFAIP3: tumor necrosis factor α 3	1.51	AI738896
Interferon/Virus-Related Genes			
Hs 83795	IRF 2: interferon regulatory factor 2	1.33	NM_002199
Hs 115541	JAK2: Janus kinase 2	2.00	AF001362
Hs.86958	IR-2: interferon receptor 2	>2	L41944
Hs.179972	IFI α: interferon α-induced protein	1.30	NM_018011
Hs.50651	JAK 1: Janus kinase 1	<0.5[a]	
Hs.82396	2 , 5′ OAS1: 2′, 5′-oligoadenylate synthetase 1	0.43	NM_002534
Apoptosis			
Hs.381231	caspase 8	>2	NM_00128
Hs.9216	caspase 7	1.75	NM_001227
Others			
Hs.234642	APQ3: aquaporin 3	0.47	NM_004925
Hs.89603	MUC1: mucin 1	0.37	NM_002456

[a] Ratio from cDNA microarray data. Gene expression level is below detection limit on Affymetrix genechip. All other ratios are from Affymetrix genechip.

analyzed in whole-cell extract (WCE) by electrophoretic mobility shift assay (EMSA). In contrast to previous reports of reduced IRF-1 expression in whole lungs of CF mice (Kelley and Elmer, 2000; Widdicombe, 2000), IRF-1 was strongly activated by IFN-γ in both CF and NL. Its activation by TNF-α or polyIC was weaker but similar in CF and NL (Figure 5A). Similarly, NF-κB was activated by dsRNA or TNF-α in both CF and NL (Figure 5B). Quantitation of total NF-κB (p65 and p50) showed no difference between CF and NL (NF-κB relative units: nonstimulated, CF 990 ± 380, NL 1090 ± 360; IFN-γ, CF 970 ± 490, NL 1240 ± 350; polyIC, CF 2000 ± 310, NL 2670 ± 280; TNF-α CF 3250 ± 140, NL 4130 ± 790; $n = 3$, all $p > 0.05$).

Activation of STAT1 is essential for NOS2 expression and the antiviral response (Gao et al., 1997; Guo et al., 1997; Heitmeier et al., 1999). To evaluate STAT1, CF and NL were exposed to IFN-γ (10^3 U/ml) for 30 min, then WCE collected and analyzed by EMSA with ^{32}P-labeled GAS oligo duplex. CF had lower STAT1 activation compared to NL (Figure 5C). Impairment of STAT1 activation was consistent in CF, and ~60% of NL (Figure 5D). STAT1 is important for not only NOS2 expression, but also for STAT1 itself. To evaluate STAT1 production in CF, CF and NL cells exposed to IFN-γ for 24 hr were evaluated by Western blot using rabbit polyclonal anti-STAT1 Ab. 2fTGH and U3A, human fibroblast cell lines with and without expression of STAT1 (Muller et al., 1993), were used as positive and negative controls for STAT1 expression. Baseline STAT1 protein in CF was less than NL, and 24 hr after IFN-γ, NL expressed more STAT1 than CF (Figure 5E). STAT1 protein in CF was only 53% of that in NL (CF = 1.6 ± 0.7, NL = 3.0 ± 1.3, $n = 4$, $p < 0.05$). Furthermore, after IFN-γ stimulation, STAT1 in CF was significantly lower than NL (CF = 5.1 ± 0.6, NL = 10.6 ± 2.0, $p < 0.01$) (Figure 5F).

Overexpression of NOS2 or NO Donor Protects CF from Virus

Previous work suggests that loss of NOS2 expression in cells leads to increased susceptibility to viral infection (Flodstrom et al., 2001; Karupiah et al., 1998; Noda et al., 2001). Induction of NOS2 prior to infection is associated with inhibition of viral replication (Reiss and Komatsu, 1998; Sanders, 1999). Since CF cells are unable to express NOS2, NOS2 expression construct or NO donors were used to correct the NO deficiency. We introduced NOS2-transgene into CF cells by transfecting the cells with NOS2 expression plasmid (pCCF37). Control CF cells were transfected with reverse sequence NOS2 (R-NOS2) plasmid (pCCF38), or liposome reagent without plasmid, or left untreated. All cells were infected with HPIV3 (0.5 moi) 24 hr after transfection. Alternatively, two types of NO donors, S-nitroso-N-acetyl penicillamine (SNAP) or deta NONOate, were added to cells at the time of viral infection. NOS2 was expressed in CF transfected with pCCF37 but not in control CF cells (Figure 6A). Indicative of viral production, HPIV3 NP was present in untreated and control transfected cells but not in CF cells expressing the NOS2 transgene. Quantitated as nitrite and nitrate in the media, NO production in CF cells transfected with NOS2 transgene was similar to levels produced by NL cells stimulated with IFN-γ [$NO_2^- + NO_3^-$ (μM): CF cells + NOS2 transgene, 8.0 ± 1.0; NL cells + IFN-γ, 9.5 ± 0.5]. NO donor compounds produced higher levels of NO in the media [$NO_2^- + NO_3^-$ (μM): SNAP, 50 ± 20; detaNO, 29 ± 1]. NO donors SNAP and deta NONOate, decreased viral load ~2.5-fold. Strikingly, CF cells transfected with NOS2 transgene (pCCF37) had nearly undetectable infectious virus in the overlying media (Figure 6B). NOS2 overexpression may be more efficient than NO donors because NOS2 transgene provides continuous generation of intracellular NO.

Discussion

Here, CF airway epithelial cells are shown at the cellular level to be more susceptible to HPIV3 infection than NL. Increased virus is due to lack of specific antiviral host defense in CF, including NOS2 and 2′, 5′ OAS 1 which may be attributed to impairment of activation of STAT1. In support of the biological relevance of ~6-fold increase of virus, murine studies have shown that loss of innate host defenses leads to a moderate increase in virus, but significantly more severe clinical outcomes (Flodstrom et al., 2001; Kosugi et al., 2002; Noda et al., 2001; Xiang et al., 2002; Zhou et al., 1999). For example, even though the increase of virus is modest in organs of NOS2-deficient (NOS2 $^{-/-}$) mice with cytomegalovirus (Noda et al., 2001) or coxsackievirus B4 (Flodstrom et al., 2001) as compared to wild-type, the NOS2 knockout mice have higher mortality and decreased virus clearance. Likewise, CMV replication is only moderately enhanced as evidenced by 5-fold increase in viral titers in mice pretreated with a specific inhibitor of NOS2, but this results in viral persistence and latency (Kosugi et al., 2002). Mice triple deficient in Mx, RNase L, and PKR have increased susceptibility to virus, although viral titers are not significantly elevated in tissues (Xiang et al., 2002; Zhou et al., 1999). More severe clinical outcomes with modest increase of virus may occur due to inherent viral properties and/or altered host cellular response (Garcia-Sastre, 2001, 1998; Seo et al., 2002). For example, virulence may be increased with moderately higher titers due to more efficient inhibition of host antiviral pathways. Conversely, greater activation of signaling pathways, such as NF-κB, due to increased dsRNA produced during increased viral replication, may amplify proinflammatory cytokine production (Matsukura et al., 1996; Zhu et al., 1996). In this study, CF cells released more IL-6 and IL-8 than NL in response to virus. Higher levels of IL-6 and IL-8, which are involved in neutrophil accumulation and degranulation and contribute to greater airway inflammation and more severe respiratory symptoms with virus (Matsukura et al., 1996; Zhu et al., 1996). For example, severity of clinical symptoms with rhinovirus is primarily related to high levels of IL-6 in nasal secretions (Zhu et al., 1996). CF airways, even in infants, contain higher levels of proinflammatory cytokines, particularly IL-6 and IL-8, irrespective of bacterial colonization (Aldallal et al., 2002; Noah et al., 1997). Thus, it has been hypothesized that inflammation is intrinsic to the CF neonatal airway prior to infection. Here, baseline IL-6 and IL-8 secretion are similar in CF and

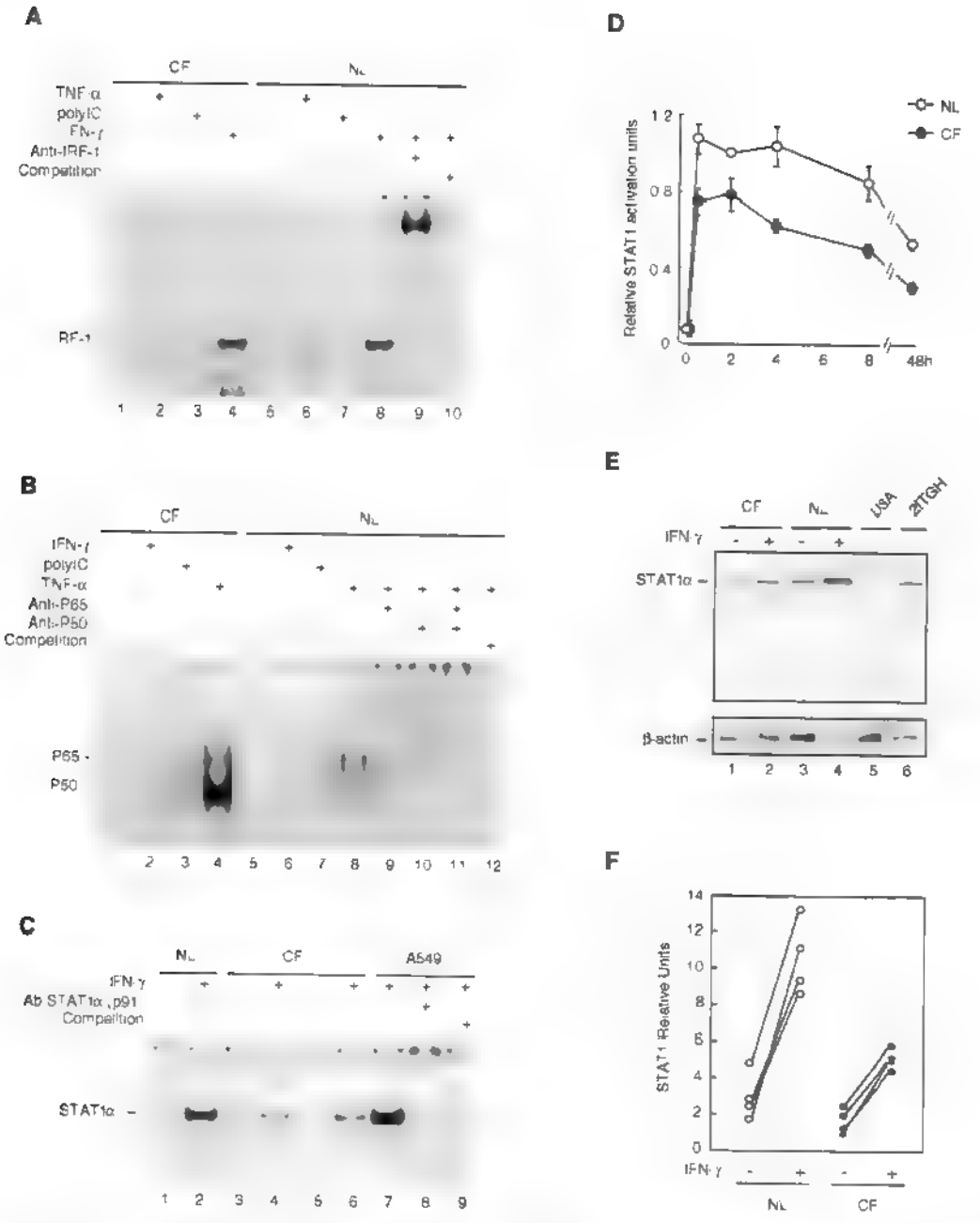

Figure 5. Activation and Expression of Transcription Factors in CF Cells

(A) WCE (4 μg) from CF and NL cells, untreated or treated with TNF-α, polyIC, or by IFN-γ for 3 hr were evaluated for IRF-1 by EMSA (n = 4).

(B) NF-κB activation was evaluated by EMSA in cells stimulated with TNF-α, polyIC, or by IFN-γ for 1 hr (n = 3).

(C) CF and NL cells were stimulated with IFN-γ for 30 min and WCE collected to evaluate for STAT1 activation by EMSA. IFN-γ-stimulated A549 was a positive control, and supershift with anti-STAT1 (p91) and competition with unlabeled GAS probe confirmed presence of STAT1 in the complex.

(D) STAT1 activation at different times was quantitated in four independent EMSA experiments, which were averaged and expressed as relative units normalized to NL value at 2 hr.

(E) Cell lysate (20 μg total protein/lane) from CF or NL 24 hr after IFN-γ stimulation was evaluated for STAT1 (p91) expression by Western analysis. Lysates from 2fTGH and U3A were used as positive and negative controls.

(F) Quantitation of Western analysis of STAT1 expression in cell lysate from four pairs of NL and CF cells, unstimulated or 24 hr after IFN-γ.

NL, but IL-6 and IL-8 mRNA are higher, which may account for the greater release of cytokines upon viral infection. Thus, virus may be one stimulus for the increased cytokine production in CF airways. Taken together, the susceptibility of CF infants to virus may be explained by increased virus and cytokine production,

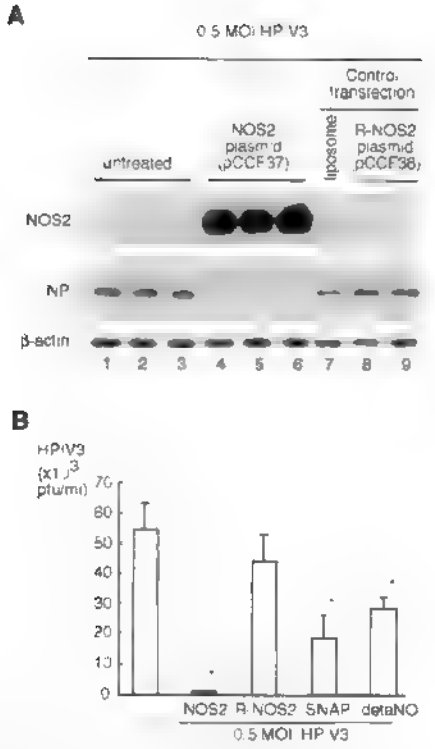

Figure 6. NOS2 Overexpression or NO Donors Protect CF Cells from HPIV3 Infection

(A) Western analysis for NOS2 and HPIV3 NP in CF cells infected by HPIV3, transfected with NOS2 expression construct (NOS2, pCCF37), exposed to reagent alone, or transfected with reverse sequence NOS2 expression construct (R-NOS2, pCCF38) 24 hr prior to infection (n = 2).

(B) Plaque assay using media overlying CF cells 24 hr after HPIV3 infection (0.5 moi). 24 hr prior to infection, CF cells were transfected with NOS2 expression construct (NOS2, pCCF37), reverse sequence NOS2 expression construct (R-NOS2, pCCF38), reagent alone (liposome), or left untreated. At the time of infection, some untreated CF cells were exposed to NO donors, SNAP, or deta NONOate (detaNO). Untreated cells have higher titer of infectious virus production than cells with NOS2-transgene or with NO donors [n = 3, *p < 0.02].

which results in greater airway inflammation and the severe respiratory symptoms of CF infants with virus infection.

Despite defects in antiviral defenses, pretreatment with IFNs protected CF from virus. The biologic consequences, including antiviral effects, of IFN are mediated by multiple independent genes. Induction of over 600 genes has been identified in response to IFNs (de Veer et al., 2001). Thus, it is difficult to assign IFN antiviral action to any specific gene. Redundancy of antiviral defense is supported by the fact that pretreatment with exogenous IFN leads to a protective antiviral state despite defects in various antiviral pathways. However, it is clear that if the early antiviral defenses are lacking, using a strategy of knockout of specific antiviral genes, virus infection can lead to devastating effects despite the presence of intact IFN pathways (Kosugi et al., 2002; Noda et al., 2001; Xiang et al., 2002; Zhou et al., 1999). For example, mice deficient in Mx, RNase L, and PKR, which are markedly susceptible to viral infections, are nevertheless rescued by pretreatment with IFN (Zhou et al., 1999). Thus, virus-inducible, cell-autonomous innate defenses are important to inhibiting virus, and indeed may be crucial to host defense against viruses with strategies that interfere with IFN signaling, such as HPIV3.

STAT1 is required for IFN signal transduction in the cell and essential for the survival response to virus infection (Durbin et al., 1996; Meraz et al., 1996). Despite numerous downstream targets of STAT1 activation, loss of NOS2 has been identified as a primary factor in the susceptibility of STAT1 null animals to virus (Karupiah et al., 1993). Although not clearly understood, decreased STAT1 also produces a deficient antiviral state and loss of NOS2, while other IFN-mediated genes respond normally (Briscoe et al., 1996, Karaghiosoff et al., 2000). In two prior studies, nonfunctional JAK1 or Tyk2, receptor-associated kinases in the IFN signaling pathway, resulted in decreased STAT1 protein and activation, and a defective antiviral state, although the response to IFN-α or -γ was intact (Briscoe et al., 1996; Karaghiosoff et al., 2000). The Tyk2-deficient cells displayed a phenotype remarkably similar to the CF cells: increased virus replication in cells, impairment of STAT1 activation, with almost all IFN-dependent pathways intact except for NOS2. Altogether, these and the present study suggest that a threshold of STAT 1 may be required for the antiviral state, expression of NOS2, and perhaps other antiviral genes, such as 2′, 5′ OAS. Alternatively, a JAK1- or Tyk2-dependent signal may be required, in addition to STAT1, for expression of NOS2, and for the antiviral state (Briscoe et al., 1996).

Because IFN/STAT1 pathways are so effective in preventing viral infection, many viruses have developed mechanisms to evade the interferon system of the host. All members of the paramyxovirus family interfere with IFN signaling, although by different mechanisms (Andrejeva et al., 2002; Young et al., 2000). HPIV3 inhibits IFN signaling, through specific reduction of serine phosphorylation of STAT1α (Young et al., 2000) Serine phosphorylation is intact in CF (data not shown), but CF cells with impaired IFN activation of STAT1 may be particularly vulnerable to serine phosphorylation block by HPIV3, resulting in more effective interference with IFN signaling. While interference with IFN signaling is a common strategy by which paramyxovirus circumvents antiviral defenses (Andrejeva et al., 2002; Young et al., 2000), viral proteins which block NOS pathways have not been reported. Our data support that HPIV3 may not have specific strategies to escape NO effects. NO inhibits virus replication and even latency of virus, including coxsackievirus, influenza A & B, murine cytomegalovirus, vaccinia, ectromelia, and herpes simplex-1 (Croen, 1993; Flodstrom et al., 2001; Karupiah et al., 1998; Karupiah and Harris, 1995; Rimmelzwaan et al., 1999; Saura et al., 1999; Zaragoza et al., 1997). Here, HPIV3 is also shown to be inhibited by NO Two specific virus targets of NO, ribonucleotide reductase and viral protease, have been suggested on the basis of in vitro exposure of viral protein to NO donors in cell free systems (Croen, 1993; Lepoivre et al., 1991; Saura et al., 1999). These two known targets are absent in HPIV3. Although viral proteins may be targets of NO, NO also affects host proteins, which is relevant to HPIV3 since it requires host

proteins for transcription and replication (De et al., 1993). Known targets for NO modification include thiol groups and tyrosine, and NO may bind to heme iron in proteins (Grisham et al., 1999). In lung epithelial cells, over 40 cellular proteins are modified by tyrosine nitration, with consequences on activity and function (Aulak et al., 2001). Tyrosine nitration is decreased by NOS inhibitors and in NOS2 knockout cells; thus, NO modification of both host and viral proteins and subsequent effects on protein expression and activity are also likely reduced in CF cells which lack NOS2.

It is interesting to speculate about whether CFTR has a direct effect or is a modifier gene for expression of STAT1, 2′, 5′ OAS1, or NOS2. Inhibition of CFTR function results in reduced NOS2 mRNA in human tracheal epithelial cell lines, while overexpression of human CFTR in CF mice intestinal epithelium leads to NOS2 expression in the ileum (Steagall et al., 2000). These results suggest that NOS2 expression may be directly related to the presence of functional CFTR. In addition, the present findings suggest that STAT1 and NOS2 may be potential gene modifiers of the disease severity in CF lung disease. An important component of the innate host defense in the airway is the ability of respiratory epithelial cells to produce NO continuously in vivo (Sanders et al., 1998). The continuous production of NO in the airways is due in part to expression of NOS2 (Guo et al., 1995). CF infants at birth prior to the onset of respiratory symptoms/infection have exhaled NO 3-fold lower than in healthy controls, suggesting that the defect in NOS2 expression occurs prior to onset of recurrent infections (Elphick et al., 2001). Here, NOS2 is conclusively shown to be sufficient for antiviral defense in human airway epithelial cells. The success of overexpression of NOS2 in CF cells, or pretreatment with IFN, in protection from viral infection indicates that these approaches are promising in prevention of CF lung infection. Although less effective, provision of NO donors provided significant reduction of viral production and may be an alternative strategy for treatment of CF patients.

Experimental Procedures

Cell Culture, Virus, and Cytokines

HAEC were obtained through bronchoscopy brushing, from explanted lungs, or from segments of bronchus obtained from surgery and cultured by methods previously described (Guo et al., 2000; Uetani et al., 2000). An aliquot of cultured cells was immunostained to confirm epithelial phenotype. In addition, all cells were genotyped for 86 common *CFTR* mutations by Genzyme Genetics (Boston, Massachusetts). All eight samples from explant CF lungs were confirmed to be homozygous *ΔF508/ΔF508*. Eleven samples from control non-CF lungs were all wild-type *CFTR*.

A549 cells and CV-1 cells were maintained as previously described (Choudhary et al., 2001, Guo et al., 2000). HPIV3 (HA-1, NIH 47885) was a kind gift from Dr. De. Human IFN-γ was a gift from Genentech Inc. (South San Francisco, California). The IFN-α was purchased from Sigma-Aldrich (St. Louis, Missouri). Recombinant human IL-1β and TNF-α were from Genzyme.

RNA Isolation and Northern Analysis

Total RNA was extracted by GTC-CsCl gradient method (Erzurum et al., 1993a). Northern analysis was carried out using ^{32}P-dCTP-labeled human NOS2 cDNA by methods previously described (Uetani et al., 2000).

Plaque Assay and Immunofluorescent Staining

Culture supernatants were collected, and the yield of infectious HPIV3 in cells that underwent specific treatments was measured by plaque assay on CV-1 cells as previously described (De et al., 1995). 24 hr postinfection, cells cultured on cover slides were stained for HPIV3 by the method previously described (Choudhary et al., 2001).

^{35}S-Methionine Labeling and Immunoprecipitation

CF and NL cells in 12-well plate were infected with HPIV3 at 0.1 moi. At 12 hr postinfection, the medium was replaced with methionine-free DMEM and incubation was continued in 37°C. At 14 hr postinfection, the cells were labeled with 50 μCi of ^{35}S-methionine in 1 ml methionine-free DMEM for 6 hr. Cells were washed with DPBS and cell lysates were prepared and 20 μg of protein was immunoprecipitated by antibody against HPIV3 N-protein as previously described (De et al., 2000) and analyzed in an SDS-10% polyacrylamide gel.

IL-6 and IL-8 ELISA

Production of human IL-6 and IL-8 in the supernatant from CF and NL cells 24 hr after HPIV3 infection was evaluated using Quantikine human IL-6 and IL-8 ELISA (R&D Systems, Minneapolis, Minnesota). All samples were diluted ten times using appropriate calibration buffer.

Custom cDNA Microarray and Affymetrix Gene Array

RNA extracted from CF and NL cells at baseline or after 8 hr IFN treatment were evaluated for gene expression profile using custom-constructed cDNA microarray as previously described (Frevel et al., 2003). The ISG/AU/dsRNA array used in this study contains 1013 ISGs, 1464 AU-rich genes, 18 genes potentially involved in AU directed mRNA decay, 54 ribosomal genes, 288 dsRNA-responsive genes, and 84 housekeeping genes (NOS2 is not on this array).

Affymetrix HG-U133A GeneChips were also used in this study to evaluate baseline gene expression in CF and NL cells as previously described (Lipshutz et al., 1999; Yang et al., 2000).

Western Analysis

Whole-cell lysates were prepared and Western analysis performed as previously described (Uetani et al., 2000). The primary antibodies used included rabbit polyclonal antibody against NOS2 (Merck, Rahway, New Jersey), rabbit polyclonal antibody against C terminus of IRF-1 (Santa Cruz Biotechnology, Santa Cruz, California), rabbit polyclonal antibody against PKR (Carpick et al., 1997), mouse monoclonal antibody against RNase L (Dong and Silverman, 1995), rabbit polyclonal antibodies against MxA and HPIV3 N-protein (Choudhary et al., 2001), and rabbit polyclonal antibody against 2′, 5′ OAS1 (Ghosh et al., 2001).

WCE and EMSA

WCE were prepared and EMSA performed by methods previously described (Guo et al., 1997; Uetani et al., 2000). To specifically identify NF-κB, IRF-1, and STAT1α (p91) proteins in binding complexes, 2–4 μg of rabbit anti-p65, anti-p50, anti-IRF-1, or anti-STAT1α (p91) polyclonal Ab (Santa Cruz Biotechnology) was added to the binding reaction mix and incubated for 30 min at room temperature before adding the ^{32}P-labeled oligonucleotide.

NOS2 Expression Construct and Transient Transfection

Human NOS2 expression construct was made by inserting full-length NOS2 cDNA into a pAVS6 vector (Erzurum et al., 1993b). A control construct was also made by inserting reverse sequence NOS2 cDNA into a pAVS6 vector. Transient transfection was performed on cells at 90% confluence using LipofectAMINE PLUS reagent (Invitrogen Corporation, Carlsbad, California).

Nitrite and Nitrate Quantitation

NO production was quantitated by measuring total nitrite and nitrate in the media, using ISO-NO Markll isolated nitric oxide meter and nitric oxide sensor (ISO-NOP) (World Precision Instruments, Inc., Sarasota, Florida). Data were collected and analyzed by Duo18.

Statistical Analysis

The data are reported as means ± standard deviation of the mean (SD). Two-tailed t test statistics or the Mann-Whitney test was used as appropriate at a significance level of 0.05.

Acknowledgments

Thanks to C. Bevins, R. Silverman, and J. Durbin for helpful discussions, J. Lang for artwork, J. Foertch for assistance with clinical samples, and R. Silverman, J. Humes, and G.C. Sen for primary antibodies. This work was supported in part by HL60917, DIAMID 017-01-C-0065, NIH P50 DK56490, and the CF Foundation.

Received: September 11, 2002
Revised: March 6, 2003
Accepted: March 12, 2003
Published: May 13, 2003

References

2000. Cystic Fibrosis Foundation. Patient Registry 2000 Annual Report (Bethesda, Maryland, Cystic Fibrosis Foundation), pp. 1.

Aldallal, N., McNaughton, E.E., Manzel, L.J., Richards, A.M., Zabner, J., Ferkol, T.W., and Look, D.C. (2002). Inflammatory response in airway epithelial cells isolated from patients with cystic fibrosis. Am. J. Respir. Crit. Care Med. *166*, 1248–1256.

Anderson, M.P., Rich, D.P., Gregory, R.J., Smith, A.E., and Welsh, M.J. (1991). Generation of cAMP-activated chloride currents by expression of CFTR. Science *251*, 679–682.

Andrejeva, J., Young, D.F., Goodbourn, S., and Randall, R.E. (2002). Degradation of STAT1 and STAT2 by the V proteins of simian virus 5 and human parainfluenza virus type 2, respectively: consequences for virus replication in the presence of alpha/beta and gamma interferons. J. Virol. *76*, 2159–2167.

Armstrong, D., Grimwood, K., Carlin, J.B., Carzino, R., Hull, J., Olinsky, A., and Phelan, P.D. (1998). Severe viral respiratory infections in infants with cystic fibrosis. Pediatr. Pulmonol. *26*, 371–379.

Aulak, K.S., Miyagi, M., Yan, L., West, K.A., Massillon, D., Crabb, J.W., and Stuehr, D.J. (2001). Proteomic method identifies proteins nitrated in vivo during inflammatory challenge. Proc. Natl. Acad. Sci. USA *98*, 12056–12061.

Biron, C.A. (1999). Initial and innate responses to viral infections–pattern setting in immunity or disease. Curr. Opin. Microbiol. *2*, 374–381.

Briscoe, J., Rogers, N.C., Witthuhn, B.A., Watling, D., Harpur, A.G., Wilks, A.F., Stark, G.R., Ihle, J.N., and Kerr, I.M. (1996). Kinase-negative mutants of JAK1 can sustain interferon-gamma-inducible gene expression but not an antiviral state. EMBO J. *15*, 799–809.

Carpick, B.W., Graziano, V., Schneider, D., Maitra, R.K., Lee, X., and Williams, B.R. (1997). Characterization of the solution complex between the interferon-induced, double-stranded RNA-activated protein kinase and HIV-I trans-activating region RNA. J. Biol. Chem. *272*, 9510–9516.

Choudhary, S., Gao, J., Leaman, D.W., and De, B.P. (2001). Interferon action against human parainfluenza virus type 3: involvement of a novel antiviral pathway in the inhibition of transcription. J. Virol. *75*, 4823–4831.

Croen, K.D. (1993). Evidence for antiviral effect of nitric oxide. Inhibition of herpes simplex virus type 1 replication. J. Clin. Invest. *91*, 2446–2452.

De, B.P., Burdsall, A.L., and Banerjee, A.K. (1993). Role of cellular actin in human parainfluenza virus type 3 genome transcription. J. Biol. Chem. *268*, 5703–5710.

De, B.P., Gupta, S., and Banerjee, A.K. (1995). Cellular protein kinase C isoform zeta regulates human parainfluenza virus type 3 replication. Proc. Natl. Acad. Sci. USA *92*, 5204–5208.

De, B.P., Hoffman, M.A., Choudhary, S., Huntley, C.C., and Banerjee, A.K. (2000). Role of NH(2)- and COOH-terminal domains of the P protein of human parainfluenza virus type 3 in transcription and replication. J. Virol. *74*, 5886–5895.

de Veer, M.J., Holko, M., Frevel, M., Walker, E., Der, S., Paranjape, J.M., Silverman, R.H., and Williams, B.R. (2001). Functional classification of interferon-stimulated genes identified using microarrays. J. Leukoc. Bio., *69*, 912–920.

Dong, B., and Silverman, R.H. (1995). 2–5A-dependent RNase molecules dimerize during activation by 2–5A. J. Biol. Chem. *270*, 4133–4137.

Durbin, J.E., Hackenmiller, R., Simon, M.C., and Levy, D.E. (1996). Targeted disruption of the mouse Stat1 gene results in compromised innate immunity to viral disease. Cell *84*, 443–450.

Elphick, H.E., Demoncheaux, E.A., Ritson, S., Higenbottam, T.W., and Everard, M.L. (2001). Exhaled nitric oxide is reduced in infants with cystic fibrosis. Thorax *56*, 151–152.

Erzurum, S.C., Danel, C., Gillissen, A., Chu, C.S., Trapnell, B.C., and Crystal, R.G. (1993a). In vivo antioxidant gene expression in human airway epithelium of normal individuals exposed to 100% O2. J. Appl. Physiol. *75*, 1256–1262.

Erzurum, S.C., Lemarchand, P., Rosenfeld, M.A., Yoo, J.H., and Crystal, R.G. (1993b). Protection of human endothelial cells from oxidant injury by adenovirus-mediated transfer of the human catalase cDNA. Nucleic Acids Res. *21*, 1607–1612.

Flodstrom, M., Horwitz, M.S., Maday, A., Balakrishna, D., Rodriguez, E., and Sarvetnick, N. (2001). A critical role for inducible nitric oxide synthase in host survival following coxsackievirus B4 infection. Virology *281*, 205–215.

Frevel, M.A., Bakheet, T., Silva, A.M., Hissong, J.G., Khabar, K.S., and Williams, B.R. (2003). p38 Mitogen-activated protein kinase-dependent and -independent signaling of mRNA stability of AU-rich element-containing transcripts. Mol. Cell. Biol. *23*, 425–436.

Gao, J., Morrison, D.C., Parmely, T.J., Russell, S.W., and Murphy, W.J. (1997). An interferon-gamma-activated site (GAS) is necessary for full expression of the mouse iNOS gene in response to interferon-gamma and lipopolysaccharide. J. Biol. Chem. *272*, 1226–1230.

Gao, J., De, B.P., and Banerjee, A.K. (1999). Human parainfluenza virus type 3 up-regulates major histocompatibility complex class I and II expression on respiratory epithelial cells: involvement of a STAT1- and CIITA-independent pathway. J. Virol. *73*, 1411–1418.

Garcia-Sastre, A. (2001). Inhibition of interferon-mediated antiviral responses by influenza A viruses and other negative-strand RNA viruses. Virology *279*, 375–384.

Garcia-Sastre, A., Egorov, A., Matassov, D., Brandt, S., Levy, D.E., Durbin, J.E., Palese, P., and Muster, T. (1998). Influenza A virus lacking the NS1 gene replicates in interferon-deficient systems. Virology *252*, 324–330.

Ghosh, A., Sarkar, S.N., Rowe, T.M., and Sen, G.C. (2001). A specific isozyme of 2′-5′ oligoadenylate synthetase is a dual function pro-apoptotic protein of the Bcl-2 family. J. Biol. Chem. *276*, 25447–25455.

Grandvaux, N., tenOever, B.R., Servant, M.J., and Hiscott, J. (2002). The interferon antiviral response: from viral invasion to evasion. Curr. Opin. Infect. Dis. *15*, 259–267.

Grisham, M.B., Jourd'Heuil, D., and Wink, D.A. (1999). Nitric oxide. I. Physiological chemistry of nitric oxide and its metabolites:implications in inflammation. Am J. Physiol. *276*, G315–G321.

Guo, F.H., De Raeve, H.R., Rice, T.W., Stuehr, D.J., Thunnissen, F.B., and Erzurum, S.C. (1995). Continuous nitric oxide synthesis by inducible nitric oxide synthase in normal human airway epithelium in vivo. Proc. Natl. Acad. Sci. USA *92*, 7809–7813.

Guo, F.H., Uetani, K., Haque, S.J., Williams, B.R., Dweik, R.A., Thunnissen, F.B., Calhoun, W., and Erzurum, S.C. (1997). Interferon gamma and interleukin 4 stimulate prolonged expression of inducible nitric oxide synthase in human airway epithelium through synthesis of soluble mediators. J. Clin. Invest. *100*, 829–838.

Guo, F.H., Comhair, S.A., Zheng, S., Dweik, R.A., Eissa, N.T., Thomassen, M.J., Calhoun, W., and Erzurum, S.C. (2000). Molecular mechanisms of increased nitric oxide (NO) in asthma: evidence for transcriptional and post-translational regulation of NO synthesis. J. Immunol. *164*, 5970–5980.

Haque, S.J., and Williams, B.R. (1998). Signal transduction in the interferon system. Semin. Oncol. *25*, 14–22.

Heitmeier, M.R., Scarim, A.L., and Corbett, J.A. (1999). Prolonged STAT1 activation is associated with interferon-gamma priming for interleukin-1-induced inducible nitric-oxide synthase expression by islets of Langerhans. J. Biol. Chem. *274*, 29266–29273.

Hiatt, P.W., Grace, S.C., Kozinetz, C.A., Raboudi, S.H., Treece, D.G., Taber, L.H., and Piedra, P.A. (1999). Effects of viral lower respiratory tract infection on lung function in infants with cystic fibrosis. Pediatrics *103*, 619–626.

Hordvik, N.L., Konig, P., Hamory, B., Cooperstock, M., Kreutz, C., Gayer, D., and Barbero, G. (1989). Effects of acute viral respiratory tract infections in patients with cystic fibrosis. Pediatr. Pulmonol. *7*, 217–222.

Iordanov, M.S. Wong, J., Bell, J.C., and Magun, B.E. (2001). Activation of NF-kappaB by double-stranded RNA (dsRNA) in the absence of protein kinase R and RNase L demonstrates the existence of two separate dsRNA-triggered antiviral programs. Mol. Cell. Biol. *21*, 61–72.

Isaacs, A., Lindenmann, J., and Valentine, R.C. (1957). Virus interference II. Some properties of interferon. Proc. R. Soc. Lond. B *147*, 268–273.

Kamijo, R., Harada, H., Matsuyama, T., Bosland, M., Gerecitano, J., Shapiro, D., Le, J., Koh, S.I., Kimura, T., Green, S.J., et al. (1994). Requirement for transcription factor IRF-1 in NO synthase induction in macrophages. Science *263*, 1612–1615.

Karaghiosoff, M., Neubauer, H., Lassnig, C., Kovarik, P., Schindler, H., Pircher, H., McCoy, B., Bogdan, C., Decker, T., Brem, G., et al. (2000). Partial impairment of cytokine responses in Tyk2-deficient mice. Immunity *13*, 549–560.

Karupiah, G., Xie, Q.W., Buller, R.M., Nathan, C., Duarte, C., and MacMicking, J.D. (1993). Inhibition of viral replication by interferon-gamma-induced nitric oxide synthase. Science *261*, 1445–1448.

Karupiah, G., and Harris, N. (1995). Inhibition of viral replication by nitric oxide and its reversal by ferrous sulfate and tricarboxylic acid cycle metabolites. J. Exp. Med. *181*, 2171–2179.

Karupiah, G., Chen, J.H., Nathan, C.F., Mahalingam, S., and MacMicking, J.D. (1998). Identification of nitric oxide synthase 2 as an innate resistance locus against ectromelia virus infection. J. Virol. *72*, 7703–7706.

Kelley, T.J., and Elmer, H.L. (2000). In vivo alterations of IFN regulatory factor-1 and PIAS1 protein levels in cystic fibrosis epithelium J. Clin. Invest. *106*, 403–410.

Kerem, B., Rommens, J.M., Buchanan, J.A., Markiewicz, D., Cox, T.K., Chakravarti, A., Buchwald, M., and Tsui, L.C. (1989). Identification of the cystic fibrosis gene: genetic analysis. Science *245*, 1073–1080.

Kosugi, I., Kawasaki, H., Arai, Y., and Tsutsui, Y. (2002). Innate immune responses to cytomegalovirus infection in the developing mouse brain and their evasion by virus-infected neurons. Am. J. Pathol. *161*, 919–928.

Lepoivre, M., Fieschi, F., Coves, J., Thelander, L., and Fontecave, M. (1991). Inactivation of ribonucleotide reductase by nitric oxide. Biochem. Biophys. Res. Commun. *179*, 442–448.

Lipshutz, R.J., Fodor, S.P., Gingeras, T.R., and Lockhart, D.J. (1999). High density synthetic oligonucleotide arrays. Nat. Genet. *21*, 20–24.

Matsukura, S., Kokubu, F., Noda, H., Tokunaga, H., and Adachi, M. (1996). Expression of IL-6, IL-8, and RANTES on human bronchial epithelial cells, NCI-H292, induced by influenza virus A. J. Allergy Clin. Immunol. *98*, 1080–1087.

Meraz, M.A., White, J.M., Sheehan, K.C., Bach, E.A., Rodig, S.J., Dighe, A.S., Kaplan, D.H., Riley, J.K., Greenlund, A.C., Campbell, D., et al. (1996). Targeted disruption of the Stat1 gene in mice reveals unexpected physiologic specificity in the JAK-STAT signaling pathway. Cell *84*, 431–442.

Muller, M., Laxton, C., Briscoe, J., Schindler, C., Improta, T., Darnell, J.E., Jr., Stark, G.R., and Kerr, I.M. (1993). Complementation of a mutant cell line: central role of the 91 kDa polypeptide of ISGF3 in the interferon-alpha and -gamma signal transduction pathways. EMBO J. *12*, 4221–4228.

Nelson, N., Marks, M.S., Driggers, P.H., and Ozato, K. (1993). Interferon consensus sequence-binding protein, a member of the interferon regulatory factor family, suppresses interferon-induced gene transcription. Mol. Cell. Biol. *13*, 588–599.

Noah, T.L., Black, H.R., Cheng, P.W., Wood, R.E., and Leigh, M.W. (1997). Nasal and bronchoalveolar lavage fluid cytokines in early cystic fibrosis. J. Infect. Dis. *175*, 638–647

Noda, S., Tanaka, K., Sawamura, S., Sasaki, M., Matsumoto, T., Mikami, K., Aiba, Y., Hasegawa, H., Kawabe, N., and Koga, Y. (2001). Role of nitric oxide synthase type 2 in acute infection with murine cytomegalovirus. J. Immunol. *166*, 3533–3541.

Pavlovic, J., Haller, O., and Staeheli, P. (1992). Human and mouse Mx proteins inhibit different steps of the influenza virus multiplication cycle. J. Virol. *66*, 2564–2569.

Petersen, N.T., Hoiby, N., Mordhorst, C.H., Lind, K., Flensborg, E.W., and Bruun, B. (1981). Respiratory infections in cystic fibrosis patients caused by virus, chlamydia and mycoplasma–possible synergism with *Pseudomonas aeruginosa*. Acta Paediatr. Scand. *70*, 623–628.

Reiss, C.S., and Komatsu, T. (1998). Does nitric oxide play a critical role in viral infections? J. Virol. *72*, 4547–4551.

Rimmelzwaan, G.F., Baars, M.M., de Lijster, P., Fouchier, R.A., and Osterhaus, A.D. (1999). Inhibition of influenza virus replication by nitric oxide. J. Virol. *73*, 8880–8883.

Riordan, J.R., Rommens, J.M., Kerem, B., Alon, N., Rozmahel, R., Grzelczak, Z., Zielenski, J., Lok, S., Plavsic, N., Chou, J.L., et al. (1989). Identification of the cystic fibrosis gene: cloning and characterization of complementary DNA. Science *245*, 1066–1073.

Rommens, J.M., Iannuzzi, M.C., Kerem, B., Drumm, M.L., Melmer, G., Dean, M., Rozmahel, R., Cole, J.L., Kennedy, D., Hidaka, N., et al. (1989). Identification of the cystic fibrosis gene: chromosome walking and jumping. Science *245*, 1059–1065.

Ronni, T., Matikainen, S., Sareneva, T., Melen, K., Pirhonen, J., Keskinen, P., and Julkunen, I. (1997). Regulation of IFN-alpha/beta, MxA, 2′,5′-oligoadenylate synthetase, and HLA gene expression in influenza A-infected human lung epithelial cells. J. Immunol. *158*, 2363–2374.

Rosenfeld, M., and Ramsey, B. (1992). Evolution of airway microbiology in the infant with cystic fibrosis: role of nonpseudomonal and pseudomonal pathogens. Semin. Respir. Infect. *7*, 158–167.

Samuel, C.E. (1991). Antiviral actions of interferon. Interferon-regulated cellular proteins and their surprisingly selective antiviral activities. Virology *183*, 1–11.

Sanders, S.P. (1999). Asthma, viruses, and nitric oxide. Proc. Soc. Exp. Biol. Med. *220*, 123–132.

Sanders, S.P., Siekierski, E.S., Porter, J.D., Richards, S.M., and Proud, D. (1998). Nitric oxide inhibits rhinovirus-induced cytokine production and viral replication in a human respiratory epithelial cell line. J. Virol. *72*, 934–942.

Saura, M., Zaragoza, C., McMillan, A., Quick, R.A., Hohenadl, C., Lowenstein, J.M., and Lowenstein, C.J. (1999). An antiviral mechanism of nitric oxide: inhibition of a viral protease. Immunity *10*, 21–28.

Seo, S.H., Hoffmann, E., and Webster, R.G. (2002). Lethal H5N1 influenza viruses escape host anti-viral cytokine responses. Nat. Med. *8*, 950–954.

Sheppard, D.N., and Welsh, M.J. (1999). Structure and function of the CFTR chloride channel. Physiol. Rev. *79*, S23–S45.

Stark, G.R., Kerr, I.M., Williams, B.R., Silverman, R.H., and Schreiber, R.D. (1998). How cells respond to interferons. Annu. Rev. Biochem. *67*, 227–264.

Steagall, W.K., Elmer, H.L., Brady, K.G., and Kelley, T.J. (2000). Cystic fibrosis transmembrane conductance regulator-dependent regulation of epithelial inducible nitric oxide synthase expression. Am. J. Respir. Cell Mol. Biol. *22*, 45–50

Uetani, K., Der, S.D., Zamanian-Daryoush, M., de La Motte, C., Lieberman, B.Y., Williams, B.R., and Erzurum, S.C. (2000). Central role

Temporal activation of NF-κB regulates an interferon-independent innate antiviral response against cytoplasmic RNA viruses

Santanu Bose*†, Niladri Kar‡, Ratan Maitra*, Joseph A. DiDonato†‡, and Amiya K. Banerjee*†

Departments of *Virology and ‡Cancer Biology, Lerner Research Institute, Cleveland Clinic Foundation, 9500 Euclid Avenue, Cleveland, OH 44195

Edited by George R. Stark, Cleveland Clinic Foundation, Cleveland, OH, and approved July 14, 2003 (received for review May 8, 2003)

NF-κB is known to exert its antiviral innate immune response via the IFN-β-induced Janus kinase/signal transducers and activators of transcription pathway. However, our current studies have demonstrated that activated NF-κB is capable of directly establishing an antiviral state independent of IFN or secreted soluble factor(s) against two highly pathogenic respiratory RNA viruses. Human parainfluenza virus type 3, a mildly cytopathic virus that induced NF-κB very early during infection was converted to a virulent virus after NF-κB inhibition. In contrast, a highly cytopathic virus, human respiratory syncytial virus that induced NF-κB late during infection, was converted to a mildly cytopathic virus after NF-κB induction before virus replication. This interconversion of cytopathic phenotypes of viruses after NF-κB modulation was further shown to be independent of IFN and soluble secreted factors(s). Moreover, tumor necrosis factor α (TNF-α) and IL-1β elicited an antiviral response, which was NF-κB-dependent. Thus, NF-κB induction directly confers an essential innate antiviral response against human parainfluenza virus type 3 and respiratory syncytial virus, which is independent of IFN-inducible factor(s).

Innate immune response initiated by the infected host cells constitutes the first line of defense against foreign pathogens including viruses, before orchestrating a well organized adaptive immune response. NF-κB, a family of evolutionarily conserved transcription factors, represents an important modulator of innate and adaptive immune function required for optimal host defense (1–4). Viruses have evolved to activate NF-κB, either by double-stranded RNA intermediate or activation of Toll-like receptors (TLRs), leading to nuclear translocation of NF-κB (5–7). In the nucleus, NF-κB binds to its cognate promoter sites to activate an array of genes, including proinflammatory cytokines, chemokines, and adhesion molecules (7). These molecules are involved in initiating adaptive immunity process by recruiting immune cells to the site of infection. Apart from the adaptive immune responders, NF-κB's innate immune function is mediated by the activation of IFN-β, an important antiviral cytokine (8, 9), through which paracrine action activates the Janus kinase (JAK)/signal transducers and activators of transcription (STAT) antiviral pathway (8, 9).

We have used two viruses, human parainfluenza virus type 3 (HPIV-3) and human respiratory syncytial virus (RSV), to study the role of NF-κB activation in conferring essential innate antiviral response in human epithelial cells. These cells facing the luminal side (e.g., intestine, lung, and airway) have direct contact with the exterior milieu and are, therefore, the initial target for majority of pathogens, including viruses (10). Both HPIV-3 and RSV, belonging to the paramyxoviridae family, are enveloped single-stranded RNA containing viruses of negative polarity that replicates in the cytoplasm (11). These viruses are important human respiratory tract pathogens, causing high morbidity among infants, children, and immunocompromised adults manifesting disease states including, pneumonia, croup, and brochiolitis (11). To date, no effective vaccine or antiviral therapy exists for either of these viruses. Therefore, elucidation of innate immune antiviral response elicited by these viruses holds significant potential for development of effective antiviral therapies against these viruses.

In this article, we report that NF-κB is capable of signaling an innate antiviral response that is independent of IFN and the well established JAK/STAT antiviral pathway. The importance of NF-κB-mediated innate response was further borne out by our observation that the temporal nature of NF-κB induction profile exhibited by RSV and HPIV-3 had direct bearing on their respective cytopathic phenotype and replication capability. Moreover, proinflammatory cytokines like tumor necrosis factor-α (TNF-α) and IL-1β exerted a potent antiviral action, which was directly dependent on the NF-κB innate antiviral pathway. The antiviral role of NF-κB against these cytoplasmic RNA viruses is discussed.

Materials and Methods

Cells and Viruses. A549, CV-1 cells, WT and IKKγ $^{/}$ mouse embryonic fibroblasts (MEFs), and human epithelial-like fibrosarcoma cells (WT and STAT-1$^{-/-}$ cells) were cultured as described (10, 12–15). HPIV-3, RSV, and vesicular stomatitis virus (VSV) adenoviruses (Ads) were propagated in CV-1, HepG2, BHK, and HEK cells, respectively, as described (10, 14–16).

Plaque Assay. Plaque assay was performed as described (15). To visualize the cytopathic effect, the same dilutions of medium supernatants were similarly added to CV-1 cells, and the plaques were viewed by phase contrast microscopy (×10 objective). The plaque assay data shown in the figures represents the mean number of plaque-forming units/ml from three independent experiments with similar results.

Virus Infection. A549 cells pretreated with used pyrollidine dithiocarbamate (PDTC) (Calbiochem; 50 μM) for 4 h or infected with the Ads [200 multiplicity of infection (mois)] for 16 h were infected with HPIV-3 (0.1 moi) or RSV (0.1 moi), either in the absence or presence of PDTC. After 36 h postinfection, the medium supernatants were prepared for plaque assay (15). The MEFs and fibrosarcoma cells were similarly infected with HPIV-3 and RSV (0.1 moi).

Electrophoretic Mobility-Shift Assay (EMSA) and Luciferase Assay. Nuclear extracts were prepared from HPIV-3 (3 mois), RSV (1 moi) -infected A549 cells as described (17). The nuclear extracts

This paper was submitted directly (Track II) to the PNAS office.

Abbreviations: HPIV-3, human parainfluenza virus type 3; RSV, human respiratory syncytial virus; VSV, vesicular stomatitis virus; TNF-α, tumor necrosis factor α; JAK, Janus kinase; STAT, signal transducers and activators of transcription; MEF, mouse embryonic fibroblast; PDTC, pyrollidine dithiocarbamate; moi, multiplicity of infection; IκB-SR, IκB super repressor; Ad, adenovirus; L-NMMA, N^G-monomethyl-L-arginine; CM, conditioned medium; TLR, Toll-like receptor; DN-MyD88, dominant negative TLR adaptor protein MyD88; NF-κB-Luc, NF-κB-luciferase.

*To whom correspondence should be addressed: E-mail: boses@ccf.org, didonaj@ccf.org, or banerja@ccf.org.

www.pnas.org/cgi/doi/10.1073/pnas.1832775100

(8 μg of protein) were either incubated with ^{32}P-labeled NF-κB oligonucleotide probe in the presence of preimmune/normal rabbit serum (NRS) or p65 antibody (Santa Cruz Biotechnology), or incubated with a 50× molar excess of unlabeled specific WT or mutant NF-κB oligonucleotide probe, and analyzed as described (16, 17). For luciferase assay, A549 cells were transiently transfected with plasmids containing the 2× NF-κB promoter fused to the firefly luciferase gene (16) and *Renilla* luciferase (for normalization of transfection efficiencies) by using lipofectin (GIBCO/BRL) as described (16). Sixteen hours posttransfection, cells were infected with either HPIV-3 or RSV (1 moi) and 8 h (for HPIV-3) or 20 h (for RSV) postinfection, the cell lysates were prepared and assayed for firefly lucifease expression as described (16). The luciferase activity was normalized to the *Renilla* luciferase activity (dual luciferase assay from Promega). NF-κB-luciferase- (NF-κB-Luc) transfected A549 cells were also infected with Ads [Ad-GFP, IκB super repressor (Ad-IκB-SR), and Ad-expressing dominant negative TLR adaptor protein MyD88 (Ad-DN-MyD88)] for 12 h, followed by either mock infection or infection with RSV or HPIV-3 (1 moi) for 18 and 8 h, respectively. Similarly NF-κB-Luc-transfected A549 cells were infected with either Ad-GFP or Ad-IκB-SR for 12 h, followed by TNF-α or IL-1β treatment (20 ng/ml) for 2 h. The lysates from these cells were assayed for luciferase activity as described above. The luciferase assay results shown in the figures represent the average of three independent experiments and the standard deviations are shown as error bars.

Treatment of HPIV-3-Infected A549 Cells with N^G-monomethyl-L-arginine (L-NMMA), Conditioned Medium (CM), or IFN-β. A549 cells pretreated with 5 mm or 25 mM L-NMMA (Oxis International, Portland, OR) for 4 h were infected with HPIV-3 (0.1 moi) for 36 h in the absence or presence of L-NMMA. To prepare the CM, A549 cells were either mock infected or infected with HPIV-3 (0.1 or 1 moi) for 24 h. The resulting medium supernatants were added to Centricon units (Centricon Plus-20, 300,000-kDa cutoff; Millipore) and centrifuged per manufacturer's direction. After centrifugation, the membrane flow-through supernatants were checked for the absence of virus by infecting fresh A549 cells. Once the absence of virus was confirmed, the mock or the HPIV-3 CMs were added to Ad-infected cells simultaneously during adsorption (2 h at 37°C) of HPIV-3 (0.1 moi). The CM was present during the course of the infection (36 h). IFN-β (2,000 units/ml) (PBL) was similarly added to Ad-infected cells simultaneously during adsorption (2 h at 37°C) of HPIV-3 (0.1 moi), and it was present during the course of the infection (36 h). The medium supernatants from L-NMMA-, CM-, or IFN-β-treated A549 cells infected with HPIV-3 were processed for plaque assay analysis.

RSV and VSV Infection of A549 or Human Fibrosarcoma Cells Pretreated with Either TNF-α or IL-1β in the Presence of Either Ad-GFP or Ad-IκB-SR. A549 or human fibrosarcoma cells were pretreated with TNF-α or IL-1β (20 ng/ml) (R & D Systems) for either 8 or 16 h. After pretreatment, the cells were infected with RSV, HPIV-3, or VSV (0.1 moi) for 36 h in the absence of these cytokines. A549 cells were also infected with Ads (Ad-GFP or Ad-IκB-SR) for 12 h, followed by TNF-α or IL-1β pretreatment (20 ng/ml) for 16 h. These cells were then infected with either RSV or VSV (0.1 moi) for 36 h in the absence of these cytokines. The medium supernatants from these cells were then subjected to plaque assay analysis on CV-1 cells.

RSV and VSV Infection of A549 or Human Fibrosarcoma Cells Pretreated with Either TNF-α or IL-1β CM in the Presence of Anti-TNF-α or Anti-IL-1β Neutralizing Antibodies, Respectively. CM obtained from untreated and TNF-α- or IL-1β-treated (20 ng/ml) A549 (8, 16, or 24 h) or human fibrosarcoma (24 h) cells were incubated with either control or respective cytokine-neutralizing antibodies (300 ng/ml; R & D Systems) overnight at 4°C. After incubation, the medium was added to fresh A549 or human fibrosarcoma cells for 16 h pretreatment before adding RSV or VSV (0.1 moi). The medium supernatants obtained from these cells after 36 h virus infection were subjected to plaque assay analysis on CV-1 cells

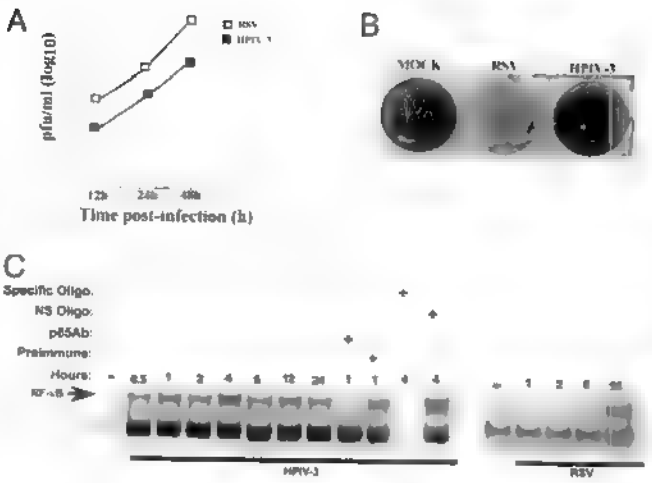

Fig. 1. Replication kinetics and NF-κB-induction profile of HPIV-3 and RSV in human lung epithelial A549 cells. (*A*) A single-step growth kinetics of HPIV-3 and RSV (0.1 moi) in A549 cells was determined by plaque assay analysis. (*B*) Cytopathic effect analysis (48 h postinfection) of HPIV-3 and RSV (0.1 moi) from infected A549 cells was determined after addition of same dilution of A549 medium supernatants to CV-1 cells for plaque assay analysis. (*C*) NF-κB EMSA using nuclear extracts from uninfected (−) and RSV-infected (1, 2, 6, and 16 h postinfection) A549 cells, and HPIV-3-infected (0.5–24 h postinfection) A549 cells in the absence or presence of NF-κB p65 antibody (Ab), preimmune serum, specific NF-κB unlabeled probe, or mutant NF-κB unlabeled probe (NS) as indicated

Results

Temporal Activation of NF-κB by HPIV-3 and RSV in Human Lung Epithelial Cells. Human lung epithelial A549 cells were initially tested for susceptibility to HPIV-3 and RSV infections. We observed that HPIV-3 is significantly less cytopathic than RSV in these cells; the cells that are the primary target of these viruses during productive infection (ref. 11 and Fig. 1 *A* and *B*). A single-step growth kinetics of these viruses (0.1 moi) at 12, 24, and 48 h postinfection revealed that HPIV-3 titer was significantly lower (two logs) compared with RSV (Fig. 1*A*). These differences can also be directly visualized by their ability to form syncytia; cytopathic effect analysis (Fig. 1*B*) of these viruses at the same dilution of medium supernatants showed few plaques for HPIV-3, whereas RSV completely disseminated the cells. These results demonstrated that HPIV-3 replicated poorly in A549 cells, whereas RSV was highly cytopathic.

We next investigated whether these viruses possessing widely different cytopathic phenotype also differ in their induction of NF-κB, which is an important innate immune responder (1–4). EMSA (Fig. 1*C*) performed with nuclear extracts obtained from RSV- or HPIV-3-infected A549 cells, revealed rapid NF-κB DNA-binding activity very early after HPIV-3 infection (30 min postinfection) before initiating its full replicative cycle (12–16 h postinfection; refs. 18 and 19). In contrast, RSV-induced NF-κB DNA-binding activity was observed considerably later (16 h) after the onset of replication (10–12 h postinfection; ref. 20), similar to that reported (21, 22). Specificity of the HPIV-3-induced NF-κB complex formation was demonstrated by super-

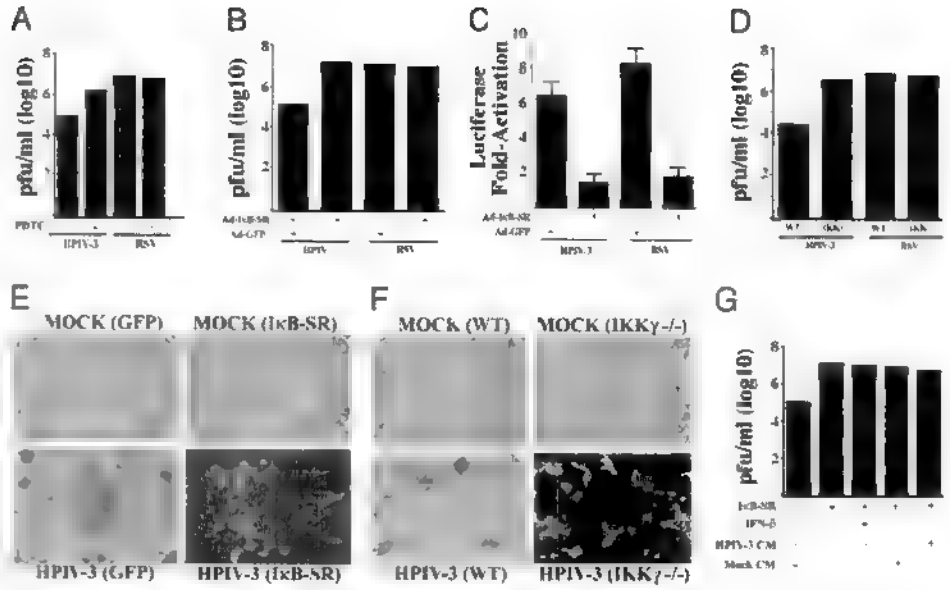

Fig. 2. Inhibition of NF-κB activation increases HPIV-3, but not RSV, replication and cytopathogenicity in an IFN- and/or soluble factor(s)-independent manner. Plaque assay analysis using medium supernatants from A549 cells mock infected or infected with either HPIV-3 or RSV in the absence or presence of PDTC (50 μM) (*A*), or A549 cells infected with HPIV-3 or RSV in the absence or presence of prior infection with Ads encoding the IκB-SR or GFP(*B*). (*C*) Expression of transfected NF-κB-Luc in A549 cells infected with HPIV-3 or RSV in the presence of IκB-SR or control GFP. (*D*) Plaque assay analysis using medium supernatants from IKKγ$^{-/-}$ or WT MEFs infected with either HPIV-3 or RSV. Phase contrast microscopic picture of CV-1 cells incubated with same dilutions of medium supernatants obtained from A549 cells infected with HPIV-3 and Ad-GFP or Ad-IκB-SR (*E*) and HPIV-3-infected WT or IKKγ$^{-/-}$ MEFs (*F*). (*G*) Plaque assay analysis using medium supernatants from A549 cells infected with HPIV-3 and Ad-GFP or Ad-IκB-SR and treated with IFN-β (2,000 units/ml). Similar analysis was performed with medium supernatants from A549 cells infected with HPIV-3 and Ad-GFP or Ad-IκB-SR in the presence or absence of either mock CM or HPIV-3 CM (cleared free of virus).

shift analysis with p65 antibody and competition with unlabeled WT, but not mutant oligonucleotide probe (Fig. 1*C*).

Inhibition of NF-κB Activation Results in Increased Replication and Cytopathogenicity of HPIV-3 Independent of IFN. The differential kinetics of NF-κB induction displayed by RSV and HPIV-3 raised the possibility that these viruses may have evolved to regulate the activation of NF-κB to strategically manipulate the antiviral defense mechanism exerted by the host for efficient replication, leading to higher cytopathic phenotype. To examine this possibility, we monitored the replication capability of HPIV-3 and RSV in cells where NF-κB was inactivated. By using PDTC, a general NF-κB inhibitor (ref. 23 and Fig. 2*A*), during infection resulted in a significant (30-fold) increase in HPIV-3 titer. In contrast, PDTC had no effect on RSV titer (Fig. 2*A*). These results were further confirmed by expressing the Ad-IκB-SR (32A/36A) (16, 24) in HPIV-3-infected cells. As shown in Fig. 2*B*, IκB-SR expression lead to dramatic increase (100-fold) in HPIV-3 titer, whereas RSV titer remained unchanged. The Ad-IκB-SR used in these studies was functional, because Ad-IκB-SR, but not control Ad-GFP, inhibited NF-κB-Luc induction by HPIV-3 and RSV in A549 cells (Fig. 2*C*). Finally, virus obtained from infected WT and IKKγ$^{-/-}$ MEFs (12) demonstrated dramatic augmentation (100-fold) of HPIV-3, but not RSV replication in IKKγ$^{-/-}$ cells (Fig. 2*D*). The significant increase in HPIV-3 cytopathogenicity and viral titer could be clearly visualized by increased syncytia formation after NF-κB inactivation (Fig. 2 *E* and *F*). The observed conversion of mildly cytopathic HPIV-3 into a virulent form, similar to RSV, after inhibition of NF-κB, suggested an important role of NF-κB in antiviral defense. These results indicate that rapid activation of NF-κB before HPIV-3 replication constitutes an essential antiviral host defense in human lung epithelial cells, as well as in mouse fibroblasts.

We next examined whether the conversion of a mildly cytopathic virus, HPIV-3, to a virulent one on NF-κB inhibition was due to the lack of IFN-β [a gene which is stimulated in HPIV-3-infected epithelial cells (25, 26)] or soluble antiviral secreted factor(s) production. As shown in Fig. 2*G*, addition of exogenous IFN-β (2,000 units/ml) to the NF-κB-inactivated cells at the time of HPIV-3 infection failed to inhibit the increased infectivity and cytopathogenicity of HPIV-3. Similar results were obtained after addition of IFN-α (data not shown). The potential involvement of putative secretory antiviral soluble factor(s) were also eliminated, because CM supernatant obtained from HPIV-3-infected A549 cells (cleared free of virus) or mock-infected cells added to Ad-IκB-SR- and HPIV-3-infected cells at the time of HPIV-3 infection, failed to repress the increased virus infectivity (Fig. 2*G*). Thus, it seems that NF-κB-mediated anti-HPIV-3 activity is conferred by establishing an intracellular antiviral state independent of IFN and/or soluble factor(s).

Inhibition of RSV Replication After Specific Induction of NF-κB by TNF-α or IL-1β. If indeed NF-κB is an essential innate antiviral mediator as shown above, we hypothesized that RSV may have maintained its highly cytopathic phenotype as a result of deregulating NF-κB activation by inducing it late in the replication cycle. If such induction constitutes the mechanism used by RSV to evade host's NF κB-dependent antiviral response for preservation of its high virulence, activation of NF-κB before the replication of RSV may confer an antiviral state. To examine this possibility, we pretreated A549 cells with TNF-α (27) or IL-1β (28), which are potent inducers of NF-κB, before RSV infection. Pretreatment of cells with TNF-α or IL-1β (Fig. 3*A*) severely restricted RSV replication with a decrease in virus titer by 1,000-fold. However, treatment of A549 cells with TNF-α or IL-1β 10–12 h postinfection (after replication initiation) failed to restrict RSV replication (data not shown). It is important to note that in these studies, TNF-α and IL-1β were present only

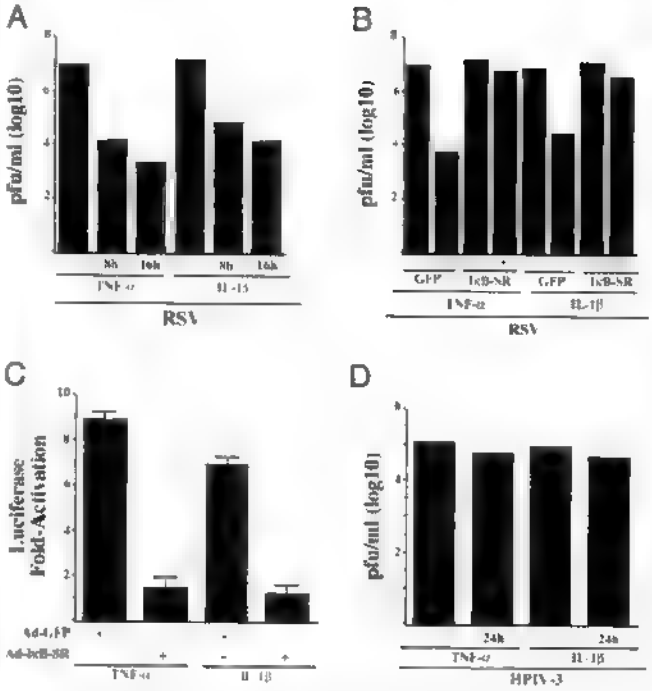

Fig. 3. Effect of TNF-α and IL-1β pretreatment on NF-κB-dependent restriction of RSV replication and cytopathogenicity (*A*) Plaque assay analysis of medium supernatants from A549 cells pretreated with 20 ng/ml TNF-α or IL 1β for 8–16 h before RSV infection (*B*) Plaque assay analysis of culture supernatants from IκB-SR or GFP expressing A549 cells, pretreated with either TNF-α or IL-1β for 16 h before RSV infection. (*C*) Expression of transfected NF-κB-Luc in A549 cells treated with either TNF-α or IL-1β (20 ng/ml for 2 h) in the presence of IκB-SR or control GFP (*D*) Plaque assay analysis of medium supernatants from A549 cells pretreated with 20 ng/ml TNF-α or IL 1β for 24 h before HPIV 3 infection

during the pretreatment period, but not during virus infection. These results strongly suggest that establishment of NF-κB-dependent antiviral state before infection was sufficient to restrict the replication of RSV.

Because TNF-α and IL-1β induces additional signaling pathways (e.g., c-Jun N-terminal kinase and extracellular signal-regulated kinase) apart from NF-κB (29, 30), we investigated whether the antiviral action of TNF-α and IL-1β is specifically mediated by activated NF-κB. Inhibition of NF-κB activation after expression of IκB-SR significantly reverted the antiviral action of TNF-α and IL-1β (Fig. 3*B*) toward RSV. In control experiments, TNF-α or IL-1β treatment of A549 cells transfected with NF-κB-Luc led to significant induction of NF-κB activity, which was inhibited when the cells were infected with Ad-IκB-SR (Fig. 3*C*). These results demonstrated the potent antiviral action of TNF-α and IL-1β is indeed mediated specifically via the NF-κB signaling pathway, and the latter pathway plays an important innate antiviral role in host cells, only when it is activated before virus replication. Interestingly, TNF-α or IL-1β (Fig. 3*D*) pretreatment failed to exert an anti-HPIV-3 activity. Presumably, HPIV-3-mediated induction of NF-κB during the normal course of infection represents the optimal threshold value for its antiviral activity, which is not augmented further by TNF-α or IL-1β treatment.

NF-κB-Dependent Antiviral Response by TNF-α and IL-1β Is Mediated Independent of IFN and Soluble Secreted Factor(s). Next, we investigated whether IFN and/or soluble factor(s) are involved in eliciting the NF-κB-dependent antiviral mechanism of TNF-α and IL-β against RSV. As shown in Fig. 4 *A* and *B*, the medium

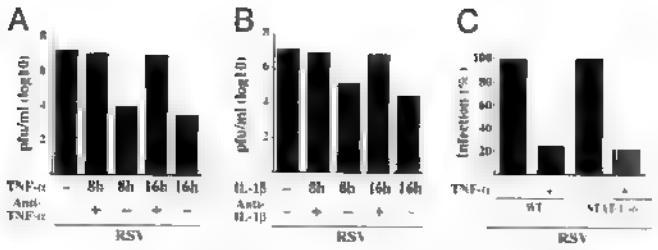

Fig. 4. The noninvolvement of IFN and/or soluble secretory factor(s) in mediating the NF-κB-dependent antiviral response elicited by TNF-α and IL-1β. Plaque assay analysis of medium supernatants from A549 cells infected with RSV after a 16-h pretreatment of A549 cells with medium obtained from TNF-α- (*A*) or IL 1β- (*B*) treated (8 or 16 h) A549 cells in the presence of control antibody or anti-TNF-α (*A*) or anti-IL-1β (*B*) neutralizing antibodies. (*C*) Plaque assay analysis using medium supernatants from WT or STAT-1$^{-/-}$ cells untreated or pretreated with TNF-α (20 ng/ml for 16 h) before infection with RSV. The percent infection indicated was calculated based on a ratio of number of plaques obtained in the presence of TNF-α over the number obtained from untreated cells

supernatant obtained from TNF-α- (Fig. 4*A*) or IL-1β- (Fig. 4*B*) treated A549 cells (cytokine CM) when treated with anti-TNF-α or anti-IL-1β neutralizing antibodies, respectively, and added to fresh A549 cells for pretreatment before virus infection, failed to inhibit RSV replication. The specificity of these cytokine-neutralizing antibodies was borne out by the observation that they failed to inhibit the antiviral action of IFN and the TNF-α and IL-1β CM retained its antiviral property even in the presence of anti-IFN neutralizing antibody (data not shown).

The noninvolvement of soluble secreted factor(s), including IFN, in exerting the NF-κB-dependent antiviral state was further shown by using WT 2fTGH- and IFN-insensitive STAT-1 null (STAT-1$^{-/-}$) U3A human epithelial-like fibrosarcoma cells (31). The lack of JAK/STAT signaling pathway was shown to have no effect on NF-κB signaling cascade induced by TNF-α treatment (32). Similar to A549 cells, TNF-α (Fig. 4*C*) or IL-1β (data not shown) pretreatment established an antiviral state for RSV in both WT and STAT-1 $^{-/-}$ cells. Moreover, additional soluble secreted factor(s) were not involved during establishment of the antiviral state in WT or STAT-1$^{-/-}$ cells, as tested by performing similar experiments described in Fig. 4 *A* and *B* (data not shown). These results suggested that IFN and/or soluble secreted factor(s) are not involved in exerting a NF-κB-dependent antiviral state.

Use of MyD88 by HPIV-3 for NF-κB Induction. Because our results have suggested that a critical time frame of NF-κB activation in infected cells dictates the antiviral function of NF-κB, we investigated the mechanism(s) that may be involved in conferring the difference in postinfection NF-κB induction profile exhibited by HPIV-3 (rapid induction) and RSV (late induction). Recently TLRs have been shown to be used by RNA cytoplasmic viruses for rapid activation of NF-κB in infected cells (5, 6, 8). Because MyD88 is an essential TLR adaptor protein required for optimal TLR-dependent NF-κB activation (33, 34), we investigated the requirement of MyD88 in transducing RSV- and HPIV-3-mediated NF-κB activation signal.

Whereas infection of A549 cells with Ad-DN-MyD88 abrogated NF-κB-Luc activation by HPIV-3, Ad-DN-MyD88 failed to inhibit NF-κB induction by RSV (Fig. 5*A*). Moreover, the requirement of MyD88 in HPIV-3-mediated induction of NF-κB was borne out by the observation that expression of DN-MyD88 resulted in drastic increase in HPIV-3 replication and cytopathogenicity (Fig. 5 *B* and *C*), which was similar to that observed after expression of IκB-SR (Fig. 2 *B* and *E*). These results indicate that in human lung epithelial cells, HPIV-3 and RSV uses two

IMMUNOLOGY

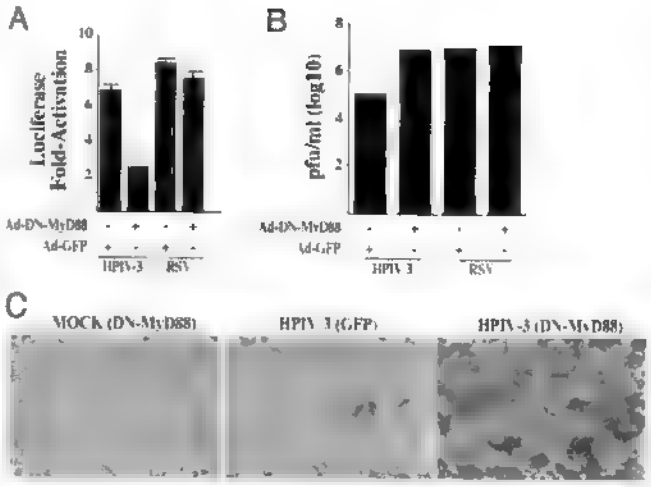

Fig. 5. Differential requirement of MyD88 for NF-κB induction by HPIV-3 and RSV. (*A*) Expression of transfected NF-κB-Luc in A549 cells infected with HPIV-3 or RSV in the presence of DN-MyD88 or control GFP. (*B*) The indicated medium supernatants from A549 cells infected with HPIV-3 or RSV in the absence or presence of prior infection with Ads encoding the DN-MyD88 or GFP were subjected to plaque assay analysis. (*C*) Phase contrast microscopic picture of CV-1 cells incubated with same dilutions of medium supernatants obtained from A549 cells infected with HPIV-3 and Ad-GFP or Ad-DN-MyD88.

alternative mechanisms, MyD88-dependent and -independent pathways, respectively, to induce NF-κB. Moreover, MyD88-dependent and -independent pathways adopted by these two viruses to either induce NF-κB rapidly (HPIV-3) or late after replication initiation (RSV), respectively, may have a direct bearing on their respective cytopathogenic phenotype.

Discussion

In this article, we have established that two medically important human respiratory tract pathogens, HPIV-3 and RSV, respond differentially to innate response elicited by NF-κB. The mildly cytopathic virus, HPIV-3 (which induces NF-κB early during infection), was converted to a virulent virus as a result of increased replication after inhibition of rapid NF-κB induction by HPIV-3. In contrast, the replication of RSV (which induces NF-κB late in infection) was not altered in NF-κB-inhibited cells. However, specific induction of NF-κB by TNF-α or IL-1β before virus replication rendered an antiviral state against RSV, converting this highly cytopathic virus to a less virulent virus. Similar results with drastic inhibition of viral replication after induction of NF-κB before virus infection were obtained when another highly cytopathic RNA cytoplasmic virus, VSV, which possesses similar high titer like RSV in A549 cells (data not shown), and fails to induce NF-κB in these cells (21) was allowed to infect TNF-α- and IL-1β-pretreated cells (see Fig. 7, which is published as supporting information on the PNAS web site, www.pnas.org). Moreover, similar to RSV, anti-VSV activity of TNF-α and IL-1β was elicited specifically by NF-κB, which is independent of IFN and soluble secreted factors (see Fig. 8, which is published as supporting information on the PNAS web site). These results demonstrated that NF-κB is also capable of conferring an essential IFN-independent antiviral activity against a virus that does not induce its activity during natural infection.

It is interesting to note that although the antiviral potential of TNF-α has been reported earlier (35, 36), the mechanism(s) involved in conferring the antiviral response was not known. In our current study, we have demonstrated that the antiviral activity of TNF-α is mediated directly by NF-κB, which is independent of IFN. In addition, we have demonstrated the ability of IL-1β to act as a potent antiviral cytokine, which exerts its IFN-independent antiviral activity by inducing NF-κB. The ability of two NF-κB-inducing cytokines to severely restrict virus replication similar to IFN demonstrated the importance of NF-κB in antiviral defense. Moreover, the noninvolvement of IFN in exerting a NF-κB-dependent antiviral response was borne out by previous reports that infection of STAT-1$^{-/-}$ cells yielded similar HPIV-3 titer compared with the WT cells (13), and RSV is insensitive to the antiviral action of IFN-α/β in A549 cells (37). Our results demonstrating that TNF-α and IL-1β exert their NF-κB-dependent antiviral action independent of IFN were recently validated, because microarray analysis did not reveal induction of IFN-α/β genes after treatment of cells with either TNF-α or IL-1β (38). In addition, nitric oxide (NO) production after inducible nitric oxide synthase (iNOS) induction through NF-κB (39) was not the antiviral factor, because A549 cells treated with the iNOS-competitive inhibitor L-NMMA during HPIV-3 infection resulted in no significant differences in HPIV-3 virus titer (data not shown). Moreover, the NF-κB-dependent antiviral action is not mediated by IFN-γ, because the nonimmune cells used in our studies are incapable of inducing IFN-γ gene.

Because NF-κB-mediated antiviral response critically relies on the time frame of its activation after virus infection, we further demonstrated that at least for RSV and HPIV-3, the temporal nature of NF-κB induction appears to depend on the use of MyD88. (33, 34). HPIV-3 used the MyD88-dependent pathway to rapidly induce NF-κB, probably after interaction of HPIV-3 envelope protein(s) with cell-surface TLRs during virus entry. In support of rapid activation of NF-κB by HPIV-3, a previous study (26) has reported the induction of MHC-I (a gene whose expression is regulated by transactivating function of NF-κB) by UV-irradiated (replication incompetent) HPIV-3 and UV-inactivated HPIV-3-induced NF-κB in A549 cells (data not shown). Further studies will be needed to identify the specific TLRs involved in NF-κB activation by HPIV-3. In contrast to HPIV-3, RSV induced NF-κB late after replication initiation via the MyD88-independent pathway. In that context, previous studies have shown that in contrast to alveolar macrophages or monocytes, RSV activated NF-κB late during infection in lung

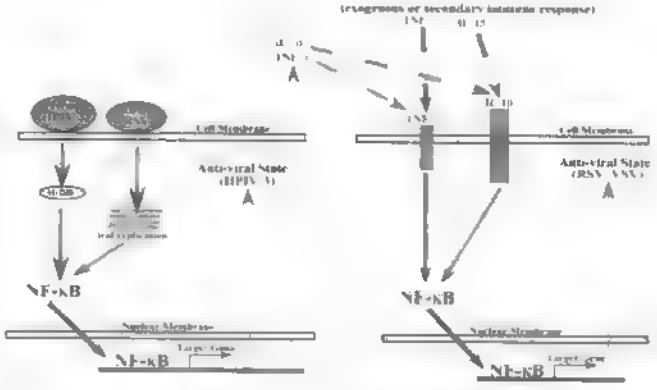

Fig. 6. A model depicting NF-κB-mediated innate antiviral response independent of IFN. Rapid activation of NF-κB by viruses like HPIV-3 via the MyD88 pathway early during infection in a replication-independent manner confers an intracellular antiviral state in the infected cells (*Left*). Similarly, viruses like RSV that induce NF-κB late after infection in a replication-dependent manner, produce TNF-α and/or IL-1β, which, by means of the paracrine mechanism, may prime uninfected cells (*Right*) after binding to its cognate receptors to establish an NF-κB-dependent antiviral state. In addition, exogenously added TNF-α or IL-1β, and the production of these cytokines after secondary adaptive response by immune cells, could prime uninfected cells to activate NF-κB-mediated antiviral response against viruses like VSV that do not induce NF-κB. TNFR, TNF-α receptor; IL-1βR, IL-1β receptor.

epithelial cells (21, 22). Moreover, the NF-κB activation by RSV in these cells were replication dependent, because UV-inactivated RSV (data not shown and ref. 40), and virus replication inhibitors (22) failed to activate RSV-dependent NF-κB induction in A549 cells. Similar to our observation, a recent study (41) has also reported TLR4-independent and replication-dependent activation of NF-κB by RSV in lung epithelial cells. In addition to MyD88, we observed a differential requirement of phosphatidylinositol 3-kinase (PI3K) (42) for induction of NF-κB by HPIV-3 and RSV. Whereas RSV failed to induce NF-κB in A549 cells after inhibition of PI3K activity (ref. 43 and data not shown), such inhibition had no effect on HPIV-3-mediated NF-κB activation (data not shown).

Based on our results, we propose a model for the direct establishment of an IFN-independent innate antiviral state after NF-κB activation (Fig. 6). Infection of human epithelial cells with HPIV-3 rapidly induces (replication independent) NF-κB via the MyD88-dependent IKK/IκB pathway, leading to the establishment of an antiviral state. HPIV-3, a mildly cytopathic, TNF-α-nonproducing virus (25, 26), thus induces the NF-κB antiviral pathway rapidly to restrict its own replication in infected cells. In contrast, NF-κB failed to exert its antiviral function against viruses, like RSV, which activated NF-κB via a MyD88-independent and replication-dependent pathway. Although RSV and VSV circumvents the antiviral activity of NF-κB in infected cells, activation of NF-κB by TNF-α and IL-1β (proinflammatory cytokines whose gene is regulated by transactivating function of NF-κB) before virus replication established an intracellular antiviral state. Thus, in the absence of IFN sensitivity (37) and evasion of NF-κB-dependent antiviral response, TNF-α and/or IL-1β produced by RSV-infected cells (44) may prime uninfected cells by means of binding to their cognate receptors, to restrict the spread of RSV by activating NF-κB. Moreover, TNF-α and/or IL-1β produced after secondary adaptive response by immune cells (45, 46), could prime uninfected cells to create an NF-κB-dependent antiviral state against viruses such as VSV, that do not induce NF-κB (21), and fail to produce IFN from infected cells (47).

In conclusion, we report an innate antiviral immune response that is independent of the well established IFN-induced JAK/STAT pathway, and demonstrate that this innate antiviral response is directly mediated by NF-κB after its activation, either by a virus or by proinflammatory cytokines like TNF-α and IL-1β. Thus, NF-κB acts as an essential host antivirulence factor to restrict the systemic spread of pathogens by not only producing IFN-β but also by being capable of directly establishing an IFN-independent intracellular antiviral state against several RNA cytoplasmic viruses by an alternative pathway.

We thank Dr. V. M. Dixit and Dr. A. Deb for the DN-MyD88 and Ad constructs; Dr. M. Karin for the gift of IKKγ knockout MEFs; Dr. R. H. Silverman for assistance with the manuscript, Dr. K. Panda for performing the iNOS assay; Dr. George R. Stark and Dr. Andrew Lerner for the STAT null cells; and The Cleveland Clinic Foundation Virus Core Facility for providing the viruses. This work was supported by a fellowship from the Morgenthaler Foundation (to S.B.) and by grants from the National Institutes of Health (to A.K.B. and J.A.D.) and the U.S. Department of Defense (to J.A.D.).

1. Baldwin, A. S. (2001) *J. Clin. Invest.* **107,** 3–6.
2. Ghosh, S. & Karin, M. (2002) *Cell* **109,** S81–S96.
3. Li, X. & Stark, G. R. (2002) *Exp. Hematol. (Charlottesville, Va.)* **30,** 285–296.
4. Li, Q. & Verma, I. M. (2002) *Nat. Rev.* **2,** 725–734.
5. Bieback, K., Lien, E., Klagge, I. M., Avota, E., Schneider-Schaulies, J., Duprex, W. P., Wagner, H., Kirschning, C. J., Ter Meulen, V. & Schneider-Schaulies, S. (2002) *J. Virol.* **76,** 8729–8736.
6. Kurt-Jones, E. A., Popova, L., Kwinn, L., Haynes, L. M., Jones, L. P., Tripp, R. A., Walsh, E. E., Freeman, M. W., Golenbock, D. T., Anderson, L. J. & Finberg, R. W. (2000) *Nat. Immunol.* **1,** 398–401.
7. Mogensen, T. H. & Paludan, S. R. (2001) *Microbiol. Mol. Biol. Rev.* **65,** 131–150.
8. Helin, E., Vainionpaa, R., Hyppia, T., Julkunen, I. & Matikainen, S. (2001) *Virology* **290,** 1–10.
9. Stark, G. R., Kerr, I. M., Williams, B. R., Silverman, R. H. & Schreiber, R. D. (1998) *Annu. Rev. Biochem.* **67,** 227–264.
10. Bose, S., Malur, A. & Banerjee, A. K. (2001) *J. Virol.* **75,** 1984–1989.
11. Lamb, R. A. & Kolakofsky, D. (2001) in *Fields Virology*, eds. Knipe, D. M. & Howley, P. M. (Lippincott, Williams & Wilkins, Philadelphia), pp. 1305–1340.
12. Makris, C., Godfrey, V. L., Krahn-Senftleben, G., Takahashi, T., Roberts, J. L., Schwarz, T., Feng, L., Johnson, R. S. & Karin, M. (2000) *Mol. Cell* **5,** 969–979.
13. Choudhary, S., Gao, J., Leaman, D. W. & De, B. P. (2001) *J. Virol.* **75,** 4823–4831.
14. Tian, B., Zhang, Y., Luxon, B. A., Garofalo, R. P., Casola, A., Sinha, M. & Brasier, A. R. (2002) *J. Virol.* **76,** 6800–6814.
15. Bose, S. & Banerjee, A. K. (2002) *Virology* **298,** 73–83.
16. Elewaut, D., DiDonato, J. A., Kim, J. M., Truong, F., Eckmann, L. & Kagnoff, M. F. (1999) *J. Immunol.* **163,** 1457–1466.
17. DiDonato, J. A., Mercurio, F., Rosette, C., Wu-Li, J., Suyang, H., Ghosh, S. & Karin, M. (1996) *Mol. Cell. Biol.* **16,** 1295–1304.
18. Sanchez, A. & Banerjee, A. K. (1985) *Virology* **143,** 45–53.
19. Gupta, S., De, B. P., Drazba, J. A. & Banerjee, A. K. (1998) *J. Virol.* **72,** 2655–2662.
20. Broughan, J. H., Randolph, V. B. & Tatem, J. M. (1997) *J. Virol.* **71,** 4962–4970.
21. Bitko, V., Velazquez, A., Yang, L., Yu-Chung, Y. & Barik, S. (1997) *Virology* **232,** 369–378.
22. Fiedler, M. A., Wernke-Dollries, K. & Stark, J. M. (1996) *J. Virol.* **70,** 9079–9082.
23. Brennan, P. & O'Neill, L. A. (1996) *Biochem. J.* **320,** 975–981.
24. Park, G. Y., Le, S., Park, K. H., Le, C. T., Kim, Y. M., Han, S. K., Shim, Y. S. & Yoo, C. G. (2001) *Eur. Respir. J.* **18,** 801–809.
25. Gao, J., Choudhary, S., Banerjee, A. K. & De, B. P. (2000) *Gene Expression* **9,** 115–121.
26. Gao, J., De, B. P. & Banerjee, A. K. (1999) *J. Virol.* **73,** 1411–1418.
27. Wallach, D., Varfolomeev, E. E., Malinin, N. L., Goltsev, Y. V., Kovalenko, A. V. & Boldin, M. P. (1999) *Annu. Rev. Immunol.* **17,** 331–367.
28. Auron, P. E. (1998) *Cytokine Growth Factor Rev.* **9,** 221–237.
29. Kyriakis, J. M. & Avruch, J. (1996) *BioEssays* **18,** 567–577.
30. Li, X., Commane, M., Jiang, Z. & Stark, G. R. (2001) *Proc. Natl. Acad. Sci. USA* **98,** 4461–4465.
31. McKendry, R., John, J., Flavell, D., Muller, M., Kerr, I. M. & Stark, G. R. (1999) *Proc. Natl. Acad. Sci. USA* **88,** 11455–11459.
32. Mukhopadhyay, A., Shishodia, S., Fu, X. Y. & Aggarwal, B. B. (2002) *J. Cell. Biochem.* **84,** 803–815.
33. Fitzgerald, K. A., Palsson-McDermott, E. M., Bowie, A. G., Jefferies, C. A., Mansell, A. S., Brady, G., Brint, E., Dunne, A., Gray, P., Harte, M. T., *et al.* (2001) *Nature* **413,** 78–83.
34. Mazio, M., Ni, J., Feng, P. & Dixit, V. M. (1997) *Science* **278,** 1612–1615.
35. Merolla, R., Rebert, N. A., Tsiviste, P. T., Hoffmann, S. P. & Panuska, J. R. (1995) *Am. J. Respir. Crit. Care Med.* **152,** 1358–1366.
36. Neuzil, K. M., Tang, Y. & Graham, B. S. (1996) *Am. J. Med. Sci.* **311,** 201–204.
37. Atreya, P. L. & Kulkarni, S. (1999) *Virology* **261,** 227–241.
38. Li, X., Massa, P. E., Hanidu, A., Peet, G. W., Aro, P., Savitt, A., Mische, S., Li, J. & Marcu, K. B. (2002) *J. Biol. Chem.* **277,** 45129–45140.
39. Asano, K., Chee, C., Gaston, B., Lilly, C. M., Gerard, C., Drazen, J. M. & Stamler, J. S. (1994) *Proc. Natl. Acad. Sci. USA* **91,** 10089–10093.
40. Garofalo, R., Sabry, M., Jamaluddin, M., Yu, R., Casola, A., Ogra, P. L. & Brasier, A. R. (1996) *J. Virol.* **70,** 8773–8781.
41. Haeberle, H. A., Takizawa, R., Casola, A., Brasier, A. R., Dieterich, H. J., Van-Rooijen, N., Gatalica, Z. & Garofalo, R. P. (2002) *J. Infect. Dis.* **186,** 1199–1206.
42. Sizemore, N., Leung, S. & Stark, G. R. (1999) *Mol. Cell. Biol.* **19,** 4798–4805.
43. Thomas, K. W., Monick, M. M., Staber, J. M., Yarovinsky, T., Carter, A. B. & Hunninghake, G. W. (2002) *J. Biol. Chem.* **277,** 492–501.
44. Tsutsumi, H., Takeuchi, R., Ohsaki, M., Seki, K. & Chiba, S. (1999) *J. Leukocyte Biol.* **66,** 99–104.
45. Bluman, E. M., Bartynski, K. J., Avalos, B. R. & Caligiuri, M. A. (1996) *J. Clin. Invest.* **97,** 2722–2727.
46. Vreugdenhil, G. R. (2000) *Cytokine* **12,** 1793–1796.
47. Ferran, M. C. & Lucas-Lenard, J. M. (1997) *J. Virol.* **71,** 371–377.

JOURNAL OF VIROLOGY, Sept. 2004, p. 8983–8993 Vol. 78, No. 17
0022-538X/04/$08.00+0 DOI: 10.1128/JVI.78.17.8983–8993.2004

Phospholipid Scramblase 1 Potentiates the Antiviral Activity of Interferon

Beihua Dong,[1] Quansheng Zhou,[2] Ji Zhao,[2] Aimin Zhou,[3] Ronald N. Harty,[4] Santanu Bose,[5] Amiya Banerjee,[5] Roger Slee,[1] Jeanna Guenther,[1] Bryan R. G. Williams,[1] Therese Wiedmer,[2] Peter J. Sims,[2]† and Robert H. Silverman[1]†*

The Departments of Cancer Biology[1] and Molecular Biology,[5] Lerner Research Institute, The Cleveland Clinic Foundation, and The Department of Chemistry, Cleveland State University,[3] Cleveland, Ohio; The Department of Molecular and Experimental Medicine, The Scripps Research Institute, La Jolla, California[2]; and The Department of Pathobiology, School of Veterinary Medicine, University of Pennsylvania, Philadelphia, Pennsylvania[4]

Received 14 March 2004/Accepted 14 April 2004

Phospholipid scramblase 1 (PLSCR1) is an interferon (IFN)- and growth factor-inducible, calcium-binding protein that either inserts into the plasma membrane or binds DNA in the nucleus depending on its state of palmyitoylation. In certain hematopoietic cells, PLSCR1 is required for normal maturation and terminal differentiation from progenitor cells as regulated by select growth factors, where it promotes recruitment and activation of Src kinases. PLSCR1 is a substrate of Src (and Abl) kinases, and transcription of the PLSCR1 gene is regulated by the same growth factor receptor pathways in which PLSCR1 potentiates afferent signaling. The marked transcriptional upregulation of PLSCR1 by IFNs led us to explore whether PLSCR1 plays an analogous role in cellular responses to IFN, with specific focus on antiviral activities. Accordingly, human cells in which PLSCR1 expression was decreased with short interfering RNA were rendered relatively insensitive to the antiviral activity of IFNs, resulting in higher titers of vesicular stomatitis virus (VSV) and encephalomyocarditis virus. Similarly, VSV replicated to higher titers in mouse *PLSCR1*$^{-/-}$ embryonic fibroblasts than in identical cells transduced to express PLSCR1. PLSCR1 inhibited accumulation of primary VSV transcripts, similar to the effects of IFN against VSV. The antiviral effect of PLSCR1 correlated with increased expression of a subset of IFN-stimulated genes (ISGs), including ISG15, ISG54, p56, and guanylate binding proteins. Our results suggest that PLSCR1, which is itself an ISG-encoded protein, provides a mechanism for amplifying and enhancing the IFN response through increased expression of a select subset of potent antiviral genes.

Interferons (IFNs) are the principal cytokines responsible for mediating innate immunity against viral infections (7). How IFNs establish an antiviral state in cells has been a subject of investigation since their discovery (21). Nevertheless, mechanisms of IFN action against viral infections remain incompletely understood. IFN antiviral studies have largely focused on several types of IFN-stimulated genes (ISGs), including the double-stranded RNA (dsRNA)-activated protein kinase (PKR), human myxovirus resistance proteins (Mx), 2′,5′-oligoadenylate synthetase (OAS) and its effector protein RNase L, ISG56 (p56), dsRNA-specific adenosine deaminase, and guanylate binding proteins (GBP) (35). Given the critical role of innate immunity in survival from infections, it is not surprising that the antiviral action of IFNs is complex and involves multiple overlapping or related pathways. For instance, mice that are triply deficient for RNase L, PKR, and Mx1 are nevertheless able to mount a substantial, residual IFN antiviral response (48). Therefore, identification of all of the antiviral ISGs is an important step toward a more complete appreciation and understanding of innate immunity. In this regard, within the past several years, global gene expression profiles from IFN-treated cells, obtained by DNA microarrays, have expanded the number of known ISGs from about 33 to >200 (12, 13).

* Corresponding author. Mailing address: Department of Cancer Biology, NB40, The Lerner Research Institute, The Cleveland Clinic Foundation, 9500 Euclid Ave., Cleveland, OH 44195. Phone: (216) 445-9650. Fax: (216) 445-6269. E-mail: silverr@ccf.org.

† These authors were equal contributors to this study.

Phospholipid scramblase 1 (PLSCR1) is a novel ISG identified as such by way of DNA microarray analysis and confirmed by detailed analysis of the PLSCR1 promoter (12, 49, 50). In fact, PLSCR1 is highly induced by IFN-α, -β, and -γ and also by various growth factors, including epidermal growth factor (EGF), stem cell factor, and granulocyte colony-stimulating factor (30, 51). PLSCR1 is a multiply palmitoylated, lipid-raft-associated endofacial plasma membrane protein, with a proline-rich cytoplasmic domain containing several SH3 and WW domain binding motifs (38). PLSCR1 is proposed to accelerate bidirectional movement of plasma membrane phospholipids during conditions of elevated calcium (50). Transmembrane movement of phospholipids in response to calcium, however, is unaffected by either IFN treatment or PLSCR1 deletion (14, 49, 51).

Although the precise biologic function(s) of PLSCR1 and its related isoforms PLSCR2 to 4 remain to be determined (38), recent studies provide intriguing evidence of a role in cell signaling, maturation, and apoptosis. For instance, proliferation and terminal differentiation of certain hematopoietic stem cells (granulocyte precursor) populations is impaired in PLSCR1-null mice (51), and in both monocytic and granulocytic lineages, expression of this protein markedly increases with terminal differentiation into polymorphonuclear leukocytes or macrophages. Conversely, mutations affecting murine PLSCR1 have been associated with a leukemogenic phenotype, which is reversed upon expression of the wild-type (full-length) protein (24, 25). PLSCR1 suppressed ovarian carci-

noma in an animal model (37), and elevated expression of PLSCR1 has been shown to be required for normal myeloid differentiation (51). Finally, there is recent evidence that the level of expression of this protein correlates with overall survival in acute myelogenous leukemia (46). PLSCR1 is phosphorylated by select protein kinases, including Abl and Src, tyrosine kinases that participate in multiple growth factor receptor signaling pathways (30, 32, 41). Tyrosine phosphorylation of PLSCR1 by c-Src occurs in response to growth factors such as EGF, resulting in association of phosphorylated PLSCR1 with Shc and the activated EGF receptor complex (30). In the absence of PLSCR1, the activation of c-Src kinase through EGF receptor (and related receptors) is markedly attenuated, suggesting that PLSCR1 plays a role in growth factor-dependent recruitment or activation of c-Src kinase, potentially through its interaction in membrane lipid rafts (30, 40). Palmitoylation of PLSCR1 is required for insertion into the plasma membrane (44). However, when palmitoylation does not occur, the importin α/β nucleopore transport system has recently been shown to import PLSCR1 into the nucleus where it binds DNA (6, 44). Accordingly, newly synthesized PLSCR1 appeared in nuclei after IFN induction of PLSCR1 in the human ovarian carcinoma cell line, Hey1B (44). PLSCR1 is the only member of the PLSCR family thus far shown to be inducible by IFNs. These findings raise the possibility that PLSCR1 may contribute to the antiviral effects of IFNs by affecting viral penetration, IFN-stimulated cell signaling pathways at the plasma membrane, the transcription of antiviral genes in the nucleus, and/or by directly blocking specific stages in the viral replication cycle. To determine the involvement of PLSCR1 in the IFN-induced antiviral state, we have compared viral replication in wild-type and PLSCR1$^{-/-}$ mouse cells as well as in human cells in which PLSCR1 levels were decreased with short interfering RNA (siRNA). Our results demonstrate a marked suppression of viral replication by PLSCR1 which is accompanied by the enhanced expression of a specific subset of antiviral ISGs.

MATERIALS AND METHODS

Cell lines. The methods for establishment of mouse embryonic fibroblasts (MEFs) from C57BL/6 × SVev129 mice were previously described (30). Briefly, primary MEFs were isolated from embryos of PLSCR1$^{-/-}$ mice (51) or wild-type mice and immortalized by transfection with plasmid simian virus 40 large T antigen cDNA-pSV2 (KO1, PLSCR1$^{-/-}$, and wild-type cells). Mouse PLSCR1 (mPLSCR1) cDNA was cloned into a modified murine stem cell virus (MSCV)-internal ribosome entry site (IRES)-green fluorescence protein (GFP) vector, MSCV-IRES-GFP (derived from a plasmid generously provided by Ruibao Ren, Brandeis University), and transfected into the packaging cell line, PT-67 (BD Clontech), to yield infectious virus. mPLSCR1 MSCV-IRES-GFP was constructed as follows. v-abl-MSCV-IRES-GFP was digested with EcoRI and BamHI to remove v-abl cDNA. An SfiI cutting site (GGCCGCCTCGGCC) was inserted into the multiple cloning site of the MSCV-IRES-GFP vector by PCR-mediated insertion. mPLSCR1 cDNA was cloned into the EcoRI and SfiI sites of the modified MSCV-IRES-GFP vector. The KO1 MEFs were infected with MSCV-mPLSCR1-IRES-GFP virus to generate KI cells, or control MSCV-IRES-GFP virus was used to infect KO1 cells to generate KO2 cells. Infected cells were sorted by flow cytometry with GFP as an indicator to collect cells with similar expression levels of GFP. The expression of PLSCR1 was confirmed by Western blotting with monoclonal antibody against mPLSCR1(1A8) (30). The human ovarian carcinoma cell line Hey1B (a gift from Alexander Marks, University of Toronto, and Yan Xu, Cleveland Clinic) (4) and mouse L929 and NIH 3T3 cells were cultured in Dulbecco's modified Eagle's medium (DMEM) supplemented with streptomycin-penicillin and 10% heat-inactivated fetal bovine serum (FBS).

Hey1B cells stably expressing siRNA were established as described previously (10). Plasmid pSUPER$_{hPLSCR1}$ was generated by cloning a 19-nucleotide sequence (beginning 92 nucleotides from the translation start site in the human PLSCR1 [hPLSCR1] mRNA) separated by a spacer from its reverse complement as a BglII/HindIII fragment (synthesized at Invitrogen) into the pSUPER vector, which directs synthesis of an RNA from the H1-RNA promoter that is processed in the cell to siRNA (10). The sequences for primers of siRNA of hPLSCR1 are 5′-GAT-CCC-CGG-ACC-TCC-AGG-ATA-TAG-TGT-TCA-AGA-GAC-ACT-ATA-TCC-TGG-AGG-TCC-TTT-TTG-GAA-A-3′ and 3′-GG-GCC-TGG-AGG-TCC-TAT-ATC-ACA-AGT-TCT-CTG-TGA-TAT-AGG-ACC-TCC-AGG-AAA-AAC-CTT-TTC-GA-5′. The sequences for primers of the mismatch control are 5′-GAT-CCC-CGG-ACG-TCC-TGG-ATT-TAG-TGT-TCA-AGA-GAC-ACT-AAA-TCC-AGG-ACG-TCC-TTT-TTG-GAA-A-3 and 3′-GG-GCC-TGC-AGG-ACC-TAA-ATC-ACA-AGT-TCT-CTG-TGA-TTT-AGG-TCC-TGC-AGG-AAA-AAC-CTT-TTC-GA-5 (mismatched nucleotides are underlined). The oligonucleotides were annealed by incubation in 100 mM potassium acetate, 30 mM HEPES-KOH (pH 7.4), and 2 mM magnesium acetate at 95°C for 4 min and then at 70°C for 10 min. The reaction mixtures were slowly cooled to 4°C, and annealed oligonucleotides were phosphorylated with T4 polynucleotide kinase at 37°C for 30 min and incubated at 70°C for 10 min. Ligation of the oligonucleotides was to pSUPER digested with BglII and HindIII. The vectors containing siRNA to hPLSCR1, the 3-base mismatch control, and empty vector were each cotransfected with plasmid pBABE containing a puromycin resistance gene (10) into Hey1B cells by using Lipofectamine 2000 (Invitrogen). Stable cell lines were selected by continuous culturing in media containing 2 μg of puromycin per ml. PLSCR1 expression levels in cell lines were determined on Western blots probed with rabbit anti-hPLSCR1 peptide 306-318 antibody (50) and anti-rabbit immunoglobulin G (IgG) horseradish peroxidase (HRP)-linked (Cell Signaling) and β-actin monoclonal antibodies (Sigma Co.). Forty-seven clones expressing siRNA to PLSCR1 were isolated and screened by Western blot assays, of which about 20 clones had PLSCR1 protein levels that were ≤2-fold that of untreated parental cells. The siRNA clone that had the lowest level of PLSCR1 was used in these studies. In addition, individual clones containing the empty vector and the vector expressing the mismatch siRNA were isolated and determined by Western blotting to have PLSCR1 levels that were similar to those of the parental cells.

VSV purification and infections. Wild-type vesicular stomatitis virus (VSV) and an M protein late-budding domain or PY motif mutant (AAPA) (both were the Indiana strain) were propagated in BHK-21 cells (17). VSV was either from infected cell supernatant or was purified by sucrose gradient sedimentation (3) as indicated in the text. Briefly, virus in culture medium was pelleted by ultracentrifugation at 80,000 × *g* in a Beckman Rotor SW 41 or SW 28 for 120 min at 4°C. Virus pellets were suspended in phosphate-buffered saline (PBS) for 16 h at 4°C, loaded onto 0 to 40% sucrose gradients in 50 mM Tris-HCl (pH 7.6), 250 mM NaCl, and 0.5 mM EDTA, and centrifuged at 35,000 × *g* in a Beckman rotor SW 41 for 90 min. The clear, white layer containing virus was collected and suspended in PBS at 4°C overnight, and the purified virus was stored at −70°C. All virus titers were determined by plaque assay (45) on soft agar overlays of L929 cells in six-well plates for incubation at 37°C for 1 to 2 days.

VSV infections were done after seeding cells in six-well plates (at 3 × 10^5 to 4 × 10^5 cells per well) and incubating them at 37°C in 5% CO_2 overnight. Cells were washed once with PBS and infected with a 0.1 multiplicity of infection (MOI) of VSV in FBS-free DMEM (Invitrogen) for 1 h followed by replacement of media with DMEM–10% FBS for different periods of time as indicated in the text. Cells were lysed with buffer containing 1% Triton X-100, 25 mM Tris-HCl (pH 8.0), 150 mM NaCl, 1% sodium deoxycholate, and 10 ng of leupeptin per ml, and extracts were centrifuged at 16,000 × *g* for 20 min. Media from infected cells were assayed for virus by plaque assays or for viral proteins in media of infected cells or supernatant of the cell lysates by Western immunoblot assays.

Immunoblots. Rabbit antibody 4720 against N-terminal residues 1 to 12 of mPLSCR1 (41) and rabbit antibody against C-terminal residues 306 to 318 of hPLSCR1 (50) were previously described (each are rabbit antipeptide antisera that are affinity purified on the peptide and thus used as affinity-purified IgG). Other antibodies used were rabbit anti-N protein of VSV (8), rabbit anti-L protein of VSV raised against a synthetic peptide corresponding to amino-terminal residues 5 to 19 of the L protein (29), mouse monoclonal anti-VSV M protein (a gift from D. S. Lyles, Winston-Salem, N.C.), mouse monoclonal anti-VSV G protein (no. 1667351, Roche), rabbit anti-p56 (a gift from Ganes Sen, Cleveland, Ohio) (16), mouse monoclonal anti-p15 (from Ernest Borden, Cleveland, Ohio) (11), rabbit anti-mGBP-2 (from Deborah Vestal, Toledo, Ohio) (42), and monoclonal anti-β-actin (catalog number A-5441, Sigma Co.). Proteins (30 to 60 μg) in cell extracts or 25 μl of medium from virus-infected cells was separated on 8 to 12% polyacrylamide–sodium dodecyl sulfate (SDS) gels and transferred onto Immobilon-P transfer membranes (Millipore Co.). Blots were

blocked with PBS containing 0.07% Tween (PBS-T) and 5% fat-free dried milk for 1 h and then incubated with primary antibodies in the same blocking buffer at room temperature for 2 h or at 4°C for 16 h. The blots were washed three times with PBS-T. After a 1-h incubation of blots with secondary antibody, anti-mouse IgG-HRP, or anti-rabbit IgG-HRP (Cell Signaling Co.) and four washes with PBS-T, protein bands were visualized with enhanced chemiluminescence detection reagents (Amersham Co.). Protein amounts were estimated with the NIH Image (version 1.61) computer program.

VSV adsorption and penetration. The ^{35}S-labeled VSV was prepared from 2×10^7 BHK-21 cells infected with VSV (MOI = 0.1) in methionine-free DMEM (Invitrogen Co.) in the absence of serum for 1 h and washed with PBS. Methionine-free DMEM containing both 3 μg of actinomycin D per ml and 1.4 mCi of [^{35}S]methionine was added to the cells, and cells were incubated for 24 h. The ^{35}S-labeled VSV in the media was purified by sucrose gradient sedimentation as described above. KO and KI cells were plated 1 day prior to infection in 12-well plates with 6×10^4 cells per well and incubated with purified ^{35}S-labeled VSV (MOI = 4) in FBS-free DMEM at 37°C for 1 h. After cells were washed twice with PBS, complete DMEM with 10% FBS was added and cells were incubated for 1.5 h. Lysis buffer was added to the cells after the cells were washed three times with PBS. The cell lysates were centrifuged at 16,000 × *g* for 20 min, the protein extracts were fractionated on 10% polyacrylamide–SDS gels, and an autoradiogram was prepared from the dried gels. Radiolabeled viral protein amounts were estimated by using NIH Image (version 1.61).

Primary VSV mRNA transcript accumulation. VSV N mRNA accumulation owing to primary transcription was measured as described previously (8). KO2 and KI cells were pretreated with 1,000 U of recombinant human IFN-α A/D (Hoffmann LaRoche, Inc.) per ml for 16 h and washed with PBS once. Cycloheximide (10 μg/ml) in DMEM with 10% FBS was added to the cells for 2.5 h followed by washing with PBS. Purified VSV at an MOI of 0.5 with FBS-free DMEM and 10 μg of cycloheximide/ml was added to the cells for 1 h. After removing the virus, cells were incubated with 10% FBS–DMEM with cycloheximide (10 μg per ml) for 3, 5, and 8 h before cells were harvested for RNA extraction with Trizol (Invitrogen). RNA (10 μg) was separated on 1.2% agarose–formaldehyde gels, transferred to a Hybond-N$^+$ membrane (Amersham Biosciences), and cross-linked with UV. The blots were incubated with ULTRAhyb (Ambion) hybridization buffer at 42°C for 4 h, prior to the addition of ^{32}P-cDNA, encoding the VSV N protein (8, 20, 33), which was labeled by using the Prime-a-Gene system (Promega) at 42°C for 16 h. The autoradiograms of the blots were prepared after washing four times at 50°C in 2× SSC (1× SSC is 0.15 M NaCl plus 0.015 M sodium citrate) with 0.1% SDS. The blots were stripped and reprobed with ^{32}P-labeled β-actin cDNA.

EMCV infections. Encephalomyocarditis virus (EMCV) (a gift of I. Kerr, London, England) was propagated by infecting L929 cells, collecting the cell supernatants, and clearing by centrifugation at 16,000 × *g* for 20 min at 4°C. Virus titers were determined by plaque assays with L929 cells. EMCV was used to infect cells at an MOI of 0.01, in FBS-free DMEM for adsorption (1 h), which was then replaced with 10% FBS–DMEM. The media containing progeny virus were collected after 24 and 40 h.

Gene expression profiling by use of custom cDNA microarrays. Cells stably expressing siRNA to hPLSCR1 and mismatch control and vector control cells were plated in triplicate at 4×10^5 cells per well in six-well plates and incubated at 37°C with 5% CO_2 for 16 h. Cells were incubated in the absence and presence of 1,000 U of human IFN-β (Interpharma) per ml for 8 h and washed with PBS. Total RNA was extracted with Trizol reagent while identically treated cells were harvested for determining PLSCR1 levels.

Array construction. The array used in this study comprised a subset of sequence-verified cDNA clones from the Research Genetics, Inc., 40,000-clone set representing 950 genes containing adenylate-uridylate-rich elements and 18 genes potentially involved in AU-directed mRNA decay as previously described (15), 855 ISGs representing an expansion of a previously described clone set containing confirmed and candidate genes stimulated by IFNs in diverse cell types (13), 288 genes responsive to the viral analog poly(I-C), and 85 housekeeping genes. DNA preparation and slide printing were as previously described except for the use of 40% dimethyl sulfoxide in place of 1.5× SSC as the printing solution (15).

Target RNA preparation. Target RNA was generated in a T7 polymerase-based linear amplification reaction based on a modified version of a published protocol (43). Two micrograms of total RNA and 5 pmol of T7-$(dT)_{24}$ primer [5′-GGCCAGTGAATTGTAATACGACTCACTATAGGGAGGCGG-$(dT)_{24}$-3′] in a total volume of 5.5 μl was incubated at 70°C for 10 min and chilled on ice. For first-strand cDNA synthesis, the annealed RNA template was incubated for 1 h at 42°C in a 10-μl reaction mixture containing first-strand buffer (Invitrogen), 10 mM dithiothreitol, 1 U of anti-RNase (Ambion) per μl, 500 μM deoxynucleoside triphosphates, and 2 U of Superscript II (Invitrogen) per μl. Second-strand synthesis was for 2 h at 16°C in a total reaction volume of 50 μl containing first-strand reaction products, second-strand buffer (Invitrogen), 250 μM deoxynucleoside triphosphates, 0.06 U of DNA ligase (Ambion) per μl, 0.26 U of DNA polymerase I (New England Biolabs) per μl, and 0.012 U of RNase H (Ambion) per μl followed by the addition of 3.3 U of T4 DNA polymerase (3 U per μl; New England Biolabs) and a further 15 min of incubation at 16°C. Second-strand reaction products were purified by phenol-chloroform-isoamyl alcohol extraction in Phaselock microcentrifuge tubes (Eppendorf) according to the manufacturer's instructions and ethanol precipitated. In vitro transcription was performed by using the T7 megascript kit (Ambion) according to a modified protocol in which purified cDNA was combined with 1 μl (each) of 10× ATP, GTP, CTP, and UTP and 1 μl of T7 enzyme mix in a 10-μl reaction volume and incubated for 9 h at 37°C. Amplified RNA was purified by using the Rneasy RNA purification kit (Ambion) according to the manufacturer's instructions.

RNA labeling. Cy3- or Cy5-labeled cDNA was prepared by indirect incorporation. Two micrograms of amplified RNA, 1 μl of dT_{12-18} primer (1 μg per μl; Invitrogen), 2.6 μl of random hexanucleotides (3 μg per μl; Invitrogen), and 1 μl of anti-RNase (Ambion) were combined in a reaction volume of 15.5 μl and incubated for 10 min at 70°C. Reverse transcription was for 2 h at 42°C in a 30-μl reaction mixture containing annealed RNA template, first-strand buffer, 500 μM (each) dATP, dCTP, and dGTP, 300 μM dTTP, 200 μM aminoallyl-dUTP (Sigma), 10 mM dithiothreitol, and 12.7 U of Superscript II per μl. For template hydrolysis, 10 μl of 0.1 M NaOH was added to the reverse transcription reaction mixture and the mixture was incubated for 10 min at 70°C, allowed to cool at room temperature for 5 min, and neutralized by the addition of 10 μl of 0.1 M HCl. cDNA was precipitated at −20°C for 30 min after the addition of 1 μl of linear acrylamide (Ambion), 4 μl of 3 M sodium acetate (pH 5.2), and 100 μl of absolute ethanol, and then resuspended in 5 μl of 0.1 M $NaHCO_3$. For dye coupling, the contents of 1 tube of *N*-hydroxysuccinimide ester containing Cy3 or Cy5 dye (product no. PA25001 and PA25002; Amersham Biosciences) was dissolved in 45 μl of dimethyl sulfoxide. Five microliters of dye solution was mixed with the cDNA and incubated for 1 h in darkness at room temperature. Labeled cDNA was purified on a QIAquick PCR purification column (QIAGEN) according to the manufacturer's instructions. Eluted cDNA was dried under a vacuum and resuspended in 30 μl of Slidehyb II hybridization buffer (Ambion). After 2 min of denaturation at 95°C, the hybridization mixture was applied to the microarray slide under a coverslip. Hybridization proceeded overnight in a sealed moist chamber in a 55°C water bath. Posthybridization, slides were washed successively for 5 min each in 2× SSC–0.1% SDS at 55°C, then in 2× SSC at 55°C, and finally, in 0.2× SSC at room temperature.

Acquisition and normalization of data. Data were acquired with a GenePix 4000B laser scanner and GenePix Pro, version 5.0, software as previously described (15). Raw data were imported into GeneSpring, version 6.0, software (Silicon Genetics) and normalized based on the distribution of all values with locally weighted linear regression before further analysis.

RESULTS

PLSCR1 contributes to antiviral activities of IFNs. To investigate the involvement of PLSCR1 in the IFN-induced antiviral state, PLSCR1 levels were stably decreased in the human ovarian carcinoma cell line Hey1B by using an siRNA approach. An siRNA against a PLSCR1 mRNA target site, 92 to 110 nucleotides 3′ to the translation start site, was generated from a DNA sequence cloned into plasmid pSUPER (10). As a control, siRNA was generated with 3 mismatched nucleotides to the same PLSCR1 sequence and with compensatory base changes in the opposite strand to maintain base pairing. In addition, cells containing the empty plasmid vector were also used as controls. Extracts of stable clones obtained by drug selection were screened for PLSCR1 expression in Western blots probed with antibodies to both PLSCR1 and β-actin. Cell lines with empty vector (vector control) and with the mismatch siRNA showed similar basal levels of PLSCR1 that increased markedly with IFN-β treatment (Fig. 1A, lanes 1 to 4). In contrast, the PLSCR1 siRNA plasmid reduced the basal expression of PLSCR1 by about 10-fold (relative to basal expression in untreated controls). Furthermore, the IFN-induced level of

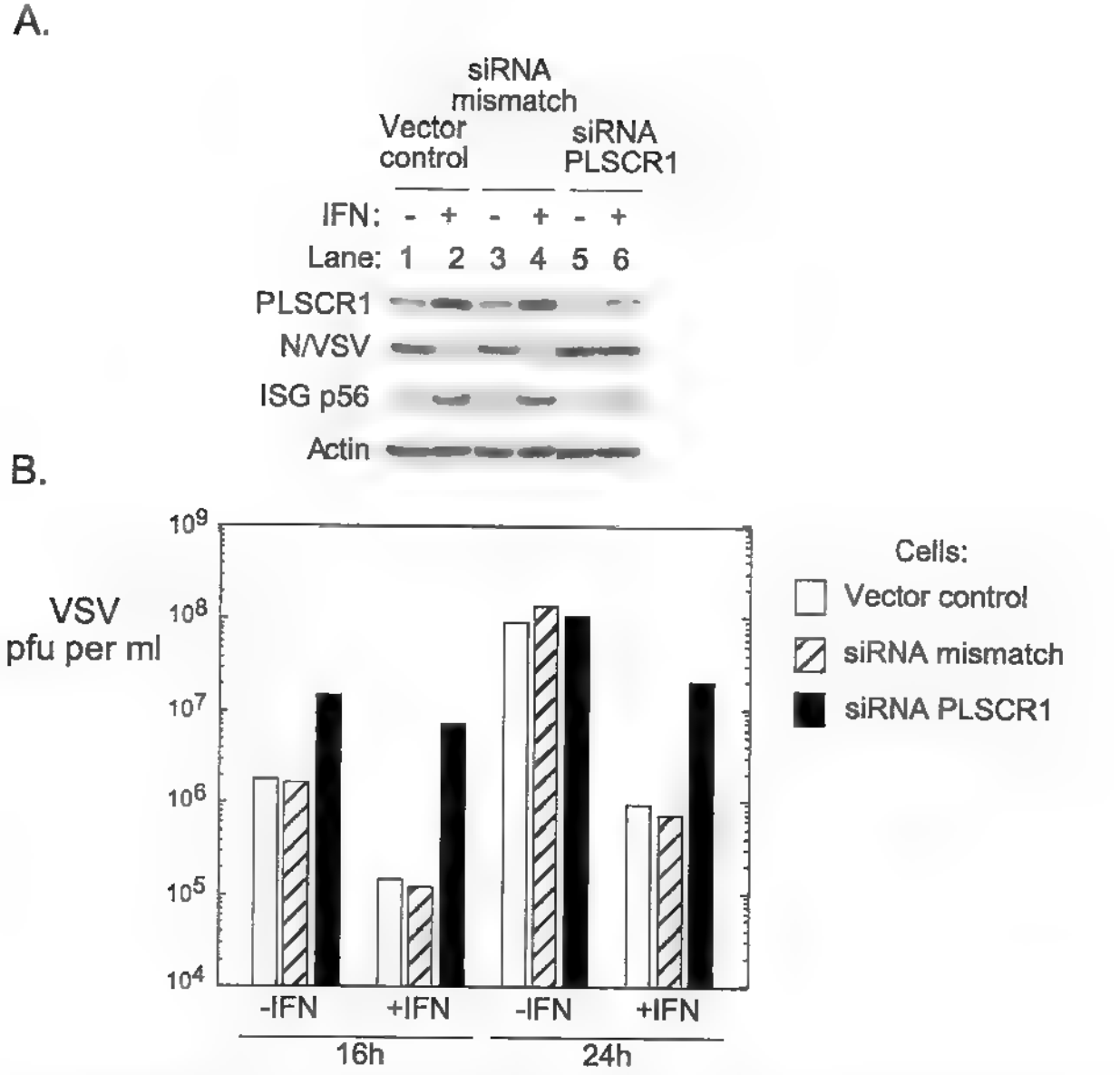

FIG. 1. Decreasing levels of PLSCR1 with siRNA suppresses the anti-VSV activity of IFN in human Hey1B cells. Hey1B cells stably transfected with pSUPER lacking insert (vector control) or pSUPER expressing the siRNA mismatch control or siRNA to PLSCR1 were incubated with or without human IFN β (1,000 U per ml) for 8 h and were then infected with purified VSV at an MOI of 0.1 for 16 and 24 h. (A) Levels of hPLSCR1, VSV N protein, p56, and β-actin were determined at 24 h postinfection from cell extracts in Western blots probed with antibodies. (B) VSV yields were determined by plaque assays after combining media from triplicate cultures of infected cells preincubated in the presence (+) or absence (−) of IFN-β (as indicated).

PLSCR1 was also suppressed severalfold through PLSCR1-specific siRNA compared to the IFN-stimulated controls not containing the PLSCR1 siRNA plasmid (Fig. 1A, top panel, compare lanes 2, 4, and 6).

To investigate the potential antiviral effect of PLSCR1, cells were incubated in the presence or absence of IFN-β (1,000 U per ml) for 8 h and subsequently infected with the VSV Indiana strain at an MOI of 0.1 (a member of the *Rhabdoviridae* family of enveloped, nonsegmented negative-strand RNA viruses). Levels of VSV N protein and p56 (encoded by an ISG) were determined at 24 h postinfection (Fig. 1A). VSV N protein amounts were greatly reduced by IFN-β in both the vector control and siRNA mismatch-expressing cells (Fig. 1A, lanes 1 to 4). Remarkably, however, N protein levels appeared only slightly decreased after IFN-β treatment of cells with siRNA to PLSCR1 (Fig. 1A, lane 6). Furthermore, reducing the PLSCR1 levels resulted in increases of VSV yields (about 1 $\log_{10}$ unit) by 16 h but not at 24 h postinfection, possibly indicating that PLSCR1 was causing a delay in the replication cycle (Fig. 1B). The antiviral effect of IFN-β at both 16 and 24 h postinfection, however, was substantially impaired when PLSCR1 levels were decreased (Fig. 1B). At 24 h postinfection, IFN-β reduced

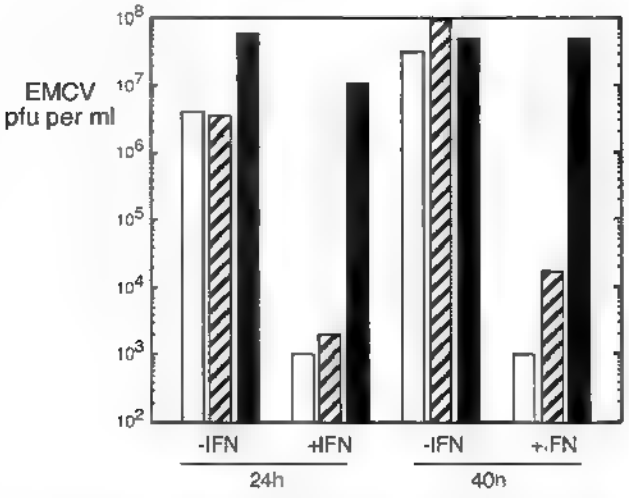

FIG. 2. PLSCR1 suppresses EMCV replication in Hey1B cells Hey1B cells stably transfected with empty vector (vector control, white bars) or with vector expressing mismatched siRNA (hatched bars) or PLSCR1 siRNA (black bars) were treated with IFN-β (1,000 U per ml) for 8 h and infected with EMCV (MOI of 0.01) for 24 and 40 h. Viral titers from combining media of triplicate infected cultures of cells were determined by plaque assays. +, present; −, absent.

VSV yields by about 200-fold in the vector control and siRNA mismatch cells, whereas the IFN effect was only 5-fold in the cells expressing PLSCR1 siRNA (Fig. 1B). To monitor IFN induction of gene expression, levels of p56 protein were measured with a monoclonal antibody. IFN-β treatment of both the empty vector and mismatch siRNA control cells induced p56 to severalfold-higher levels than in the IFN-treated PLSCR1 siRNA cells (Fig. 1A, lanes 2, 4, and 6). The effect of PLSCR1 on p56 expression required the addition of exogenous IFN and was not observed with virus alone. These results suggested a possible contribution of PLSCR1 to IFN induction of gene expression. There was no increase of p56 expression in the control siRNA-expressing cells (Fig. 1A, compare lanes 1 and 3), suggesting that pSUPER expression of siRNA in these cells did not produce an off-target, nonspecific effect on ISG expression (9, 39). This conclusion was supported by gene array results (see below).

To determine whether the antiviral activity of PLSCR1 was specific for VSV, growth of EMCV (a member of the *Picornaviridae* family of nonenveloped, positive-strand RNA viruses) was compared in the different cell lines (Fig. 2). The Hey1B cells were incubated in the presence or absence of human IFN-β (1,000 U per ml) for 8 h and then infected with EMCV at an MOI of 0.01. In the absence of IFN, suppression of basal PLSCR1 expression by specific siRNA resulted in an about 10-fold increase in viral replication at 24 h postinfection,

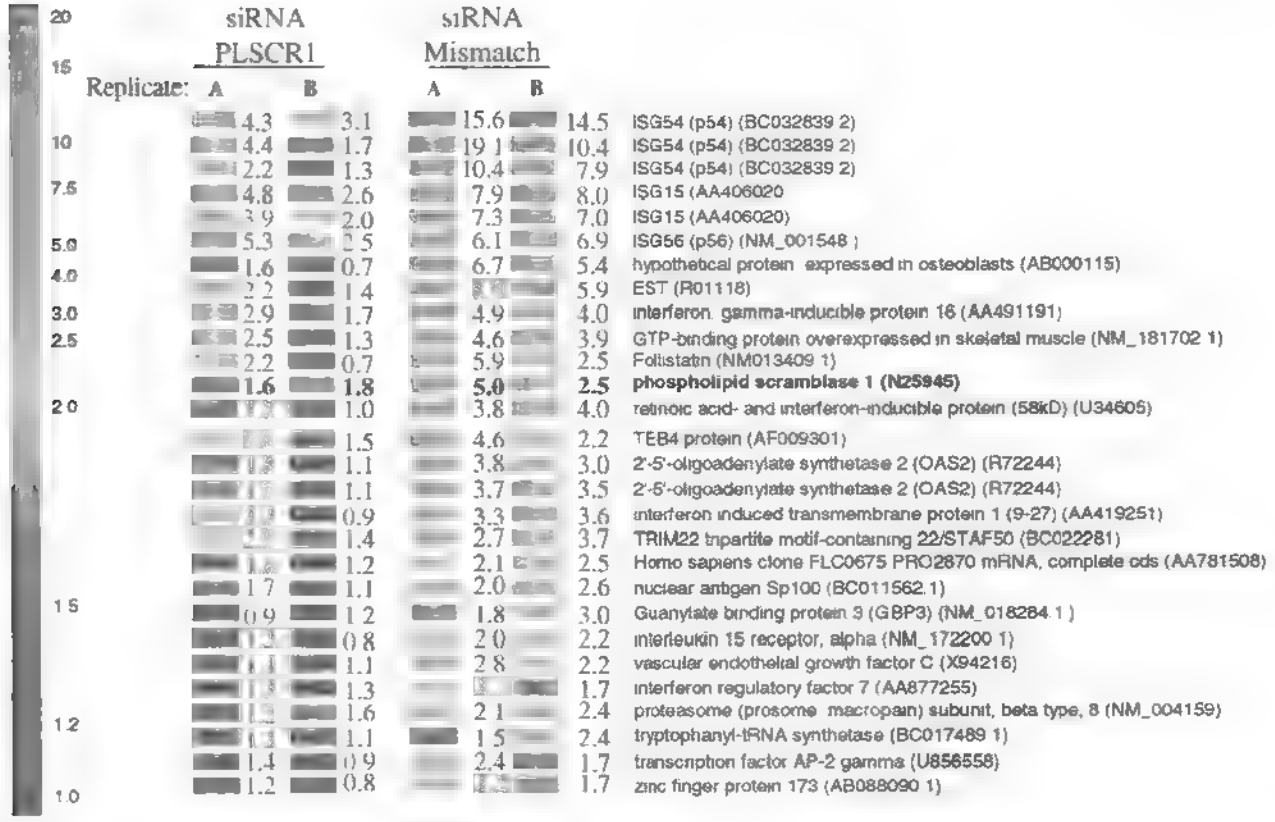

FIG. 3. PLSCR1 enhances expression of a set of ISGs as determined in DNA microarrays. Hey1B cells expressing siRNA mismatch or siRNA to PLSCR1 were incubated with or without IFN β (1,000 U/ml) for 8 h. Gene array results are from RNA samples isolated from triplicate cultures of IFN-treated or control cells. Numbers represent increases (*n*-fold) in RNA levels after IFN treatment.

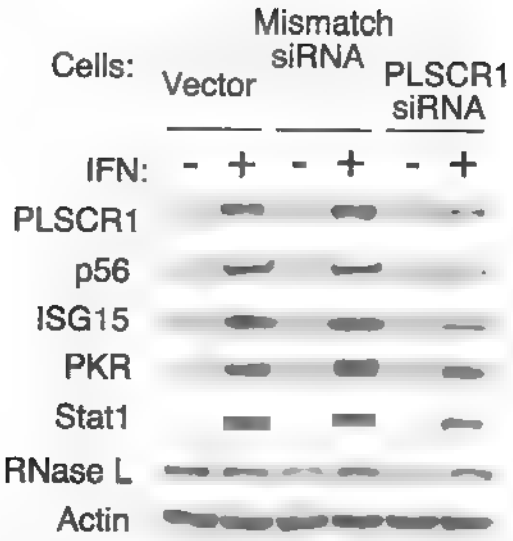

FIG. 4. PLSCR1 enhances the expression of a subset of ISGs as determined by Western immunoblots. Hey1B cells containing empty vector (vector) or expressing siRNA mismatch or siRNA to PLSCR1 were incubated with (+) or without (−) IFN-β (1,000 U/ml) for 16 h. Levels of proteins (indicated) were determined by probing Western blots of cell extracts with specific antibodies (see Materials and Methods)

although no effect was seen at 40 h, suggesting a small delay in viral replication due to PLSCR1. In contrast to these small effects in the absence of IFN, in cells pretreated with IFN, the suppression of PLSCR1 expression by specific siRNA eliminated most of the observed antiviral activity associated with addition of IFN (cf. black bars to controls in Fig. 2).

Reduced expression of ISGs in PLSCR1-deficient cells. Our findings suggest a general antiviral effect of PLSCR1 that appears related to marked enhancement of the cellular response to IFN. We therefore next compared mRNA profiles in untreated and IFN-β-treated cells by using a custom viral response cDNA microarray constructed with 855 candidate and confirmed ISGs, 950 AU-rich element genes, 288 dsRNA-stimulated genes, and 85 housekeeping genes, with the latter serving as mRNA controls (Fig. 3). Triplicate cultures of Hey1B vector control, mismatch siRNA, or PLSCR1 siRNA clones were treated with IFN-β at 8 h, and the RNA isolated from identically treated cultures was combined for microarray analysis. The experiment was independently performed twice (i.e., experiments A and B were both from RNA pools of triplicate, identically treated cultures). In addition, several of the ISGs were present at multiple positions on the array (indicated by multiple rows for the same gene in Fig. 3). Twenty-four genes were more-highly induced by IFN-β in the control cells expressing mismatched siRNA than in the cells expressing specific siRNA to PLSCR1. Twenty-one of these genes are previously identified ISGs. Three genes are newly identified ISGs from these experiments and are also AU-rich genes (hypothetical protein expressed in osteoblasts, TEB4, and transcription factor AP-2 gamma). ISG54, present at three locations on the array, was one of the most highly elevated ISGs associated with PLSCR1 expression. The average IFN induction of ISG54 was about fivefold greater in the control siRNA cells than in the PLSCR1 siRNA cells. The remaining 23 ISGs were induced 1.7- to >5-fold greater by IFN in the control siRNA cells than in the PLSCR1 siRNA-expressing cells. Our results suggest a contribution of PLSCR1, a known ISG (12, 49), to the IFN-stimulated expression of a limited subset of ISGs. However, because siRNA ablation of PLSCR1 was incomplete, the values obtained may underestimate the contribution of PLSCR1 to ISG expression. A decreased IFN induction of PLSCR1 itself was observed in the siRNA to PLSCR1 cells. PLSCR1 siRNA did not significantly affect expression of any of the 85 housekeeping genes serving as controls (data not shown).

To confirm the gene array results, immunoblot measurement of several different IFN-induced proteins was performed (Fig. 4). Deficient IFN induction of PLSCR1, p56, and ISG15 was observed; there was a small effect on Stat1 levels while PKR and RNase L amounts were essentially unaffected. The siRNAs by themselves did not induce ISG expression, as determined by both gene microarrays and Western blot assays (Fig. 4 and data not shown).

The IFN response is reduced in PLSCR1$^{-/-}$ MEFs. To perform studies in the complete absence of PLSCR1, PLSCR1 $^{-/-}$

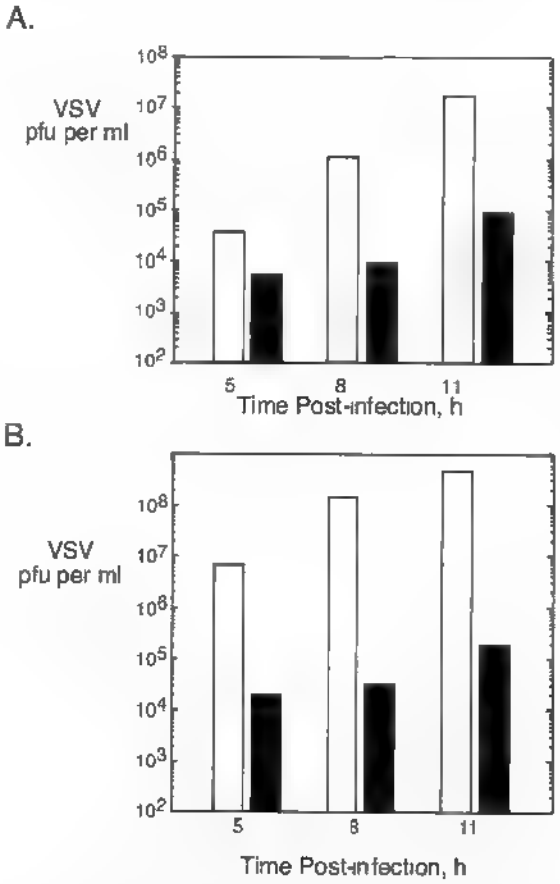

FIG. 5. VSV replicates to higher titers in MEFs lacking PLSCR1 (A) Wild-type (black bars) and PLSCR1 $^{-/-}$ KO1 (white bars) MEFs were infected with VSV at an MOI of 0.1. (B) PLSCR1 $^{-/-}$ KO2 (white bars) MEFs and reconstituted, PLSCR1-expressing knock-in KI cells (black bars) were infected with VSV at an MOI of 0.1. At different times postinfection (*x* axes), virus was harvested. Viral yields, determined by plaque assays on indicator L929 cells, were from combined triplicate cultures of infected cells.

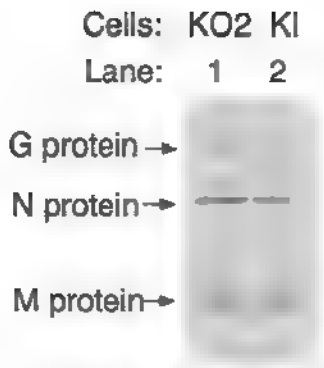

FIG. 6. Adsorption and penetration of ^{35}S-labeled VSV is unaffected by PLSCR1. KO2 (PLSCR1$^{-/-}$) and KI (PLSCR1 reconstituted) cells were infected with purified ^{35}S-VSV (MOI of 4) (see Materials and Methods). Cell-associated proteins were separated by SDS-polyacrylamide gel electrophoresis, and an autoradiogram of the dried gel was prepared. The positions of the VSV G, N, and M proteins are indicated (arrows).

MEFs immortalized with simian virus 40 large T antigen (KO1 cells) were utilized. VSV yields were increased up to about 100-fold in the KO1 cells compared to the wild-type cells (Fig. 5A). To rule out nonspecific effects owing to clonal variations, the KO1 cells were transfected with MSCV vector expressing PLSCR1 cDNA (KI cells for gene knock-in) or with an empty MSCV vector (KO2 cells). VSV yields were 3 to >4 $\log_{10}$ units higher in the KO2 cells than in KI cells (Fig. 5B). These results from KO cells deficient in PLSCR1 are consistent with results obtained with wild-type cells in which endogenous PLSCR1 expression was suppressed by siRNA, although the PLSCR1-related antiviral effect was even more apparent in the former, where PLSCR1 is completely absent.

Determining the stage(s) in the VSV replication cycle affected by PLSCR1. To examine how PLSCR1 affects VSV replication, several distinct stages in the viral life cycle were analyzed and compared in the KO2 and KI cells. Viral absorption and penetration were determined by infecting cells with purified ^{35}S-labeled VSV for 2.5 h and monitoring cell-associated proteins that originated from the input virus. After washing and lysing the infected cells, proteins were subjected to electrophoresis, transfer, and autoradiography (Fig. 6). Equivalent amounts of the ^{35}S-labeled VSV proteins, G (glycoprotein), N (nucleoprotein), and M (matrix protein), were observed associated with the KO2 and KI cells. These results suggest that PLSCR1 did not affect stages prior to viral penetration.

Primary viral transcript accumulation was monitored by measuring VSV N mRNA produced from the input genome in the presence of cycloheximide. This method relies on the fact that amplification of VSV RNA, but not primary transcription, requires ongoing protein synthesis. Previously, IFN was reported to suppress VSV replication at the level of viral primary transcription (5). In the present studies, IFN-α pretreatments effectively reduced primary viral transcript accumulation in both cell lines (Fig. 7). Furthermore, expression of PLSCR1 reduced N mRNA accumulation in either the absence or presence of prior IFN treatment. Therefore, both IFN and PLSCR1 suppressed VSV replication at the level of primary transcript accumulation. Accordingly, in cells infected in the absence of cycloheximide, VSV L, G, N, and M proteins were significantly more abundant in the media (from released virus) and from intact KO2 cells than were released virus and cell-associated virus of the KI cells (Fig. 8). An additional effect on viral protein synthesis is not ruled out by these findings (34).

To determine whether late stages in the virus replication cycles were affected by PLSCR1, release of progeny wild-type VSV and of a late-budding domain (PPPY to AAPA) M protein mutant virus into the media was compared in the KO2 and KI cells. The M protein mutation was previously observed to reduce viral release by about 1 to 2 $\log_{10}$ units (23). Similarly, the AAPA mutant form of M protein reduced viral yields by 45-fold in the KO2 cells and by 62-fold in the KI cells (Fig. 9). These results suggest that the anti-VSV effect of PLSCR1 does not depend on or require the late-budding PY domain in M protein but does not exclude the possibility that PLSCR1 may

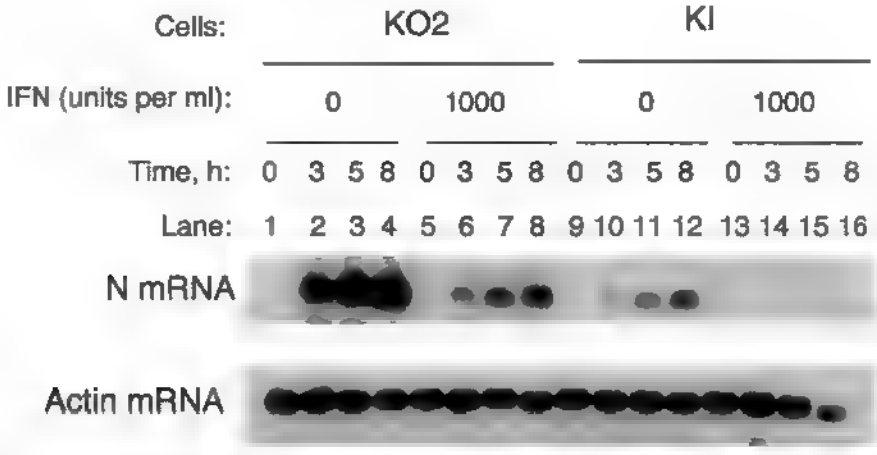

FIG. 7. PLSCR1 and IFN-α inhibit accumulation of primary VSV N transcripts. Cells were incubated with or without IFN-α A/D (1,000 U per ml) for 16 h followed by treatment with cycloheximide (3 μg/ml) for 2.5 h. Infections were with purified VSV (MOI of 0.5) for 0, 3, 5, and 8 h in the continuous presence of cycloheximide to prevent replication. The Northern blot was probed with ^{32}P-cDNA to the N gene of VSV and was normalized with a radiolabeled cDNA to β-actin.

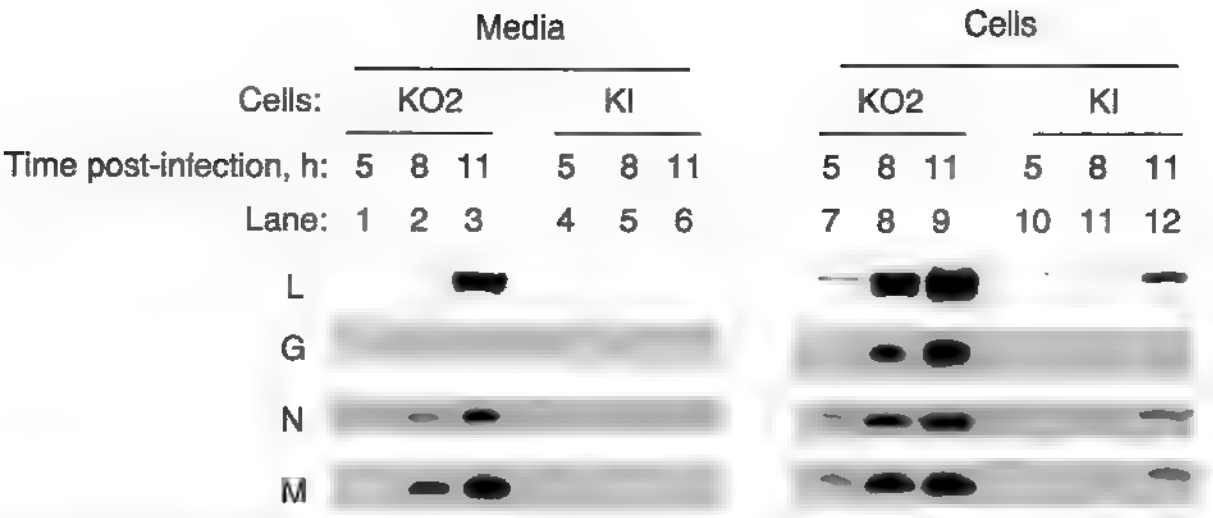

FIG. 8. VSV protein accumulation is reduced in cells expressing PLSCR1. KO2 and KI cells were infected with purified VSV at an MOI of 0.1 for 5, 8, and 11 h (as indicated). Levels of VSV proteins from released virus (Media) and associated with intact cells (Cells) were determined on Western blots probed with antibodies to the VSV L, G, N, and M proteins.

influence viral budding, for example, through effects on plasma membrane lipid organization or topology.

PLSCR1 expression was equivalent in the wild type and KI cells and was absent in the KO1 and KO2 cells (Fig. 10 and data not shown). In the wild-type cells, PLSCR1 levels were constitutively elevated and were not further increased by IFN-α treatment, perhaps due to induction by growth factors in the serum (51) (Fig. 10, lanes 4 to 6). Cell type-specific differences in basal levels of PLSCR1 may reflect inherent lineage or maturational differences in PLSCR1 expression as well as differing sensitivities of the cells to induction by growth factors or interferon. GBP-2 was induced by 10-fold-lower concentrations of IFN-α in the wild-type and KI cells than in the KO1 cells (Fig. 10) (42). However, IFN-induced levels of PKR and STAT1 were similar in the different cell lines. Basal levels of PKR, however, were modestly elevated in untreated confluent (24 h) cultures of PLSCR1-expressing cells compared with KO1 cells (Fig. 10, bottom, lanes 1, 4, and 7). These findings are consistent with the notion that PLSCR1 affects the expression of only a limited subset of ISGs.

DISCUSSION

Our results suggest that the expression of PLSCR1, an ISG, is required for maximal antiviral activity of IFN, and that this effect is mediated at least in part through potentiation of the expression of a select subset of ISGs with known or suspected antiviral activities. However, PLSCR1 is nonessential for IFN signaling because IFN strongly induces PKR and STAT1 in PLSCR1 $^{-/-}$ cells (Fig. 10). Whereas the precise mechanism by which PLSCR1 exerts these selective effects on certain ISGs remains unresolved, it is of note that (i) PLSCR1 is a palmitoylated, plasma membrane protein known to partition into lipid rafts and implicated in regulating the organization of plasma membrane phospholipids (38, 40), (ii) deletion of PLSCR1 has been shown to alter afferent signaling and cellular response to a select group of cell surface growth factor receptors with specific effects on the activation of c-Src and potentially other protein kinases (30, 32, 41), (iii) in addition to transcriptional induction by IFN, PLSCR1 expression is upregulated through each of the growth factor receptor pathways that PLSCR1 gene deletion has been shown to attenuate afferent receptor signaling (30, 51), (iv) under conditions of transcriptional induction, PLSCR1 has been shown to traffic to both the plasma membrane and the nucleus, events that appear to be regulated through its palmitoylation (44), and (v) once in the nucleus, PLSCR1, an acidic polypeptide, is found tightly bound to DNA (6). Taken together, this suggests that the observed antiviral activity of PLSCR1 and its capacity to potentiate transcription of a select subset of ISGs reflects activities of this protein at the plasma membrane that potentially influence afferent signaling through the JAK/STAT kinase pathway (or accessory signaling pathways recruited downstream of the activated receptor), resulting in alteration of the

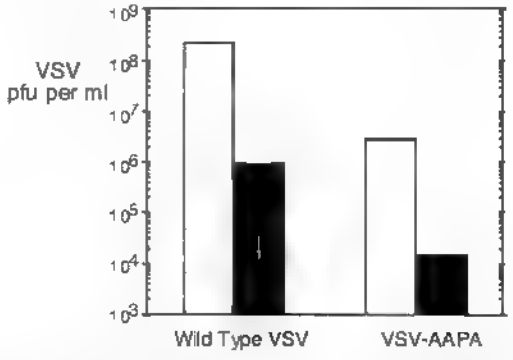

FIG. 9. Replication of VSV with a late-budding domain mutation (AAPA) in the M protein and wild type VSV were similarly inhibited by PLSCR1. KO2 (white bars) and KI (black bars) cells were infected with wild-type VSV and VSV-AAPA mutant virus (MOI of 0.1) for 16 h. The viral yields in the media combined from three separate infections of cells were determined by plaque assays on indicator cells.

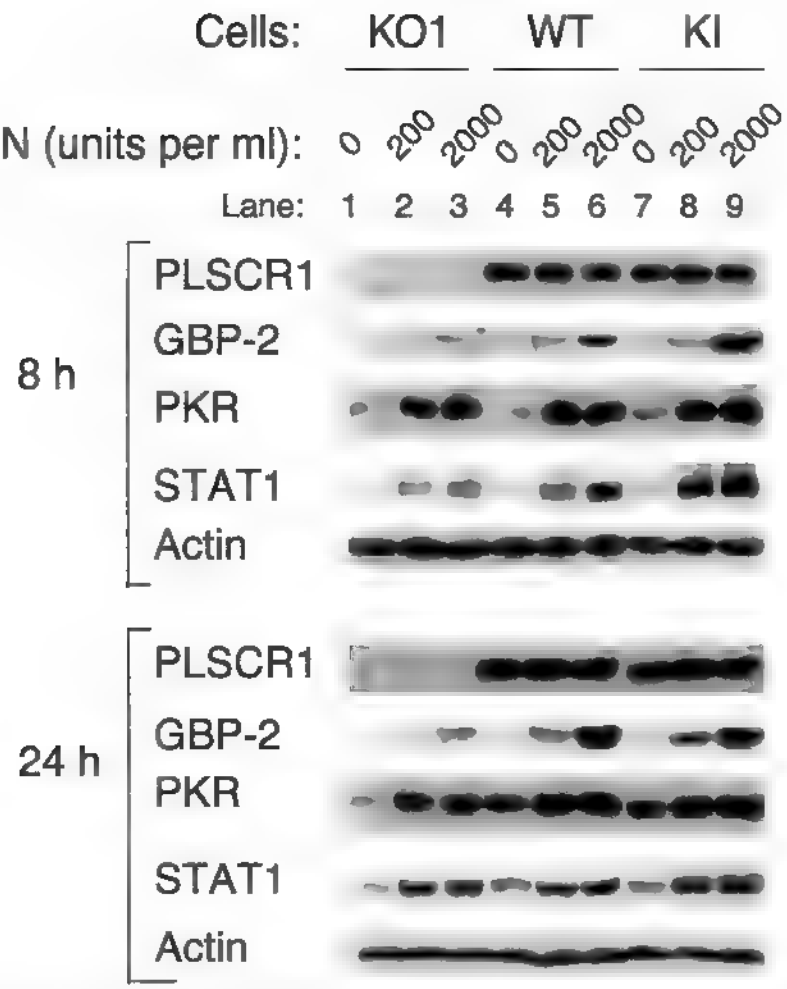

FIG. 10. IFN-induced and basal levels of PLSCR1, GBP-2, PKR, and Stat1 in IFN-treated and control MEFs that contain or lack PLSCR1. Cells were incubated for 8 or 24 h in the presence or absence of different concentrations of IFN-α A/D (as indicated). Cells harvested at 8 and 24 h were subconfluent and confluent, respectively. Western blots probed with antibodies to PLSCR1, GBP-2, PKR, and Stat1 are shown.

repertoire of activated transcription factors, and/or effects of nuclear PLSCR1 on the transcription of select ISGs.

Regarding the specific ISGs positively regulated by PLSCR1, the virus stress-inducible proteins p54 and p56 (encoded by ISG54 and ISG56, respectively) are related members of a protein family containing tetratricopeptide motifs (19). Protein p56 interacts with the protein synthesis initiation factor ε subunit of eukaryotic initiation factor 3 (eIF-3ε) and inhibits translation by interfering with the binding of eIF-2–GTP–Met-tRNA$_i$ (ternary complex) with eIF-3. Therefore, p56 has the ability to suppress translation of virus and host proteins. The functions of the other family members, p54, p58, and p60, are unknown. ISG15 contains two ubiquitin homology domains and is ligated to diverse proteins, including Jak1 and Stat1, and has been suggested to play a positive role in IFN signaling (26, 28). The NS1 protein of influenza B virus inhibits linkage of ISG15 to its target proteins, supporting an antiviral role for ISG15 (47). OAS2 is one of the upstream enzymes in the 2′,5′-oligoadenylates (2-5A)/RNase L antiviral pathway that synthesizes 2-5A in response to viral dsRNA. 2-5A activates RNase L, causing breakdown of viral and host RNA (36). RNase $L^{-/-}$ mice are partially deficient in the anti-EMCV effect of IFN-α (48). GBP-2 and GBP-3 are members of an IFN induced gene family of at least five different GBPs (31, 42). GBP-1 was shown to inhibit replication of VSV and EMCV, but the mechanism is unknown (1). Expression of PLSCR1 was also associated with enhanced basal expression of PKR in confluent, but not in subconfluent, mouse cells (Fig. 10). Therefore, PKR may also contribute to the observed antiviral effects of PLSCR1. PKR is activated by viral dsRNA to phosphorylate translation initiator factor eIF-2α, resulting in a cessation of protein synthesis. In addition, PKR is implicated in inhibiting VSV replication in mice (2). However, PLSCR1 did not affect IFN-induced levels of PKR. Expression of PLSCR1 was also associated with modestly enhanced expression of IRF7, which could potentially lead to IFN synthesis, thus further amplifying the antiviral response (Fig. 3) (27). The apparent enhancing effect of PLSCR1 on any particular gene was in the range of a 1.5- to >5-fold, with the combined effect on presumably several ISGs resulting in a significant negative impact on virus replication.

Effect of PLSCR1 on VSV replication. Although PLSCR1 appeared to enhance the expression of a number of genes, a direct effect of this protein on virus replication is also possible. Therefore, to determine how PLSCR1 was affecting VSV replication, we analyzed different stages in the virus cycle. The location of PLSCR1 in the cell membrane suggested a possible effect on virus adsorption and/or uptake. However, these steps in the virus replication cycles were unaffected by PLSCR1. In contrast, there was a substantial increase in primary (N) transcript accumulation in PLSCR1$^{-/-}$ (KO2) cells. Reduction in VSV primary transcript accumulation by IFN in either the absence or presence of PLSCR1 was substantial. The effect of PLSCR1 on VSV replication is superimposed on a larger IFN antiviral effect. As a result, we were unable to accurately determine whether the reduction by IFN in the two cell types was comparable. Our findings are consistent with a previous report demonstrating that IFN treatment affects VSV replication at the level of primary transcription (5). However, different studies localized the effect of IFN against VSV to other stages in the replication cycle, including protein synthesis (34) and virus assembly (22). Recently, it was demonstrated that IFN inhibits VSV entry into human epithelial cells by producing soluble secreted antiviral factors (S. Bose and A. K. Banerjee, unpublished data). Therefore, there are clearly cell-type-specific differences in the anti-VSV mechanism of IFNs. The present study does not rule out an effect on viral protein synthesis because it is difficult to measure an effect on protein synthesis when there is potent inhibition of viral primary transcription. IFN was able to reduce VSV primary transcript accumulation even in the PLSCR1$^{-/-}$ (KO2) cells, perhaps because the ISG(s) responsible for this effect was still induced, albeit to a lower extent than in the PLSCR1-positive KI cells (Fig. 7). Although expression of PLSCR1 was associated with modestly enhanced IFN-induction of OAS2 (encoding a 2-5A synthetase), there were no RNase L-mediated rRNA cleavage products in IFN-treated, VSV-infected KI cells (data not shown). Therefore, RNase L action against viral RNA is unlikely to be responsible for the decreased accumulation of VSV primary transcripts observed in the PLSCR1$^{-/-}$ cells (data not shown). The effect of PLSCR1 on a budding mutant of VSV was also investigated. The N-terminal, cytoplasmic domain of mPLSCR1 and hPLSCR1 contains PPXY motifs typical of WW-binding domains that could potentially interfere with virus budding. These motifs are similar to the PY motif or late-budding domain of the VSV M protein (PPPY) and of other members of the *Rhabdoviridae*, *Retroviridae*, and *Filoviridae* (18). VSV yields were compared from KO2 and KI cells infected with wild-type and mutant VSV in which the PPPY budding domain of the M protein was altered to AAPA to impair viral release (17, 23). However, yields of both wild-type and mutant VSV were similarly decreased in the KI cells compared with the KO2 cells (Fig. 9). These data suggest that, irrespective of any potential antiviral effect of PLSCR1 at the stage of virus assembly and budding from the plasma membrane, PLSCR1 must also exert an inhibitory or antiviral action prior to this terminal event in viral replication.

It was apparent from these studies that the observed antiviral effect of PLSCR1 extended beyond VSV. Replication of both VSV and EMCV were suppressed by expression of PLSCR1 in the human Hey1B cell line. In PLSCR1$^{-/-}$ MEFs, an antiviral effect of ectopically expressed PLSCR1 was observed against both VSV and the murine retrovirus Moloney murine leukemia virus (Fig. 5 and data not shown). While our results suggest that the broad antiviral effect mediated by PLSCR1 is related to enhanced expression of certain antiviral genes, the specific ISGs responsible for the inhibition of VSV, EMCV, and Moloney murine leukemia virus replication observed in this study are unknown. However, our findings indicate that PLSCR1 is an amplifying factor in the expression of certain critical antiviral genes that collectively have a large impact on virus growth. Furthermore, our gene array results provide a relatively short list of interesting candidate genes, some of which are responsible for potent inhibition of viral replication (Fig. 3). Exploring the specific functions of these genes targeted by PLSCR1 will be a new direction for investigating how IFNs protect cells against viral infections.

ACKNOWLEDGMENTS

We thank Ganes Sen, Ernest Borden (Cleveland, Ohio), and Deborah Vestal for gifts of antibodies and Jonathan Leis (Chicago, Ill.) and Xiaoxia Li (Cleveland, Ohio) for discussions.

This investigation was supported by grant CA89132 (to R.H.S. and P.J.S.) and grant P01 CA62220 (to B.R.G.W. and R.H.S.) from the National Cancer Institute, National Institutes of Health, by grant HL63819 (to P.J.S.) from the National Heart, Lung, and Blood Institute, National Institutes of Health, and by U.S. Army grant DAMD17-01-C-0065 (to B.R.G.W. and R.H.S.)

REFERENCES

1. **Anderson, S. L., J. M. Carton, J. Lou, L. Xing, and B. Y. Rubin.** 1999. Interferon-induced guanylate binding protein-1 (GBP-1) mediates an antiviral effect against vesicular stomatitis virus and encephalomyocarditis virus. Virology **256**:8–14.
2. **Balachandran, S., P. C. Roberts, L. E. Brown, H. Truong, A. K. Pattnaik, D. R. Archer, and G. N. Barber.** 2000. Essential role for the dsRNA-dependent protein kinase PKR in innate immunity to viral infection. Immunity **13**:129–141.
3. **Barenholz, Y., R. Pal, and R. R. Wagner.** 1993. Metabolic labeling of viral membrane lipids by fluorescent fatty acids: studying virus fusion with target membranes. Methods Enzymol. **220**:288–312.
4. **Baumal, R., J. Law, R. N. Buick, H. Kahn, H. Yeger, K. Sheldon, T. Colgan, and A. Marks.** 1986. Monoclonal antibodies to an epithelial ovarian adenocarcinoma: distinctive reactivity with xenografts of the original tumor and a cultured cell line. Cancer Res. **46**:3994–4000.
5. **Belkowski, L., and G. C. Sen.** 1987. Inhibition of vesicular stomatitis viral mRNA synthesis by interferons. J. Virol. **61**:653–660.
6. **Ben-Efraim, I., Q. Zhou, T. Wiedmer, L. Gerace, and P. J. Sims.** 2004. Phospholipid scramblase 1 (PLSCR1) is imported into the nucleus by a receptor-mediated pathway and interacts with DNA. Biochemistry **43**:3518–3526.
7. **Biron, C. A., and G. C. Sen.** 2001. Interferons and other cytokines, p. 321–351. *In* D. M. Knipe, P. M. Howley, D. E. Griffin, R. A. Lamb, M. A. Martin, B. Roizman, and S. E. Straus (ed.), Fields virology, 4th ed. Lippincott Williams & Wilkins, Philadelphia, Pa.
8. **Bose, S., M. Mathur, P. Bates, N. Joshi, and A. K. Banerjee.** 2003. Requirement for cyclophilin A for the replication of vesicular stomatitis virus New Jersey serotype. J. Gen. Virol. **84**:1687–1699.
9. **Bridge, A. J., S. Pebernard, A. Ducraux, A. L. Nicoulaz, and R. Iggo.** 2003. Induction of an interferon response by RNAi vectors in mammalian cells. Nat. Genet. **34**:263–264.
10. **Brummelkamp, T. R., R. Bernards, and R. Agami.** 2002. A system for stable expression of short interfering RNAs in mammalian cells. Science **296**:550–553.
11. **D'Cunha, J., S. Ramanujam, R. J. Wagner, P. L. Witt, E. Knight, Jr., and E. R. Borden.** 1996. In vitro and in vivo secretion of human ISG15, an IFN-induced immunomodulatory cytokine. J. Immunol. **157**:4100–4108.
12. **Der, S. D., A. Zhou, B. R. Williams, and R. H. Silverman.** 1998. Identification of genes differentially regulated by interferon alpha, beta, or gamma using oligonucleotide arrays. Proc. Natl. Acad. Sci. USA **95**:15623–15628.
13. **de Veer, M. J., M. Holko, M. Frevel, E. Walker, S. Der, J. M. Paranjape, R. H. Silverman, and B. R. Williams.** 2001. Functional classification of interferon-stimulated genes identified using microarrays. J. Leukoc. Biol. **69**:912–920.

14. **Fadeel, B., B. Gleiss, K. Hogstrand, J. Chandra, T. Wiedmer, P. J. Sims, J. I. Henter, S. Orrenius, and A. Samali.** 1999. Phosphatidylserine exposure during apoptosis is a cell-type-specific event and does not correlate with plasma membrane phospholipid scramblase expression. Biochem. Biophys. Res. Commun. **266**:504–511.
15. **Frevel, M. A., T. Bakheet, A. M. Silva, J. G. Hissong, K. S. Khabar, and B. R. Williams.** 2003. p38 mitogen-activated protein kinase-dependent and -independent signaling of mRNA stability of AU-rich element-containing transcripts. Mol. Cell. Biol. **23**:425–436.
16. **Guo, J., K. L. Peters, and G. C. Sen.** 2000. Induction of the human protein p56 by interferon, double-stranded RNA or virus infection. Virology **267**: 209–219.
17. **Harty, R. N., M. E. Brown, J. P. McGettigan, G. Wang, H. R. Jayakar, J. M. Huibregtse, M. A. Whitt, and M. J. Schnell.** 2001. Rhabdoviruses and the cellular ubiquitin-proteasome system: a budding interaction. J. Virol. **75**: 10623–10629.
18. **Harty, R. N., J. Paragas, M. Sudol, and P. Palese.** 1999. A proline-rich motif within the matrix protein of vesicular stomatitis virus and rabies virus interacts with WW domains of cellular proteins: implications for viral budding. J. Virol. **73**:2921–2929.
19. **Hui, D. J., C. R. Bhasker, W. C. Merrick, and G. C. Sen.** 2003. Viral stress-inducible protein p56 inhibits translation by blocking the interaction of eIF3 with the ternary complex eIF2.GTP.Met-tRNAi. J. Biol. Chem. **278**: 39477–39482.
20. **Hwang, L. N., N. Englund, T. Das, and A. K. Banerjee.** 1999. Optimal replication of vesicular stomatitis virus RNA polymerase require phosphorylation of a residue(s) at carboxy-terminal domain II of its accessory subunit, phosphoprotein P. J. Virol. **73**:5613–5620.
21. **Isaacs, A., and J. Lindenmann.** 1957. Virus interference. I. The interferon. Proc. R. Soc. Lond. B **147**:258–267.
22. **Jay, F. T., M. R. Dawood, and R. M. Friedman.** 1983. Interferon induces the production of membrane protein-deficient and infectivity-defective vesicular stomatitis virions through interference in the virion assembly process. J. Gen. Virol. **64**:707–712.
23. **Jayakar, H. R., K. G. Murti, and M. A. Whitt.** 2000. Mutations in the PPPY motif of vesicular stomatitis virus matrix protein reduce virus budding by inhibiting a late step in virion release. J. Virol. **74**:9818–9827.
24. **Kasukabe, T., H. Kobayashi, Y. Kaneko, J. Okabe-Kado, and Y. Honma.** 1998. Identity of human normal counterpart (MmTRA1b) of mouse leukemogenesis-associated gene (MmTRA1a) product as plasma membrane phospholipid scramblase and chromosome mapping of the human MmTRA1b/phospholipid scramblase gene. Biochem. Biophys. Res. Commun. **249**:449–455.
25. **Kasukabe, T., J. Okabe-Kado, and Y. Honma.** 1997. TRA1, a novel mRNA highly expressed in leukemogenic mouse monocytic sublines but not in non-leukemogenic sublines. Blood **89**:2975–2985.
26. **Kim, K. I., and D. E. Zhang.** 2003. ISG15, not just another ubiquitin-like protein. Biochem. Biophys. Res. Commun. **307**:431–434.
27. **Levy, D. E., I. Marie, E. Smith, and A. Prakash.** 2002. Enhancement and diversification of IFN induction by IRF-7-mediated positive feedback. J. Interferon Cytokine Res. **22**:87–93.
28. **Malakhova, O. A., M. Yan, M. P. Malakhov, Y. Yuan, K. J. Ritchie, K. I. Kim, L. F. Peterson, K. Shuai, and D. E. Zhang.** 2003. Protein ISGylation modulates the JAK-STAT signaling pathway. Genes Dev. **17**:455–460.
29. **Mathur, M., T. Das, and A. K. Banerjee.** 1996. Expression of L protein of vesicular stomatitis virus Indiana serotype from recombinant baculovirus in insect cells: requirement of a host factor(s) for its biological activity in vitro. J. Virol. **70**:2252–2259.
30. **Nanjundan, M., J. Sun, J. Zhao, Q. Zhou, P. J. Sims, and T. Wiedmer.** 2003. Plasma membrane phospholipid scramblase 1 promotes EGF-dependent activation of c-Src through the epidermal growth factor receptor. J. Biol. Chem. **278**:37413–37418.
31. **Nguyen, T. T., Y. Hu, D. P. Widney, R. A. Mar, and J. B. Smith.** 2002. Murine GBP-5, a new member of the murine guanylate-binding protein family, is coordinately regulated with other GBPs in vivo and in vitro. J. Interferon Cytokine Res. **22**:899–909.
32. **Pastorelli, C., J. Veiga, N. Charles, E. Voignier, H. Moussu, R. C. Monteiro, and M. Benhamou.** 2001. IgE receptor type I-dependent tyrosine phosphorylation of phospholipid scramblase. J. Biol. Chem. **276**:20407–20412.
33. **Pattnaik, A. K., and G. W. Wertz.** 1990. Replication and amplification of defective interfering particle RNAs of vesicular stomatitis virus in cells expressing viral proteins from vectors containing cloned cDNAs. J. Virol. **64**:2948–2957.
34. **Sahni, G., and C. E. Samuel.** 1986. Mechanism of interferon action. Expression of vesicular stomatitis virus G gene in transfected COS cells is inhibited by interferon at the level of protein synthesis. J. Biol. Chem. **261**:16764–16768.
35. **Sen, G. C.** 2001. Viruses and interferons. Annu. Rev. Microbiol. **55**:255–281.
36. **Silverman, R. H.** 2003. Implications for RNase L in prostate cancer biology. Biochemistry **42**:1805–1812.
37. **Silverman, R. H., A. Halloum, A. Zhou, B. Dong, F. Al-Zoghaibi, D. Kushner, Q. Zhou, J. Zhao, T. Wiedmer, and P. J. Sims.** 2002. Suppression of ovarian carcinoma cell growth in vivo by the interferon-inducible plasma membrane protein, phospholipid scramblase 1. Cancer Res. **62**:397–402.
38. **Sims, P. J., and T. Wiedmer.** 2001. Unraveling the mysteries of phospholipid scrambling. Thromb. Haemost. **86**:266–275.
39. **Sledz, C. A., M. Holko, M. J. de Veer, R. H. Silverman, and B. R. Williams.** 2003. Activation of the interferon system by short-interfering RNAs. Nat. Cell Biol. **5**:834–839.
40. **Sun, J., M. Nanjundan, L. J. Pike, T. Wiedmer, and P. J. Sims.** 2002. Plasma membrane phospholipid scramblase 1 is enriched in lipid rafts and interacts with the epidermal growth factor receptor. Biochemistry **41**:6338–6345.
41. **Sun, J., J. Zhao, M. A. Schwartz, J. Y. Wang, T. Wiedmer, and P. J. Sims.** 2001. c-Abl tyrosine kinase binds and phosphorylates phospholipid scramblase 1. J. Biol. Chem. **276**:28984–28990.
42. **Vestal, D. J., V. Y. Gorbacheva, and G. C. Sen.** 2000. Different subcellular localizations for the related interferon-induced GTPases, mGBP-1 and mGDP-2: implications for different functions? J. Interferon Cytokine Res. **20**:991–1000.
43. **Wang, E., L. D. Miller, G. A. Ohnmacht, E. T. Liu, and F. M. Marincola.** 2000. High-fidelity mRNA amplification for gene profiling. Nat. Biotechnol. **18**:457–459.
44. **Wiedmer, T., J. Zhao, M. Nanjundan, and P. J. Sims.** 2003. Palmitoylation of phospholipid scramblase 1 controls its distribution between nucleus and plasma membrane. Biochemistry **42**:1227–12233.
45. **Xiang, Y., R. C. Condit, S. Vijaysri, B. Jacobs, B. R. G. Williams, and R. H. Silverman.** 2002. Blockade of interferon induction and action by the E3L double-stranded RNA binding proteins of vaccinia virus. J. Virol. **76**:5251–5259.
46. **Yokoyama, A., T. Yamashita, E. Shiozawa, A. Nagasawa, J. Okabe-Kado, T. Nakamaki, S. Tomoyasu, F. Kimura, K. Motoyoshi, Y. Honma, and T. Kasukabe.** 2004. MmTRA1b/phospholipid scramblase 1 gene expression is a new prognostic factor for acute myelogenous leukemia. Leuk. Res. **28**:149–157.
47. **Yuan, W., and R. M. Krug.** 2001. Influenza B virus NS1 protein inhibits conjugation of the interferon (IFN)-induced ubiquitin-like ISG15 protein. EMBO J. **20**:362–371.
48. **Zhou, A., J. M. Paranjape, S. D. Der, B. R. Williams, and R. H. Silverman.** 1999. Interferon action in triply deficient mice reveals the existence of alternative antiviral pathways. Virology **258**:435–440.
49. **Zhou, Q., J. Zhao, F. Al-Zoghaibi, A. Zhou, T. Wiedmer, R. H. Silverman, and P. J. Sims.** 2000. Transcriptional control of the human plasma membrane phospholipid scramblase 1 gene is mediated by interferon-alpha. Blood **95**:2593–2599.
50. **Zhou, Q., J. Zhao, J. G. Stout, R. A. Luhm, T. Wiedmer, and P. J. Sims.** 1997. Molecular cloning of human plasma membrane phospholipid scramblase. A protein mediating transbilayer movement of plasma membrane phospholipids. J. Biol. Chem. **272**:18240–18244.
51. **Zhou, Q., J. Zhao, T. Wiedmer, and P. J. Sims.** 2002. Normal hemostasis but defective hematopoietic response to growth factors in mice deficient in phospholipid scramblase 1. Blood **99**:4030–4038.

BMC Microbiology

BioMed Central

Research article

Open Access

Flagellin acting via TLR5 is the major activator of key signaling pathways leading to NF-κB and proinflammatory gene program activation in intestinal epithelial cells

Thomas Tallant[†1], Amitabha Deb[†1,2], Niladri Kar[1], Joseph Lupica[1], Michael J de Veer[1,3] and Joseph A DiDonato*[1]

Address [1]Deparment of Cancer Biology The Lerner Research Institute at the Cleveland Clinic Foundation 9500 Euclid Avenue. Cleveland, OH 44195, USA, [2]Amitabha Deb Massachusetts Biologics Labs, University of Massachusetts Medical School, 305 South Street, Jamaica Plain, MA 02130-3597, USA and [3]Michael de Veer, Centre for Animal Biotech Department of Veterinary Science, Melbourne University, Parkville, Victoria, 3010, Australia

Email: Thomas Tallant - tallant@ccf.org; Amitabha Deb - amitabha.deb@usmed.edu, Niladri Kar - karn@ccf.org; Joseph Lupica - lupicaj@ccf.org; Michael J de Veer - mdeveer@unimelb.edu.au, Joseph A DiDonato* - didonaj@ccf.org

* Corresponding author †Equal contributors

Published: 23 August 2004

BMC Microbiology 2004, 4:33 doi:10.1186/1471-2180-4-33

Received: 06 May 2004

Accepted: 23 August 2004

This article is available from: http://www.biomedcentral.com/1471-2180/4/33

Abstract

Background: Infection of intestinal epithelial cells by pathogenic *Salmonella* leads to activation of signaling cascades that ultimately initiate the proinflammatory gene program. The transcription factor NF-κB is a key regulator/activator of this gene program and is potently activated. We explored the mechanism by which *Salmonella* activates NF-κB during infection of cultured intestinal epithelial cells and found that flagellin produced by the bacteria and contained on them leads to NF-κB activation in all the cells; invasion of cells by the bacteria is not required to activate NF-κB.

Results: Purified flagellin activated the mitogen activated protein kinase (MAPK), stress-activated protein kinase (SAPK) and Ikappa B kinase (IKK) signaling pathways that lead to expression of the proinflammatory gene program in a temporal fashion nearly identical to that of infection of intestinal epithelial cells by *Salmonella*. Flagellin expression was required for *Salmonella* invasion of host cells and it activated NF-κB via toll-like receptor 5 (TLR5). Surprisingly, a number of cell lines found to be unresponsive to flagellin express TLR5 and expression of exogenous TLR5 in these cells induces NF-κB activity in response to flagellin challenge although not robustly. Conversely, overexpression of dominant-negative TLR5 alleles only partially blocks NF-κB activation by flagellin. These observations are consistent with the possibility of either a very stable TLR5 signaling complex, the existence of a low abundance flagellin co-receptor or required adapter, or both.

Conclusion: These collective results provide the evidence that flagellin acts as the main determinant of *Salmonella* mediated NF-κB and proinflammatory signaling and gene activation by this flagellated pathogen. In addition, expression of the *fli C* gene appears to play an important role in the proper functioning of the TTSS since mutants that fail to express *fli C* are defective in expressing a subset of Sip proteins and fail to invade host cells. Flagellin added in *trans* cannot restore the ability of the *fli C* mutant bacteria to invade intestinal epithelial cells. Lastly, TLR5 expression in weak and non-responding cells indicates that additional factors may be required for efficient signal propagation in response to flagellin recognition.

Background

Intestinal epithelial cells serve as a barrier between the luminal microflora and the body and as such are perfectly positioned to monitor the approach/invasion of pathogens. These intestinal epithelial cells (IECs) serve as innate immune sentinels and monitor their environment and constantly give out innate host defense instruction to local immune effector cells [1,2]. Pathogens such as *Salmonella* and other enteroinvasive pathogenic bacteria such as enteroinvasive *E. Coli*, *Shigella* and *Yersinia* upon infection of IECs leads to the up-regulation of the expression of host genes, the products of which activate mucosal inflammatory and immune responses and alter epithelial cell functions [3-6]. Previously we and others demonstrated that IKK via NF-κB and the SAPK signaling pathways via Jun N-terminal kinase (JNK) and p38 kinase were key regulators of the up-regulation of the proinflammatory gene program [3,7-9], with NF-κB appearing to be the most critical [3]. Typically *Salmonella* infects thirty-forty percent of IECs in culture models of infection [10], however, we and others have found that *Salmonella* infection activates NF-κB DNA binding activity to levels equivalent to that of TNFα which activates NF-κB in all of the cells [3]. Previous studies examining NF κB activation by *Salmonella* in HT29 colonic intestinal epithelial cells, which serve as model colonic epithelial cells in culture, indicated that delivery of *Salmonella* proteins into the host cell via its type III secretion system (TTSS), such as SopE and SopE2, the bacterially encoded exchange factors for the Rho-family members Rac1 and CdC42, result in exchange factor activation, cytoskeletal rearrangements and activation of the MAPK, SAPK and NF-κB signaling pathways [7,8,11-15]. Recent observations that utilized *Salmonella* strains that were defective in invasion and delivery of invasion proteins by the TTSS but not attachment indicated that additional factors other than those delivered by the TTSS could lead to NF-κB activation [16] Presently it is not clear what protein(s) dictate the activation of key signaling pathways that lead to the temporal expression of the proinflammatory gene program, although the SopE proteins have been given extreme attention recently [7,8,15]

In searching for additional *Salmonella* proteins that could activate the proinflammatory gene expression program, bacterial flagellin was recently found to be such a protein [16-19] and had been shown previously to activate IL-8 expression in monocytes [19-21]. Flagellin was found to activate NF-κB in polarized epithelial cells only when flagellin was present on their basolateral surface [22] consistent with the idea that a cell surface receptor was present there and could recognize it. The toll-like receptors (TLRs) have been found to recognize pathogen associated molecular patterns (PAMPs) reviewed in [23-26]. TLR2 interacts with TLR1 and TLR6 to recognize bacterial lipopeptides and zymosan respectively [27,28]. TLR4 recognizes LPS only when associated with its co-receptor MD2 and CD14 [29-32] Recently, flagellin was demonstrated to be recognized by TLR5 and activate an innate host response [22,33]. However, little was known or demonstrated about the endogenous levels of TLR5 in cells used in those studies and why those cells failed to respond to flagellin. Here we have identified flagellin as the primary initiator and temporal regulator of not only the major signaling pathways activated during *Salmonella* infection but also of key target genes of the proinflammatory gene program too. We have also found flagellin expression to be required for *Salmonella* bacterial invasion. Independently we found TLR5 recognizes flagellin but its signaling activity toward this PAMP is consistent with either the aid of another flagellin-recognizing co-receptor (as TLR4 utilizes for LPS) or the use of another adapter protein, perhaps similar to MyD88, that is absent or present at low levels in flagellin non-or low-responding cells

Results

Salmonella infection leads to a minority of cells invaded but activates NF-κB in nearly all cells

Previously, we have noted that pathogenic *Salmonella sp.* infection leads to potent IKK and NF-κB activation and activation of the proinflammatory gene program [3]. Previous studies suggest that about thirty-forty percent of the intestinal epithelial cells are infected during a typical *Salmonella* infection in cultured intestinal epithelial cells [10] We wished to address the question of how bacterial infection of about thirty percent of the host cells could give rise to NF-κB DNA binding activity equivalent to activation of NF-κB in nearly all of the host cells as TNFα treatment of the cells does. To examine this phenomenon in detail HT29 cells either mock-infected or infected at a MOI of fifty for one-hour with wild-type *S. typhimurium* that had been transformed with the plasmid pFM10.1, that encodes green fluorescent protein (GFP) under the control of the *Salmonella* ssaH promoter and only functions once the bacteria has invaded the host cell [34]. As can be seen in Fig. 1A, GFP expression occurs in about thirty to forty percent of the cells. We next examined the localization of the NF-κB subunit p65 (RelA) in non-treated (mock-infected), *Salmonella* infected or TNFα (10 ng/ml) stimulated cells and found that p65 (RelA) was localized to the cytoplasm in non-treated cells whereas, in *Salmonella* infected cells or in TNFα treated cells p65 (RelA) had localized to the nucleus (Fig. 1B). These results demonstrate that *Salmonella* infection activates NF-κB in virtually all of the cells even though only a minority of them become infected and is consistent with and aids in explanation of our previous results examining *Salmonella* infection and NF-κB activation [3].

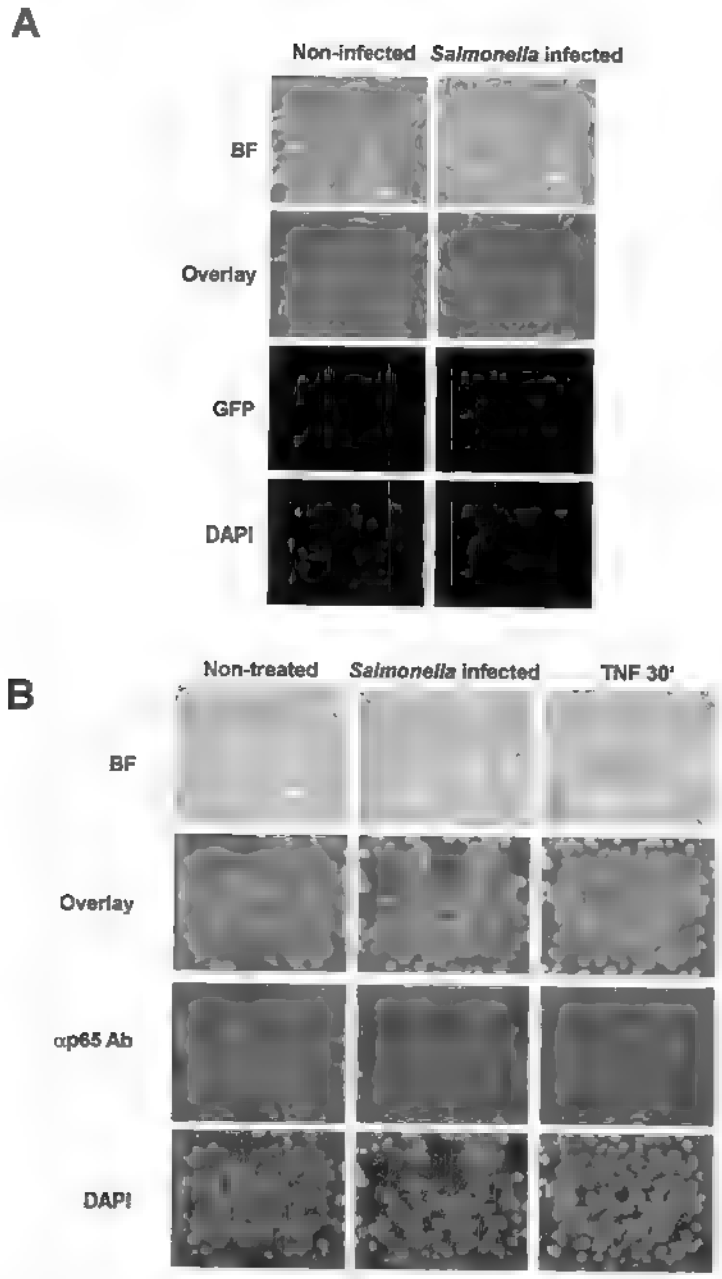

Figure 1

Salmonella infection leads to NF-κB nuclear localization even in non-infected cells HT29 cells were grown on glass coverslips and either mock-infected, left untreated, infected with *Salmonella typhimurium*, or treated with TNFα (10 ng/ml) Cells fixed after 30 min (TNF) and 1 h (*Salmonella*) as described in Experimental Procedures and *Salmonella* that had invaded HT29 cells were detected by direct fluorescence microscopy of GFP expression, p65(RelA) localization was monitored by indirect immunofluorescence of rabbit anti-p65 antibody detected with FITC-conjugated donkey anti-rabbit antibody. DAPI was used to stain nuclei. A, HT29 cells were mock-infected or infected at an MOI of 50 with *Salmonella typhimurium* strain SJW1103G which expresses GFP from the ssaH promoter that is only active inside infected host cells [10,34]. Cells were photographed using bright field microscopy (BF), and immunofluorescence to detect GFP or DAPI staining as indicated. Images were merged (overlay) to reveal cells that were infected. B, HT29 cells were left untreated, infected with *Salmonella typhimurium* strain 1103 or treated with TNFα. NF-κB p65(RelA) localization under various conditions as indicated was monitored by indirect immunofluorescence. Cells were visualized by bright field microscopy (BF), cell nuclei were stained with DAPI and p65(RelA) was visualized with FITC. DAPI staining was falsely colored red to make visualization of the merge (overlay) easier to distinguish.

Soluble bacterial product identified as flagellin can activate NF-κB in intestinal epithelial cells

Since *Salmonella sp.* infection of intestinal epithelial cells in culture led to only roughly thirty percent infection but activation of NF-κB in nearly all of the cells, we anticipated that NF-κB activation was in response to host cell recognition of bacteria structural components or products produced by the bacteria and not by the invasion process. Invasion itself has been demonstrated not to be required for activation of the proinflamatory gene program as had previously been thought [16]. To investigate this possibility sterile-filtered *S dublin* culture broth left either untreated or boiled for twenty minutes was used to challenge HT29 intestinal epithelial cells and NF-κB DNA binding activity was monitored by electromobility shift assays (EMSAs) of whole cell extracts (WCE) prepared forty five minutes after exposure [3,35]. Potent activation of NF-κB in response to the broth under both conditions was observed indicating the activating factor was heat stable (AD, TT and JD, personal observations) and is not LPS since HT29 cells are not responsive to LPS [3,35]

The native sterile-filtered concentrated broth was subsequently treated with DNase, RNase, proteinase K or crudely size fractionated on 100 kDa centricon filters The variously treated broths were then used to challenge HT29 intestinal epithelial cells and WCEs were prepared after forty five minutes and NF-κB DNA binding activity was analyzed by EMSA (Fig 2A). Direct infection of HT29 cells by *S. typhimurium* 1103 or exposure to the culture broths (supt), as indicated, induced NF-κB DNA binding activity, while the activity-inducing factor was found to be sensitive to protease digestion and was retained by a 100 kDa filter (Fig. 2A). To further determine the identity of the NF-κB inducing activity, sterile filtered concentrated broth culture was fractionated by Superose 12 gel permeation chromatography (Fig. 2B) and by anion exchange chromatography (Fig. 2C). Aliquots of chromatography fractions were assayed for their ability to activate NF-κB in HT29 cells and analyzed by EMSA. As can be seen from the Coomassie blue stained gel (Fig. 2B, top panel) increased NF-κB DNA binding activity (Fig. 2B, lower panel lanes 4–6) corresponded to the increased abundance of an approximately 55 kDa protein. Anion exchange chromatography on POROS HQ matrix and elution of bound proteins with an increasing salt gradient as indicated (Fig. 2C) demonstrated that NF-κB DNA binding-inducing activity corresponded to chromatographic fractions containing an increased abundance of the 55 kDa protein (Fig. 2C top panel, and data not shown). Eluted fractions observed in Fig. 2C were concentrated and fractionated on preparative 12% SDS-PAGE gels and bands corresponding to B1-B6 were cut from the gels and the proteins eluted, precipitated and renatured as described in Experimental Procedures and used to stimulate HT29 cells. Whole cell extracts from these cells were assayed for NF-κB DNA binding-inducing activity by EMSA and only band 2 (B2) corresponding to the 55 kDa protein (Fig. 2C lower panel) was able to elicit NF κB DNA binding activity while buffer from the beginning or end of the salt gradient failed to activate NF-κB DNA binding activity.

Proteins corresponding to protein bands B1-B6 and blank areas of the gel were further processed for peptide sequencing as described in Experimental Procedures. Trypsin digestion of the protein corresponding to B2 and analysis by electrospray ion trap LC/MS identified the amino acid sequence of twenty-one peptides. Flagellin (seventy-five percent coverage by the twenty-one peptides) was unambiguously identified as the protein consistent with inducing NF-κB DNA binding activity (Fig 3)

Flagellin is required to activate NF-κB in intestinal epithelial cells

To determine if flagellin was indeed the factor that was responsible for triggering activation of NF-κB after exposure of intestinal epithelial cells to direct bacterial infection or to filtered culture broths of pathogenic *Salmonella sp* we prepared infectious bacteria and boiled and filtered culture broths from the non-flagellated E. Coli DH5α, pathogenic *S. dublin* strain 2229, an isogenic *S. dublin* 2229 SopE⁻ mutant, isogenic *S. dublin* 2229 SopB⁻ mutant, isogenic *S. dublin* 2229 double SopE⁻/SopB⁻ mutant (strain SE1SB2), *S. typhimurium* strain 1103, and isogenic *S. typhimurium* fliC⁻ Tn*10* insertion mutant (strain 86) and a *S. typhimurium* 1103 isogenic double mutant fliC⁻/fljB⁻ and were used to challenge HT29 cells. Bacteria and culture broths were used to challenge HT29 intestinal epithelial cells and WCE extracts were prepared after forty-five minutes and analyzed for NF-κB DNA binding activity by EMSA. *Salmonella* strains could activate NF-κB, while *Salmonella* strains failing to produce flagellin (fliC and fliC⁻/fljB⁻ mutants as indicated) also failed to activate NF-κB (Fig. 4A &4B). *E. Coli* DH5α is non-flagellated and does not produce flagellin failed to activate NF-κB. We also noticed through numerous experiments that *S. dublin* direct infections always activated NF-κB to a greater extent than *S. typhimurium* as observed in Fig. 4A while culture broths from both species activated NF-κB almost equally well (Fig. 4B) We believe this difference is due perhaps to *S. dublin* releasing more flagellin into the cell culture media than *S. typhimurium* during infection since purification of flagellin from both *S. dublin* and *S. typhimurium* and addition of equivalent amounts of chromatographically purified flagellin gave similar NF-κB activation profiles (TT & JD, unpublished observations).

Of note is the total failure of the double flagellin gene mutants to activate NF-κB as compared to the very minor

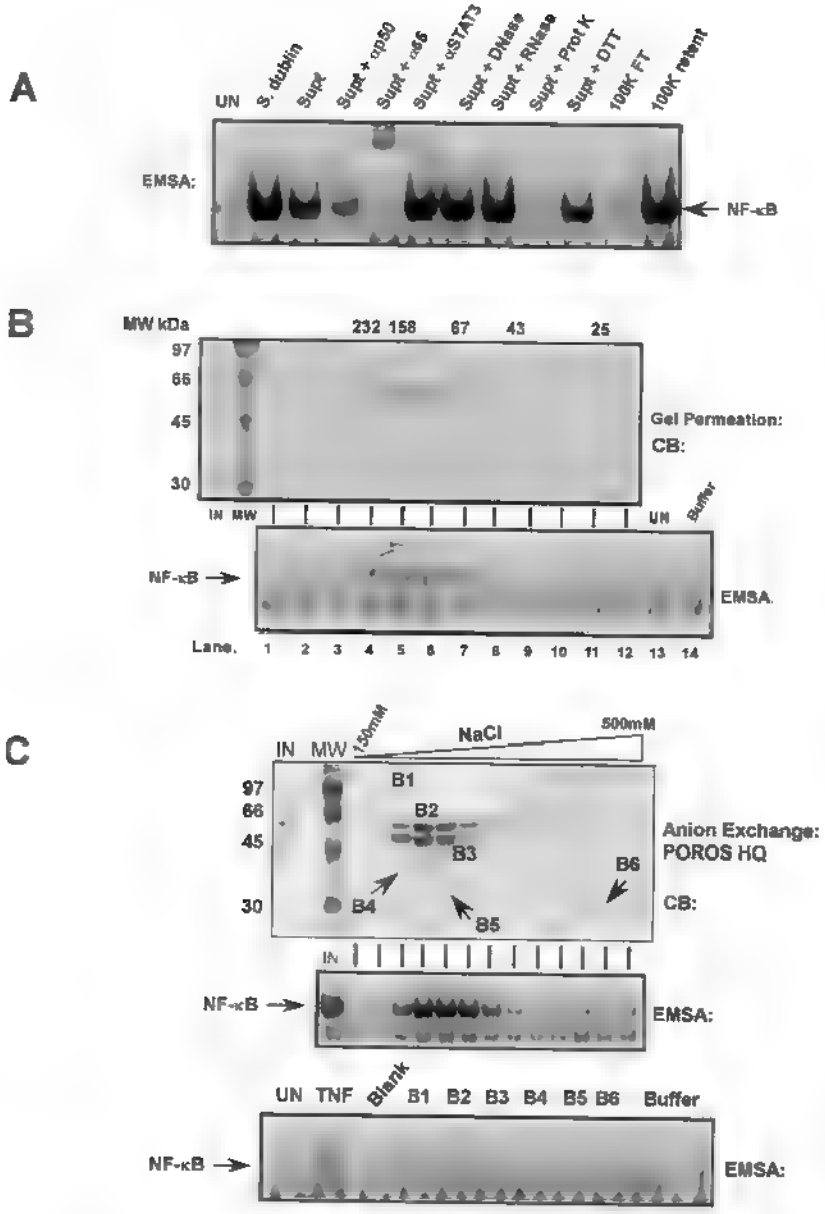

Figure 2

Protein factor in *Salmonella* culture broth leads to NF-κB activation. A, *Salmonella dublin* culture broth concentrated 100-fold was treated as indicated or infectious bacteria, as indicated was used to challenge HT29 cells. NF-κB DNA binding activity was assayed by EMSA from whole cell extracts prepared 45 min after treatment. Authenticity of the NF-κB DNA:protein complex was determined using p65(RelA)-specific and p50-specific antibody supershifts B, Concentrated *Salmonella dublin* culture broth (IN) was chromatographed by gel permeation on a Superose 12 column. Eluted protein fractions were analyzed by fractionation on 10% SDS-PAGE and visualized by Coomassie blue (CB) staining. Molecular weight markers for chromatography and on the gels are indicated Aliquots of each fraction as indicated was used to stimulate HT29 cells and resultant WCEs were analyzed by EMSA for NF-κB DNA binding activity. C, Concentrated *Salmonella dublin* culture broth (IN) was chromatographed by anion exchange chromatography on POROS HQ matrix. Proteins were eluted with an increasing NaCl gradient as indicated and analyzed on 10% SDS-PAGE and visualized by Coomassie blue (CB) staining. Input and aliquots of each fraction as indicated was used to stimulate HT29 cells and resultant WCEs were analyzed by EMSA for NF-κB DNA binding activity Eluted material corresponding to protein bands B1-B6, a blank portion of the gel was isolated from a duplicate 10% SDS-PAGE gel as described in Experimental Procedures along with buffer samples from the beginning and end NaCl buffer gradient and used to stimulate HT29 cells and resultant WCEs were analyzed by EMSA for NF-κB DNA binding activity.

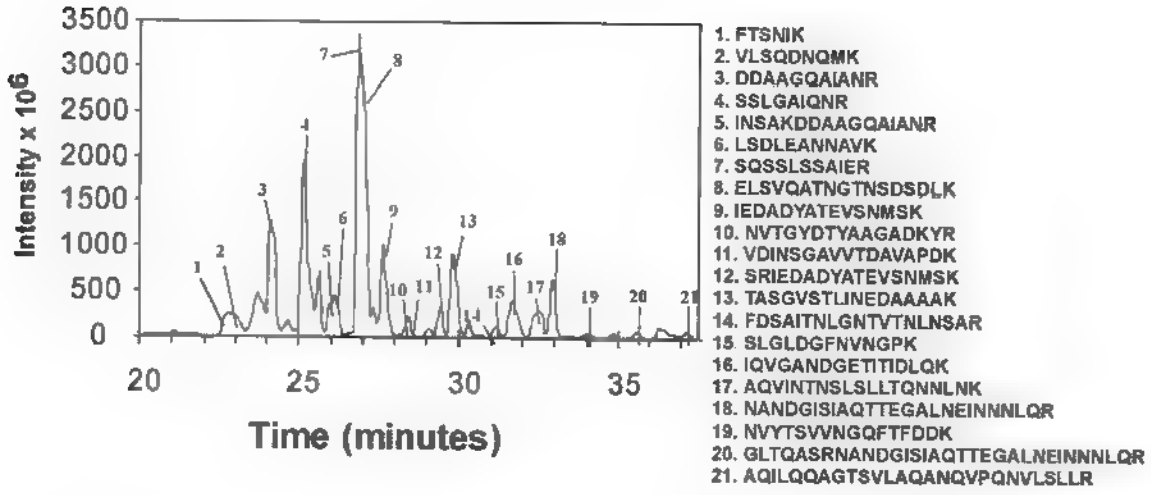

Figure 3
Identifcation by mass spectrometry of flagellin as the NF-κB activating factor in *Salmonella* culture broth. Microcapillary HPLC tandem mass spectrometry of Band 2 digested by trypsin. Peaks corresponding to *Salmonella* peptides are numbered and identified with the corresponding numbered peptide sequence to the right.

activation observed in the single Phase I flagellin fliC..Tn*10* insertion mutant (next to last lanes in Fig. 4A &4B) which likely is due to the extremely limited expression of the phase II flagellin (from fljB), although the strains of *Salmonella* used here genetically are unable or rarely shift phases of flagellin production. These results are consistent with previous reports identifying flagellin as a potent inducer of the proinflammatory response and IL-8 production [16-19]. Since flagellin appears required for activation of the NF-κB pathway upon direct infection of intestinal epithelial cells it appeared possible that flagellin may also be the major determinant of other major mitogenic and stress activated signaling pathways activated upon pathogenic *Salmonella* infection of intestinal epithelial cells. Previously others and we have demonstrated that direct *Salmonella* infection of intestinal epithelial cells results in JNK activation [8] and also the activation of NF-κB via IKK [3]. The identification of flagellin as a potent NF-κB activator is significant since SopE had previously been shown to be a pathogenic *Salmonella* bacteriophage encoded protein that is injected into the host cell and acts as an exchange factor for the small Rho GTPases Rac1 and CdC42 initiating cytoskeleton rearrangements and eventual activation of the MAPK, SAPK and NF-κB pathways [7,15], while SopB is a *Salmonella* protein that functions as an inositol phosphate phosphatase and participates in cytoskeletal rearrangements and stimulates host cell chloride secretion [36].

Flagellin triggers activation of the mitogen activated protein kinase, stress activated protein kinase and IKK signaling pathways

Intestinal epithelial cells act as sentinels for invasion of luminal surfaces and orchestrate the attraction of effector immune cells to the area by production of chemokine genes like IL-8 and macrophage chemoattractant protein 1 (MCP1) proinflammatory cytokine genes such as TNFα, IL-1 and IL-6 [1,4-6]. Expression of these genes primarily depends upon the action of transcription factors that are activated in response to the transmission of signals via the MAPK, SAPK and IKK signaling pathways. Since NF-κB is considered a central regulator/activator of the proinflammatory gene program we decided to examine the effect that non-flagellin producing mutant strains of *Salmonella* had on activation of the MAPK, SAPK and IKK signaling pathways compared to infection of intestinal epithelial cells with wild-type *Salmonella* or by exposure of the intestinal epithelial cells to purified flagellin. Infection of HT29 cells with wild-type *S. typhimurium* resulted in activation of MAPKs ERK1&2, the SAPKs p38, JNK and IKK (Fig. 5) as determined by use of activation-indicating phospho-specific antibodies in immunoblot (IB) analysis or antibody-specific immuno kinase assays (KA) for JNK and IKK using their respective substrates GST-cJun 1–79 and GST-IκBα1–54 [37-39]. Interestingly, MAPK stimulation is transient in nature as activation declines beginning at forty-five minutes while p38, JNK and IKK activity

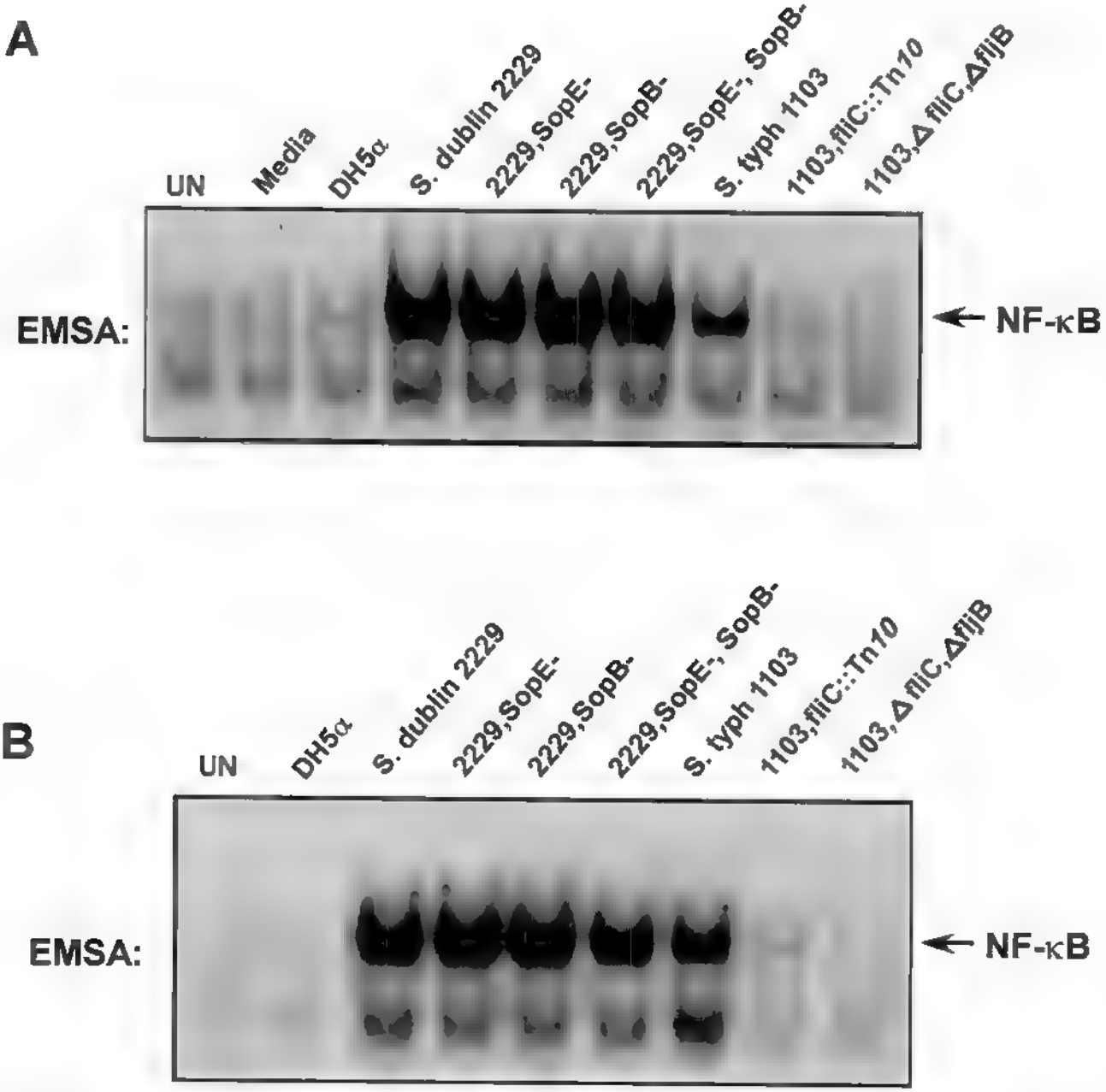

Figure 4
Flagellin mutants fail to activate NF-κB. EMSAs assaying for NF-κB DNA binding activity in WCEs prepared 45 min from non-infected cells (UN) and after direct infection of HT29 cells with wild-type *E. coli* DH5α, wild-type *Salmonella dublin* or SopE⁻ mutant, SopB⁻ mutant, the SopE⁻/SopB⁻ double mutant, wild-type *Salmonella typhimurium* strain 1103, the fliC⁻ mutant (fliC::Tn*10*), the fliC⁻/fljB⁻ double mutant as indicated at an MOI of 50. B, EMSAs assaying for NF-κB DNA binding activity in WCEs prepared 45 min after challenge of HT29 cells from non-infected cells (UN) or with sterile-filtered concentrated culture broths from wild-type and mutant bacteria as indicated.

increases with time through one hour. As seen in Fig. 4, the fliC⁻/fljB double mutant *Salmonella* also failed to induce IKK and NF-κB activity (Fig. 5 as indicated). Surprisingly, the fliC⁻/fljB double mutant *Salmonella* failed to

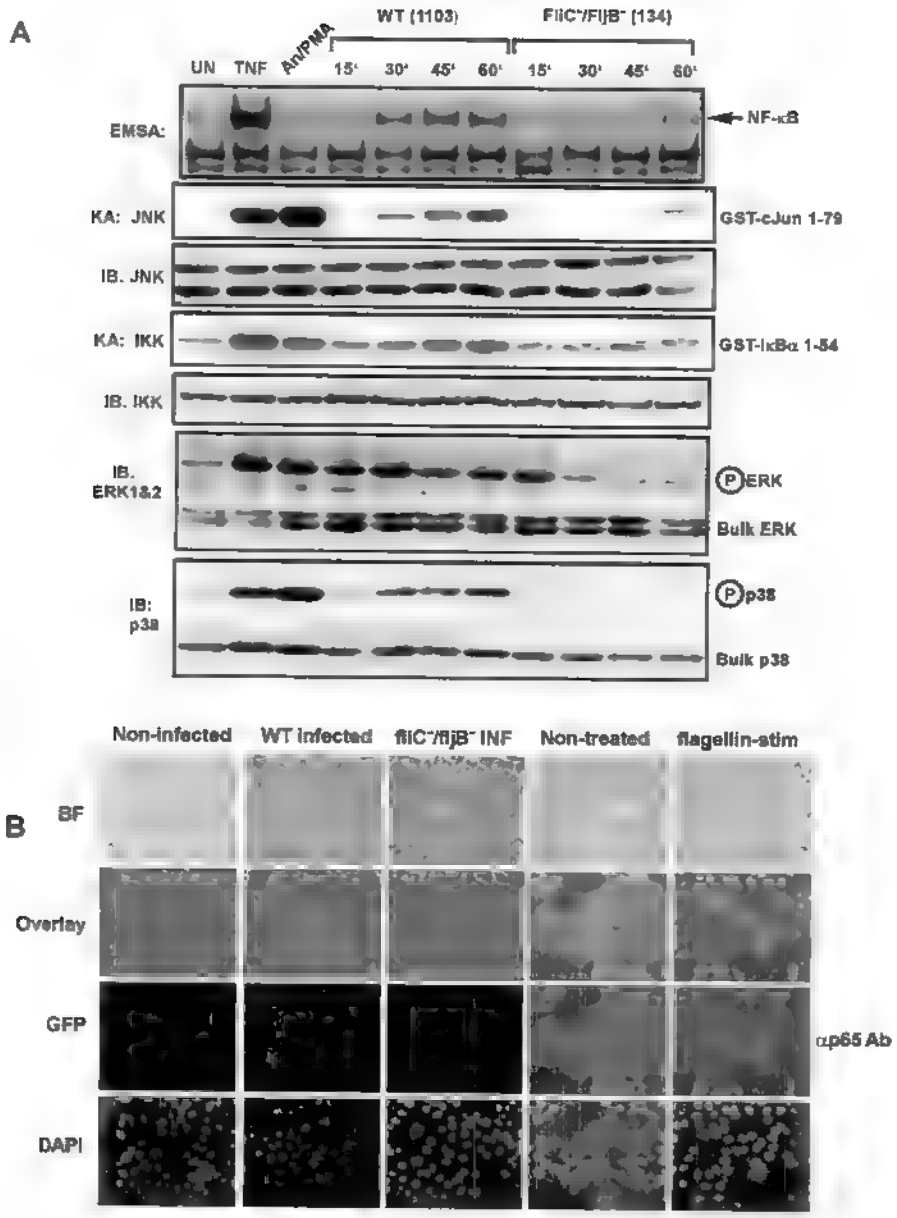

Figure 5

Flagellin is required for activating multiple signaling pathways during *Salmonella* infection and leads to nuclear localization of NF-κB. HT29 cells were left untreated, stimulated with TNFα (10 ng/ml) or a cocktail of anisomycin [An] (20 μg/ml)/PMA (12.5 ng/ml) for 15 min, or infected with either wild-type (WT) *Salmonella typhimurium* strain 1103 or the *Salmonella typhimurium* double fliC⁻/fljB⁻ mutant strain 134 as indicated. WCE were prepared at the indicated times or at 10 min for TNF-treated cells or 15 min for anisomycin/PMA treated cells and used in EMSAs to analyze NF-κB DNA binding activity, or in immuno-kinase assays (KA) using anti-IKK or anti-JNK antibodies to measure IKK and JNK kinase activity on their respective substrates GST-IκBα 1–54 and GST-cJun 1–79 (as indicated). Immunoblot (IB) analysis of equivalent amounts (40 μg) of protein from each extract was fractionated on SDS-PAGE gels and transferred to PVDF membranes and probed with the indicated antibodies to detect bulk IKK, JNK, ERK and p38 as indicated. Immunoblot analysis using phospho-specific antibodies for ERK and p38 to detect activated ERK and p38 are indicated B, Immunofluorescence demonstrating that flagellin mutant Salmonella fail to infect HT29 cells and that purified flagellin stimulation of HT29 cells leads to NF-κB nuclear p65 (RelA) localization as determined by indirect immunofluorescence. Imaging of the treatment indicated HT29 cells grown on coverslips was essentially the same as in Fig. 1A & 1B. False coloring of the DAPI stain was used to enhance the visualization of both DAPI stained nuclei and p65 nuclear localization.

induce the SAPKs p38 and JNK and only briefly (fifteen minutes) activated MAPK. This result is puzzling since other *Salmonella* proteins such as SopE and SopE2 can activate the small GTPases Rac and CdC42, and these Rho family GTPases have been linked to JNK and p38 activation [7,8,14,15] yet appear not to function in the flagellin minus strain.

The fliC /fljB- double mutant *Salmonella* failed to invade HT29 cells compared to the wild-type *Salmonella* strain as determined by gentamycin protection/invasion assay (see Experimental Procedures). The flagellin fliC-/fljB- double mutant displayed a four orders of magnitude difference in its ability to invade HT29 cells (TT & JD, unpublished observations). To demonstrate this point further, we infected HT29 cells with either wild type *Salmonella* or the fliC /fljB- double mutant *Salmonella* (strain 134), both strains were transformed with the plasmid pFM10.1 that encodes GFP under the control of the Salmonella ssaH promoter and only functions once the bacteria has invaded the host cell [10,34]. The wild type *Salmonella* clearly was able to infect HT29 cells (GFP, Fig. 5B) while the flagellin mutant bacteria failed to invade HT29 cells as evidenced by the lack of GFP expression (Fig. 5B). To determine if flagellin is sufficient or that other bacterially produced proteins are required for invasion, we added either purified flagellin or sterile-filtered culture broths or a combination of both to HT29 cells that were challenged with the *Salmonella* fliC-/fljB- double mutant and assayed for invasion. Intestinal epithelial cells failed to be invaded using all tested combinations of purified flagellin and/or culture broths with the fliC /fljB- double mutant strain (TT & JD, unpublished observations). To our knowledge there is no known direct connection between expression of flagellin genes and the effectiveness of the type III secretion system to deliver bacterially produced proteins such as SopE, SopE2 and SipA or other Sip or Sop proteins [7,14,15,40,41] that play important roles in initiating bacterial internalization. Furthermore, to evaluate the effectiveness of flagellin to stimulate p65 (RelA) nuclear localization in intestinal epithelial cells we challenged HT29 cells with purified flagellin and examined p65 (RelA) localization using indirect immunofluorescence and found p65 (RelA) nuclear localization in nearly every cell (Fig. 5B as indicated).

Purified flagellin (0.5 μg/ml) was added to the culture media of HT29 cells and WCE were prepared at various times as indicated after exposure and assayed for NF-κB DNA binding activity in EMSAs (Fig. 6A). Flagellin potently activated NF-κB in a time dependent manner similar to that observed for TNF (10 ng/ml) treatment of HT29 cells (Fig. 6A). Analysis of the MAPK, SAPK and IKK signaling pathways (Fig. 6B) at various times after flagellin treatment of HT29 cells using activation-specific phospho-antibodies to monitor MAPK and p38 kinase activation or antibody-specific immunoprecipitation kinase assays for JNK and IKK activities demonstrated that JNK and IKK activity increased through time to one-hour while p38 and MAPK (ERK1&2) activity peaked at thirty minutes and began to decline to noticeably lower levels by one-hour (Fig 6B as indicated). The activation profile of the MAPK, SAPK and IKK signaling molecules ERK1&2, p38, JNK and IKK in intestinal epithelial cells in response to purified flagellin exposure remarkably resembled that of intestinal epithelial cells infected with wild-type *Salmonella* (Fig. 5A). From these observations we conclude that the temporal activation of the signaling pathways examined here (MAPK, SAPK and IKK), which reflect early events in *Salmonella* infection, are determined almost exclusively by recognition and response of intestinal epithelial cells to flagellin

We wished to further examine the effect of purified flagellin and flagellin present on *Salmonella* on the temporal pattern of proinflammatory cytokine gene expression in intestinal epithelial cells in order to differentiate the effects of flagellin alone vs. flagellated *Salmonella* or non-flagellated *Salmonella* infection. HT29 cells were left untreated, stimulated with TNFα (10 ng/ml), or stimulated with flagellin (0 5 ug/ml), or infected with wild-type *Salmonella* typhimurium or the *Salmonella* fliC/fljB double mutant (at MOI of 50). After the indicated times after treatment or infection, HT29 cells were harvested in ice-cold PBS and the cell pellets lysed in Trizol and RNA was purified and used to prepare first-strand cDNA (see Experimental Procedures). Aliquots of the cDNA were used in semi-quantitative RT-PCR reactions using IL1α, IL-1β, IL-8, TNFα, MCP1 and β-actin gene specific primers (sequences available upon request) and the products were fractionated on ethidium bromide containing 1.2% agarose gels. Expression of the known NF κB target genes IL-1β, IL-8, TNFα and MCP1 was increased in response to TNFα or purified flagellin exposure (Fig. 6C). Wild-type *Salmonella* infection also led to activation of these same genes although the expression of TNFα and MCP1 was transient in comparison and occurred immediately after infection. The *Salmonella* fliC /fljB- double mutant failed to induce IL-1β, IL-8 and TNFα expression, however MCP1 expression was induced, although at lower levels than that induced by wild-type *Salmonella*, and also, the expression of MCP1 was not transient in nature and continued throughout the time course (9 h) (Fig. 6C). The expression level of β-actin served as an internal standard for comparison. Interestingly, IL-1α, which is not an NF-κB target gene was stimulated in response to HT29 cell challenge by all of the treatments. Obviously, the *Salmonella* fliC /fljB- double mutant can activate other signaling pathways leading to IL-1α

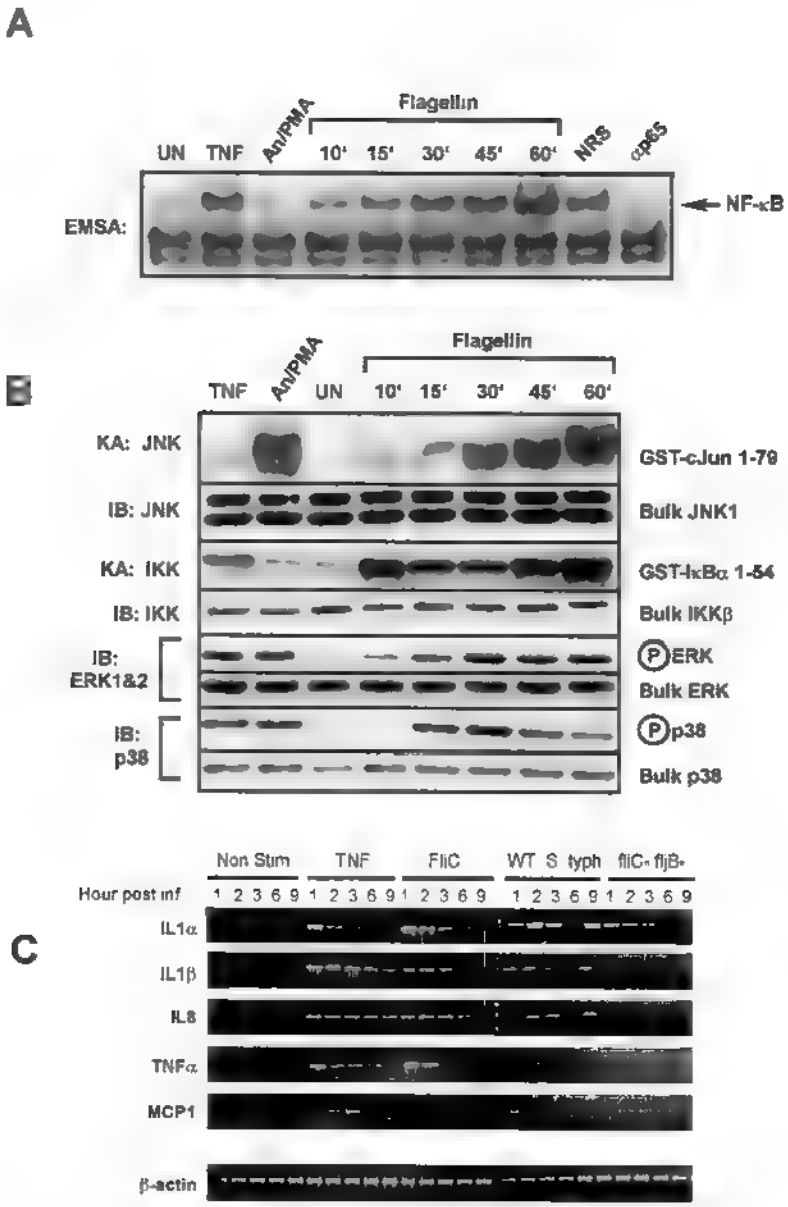

Figure 6

Purified flagellin activates signaling pathways and proinflammatory gene expression in intestinal epithelial cells mimicking that of wildtype a wild-type *Salmonella* infection. HT29 cells were left untreated or treated with TNFα (10 ng/ml) or a cocktail of anisomycin [An] (20 μg/ml)/PMA (12.5 ng/ml) for 10 min, or with flagellin (1 μg/ml) for the indicated times. WCE were prepared and analyzed by EMSA for NF-κB DNA binding activity, immuno-kinase assays (KA) or immunoblot analysis using phospho-specific antibodies for ERK or p38 to detect activation and with kinase-specific antibodies as described in Fig. 5A to detect bulk kinase abundance as indicated. A, EMSA to detect NF-κB DNA binding activity. Authenticity of the NF-κB bandshift was tested with supershift of the complex with p65(RelA)-specific antibody (α p65). normal rabbit serum (NRS) served as an irrelevant antibody control. B, immunoblot and kinase assays to detect IKK, JNK, ERK and p38 kinase activities and protein abundance as in Fig. 5A. C, semi-quantitative RT-PCR of proinflammatory gene expression of non-treated, wild-type and flagellin double mutant Salmonella typhimurium infected, TNFα (10 ng/ml) or flagellin (1 μg/ml) stimulated cells. HT29 cells were harvested at the indicated times after the indicated treatments and isolated RNA was used to make first strand cDNA that subsequently used in RT-PCR reactions (as described in Experimental Procedures) using gene-specific primers for IL1α, IL1β, IL-8, TNFα, MCP1 and β-actin. β-actin was used as a standard for normalizing expression patterns. Resulting PCR products were fractionated on 2% agarose gels and visualized by eithidium bromide staining.

expression. We presently do not know what these signaling pathways are.

Flagellin activates NF-κB DNA binding in a MyD88-dependent manner

Flagellin was capable of activating the requisite signaling pathways consistent with proinflammatory gene activation similar to that of a cytokine like TNFα that activates all cells on which a functional cell surface receptor for it is present (see p65 [RelA] nuclear localization in Fig. 1 and Fig. 5C) we decided to examine the potential of the Toll-like receptors, to activate the NF-κB pathway in response to flagellin exposure. To quickly test this hypothesis we examined the effect that a dominant negative MyD88 (aa 152–296) [42] expressing adenovirus had on flagellin mediated NF-κB activation in HT29 cells. MyD88 is an adapter protein utilized by the IL-1 receptor and all of the known TLRs, which share homology to IL-1 through their cytoplasmic signaling domain and is required for immediate activation of the NF-κB pathway [43,44]. We found that expression of DN-MyD88 in HT29 cells blocked the activation of NF-κB DNA binding activity assayed by EMSA analysis in response to IL-1 or flagellin exposure, consistent with the action of a TLR-mediated activation of NF-κB (TT & JD, unpublished observations) To examine this possibility further we initially used wild-type, MyD88 $^{-/-}$ and TLR2$^{-/-}$/TLR4$^{-/-}$ MEFs (a gift of S. Akira, Univ. of Osaka, JA) to verify the role of MyD88 and to examine the potential role of two of the TLRs to respond to flagellin or to direct wild-type *Salmonella* infection and lead to NF-κB activation (Fig. 7). Wild-type *Salmonella* infection activates NF-κB potently in both the wild-type and TLR deficient MEFs (lanes 2 & 15) but this activation is somewhat defective in the MyD88 deficient MEFs (lane 10). Challenge of all three types of cells with concentrated sterile-filtered wild-type *S. dublin* or the double SopE / SopB^{-} isogenic mutant *S. dublin* strain SE1SB2 culture broths activated NF-κB in wild-type MEFs and TLR2/4 double deficient cells but failed to activate NF-κB in MyD88 deficient cells (compare lanes 11 and 12 with lanes 3, 4, 6, 7, 16 and 17). NF-κB was potently activated in wild-type MEFs by exposure to purified flagellin (0 5 μg/ml) and therefore eliminated the possibility that LPS played a role in NF-κB activation in these experiments. The exclusion of LPS as a major contributor to NF-κB activation is also provided by the potent activation of the TLR2/4 double deficient MEFs (lanes 16 & 17). TLRs 2 and 4 respond to bacterial lipopeptides, peptidoglycans, certain LPSs and gram negative LPS respectively [45-47]. IL-1 stimulation verified the functional requirement of MyD88 in transmission of IL-1 and flagellin-mediated signals

To further define a possible role for the TLRs in flagellin recognition we assayed for the ability of overexpressed TLRs to activate NF-κB in cells that normally respond poorly to flagellin exposure. Choosing cells that responded slightly to purified flagellin ensured that the signaling components and adapters that flagellin uses were present and functional and that the limiting factor was likely only to be the receptor that responds to flagellin. We found that HeLa cells and HEK293T cells activated NF-κB DNA binding activity in response to IL-1 stimulation but poorly to flagellin exposure (TT & JD, unpublished observations) (but see Fig. 9B) and we chose HEK293T cells to use further because of their greater transfection efficiency Amino-terminus FLAG epitope-tagged TLRs 1–9 (kind gifts of R. Medzhitov, Yale Univ. and R. Ulevitch, TSRI) [48,49] were overexpressed in HEK 293T cells in transient transfections along with the 2×-NF-κB-dependent promoter driven luciferase reporter gene [50] and the expression of luciferase in response to no treatment, flagellin (0.5 μg/ml) or TNFα (10 ng/ml) was determined. TLR5 was the only TLR whose expression resulted in a noticeable response to flagellin challenge of the cells (Table 1).

To further determine the likelihood of TLR5 being the TLR through which flagellin activated NF-κB, we constructed dominant-negative signaling mutations by deletion of the carboxyl portion of each TLR to a conserved tryptophan in the TIR domain (see Materials and Methods) A similar mutation in the IL-1 receptor abrogates its ability to lead to NF-κB activation [51,52]. Each DN-TLR along with a reverse cloned TLR5 (AS-TLR5) were cloned into the mammalian expression vector pCDNA3.1 (Invitrogen, Carlsbad, CA). All mutant proteins were expressed well (TT & JD unpublished observations). Each DN-TLR mammalian expression vector and empty expression vector along with 2× NF-κB Luc was transfected as previously described [3] into HT29 cells which respond very well to flagellin. The transfected cells were left untreated, stimulated with TNFα (10 ng/ml) or with purified flagellin (0.5 μg/ml). Reporter gene expression was observed not to be affected by DN-TLR expression in response to TNFα stimulation of transfected cells (Fig. 8A) however, only expression of either the DN-TLR5 or an antisense TLR5 construct resulted in a nearly fifty percent and twenty-five percent inhibition of flagellin-mediated reporter gene activation respectively (Fig. 8B), while DN-TLR2 also was found to mildly inhibit flagellin-mediated reporter expression. These results imply that TLR5 takes part in cell surface recognition of flagellin and initiates the signaling pathway leading to NF-κB activation. The effect of DN-TLR2 on NF-κB-dependent reporter gene activation may be non-specific since its expression also inhibited TNFα-mediated reporter activation as compared to the other DN-TLRs. DN-TLR2 may also compete for an unknown adapter protein that both TLR2 and TLR5 might share. In any event, TLR2 and TLR4 were shown by the results presented in

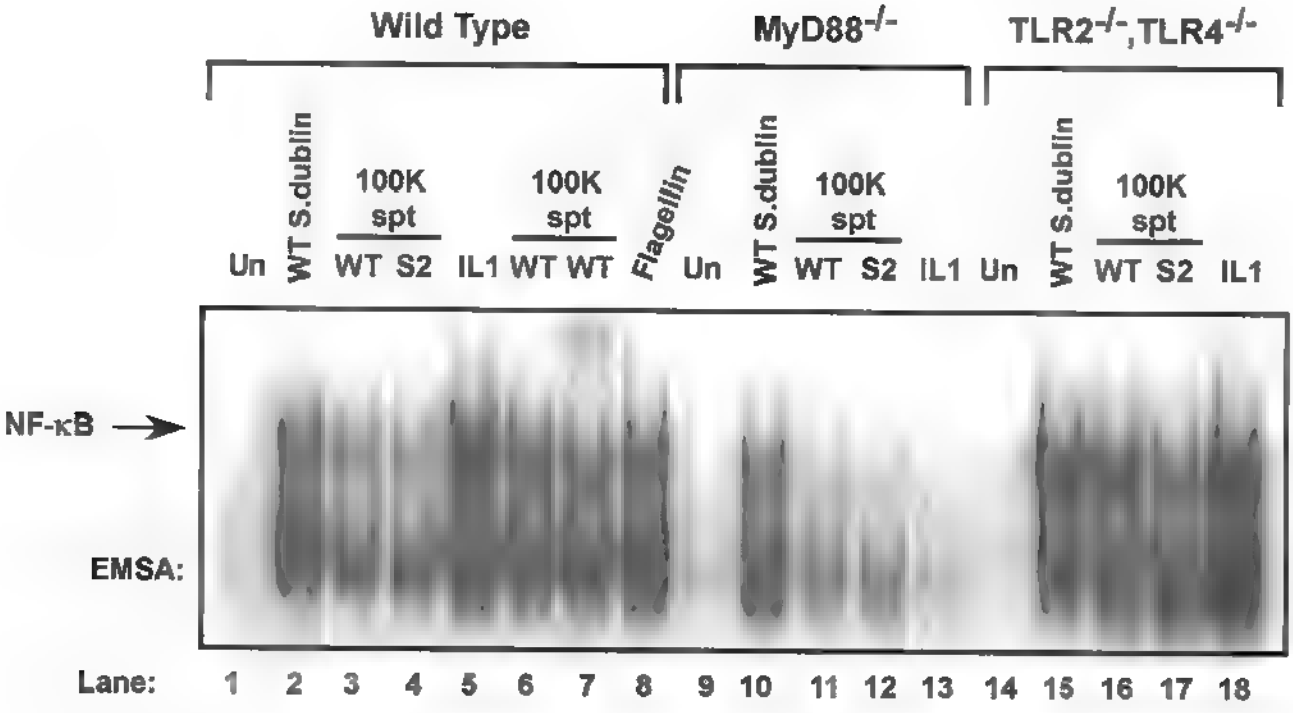

Figure 7

Flagellin-mediated activation of NF-κB is MyD88 dependent. Infectious wild-type *Salmonella Dublin* (MOI of 100), IL-1 (20 ng/ml), purified flagellin (1 μg/ml) (as indicated), sterile-filtered and concentrated 100 kDa filter retentate supernatant (spt) from wild-type *Salmonella dublin* and SopE⁻/SopB⁻ double mutant *Salmonella dublin* strain SE1SB2 (S2, as indicated) was used to challenge wild-type, MyD88⁻/⁻ knockout or TLR2⁻/⁻/TLR4⁻/⁻ double knockout MEFs as indicated. WCEs were prepared 45 min after treatments and examined by EMSA to analyze NF-κB DNA binding activity. IL-1 (20 ng/ml) was used as a positive control to monitor MyD88 function

Fig. 7 not to be required for flagellin-mediated activation of NF-κB.

Flagellin-mediated activation of NF-κB in intestinal epithelial cells leads to increased and decreased expression of a subset of TLRs

Stimulation of intestinal epithelial cells with *S. typhimurium* or with purified flagellin led to activation of the proinflammatory gene program (Fig. 6C). We wished to examine whether or not expression of TLR genes would also be altered in flagellin stimulated cells. HT29 cells were treated or not with purified flagellin (0.5 μg/ml) or with TNFα (10 μg/ml) and total RNA was isolated from non-treated and treated cells three hours after stimulation and used to make first-strand cDNA. Real-time RT-PCR using gene-specific primers for each of the TLRs (Superarray, Frederick, MD) and first-strand cDNA prepared from non-stimulated or flagellin stimulated cells was used to generate SYBR green (Perkin-Elmer) labeled DNA products that were detected in an iCycler™ (Bio-Rad). Interestingly, flagellin only mildly activated the expression of TLR2, while expression levels of TLRs 5, 6, 9 and 10 were decreased by 2-fold (Table 2). Contrastingly, TNF stimulation led to increased expression of TLRs 3 and 4 (1.6- and 3.5-fold respectively), while TLRs 2, 9 and 10 were decreased by approximately 2-, 5- and 3-fold respectively. GAPDH expression served as comparative standard

TLR5 is expressed in cells that don't respond well to flagellin

This study and others [22,33] have identified TLR5 as the likely TLR through which flagellin activates NF-κB. Previous reports made no determination on the presence or abundance of TLR5 in the cells that they used to ascertain its function [22,33]. We wished to determine if TLR5 protein abundance was absent or greatly decreased in cells that failed to respond or responded poorly to challenge by flagellin. TLR5 abundance in a number of cell lines was examined by immunoblot analysis using a TLR5 specific

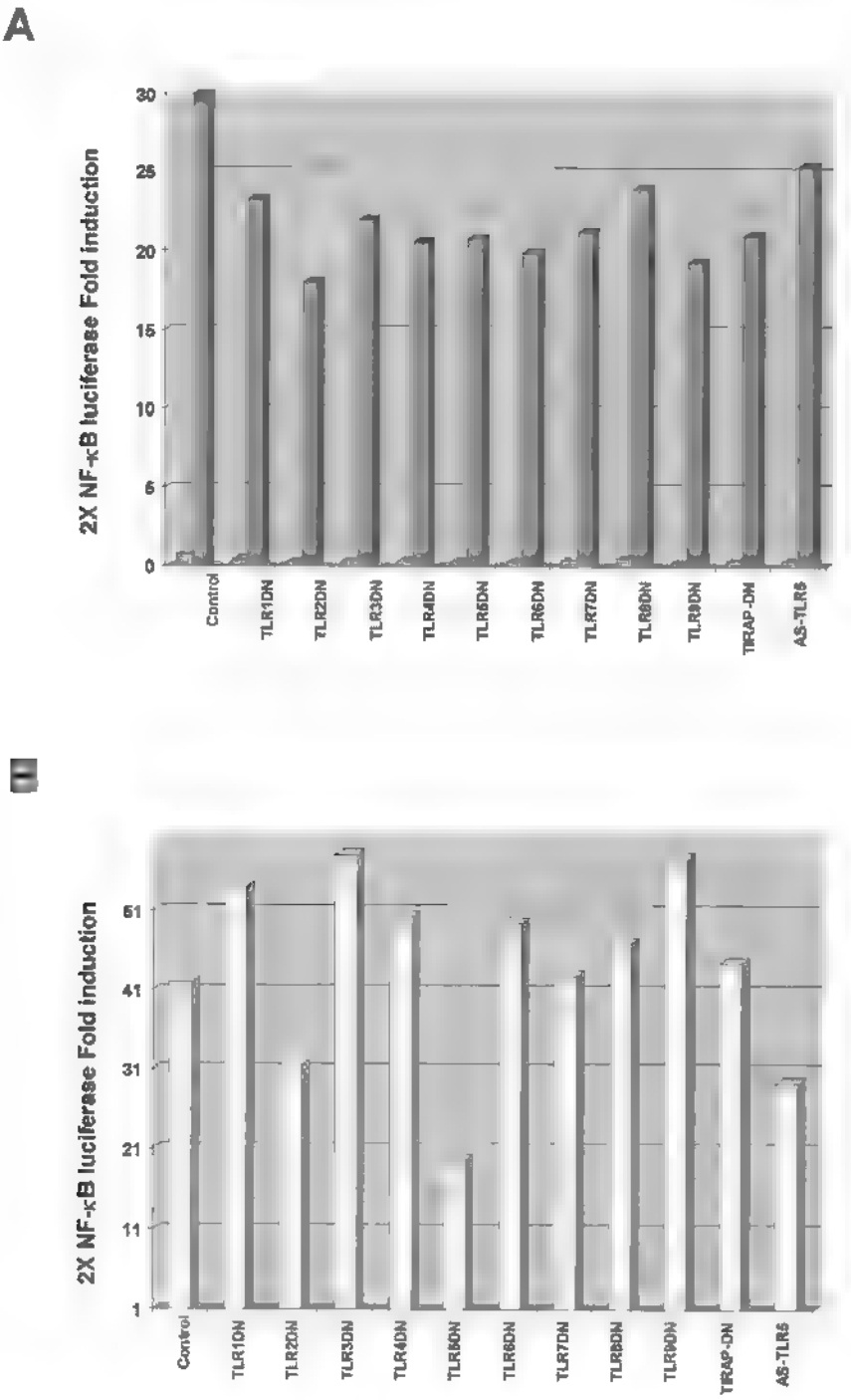

Figure 8
TLR5 inhibits flagellin-mediated NF-κB reporter gene activity. HT29 cells were transfected in triplicate in 6-well dishes using the indicated DN-TLR mammalian expression vectors or antisense TLR5 (AS TLR5) (2 μg/well), 2× NF-κB Luc reporter gene (100 ng/well), pRL-TK Renilla luciferase for normalization (50 ng/well) adjusted to 4 μg total DNA/well with empty vector pCDNA3.1 DNA. A, Fold-induction of 2× NF-κB Luc reporter gene in non-stimulated cells (light shading) and in TNFα (10 ng/ml) treated cells (dark shading). Lysates were prepared 12 h after stimulation. Results of a representative experiment are shown. B, HT29 cells transfected as in A were treated with flagellin (1 μg/ml) and cell lysates were prepared and analyzed as in Fig. 8A. Results of a representative experiment are shown.

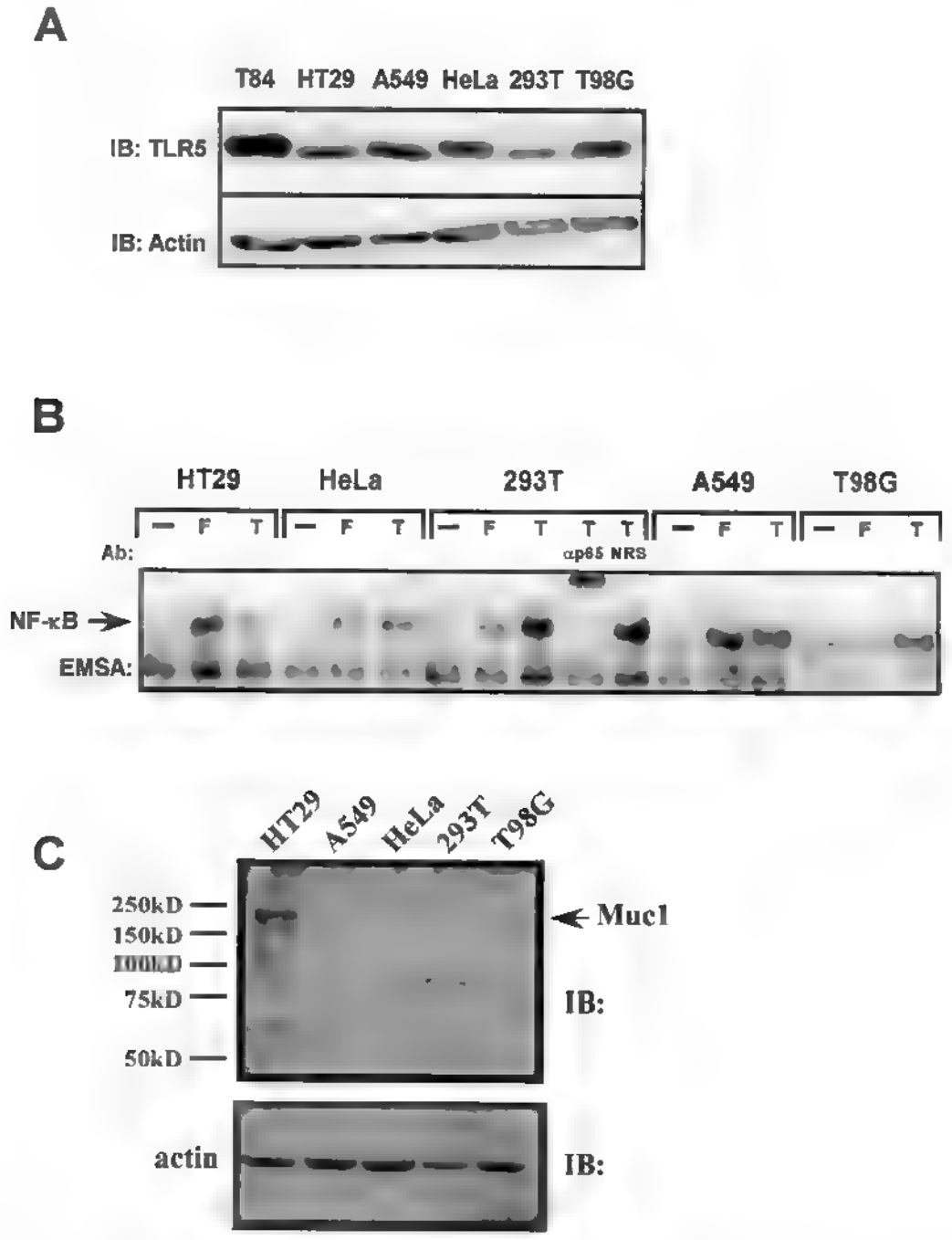

Figure 9

TLR5 is expressed in numerous cell types and has variable responses to flagellin. A, whole cell extracts were prepared from non-stimulated T84, HT29, A549, HeLa, 293T and T98G cells and fractionated on a 8% SDS-PAGE gel, proteins were transferred to PVDF membrane and probed with anti-TLR5 antibody for immunoblot analysis (IB). Protein loading was examined by probing with anti-actin antibody. B, HT29, A549, HeLa, 293T and T98G cells were left untreated (–), treated with flagellin (F) or TNFα (T) and WCEs were prepared after 45 min and used in EMSA to monitor NF-κB DNA binding activity. Authenticity of the NF-κB bandshift was tested with supershift of the complex with p65(RelA)-specific antibody (αp65), normal rabbit serum (NRS) served as an irrelevant antibody control. C, HT29, A549, HeLa, 293T and T98G cells WCEs (50 μg) were fractionated on a 8% SDS-PAGE gel, proteins transferred to Immobilon P and immunoprobed with anti-muc1 (1:450, Santa Cruz). Size markers are listed and muc1 position is indicated with an arrow.

Table 1: TLR5 reponds to flagellin and activates NF-κB

	No Stim	TNF	Flic
Vector	1	13.5	4.9
TLR1	1.7	ND	5.1
TLR2	1.6	ND	5.3
TLR3	1.5	ND	5.0
TLR4	1.8	ND	5.4
TLR5	1.6	ND	9.2*
TLR7	1.5	ND	5.2
TLR8	1.4	ND	5.0
TLR9	1.5	ND	5.1

293T cells were transfected with empty vector (pCDNA3.1) or the individual listed wild-type TLR alleles in triplicate in 6-well dishes. Cells were left untreated (No Stim), TNFα (10 ng/ml) or flagellin (1 μg/ml). NF-κB reporter activity was adjusted by normalizing expression to control Renilla luciferase activity and fold induction was calculated as reporter gene activity in treated cells/reporter gene activity in non-stimulated cells. ND is not determined.

Table 2: Change in TLR mRNA levels following TNFα or FliC stimulation.

Gene	Fold change TNFα stimulated	Fold change FliC stimulated
TLR1	ND	ND
TLR2	0.6	1.3
TLR3	1.6	0.6
TLR4	3.5	1.1
TLR5	0.9	0.5
TLR6	0.9	0.6
TLR7	M	M
TLR8	ND	ND
TLR9	0.2	0.5
TLR10	0.3	0.5
GAPDH	1.0	1.0

ND None detected by RT²PCR

M None detected above level of minus RT control.

Reverse Transcription and Real Time PCR (RT²PCR)-RNA was prepared from cells left untreated, stimulated with TNFα (10 ng/ml) or flagellin (1 μg/ml) for 3 h. RT²PCR was performed with an iCycler (Bio-Rad) to quantify SYBR-green labeled products generated from PCR products of 1st strand cDNA prepared from TLR1 through TLR10 mRNA, 18S rRNA, and GAPDH mRNA. RT²PCR (25 ul reaction volume) was performed with the appropriate primers (SuperArray) in triplicate with HotStart Taq DNA polymerase (SuperArray) at 95°C for 5 min to activate Taq and amplified for 40 cycles (95°C, 30 sec, 55°C, 30 sec, 72°C, 30 sec) RT²PCR was performed on the minus RT controls with TLR5 primers to detect DNA contamination. Fold change in mRNA expression was expressed as $2^{\Delta\Delta Ct}$. ΔCt is the difference in threshold cycles for the TLR mRNAs and 18S rRNA. ΔΔCt is the difference between ΔCt non-simulated control and ΔCt stimulated sample.

antibody and compared with the ability of purified flagellin to induce NF-κB DNA binding activity of WCEs prepared from them. Intestinal epithelial cell lines T84 and HT29 were used as was the lung adenocarcinoma cell line A549, the human cervical adenocarcinoma cell line HeLa, the human embryonic kidney cell line expressing large T antigen HEK293T, and the glioblastoma cell line T98G TLR5 protein was detected in all cell lines examined by immunoblot with TLR5-specific antibody (Fig. 9A) T84 cells exhibited the highest abundance while expression levels of the other cell lines were similar and appeared not to differ by more than two-fold (Fig. 9A). NF-κB DNA binding activity in non-stimulated, TNFα and flagellin stimulated cells was analyzed by EMSA assays of WCEs prepared from each cell type (Fig 9B). HT29 and A549 cells responded strongly to flagellin and to TNFα stimulation while HeLa, 293T and T98G cells responded poorly (HeLa, 293T) or not at all (T98G) to flagellin stimulation. The authenticity of the NF-κB DNA binding complex was determined using p65-specific antibody to supershift the NF-κB DNA:protein complex. It is of interest that some cells that express TLR5 either do not respond at all or do so very poorly. This may be due to either lack of receptor presence at the plasma membrane and intrac-

ellular localization, inactivating or detrimental mutations in the TLR5 gene in these cell lines or lack of or low abundance of a required co-receptor or adapter protein (as is the case in some cells for TLR4 and its co-receptor/adapter MD2 [30,53,54]). IL-1 can activate NF κB DNA binding activity in all of the examined cell lines so it appears that the signaling apparatus downstream of MyD88 to NF-κB is intact.

Recently Muc1 a secreted and membrane bound mucin protein was shown to serve as a receptor that bound *Pseudomonas aeruginosa* and its flagellin, leading to activation of the MAPK pathway [55,56] although NF-κB activity was not examined. We examined the muc1 abundance levels in HT29 (strong flagellin responder), A549 (strong flagellin responder), HeLa, 293T (both weak flagellin responders) and T98G (no flagellin response) to determine if its expression correlated with the activation profile of NF-κB and MAPK in these cells in response to flagellin [55]. Should this be the case then muc1 might serve as a viable co-receptor for TLR5 in propagating activation signals leading to NF-κB activation. We observed that only HT29 cellular proteins gave a strong signal by immunoblot analysis using an muc1-specific antibody while muc1 was barely detectable in the other cell lines (Fig. 9C). These results suggest that muc1 does not serve the role of a TLR5 co-receptor that leads to NF-κB activation and likely plays little to no role activating MAPK pathways in A549 cells where we have observed similar temporal MAPK activation in response to flagellin exposure as we do in HT29 cells (TT and JD, unpublished results). Further examination of muc1's role in HT29 cells in regards to NF-κB and MAPK signaling using siRNA is warranted.

Discussion

Intestinal epithelial cells at mucosal surfaces serve as innate immune sentinels controlling the innate host defense instruction to the immune effector cells inside the body in response to the external environment [1,2]. Previous studies examining pathogenic *Salmonella* invasion of intestinal epithelial cells demonstrated activation of the proinflammatory gene program and invasion of only a minor portion of the cells [10]. We previously demonstrated that NF-κB is as potently induced in pathogenic *Salmonella .sp* infected cells similar to those treated with the proinflammatory cytokines that are potent NF-κB activators such as TNFα and IL-1β and that this activity was IKK-mediated [3]. Here we examined how bacterial invasion of only a third of the cells could give rise to NF κB activity profiles consistent with activation of NF-κB in every cell such as the profile TNFα stimulation provides. We found that bacterial infection activates nuclear translocation of p65 (RelA) in nearly all of the intestinal epithelial cells consistent with the hypothesis that a cell surface receptor was recognizing either a soluble product that bacteria were producing, or a bacterial product on the bacteria, or both. We examined bacterial culture broths and found a bacterial product that was protein in composition and when used to challenge intestinal epithelial cells it potently activated NF-κB DNA binding activity (Fig. 2A). We further purified this protein by gel permeation and anion exchange chromatography and found the protein to be flagellin by electrospray ion trap mass spectroscopy (Fig. 2B &2C and Fig. 3). While our studies were in progress, flagellin was identified as being a potent proinflammatory mediator leading to IL-8 production and secretion [16-18]. We demonstrate in this study that flagellin appears to be exclusively responsible for activating NF κB in intestinal epithelial cells since flagellin mutant strains do not activate NF-κB (Fig. 4) nor lead to their internalization (Fig. 5B). Furthermore, flagellin challenge of intestinal epithelial cells leads to p65 (RelA) nuclear localization in nearly all of the treated cells (Fig. 5B). Transcription factors like activator protein 1 (AP-1) and NF-κB, which are key regulators/activators of the proinflammatory gene program [57,58] are activated by engagement of the MAPK, SAPK and IKK signaling pathways. We demonstrate that the MAPK, SAPK and IKK signaling pathways activation fails to occur in host cells by infection/exposure to *Salmonella* strains devoid of flagellin or products in the culture broths derived from those mutant *Salmonella* strains (Figs. 5A and 6B). We also demonstrate here that combined mutants of both fliC and fljB exhibit a severe lack of invasion (10^{-4} less than wild-type) and failure to activate stress response signaling, which has not been revealed previously. It is likely that the lack of flagellin production interferes with the functioning of the type III secretion system (TTSS) although flagellin is not known to effect expression of TTSS-required gene products. This hypothesis seems credible since supply of flagellin or bacterial culture components from wild-type *Salmonella* cultures in *trans* to the double fliC /fljB mutant bacteria fails to compliment their lack of infectivity in gentamycin invsion assays (TT & JD, unpublished observations and see Fig. 5B). In fact, we found the abundance of a subset of Sip and Sop proteins (SipA and SopD) released into the bacterial culture media to be drastically reduced in the flagellin mutant strains used here (TT & JD, unpublished observations). These two proteins have not previously been identified as activators of NF-κB nor are they considered as such here.

The TTSS translocates the *Salmonella* invasion proteins (Sips) and the SopE proteins into the host cell initiating cytoskeletal rearrangements that ultimately lead to bacterial internalization, [11,12,41] In any event, it is clear that purified flagellin activates a similar cadre of proinflammatory genes as does infection of intestinal epithelial cells with wild-type flagellated *Salmonella*. The temporal expression pattern of these genes was found to be

remarkably similar (Fig. 6C) indicating that flagellin mediated temporal activation of the MAPK, SAPK and IKK signaling pathways can suffice for signaling pathways activated by Sips or SopE and SopE2 and largely recapitulates the temporal activation of key proinflammatory genes as does infection of intestinal epithelial cells with wild-type flagellated *Salmonella*.

The rapid, and potent activation of the MAPK, SAPK and IKK signaling pathways by flagellin was consistent with and indicative of the activation of a cell surface receptor. In this study and in other studies TLR5 has been demonstrated to play an integral role in the recognition of flagellin leading to activation of NF-κB and expression of the IL-8 gene (Fig. 6C) [22,33]. Identification of TLR5 utilized transfection of TLRs 1 – 9 into cell lines which responded poorly to flagellin (this study) or not at all [22,33] and challenging the transfectants with flagellin to identify which TLR responded to this PAMP. Previous studies that identified TLR5 as the receptor for flagellin did not examine the abundance of TLR5 in these cells or account for the lack of TLR5-mediated signaling in response to flagellin [22,33]. We demonstrate here that cells which respond poorly (HeLa and HEK293T) or not at all (T98G) contain TLR5 in at least equivalent abundance as HT29 cells which are highly responsive to flagellin. We propose at least three possibilities to account for this discrepancy, first, this may be due to either lack of TLR5 receptor presence at the plasma membrane and intracellular localization; second, inactivating or detrimental mutations in the TLR5 gene in these cell lines; and lastly, lack of or low abundance of a required co-receptor or adapter protein required for either efficient ligand recognition and/or signaling. These possibilities are currently being investigated. We favor the last possibility since surface biotinylation experiments indicate that TLR5 is present on the cell surface in both flagellin responding cells and in non-responders mentioned above (data not shown). Invocation of the second hypothesis would require inactivating mutations be present in three different cell lines, a highly improbable outcome.

How do the findings presented here correlate with events during a "normal" *Salmonella* infection? We have indicated in this study that defective type III secretion system functioning leads to loss of host cell infectivity and underscores the importance of this system in the normal course of infection. In the *in vivo* setting, polarized epithelial cells express TLR5 on the basolateral surface [48] and flagellin can only reach the receptor either after either breaching the tight junction barrier by physical damage or by loosening of the junctions in response to Sips and Sops delivered into the intestinal epithelial cells by the TTSS or by delivery of flagellin across the intestinal epithelial cell by the bacteria itself [17,59-61]. This scenario would imply the main function of the type III secretion system would be to trigger stress response signaling facilitating invasion and lead to loosening the tight junctions and result in flagellin/ flagellated bacteria to passing through the junctions and infected cells allowing access the basolateral surface and then systemic dispersion. TLR5 on the basolateral surface of the intestinal epithelial cells, in response to flagellin, could then lead to activation of NF-κB and the proinflammatory gene program and host protection. This model is consistent with activation of the proinflammatory gene program observed in response to flagellated *Salmonella sp.* infection in many reports too numerous to cite here and would allow the innate host defense system a fail-safe way to recognize pathogen exposure. In instances where infection of intestinal epithelial cells by naturally occurring non-flagellated *Salmonella* occurs, a strong proinflammatory response would not initially be presented but the *Salmonella* would instead lead to systemic infection as is the case in chickens with *S. galinarum* and *S. pollorum* and result in typhoid like disease [62]. Infection of chicken epithelial cells does not lead to proinflammatory gene expression by these non-flagellated pathogens but does when infected with *S. typhimurium* or *S. dublin* [62]

Argument for the existence of an additional TLR5 co-receptor/adapter being in limited abundance or absent might be in evidence from the transfection results presented in Table 1 which demonstrated that overexpression of cell surface localized FLAG-tagged TLR5 only resulted in slightly over a two-fold increase in NF-κB reporter gene expression in response to flagellin. If only TLR5 was required for activation of the signaling pathway should not a much more robust response been observed? We have also used DN TLR5 transfections and NF-κB-dependent reporter gene assays or overexpresssion of DN-TLR5 using recombinant adenoviruses and analysis of resulting NF-κB DNA binding activity in response to flagellin to examine its effectiveness to completely inhibit TLR5-mediated flagellin activation of NF-κB. We have found it difficult to gain more than a fifty-percent reduction in either reporter gene activation or NF-κB DNA binding activity in HT29 cells (TT, AD & JD, unpublished observations) These results suggest that the resting TLR5 signaling complex may be quite stable as has recently been suggested [63] Should the endogenous TLR5 signaling complex be extremely stable it would therefore be expected that titration of a required pre-stimulus bound adapter or co-receptor away would be inefficient and this is what we have observed. Expression of a DN-MAL (TIRAP), a MyD88-related TLR adapter [64,65] had little to no effect on flagellin-mediated NF-κB activity in transient transfection NF-κB reporter gene assays (TT & JD, unpublished observations). Recently, TLR5 has been shown to bind flagellin [66-68] and that this is likely a

direct interaction due to failure of the human TLR5 to respond to a purified flagellin derived from a mouse-specific *Salmonella* strain [68]. These observations still do not preclude the existence of a co-receptor or adapter that is critical for signal transmission. Detailed biochemical characterization of the TLR5 signaling complex will resolve this issue. Muc1, a recently described flagellin interacting membrane protein by virtue of its ability to trigger activation of the MAPK pathway in response to flagellin exposure [55] was considered a viable candidate for such a co-receptor but our observations suggest that it can not serve as the putative TLR5 co-receptor as it is expressed at similar levels in flagellin non-responding cell lines examined here as it is in A549 cells which respond strongly to flagellin and both cell line types express similar levels of TLR5 (Fig. 9).

Conclusion

In conclusion, our data clearly demonstrates that flagellin can act as the major determinant in activating key stress response signaling pathways and proinflammatory gene program expression in a temporal and qualitative fashion as observed during infection of intestinal epithelial cells by wild-type *Salmonella sp.* that express flagellin, a point that was not well established until this study. In addition, expression of the *fli C* gene appears to play an important role in the proper functioning of the TTSS since mutants that fail to express *fli C* are defective in expressing a subset of Sip proteins and fail to invade host cells. Flagellin added in *trans* cannot restore the ability of the *fli C* mutant bacteria to invade intestinal epithelial cells. Flagellin is "sensed" by TLR5 and in response propagates signaling pathways culminating in potent proinflammatory gene expression. Interestingly we found that TLR5 is expressed in weakly responding and also in some flagellin non responding cells, 293T, HeLa and T98G cells respectively at levels similar to cells such as HT29 and A549 cells that respond strongly to flagellin and can be found on the cell surface, raising a strong possibility that productive TLR5 signaling may require an additional factor/adaptor other than those already known to be key in the IL-1 signaling pathway, which shares extensive similarities to the TLRs signaling pathways.

Methods

Materials

Human tumor necrosis factor alpha (TNFα) and human IL-1 were purchased from R&D Systems (Minneapolis, MN). Tris [hydroxymethyl]aminomethane (Tris) was purchased from Fisher Scientific (Fairlawn, NJ). Fetal calf serum was purchased from US Biotechnologies Inc. (Parkerford, PA). Para-nitro-phenylphosphate (PNPP) was purchased from Aldrich Chemical (Milwaukee, WI). The Polyacrylamide gel electrophoresis (PAGE) supplies: acrylamide, bis-acrylamide, sodium dodecyl sulfate (SDS), TEMED, and ammonium persulfate were purchased from Bio-Rad Laboratories (Hercules, CA). Dulbecco's modified essential medium (DMEM), DMEM:F12, phosphate buffered saline (PBS), glutamine, penicillin G, streptomycin, amphotericin B, and Grace's Insect medium were purchased from Invitrogen (Carlsbad, CA). Luria Broth (LB) was purchased from Becton Dickson and Co (Sparks, MD). The protease inhibitors: aprotinin, bestatin, leupeptin, pepstatin A, and phenylmethylsulfonyl fluoride (PMSF) were purchased from Cal Biochem (La Jolla, CA). Protease inhibitor cocktail contained 10 μg/ml aprotinin, 2.5 μg/ml leupeptin, 8.3 μg/ml bestatin, and 1.7 μg/ml pepstatin A. Phorbol 12-myristate 13 acetate (PMA), N-[2-hydroxyethyl]piperazine-N'-[2-ethanesulfonic acid] (Hepes), anisomycin, and 2-[N morpholino]ethanesulfonic acid (MES) were purchased from Sigma Chemical (St. Louis, MO). All other reagents were purchased from Sigma Chemical or Fisher Scientific unless stated otherwise.

Cell culture

HT29 human intestinal (colorectal adenocarcinoma) epithelial cells (ATCC HTB-38), HeLa cervical epithelial adenocarcoma cells (ATCC CCL-2), 293T kidney cells (CRL-11268), A549 lung carcinoma cells (ATCC-185), and T98G glioblastoma cells (ATCC CRL-1690) were cultured in DMEM with 2 mM glutamine, 10% Fetal Calf Serum, 100 Units/ml Penicillin G, and 100 μg/ml Streptomycin at 37°C in a humidified 5% CO_2 atmosphere. T84 colorectal carcinoma cells (ATCC CCL-248) were cultured in DMEM:F12 with 2 mM glutamine, 5% Fetal Calf Serum, 100 Units/ml Penicillin G, and 100 μg/ml Streptomycin at 37°C in a humidified 5% CO_2 atmosphere. H5 insect cells (Invitrogen) were cultured in Grace's medium with 2 mM glutamine, 10% Fetal Calf Serum, 100 Units/ml Penicillin G, 100 μg/ml Streptomycin, and 0.25 μg/ml amphotericin B at 28°C MyD88$^{-/-}$ & TLR2$^{-/-}$/TLR4$^{-/-}$ double knockout cells were obtained from Shizuo Akira and Osamu Takeuchi (Univ. of Osaka, Japan) and grown in DMEM with 2 mM glutamine, 10% Fetal Calf Serum, 100 Units/ml Penicillin G, and 100 μg/ml Streptomycin at 37°C in a humidified 5% CO_2 atmosphere.

Bacterial strains

Salmonella typhimurium strain SJW1103 (FliC, phase 1 flagellin, stabilized) [69] is a wild type *Salmonella typhimurium* and can only express the Phase I fliC flagellin, SJW86 (SJW1103 FliC::TN10), and SJW134 (SJW1103 FliC and FljB deletions) were obtained from Robert Macnab (Yale Univ., Conn) and have been described [70]. *Salmonella* serovar dublin strain 2229, strain SE1 (2229 SopE mutant), strain SB2 (2229 SopB mutant), and SE1SB2 (2229 SopE and SopB mutant) were obtained from Edward Galyov (Compton Laboratory, Berkshire, UK) and have been described [14,15]. *Salmonella* strains for

stimulation were grown in LB at 37°C without agitation for 16 hours, centrifuged at 6,000 × g for 1 minute, gently washed with PBS, and gently suspended in DMEM to maintain cells with attached flagella.

Plasmid pFM10.1 (ampicillin resistance), encodes a green fluorescent protein (GFP) expressed after the *Salmonella* host is internalized by mammalian cells, obtained from Stanley Falkow (Stanford Univ, Stanford, CA) [10,34] and was transformed into strains SJW1103 and SJW134 by electroporation. Strains containing pFM10 1 were designated SJW1103G and SJW134G.

Preparation and analysis of Salmonella cell free culture supernatant

Native flagellin was harvested from *S dublin* 2229 or *S. typhimurium* SJW1103. Starter cultures were grown in Luria broth (LB) for 18 hours at 37°C with aeration, diluted 1:5000 in fresh LB, and grown for 12 hours under the same conditions. All subsequent procedures were performed at 4°C. Cells were removed from the medium by centrifugation at 10,000 × g for 5 min and discarded. The supernatant containing flagellin was filtered through a 0.8 micron filter (Millipore, Bedford, MA) to remove residual cells. Supernatant was concentrated 100 fold using an Amicon 100 kiloDalton (kDa) cutoff membrane (Millipore). Initial studies used concentrated culture supernatant from *S. dublin* strain 2229 that was treated with DNase, RNase, Protease K, boiled for 20 min or 100 mM DTT at 37°C for 2 hours and used for stimulation of cultured cells

Concentrated *S. typhimurium* 1103 bacterial culture supernatant was washed 4 times by 1:10 dilution with 50 mM MES, pH 6.0, 50 mM NaCl and re-concentrated. Material not retained by the 100 kDa membrane was discarded. Washed culture supernatant was fractionated by gel permeation or anion exchange chromatography for analysis. For long-term storage, washed culture supernatant was supplemented with protease cocktail and stored at -20°C.

Fractionation by gel permeation chromatography was performed with a Superose 12HR column (Pharmacia) on a Bio-Logic system (Bio-Rad). One-half milliliter of 100× washed supernatant (equivalent of 50 ml original culture supernatant) was separated on the column at 0.4 ml/minute in 50 mM Hepes, pH 7.4, 200 mM NaCl Fractions (0.5 ml) were collected, and 50 µl was fractionated by SDS-PAGE and stained with Bio Safe Coomassie (Bio-Rad). Thirty microliters of each fraction was used for stimulation of HT29 cells (60 mm dishes) for 45 min and NF-κB DNA binding activity in the resulting whole cell extracts extracts were assayed by EMSA. The column was standardized with catalase (232 kDa), aldolase (158 kDa), abumin (67 kDa), ovalbumin (43 kDa), and Chymotripsinogen A (25 kDa), all obtained from Amersham-Pharmacia

Fractionation by anion exchange chromatography was performed with Poros HQ matrix (2 ml column, PerSeptive Biosystems, Farmingham, MA) on a Bio-Logic system Five mililiters of 100× washed supernatant (equivalent of 500 ml original culture supernatant) was separated at 1 ml/minute in 50 mM Hepes, pH 7.4, and a NaCl gradient from 50–500 mM. Fractions were collected and 5 µl of each fraction was examined by 10% SDS-PAGE. Proteins were fractionated on duplicate 10% SDS-PAGE precast gels (BioRad). One gel was stained with Bio Safe Coomassie (Bio-Rad) and the protein bands were isolated for Mass Spectroscopy analysis (CCF Mass spectroscopy core facility) from the other identical non-stained gel, by electro elution with a whole gel eluter (Bio Rad) and SDS was removed with SDS-Out (Pierce, Rockland, IL) per the manufacturers directions. Proteins isolated from bands B1 to B6 were acetone precipitated by addition of 20 µg Aprotinin and 5 µg of BSA to each eluted fraction, ice-cold acetone (-20°C) was added to 80%, mixed well and precipitated overnight at 20°C. Proteins were pelleted by centrifugation at 14,000 × g in the cold for 30 min, acetone/liquid was removed and the pellets washed 2× with 1 ml acetone (-20°C). After removal of the acetone, protein pellets were air dried and then resuspended and denatured in 5 µl of 6 M guanidinium hydrochloride (Gu-HCl) at room temperature for 30 min. Resuspended proteins were two-fold serially diluted in DMEM to a final Gu-HCl concentration of 55 mM to renature the proteins. Two hundred fifty microliters of individual renatured proteins/DMEM were added per ml to HT29 cells (60 mm dishes) and whole cell extracts were prepared 45 min after stimulation and were assayed for NF-κB DNA binding activity by EMSA.

Purification of flagellin (purified flagellin)

The washed and concentrated culture supernatant from *S. typhimurium* 1103 containing flagellin was boiled for 20 minutes and precipitants removed by centrifugation at 15,000 × g. The supernatant containing flagellin was diluted 1:2 with 50 mM MES, pH 6.0, 50 mM NaCl and mixed with 2 ml Poros SP cation exchange matrix (PerSeptive Biosystems) per 1 liter of original culture. The Poros SP matrix was prepared as a 50% slurry and equilibrated with 50 mM MES, pH 6.0 The flagellin preparation and matrix were mixed on a roller at 12 to 14 RPM for 2 hours. The matrix along with bound contaminants was removed by filtration through a 0.85 micron filter and discarded, flagellin failed to bind to the cation exchange matrix at pH 6.0 and eluted in the flowthrough and was collected.

The pH of the flowthrough was adjusted by five-fold dilution of the sample with 50 mM Hepes, pH 7.8, 50 mM

NaCl, and loaded onto a Poros HQ anion exchange column (2 ml column, PerSeptive Biosystems) equilibrated with 50 mM Hepes, pH 7.4, 50 mM NaCl. The column was washed with 2 volumes 50 mM Hepes, pH, 7.4, 50 mM NaCl, and eluted with a 10 column volume linear gradient of 50–500 mM NaCl in 50 mM Hepes, pH 7.4. Flagellin eluted from the column between 200–275 mM NaCl. Fractions containing flagellin were pooled and concentrated. The preparation was determined to be pure by electrophoresis of 5 μg protein by SDS-PAGE and stained with Bio-Safe Coomassie (Bio-Rad) Samples were stored at 80°C in 50 mM Hepes, pH 7.4, approx 225 mM NaCl, 10% glycerol and protease cocktail. A 4 liter preparation of culture supernatant yielded 2 mg purified flagellin.

In-gel tryptic digestion and protein identification by LC-MS

Gels were fixed and stained (Bio Safe Blue, BioRad). All of the following procedures were performed by the CCF Mass spectroscopy core facility. Excised gel bands were reduced (100 mM DTT), and alkylated (100 mM iodoacetamide). Proteins in the gel bands were digested with modified trypsin (Promega, 20 μg/mL) with an overnight incubation at 37°C. Tryptic peptides were extracted from the gel with 50% acetonitrile, 0.1% acetic acid, concentrated in a SpeedVac (Thermo Savant) to remove acetonitrile, and reconstituted to 20 uL with 0 1% acetic acid. Extracted peptides were subjected to reversed phase (50 uM ID packed with Phenomenex Jupiter C18, 6 cm capillary column) liquid chromatography (2%–70% solvent B; Solvent A, 50 mM acetic acid, aqueous, Solvent B acetonitrile), coupled to a Finnigan LCQ DECA ion trap mass spectrometer for peptide sequencing, as described [38]

Preparation of GST-IκBα1-54 and GST-cJUN1-79 kinase substrates

IκBα amino acids 1 to 54 fused to GST or cJUN amino acids 1–79 fused to GST were prepared as previously described [37-39] and stored in kinase buffer (20 mM Hepes, pH 7.6, 10 MM MgCl2, 10 mM NaCl, 2 mM beta-glycerophosphate, 10 mM PNPP)

Preparation of cells for microscopy

HT29 cells for microscopic examination were grown in 6 well plates on sterile cover slips to a density of 50–75% Cells were stimulated as described above. After stimulation, cover slips with HT29 cells were washed 2 times with ice cold PBS and fixed with 4% w/v formalin at room temperature for 20 minutes. Cells were washed 4 times with PBS prior to mounting for visualization of *Salmonella* invasion. Cover slips were mounted with Vectashield mounting medium with DAPI (Vector Laboratories, Burlingame, CA), and cover slips sealed to slides.

Cells for antibody staining were treated with absolute methanol for 20 minutes following formalin fixation, then washed 3 times with PBS supplemented with 0.1% BSA (PBSB) and used directly or stored in the cold after azide was added to 0.02%. For p65(RelA) localization, cells on coverslips were blocked for 1 h at 37°C with PBS supplemented with 1% BSA. The PBSB was removed, washed once with PBSB and coverslips were placed cell-side down onto 150 μl of p65 antibody (Zymed, South San Francisco, CA) diluted 1:1500 in PBSB on a square of parafilm and placed in a humidified chamber at 37°C for 1.5 h. Coverslips were removed and placed cell-side up in 6-well dishes and washed 3 × 5 min with PBSB. Coverslips were then removed and placed cell-side down onto 150 μl of FITC labeled donkey anti rabbit secondary antibody (Jackson Immunoresearch Laboratories, West Grove, PA) (1:300 in PBSB) on a square of parafilm and placed in a humidified chamber at 37°C for 1.5 h. Coverslips were removed and placed cell-side up in 6-well dishes and washed 5 × 5 min with PBSB, removed and placed cell-side down onto slides mounted with Vectashield (Vector Laboratories, Burlingame, CA) with DAPI and then sealed. NF-κB localization was determined by indirect immunofluorescence. Samples were observed on a Leica DMR upright microscope (Leica Microsystems Inc., Heidelberg, Germany) at 400× with oil immersion and equipped with FITC and UV filters. Images were collected with a MicroMax RS camera (Princeton Instruments Inc., Princeton, NJ), and Image Pro plus, version 4.5, software (Media Cybernetics Inc., Carlsbad, CA). Color enhancements were performed with Image Pro plus software. Visible light plus color overlays for Fig. 1 and Fig. 5B were performed with MetaMorph Software (Universal Imaging Corp., Downington, PA).

Bacterial infection and cell stimulation

Mouse embryo fibroblasts (MEFs) or HT29 cells were grown in DMEM as above to a density of 90% prior to stimulation. All cells were washed with warm PBS and supplemented with DMEM without serum or antibiotics in preparation for stimulation. Cells were stimulated with; 10 ng/ml TNFα, 1 μg/ml flagellin unless specified otherwise, 20 μg/ml Anisomycin, 12 5 ng/ml PMA, or 10^8 *Salmonella*/ml at 37°C for desired times and extracts prepared as below. Cells harvested beyond one hour were washed with warm PBS and supplemented with warm DMEM, 2 mM glutamine, and 200 ug/ml gentamycin after 1 hour and returned to 37°C until extract preparation desired

Whole cell extract preparation

Cells were washed with ice-cold PBS and all subsequent steps carried out at 4°C or on ice. Cells were scraped from the dish in ice-cold PBS, and collected by centrifugation at 1000 × g for 1 minute. Cells were lysed by suspension in

50 mM Tris-HCl, pH 7.6, 400 mM NaCl, 25 mM beta glycerol phosphate, 25 mM NaF, 10 mM PNPP, 10 % glycerol, 0.5 mM sodium orthovanadate, 0.5% nonidet 40 (NP-40), 5 mM benzamidine, 2.5 mM metabisulfite, 1 mM PMSF, 1 mM DTT and protease inhibitor cocktail as described [3].

Electromobility shift assays (EMSA)

NF κB DNA binding assays were carried out as previously described [3,35,38]. Anti-p65 antibody (Zymed, South San Francisco), anti-p50 antibody (Santa Cruz Biotechnologies, Santa Cruz, CA), and anti-STAT3 antibody (Santa Cruz) were used for EMSA supershifts.

Invasion assay

HT29 cells, 90–95% confluent in 35 mm round dishes, were prepared for stimulation as above and treated with a 1 ml suspension of Salmonella SJW1103 or SJW134 or left untreated in triplicate as above. After one hour, HT29 cells were washed 4× with warm PBS, supplemented with warm DMEM, 2 mM glutamine, and 200 μg/ml gentamycin, and incubated at 37°C for 4 hours. Cells were then harvested as above and lysed by suspension in 1 ml sterile distilled water. Ten-fold serial dilutions were prepared in PBS and 100 μl of each dilution was plated on LB agar plates and grown at 37°C for 20 hours. Colonies were counted and averaged.

Kinase assays

Whole cell extracts (250 μg) were supplemented with 150 μl of Buffer A (20 mM Hepes, pH 7.9, 20 mM beta-glycerophosphate, 10 mM NaF, 0.1 mM orthovanadate, 5 mM PNPP, 10 mM 2-mercaptoethanol, 0.5 mM PMSF, and protease inhibitor cocktail), and immuno precipitation kinase assays carried out as described [3] using either IKKα monoclonal antibody (PharMingen – Becton Dickson), anti-JNK1 (Santa Cruz Biotechnologies, Santa Cruz, CA), or anti-hemagglutinin (HA) epitope antibody (Covence Antibodies, Princeton, NJ) as indicated. Protein G immunopellets were collected by centrifugation at 500 × g for 30 sec, washed 3 times with Buffer B (Buffer A plus 250 mM NaCl), and one time with Buffer C (Buffer A plus 50 mM NaCl and 10 mM $MgCl_2$). Immunopellets were resuspended in 30 μl Kinase buffer with 0.1 mM orthovanadate, 50 μM "cold" ATP, 5 μCi γ-^{32}P-ATP, 2 mM DTT, and 2 μg of soluble GST IκBα1–54 or GST-cJUN1-79, and incubated at 30°C for 30 minutes. Reactions were stopped by the addition of 15 μl 4× SDS-PAGE loading buffer, heated at 95°C for 5 minutes, and resolved on 10% SDS-PAGE gels by standard procedures. Gels were rinsed, stained with Bio-Safe Coomassie (Bio-Rad) to visualize protein bands, rinsed, photographed then dried and exposed to Kodak X-OMAT AR film (Eastman Kodak Co., Rochester, NY) to detect substrate phosphorylation.

Immunoblotting

Protein samples (40 μg) were resolved by SDS-PAGE on a 10% acrylamide gels by standard procedures, and proteins transferred to PVDF membrane (Millipore) and probed with antibodies as described [3]. Membranes were washed 3× briefly with TBST, incubated with a 1:1000 dilution (1:800 for anti-TLR5) of the primary antibody in TBST, 1% non-fat milk for 1 hour, washed 3 × 5 min with TBST, and then incubated with a 1:2000 dilution of the appropriate HRP-conjugated secondary antibody in TBST, 0.5% non-fat milk for 1 hour. Primary antibodies used were: anti-IKKα/β (H-470, Santa Cruz), anti-JNK1, anti-ERK2 (K-23, Santa Cruz), anti-phospho-ERK (E-4, Santa Cruz), anti-p38MAPK (Cell Signaling Technologies, Beverly, MA), anti-phosopho-p38MAPK (Cell Signaling), anti-TLR5 (H-127, Santa Cruz), anti-muc1 (H-295, Santa Cruz) and anti-actin (C-11, Santa Cruz). Secondary antibodies used were: anti-mouse IgG HRP conjugate (Amersham-Pharmacia), anti-rabbit IgG HRP conjugate (Amersham-Pharmacia), anti-goat IgG-HRP conjugate (Santa Cruz). HRP activity was detected by ECL (Amersham Pharmacia) as per manufacturers instructions, on Kodak X-OMAT AR film.

Construction of dominant-negative TLRs

All DN-TLRs were constructed using PCR. The universal 5' primer consisted of a 5'KPN I restriction site followed by sequences encoding the kozak sequence, translational start site, and preprotrypsin leader sequence of pCMV-1 (Sigma) that all the wild type TLRs were initially cloned into. The 3' anti-sense (AS) primers were human TLRgene-specific primers (sequences available upon request) that created a stop codon immediately after a conserved tryptophan in Box 9 of the TLR TIR homology domain according to Bazan [71], thus creating carboxy terminus deletions. The 5' end of the AS primer contained a number of convenient restriction sites to allow directional cloning. PCR was performed with turbo-Pfu polymerase (Stratagene, La Jolla, CA) using standard procedures on individual wild-type TLR pCMV-1 plasmid DNAs (5 ng each, kind gifts of R. Medzhitov, Yale Univ. and R. Ulevitch, TSRI) [48,49] with the 150 ng each of the universal 5' sense primer and individual gene-specific TLR 3' primers. PCR products were cleaned up with PCR cleanup kit (Qiagen, Germany) digested with appropriate restriction enzymes, gel purified and then ligated into the mammalian expression vector pCDNA3.1 (Invitrogen). Positive clones were sequenced to verify the mutations and tested for expression in transient expression assays and detected on immunoblots by probing with anti FLAG M2 monoclonal antibody (Sigma). All wild-type and DN-TLR alleles are amino terminus FLAG epitope-tagged.

2. Eckmann L, Kagnoff MF, Fierer J: **Intestinal epithelial cells as watchdogs for the natural immune system.** *Trends Microbiol* 1995, **3**:118-120.
3. Elewaut D, DiDonato JA, Kim JM, Truong F, Eckmann L, Kagnoff MF: **NF-kappa B is a central regulator of the intestinal epithelial cell innate immune response induced by infection with enteroinvasive bacteria.** *J Immunol* 1999, **163**:1457-1466.
4. Witthoft T, Eckmann L, Kim JM, Kagnoff MF: **Enteroinvasive bacteria directly activate expression of iNOS and NO production in human colon epithelial cells.** *Am J Physiol* 1998, **275**:G564-G571.
5. Eckmann L, Stenson WF, Savidge TC, Lowe DC, Barrett KE, Fierer J, Smith JR, Kagnoff MF: **Role of intestinal epithelial cells in the host secretory response to infection by invasive bacteria. Bacterial entry induces epithelial prostaglandin h synthase-2 expression and prostaglandin E2 and F2 alpha production.** *J Clin Invest* 1997, **100**:296-309.
6. Jung HC, Eckmann L, Yang SK, Panja A, Fierer J, Morzycka-Wroblewska E, Kagnoff MF: **A distinct array of proinflammatory cytokines is expressed in human colon epithelial cells in response to bacterial invasion.** *J Clin Invest* 1995, **95**:55-65.
7. Hardt WD, Chen LM, Schuebel KE, Bustelo XR, Galan JE: **S. typhimurium encodes an activator of Rho GTPases that induces membrane ruffling and nuclear responses in host cells.** *Cell* 1998, **93**:815-826.
8. Hobbie S, Chen LM, Davis RJ, Galan JE: **Involvement of mitogen-activated protein kinase pathways in the nuclear responses and cytokine production induced by Salmonella typhimurium in cultured intestinal epithelial cells.** *J Immunol* 1997, **159**:5550-5559.
9. Chen LM, Hobbie S, Galan JE: **Requirement of CDC42 for Salmonella-induced cytoskeletal and nuclear responses.** *Science* 1996, **274**:2115-2118.
10. Valdivia RH, Hromockyj AE, Monack D, Ramakrishnan L, Falkow S: **Applications for green fluorescent protein (GFP) in the study of host-pathogen interactions.** *Gene* 1996, **173**:47-52.
11. Galan JE: **Salmonella interactions with host cells: type III secretion at work.** *Annu Rev Cell Dev Biol* 2001, **17**:53-86.
12. Galan JE, Collmer A: **Type III secretion machines: bacterial devices for protein delivery into host cells.** *Science* 1999, **284**:1322-1328.
13. Kubori T, Galan JE: **Salmonella type III secretion-associated protein InvE controls translocation of effector proteins into host cells.** *J Bacteriol* 2002, **184**:4699-4708.
14. Bakshi CS, Singh VP, Wood MW, Jones PW, Wallis TS, Galyov EE: **Identification of SopE2, a Salmonella secreted protein which is highly homologous to SopE and involved in bacterial invasion of epithelial cells.** *J Bacteriol* 2000, **182**:2341-2344.
15. Wood MW, Rosqvist R, Mullan PB, Edwards MH, Galyov EE: **SopE, a secreted protein of Salmonella dublin, is translocated into the target eukaryotic cell via a sip-dependent mechanism and promotes bacterial entry.** *Mol Microbiol* 1996, **22**:327-338.
16. Eaves-Pyles T, Szabo C, Salzman AL: **Bacterial invasion is not required for activation of NF-kappaB in enterocytes.** *Infect Immun* 1999, **67**:800-804.
17. Gewirtz AT, Simon PO Jr, Schmitt CK, Taylor LJ, Hagedorn CH, O'Brien AD, Neish AS, Madara JL: **Salmonella typhimurium translocates flagellin across intestinal epithelia, inducing a proinflammatory response.** *J Clin Invest* 2001, **107**:99-109.
18. Gewirtz AT, Rao AS, Simon PO Jr, Merlin D, Carnes D, Madara JL, Neish AS: **Salmonella typhimurium induces epithelial IL-8 expression via Ca(2+)-mediated activation of the NF-kappaB pathway.** *J Clin Invest* 2000, **105**:79-92.
19. McDermott PF, Ciacci-Woolwine F, Snipes JA, Mizel SB: **High-affinity interaction between gram-negative flagellin and a cell surface polypeptide results in human monocyte activation.** *Infect Immun* 2000, **68**:5525-5529.
20. Ciacci-Woolwine F, Blomfield IC, Richardson SH, Mizel SB: **Salmonella flagellin induces tumor necrosis factor alpha in a human promonocytic cell line.** *Infect Immun* 1998, **66**:1127-1134.
21. Moors MA, Li L, Mizel SB: **Activation of interleukin-1 receptor-associated kinase by gram-negative flagellin.** *Infect Immun* 2001, **69**:4424-4429.
22. Gewirtz AT, Navas TA, Lyons S, Godowski PJ, Madara JL: **Cutting edge: bacterial flagellin activates basolaterally expressed TLR5 to induce epithelial proinflammatory gene expression.** *J Immunol* 2001, **167**:1882-1885.
23. Akira S: **Toll-like receptors and innate immunity.** *Adv Immunol* 2001, **78**:1-56.
24. Akira S, Hemmi H: **Recognition of pathogen-associated molecular patterns by TLR family.** *Immunol Lett* 2003, **85**:85-95.
25. Medzhitov R, Janeway C Jr: **The Toll receptor family and microbial recognition.** *Trends Microbiol* 2000, **8**:452-456.
26. O'Neill L: **Specificity in the innate response: pathogen recognition by Toll-like receptor combinations.** *Trends Immunol* 2001, **22**:70.
27. Hajjar AM, O'Mahony DS, Ozinsky A, Underhill DM, Aderem A, Klebanoff SJ, Wilson CB: **Cutting edge: functional interactions between toll-like receptor (TLR) 2 and TLR1 or TLR6 in response to phenol-soluble modulin.** *J Immunol* 2001, **166**:15-19.
28. Ozinsky A, Underhill DM, Fontenot JD, Hajjar AM, Smith KD, Wilson CB, Schroeder L, Aderem A: **The repertoire for pattern recognition of pathogens by the innate immune system is defined by cooperation between toll-like receptors.** *Proc Natl Acad Sci U S A* 2000, **97**:13766-13771.
29. Kawasaki K, Akashi S, Shimazu R, Yoshida T, Miyake K, Nishijima M: **Involvement of TLR4/MD-2 complex in species-specific lipopolysaccharide-mimetic signal transduction by Taxol.** *J Endotoxin Res* 2001, **7**:232-236.
30. Nagai Y, Akashi S, Nagafuku M, Ogata M, Iwakura Y, Akira S, Kitamura T, Kosugi A, Kimoto M, Miyake K: **Essential role of MD-2 in LPS responsiveness and TLR4 distribution.** *Nat Immunol* 2002, **3**:667-672.
31. Backhed F, Normark S, Richter-Dahlfors A: **TLR4-dependent lipopolysaccharide signalling in epithelial cells is independent of extracellular protease activity.** *Cell Microbiol* 2002, **4**:297-303.
32. da Silva CJ, Soldau K, Christen U, Tobias PS, Ulevitch RJ: **Lipopolysaccharide is in close proximity to each of the proteins in its membrane receptor complex. transfer from CD14 to TLR4 and MD-2.** *J Biol Chem* 2001, **276**:21129-21135.
33. Hayashi F, Smith KD, Ozinsky A, Hawn TR, Yi EC, Goodlett DR, Eng JK, Akira S, underhill DM, Aderem A: **The innate immune response to bacterial flagellin is mediated by Toll-like receptor 5.** *Nature* 2001, **410**:1099-1103.
34. Valdivia RH, Falkow S: **Fluorescence-based isolation of bacterial genes expressed within host cells.** *Science* 1997, **277**:2007-2011.
35. DiDonato JA, Mercurio F, Karin M: **Phosphorylation of I kappa B alpha precedes but is not sufficient for its dissociation from NF-kappa B.** *Mol Cell Biol* 1995, **15**:1302-1311.
36. Norris FA, Wilson MP, Wallis TS, Galyov EE, Majerus PW: **SopB, a protein required for virulence of Salmonella dublin, is an inositol phosphate phosphatase.** *Proc Natl Acad Sci U S A* 1998, **95**:14057-14059.
37. DiDonato JA: **Assaying for I kappa B kinase activity.** *Methods Enzymol* 2000, **322**:393-400.
38. DiDonato JA, Hayakawa M, Rothwarf DM, Zandi E, Karin M: **A cytokine-responsive IkappaB kinase that activates the transcription factor NF-kappaB.** *Nature* 1997, **388**:548-554.
39. Hibi M, Lin A, Smeal T, Minden A, Karin M: **Identification of an oncoprotein and UV-responsive protein kinase that binds and potentiates the c-Jun activation domain.** *Genes Dev* 1993, **7**:2135-2148.
40. Galkin VE, Orlova A, VanLoock MS, Zhou D, Galan JE, Egelman EH: **The bacterial protein SipA polymerizes G-actin and mimics muscle nebulin.** *Nat Struct Biol* 2002, **9**:518-521.
41. Wallis TS, Wood M, Watson P, Paulin S, Jones M, Galyov E: **Sips, Sops, and SPIs but not stn influence Salmonella enteropathogenesis.** *Adv Exp Med Biol* 1999, **473**:275-280.
42. Muzio M, Ni J, Feng P, Dixit VM: **IRAK (Pelle) family member IRAK-2 and MyD88 as proximal mediators of IL-1 signaling.** *Science* 1997, **278**:1612-1615.
43. Takeuchi O, Akira S: **MyD88 as a bottle neck in Toll/IL-1 signaling.** *Curr Top Microbiol Immunol* 2002, **270**:155-167.
44. Medzhitov R, Preston-Hurlburt P, Kopp E, Stadlen A, Chen C, Ghosh S, Janeway CA Jr: **MyD88 is an adaptor protein in the hToll/IL-1 receptor family signaling pathways.** *Mol Cell* 1998, **2**:253-258.
45. Yoshimura A, Lien E, Ingalls RR, Tuomanen E, Dziarski R, Golenbock D: **Cutting edge: recognition of Gram-positive bacterial cell wall components by the innate immune system occurs via Toll-like receptor 2.** *J Immunol* 1999, **163**:1-5.

Transfections

HT29 cells were transfected with Lipofectamine Plus (Invitrogen) as previously described [3]. In transfections monitoring reporter gene expression, transfections were performed at least three times in 6 well dishes in triplicate with the total DNA mass kept constant at 4 μg (2 μg effector plasmid DNA, 100 ng 2× NF-κB Luc reporter gene, 50 ng pRL-TK, a thymidine kinase promoter driven *Renilla* luciferase normalization reporter and 1.85 μg pCDNA3.1 plasmid DNA as bulk filler DNA) and fire-fly luciferase expression was normalized to *Renilla* luciferase expression using the dual-luciferase assay (Promega, Madison, WI). Fold inductions were calculated and values between experiments did not vary more than 15%, a representative experiment is presented. Transfection of 293T cells was performed with lipofectamine 2000 (Invitrogen) in 6-well dishes in triplicate as per the manufacture's protocol. TLR expression plasmids were added at 2 μg/well, and NF κB and normalization control plasmids were as above with HT29 cells and pCDNA3.1 plasmid DNA as bulk filler DNA to a final DNA mass of 4 μg/well. Fold inductions were calculated and values between experiments (N of 3) did not vary more than 10%, a representative experiment is presented

Real Reverse Transcription and Real Time PCR (RT²PCR)

Cells (N = 3) were stimulated 3 hours at 37°C with TNFα or FliC or left untreated and harvested for total RNA isolation. Total cellular RNA was extracted from cells with Trizol reagent (Invitrogen) [3] and reverse transcribed with ReactionReady first strand cDNA synthesis kit (SuperArray Bioscience Corp., Fredrick, MD). RNA (2.5 ug per 20 ul reaction) was reverse transcribed using random primers and Moloney murine leukemia virus reverse transcriptase per manufacturer specified conditions. Controls without reverse transcriptase (minus RT) was also generated for each RNA sample. RT²PCR was performed with an iCycler (Bio-Rad) to quantify TLR1 through TLR10 mRNA, 18S rRNA, and GAPDH mRNA. RT²PCR (25 ul reaction volume) was performed with the appropriate primers (SuperArray) per manufacturers instructions in triplicate with HotStart Taq DNA polymerase (SuperArray) at 95°C for 15 min to activate Taq and amplified for 40 cycles (95°C, 30 sec, 55°C, 30 sec, 72°C, 30 sec). RT²PCR was performed on the minus RT controls with TLR5 primers to detect DNA contamination. Real-time PCR analysis was performed using SYBR-green (Perkin-Elmer) according to manufacture's instructions with the specific primer pairs indicated above and primer pairs for 18S ribosomal RNA as reference RNA (Classic 18S primer pairs – Ambion Inc) Cycle time (Ct) was measured using the iCycler™ and its associated software (Bio-Rad). Relative transcript quantities were calculated by the ΔΔCt method using 18S ribosomal RNA as a reference amplified from samples using the Classic 18S primer pairs from Ambion, Inc (Austin, TX). Normalized samples were then expressed relative to the average ΔCt value for untreated controls to obtain relative fold-change in expression levels. Fold change in mRNA expression was expressed as $2^{-\Delta\Delta Ct}$. ΔCt is the difference in threshold cycles for the TLR mRNAs and 18S rRNA. ΔΔCt is the difference between ΔCt non-simulated control and ΔCt stimulated sample. Values for fold-induction varied less than 5% among replicates.

Abbreviations

The abbreviations used are: FBS, fetal bovine serum; IL-1, interlukin-1, SDS, sodium dodecyl sulfate; PAGE, polyacrylamide gel electrophoresis, EMSA, electromobility shift assay; IB, immunoblot, KA, kinase assay; GST, glutathione S-transferase; PBS, phosphate-buffered saline; TNFα, tumor necrosis factor α; NF-κB, nuclear factor kappa B; IKK, Ikappa B kinase; IκB, Ikappa B; PCR, polymerase chain assay; RT-PCR, reverse transcription polymerase chain assay; Gu-HCl, guanidinium hydrochloride ; MAPK, mitogen activated protein kinase; SAPK, stress-activated protein kinase; ERK, extracellular regulated kinase; TLR, toll like receptor; DN, dominant negative; JNK, Jun N-terminal kinase; AP-1, activator protein-1; MEF, mouse embryo fibroblast; WCE, whole cell extract; IEC, intestinal epithelial cell; MCP1, macrophage chemoattractant protein 1; TTSS, type III secretion system; Sip, *Salmonella* invasion protein; PMA, phorbol 12-myristate 13 acetate; PNPP, para nitrophenyl phosphate; TK, thymidine kinase; BF, bright field; NP-40, nonidet-40; NRS, normal rabbit serum; IN, input; Ct, cycle time.

Authors' contributions

TT and AD initiated the study and performed the majority of the experiments and contributed equally and were assisted by NK and JL. MD constructed a number of DN-TLRs and JD developed the study, provided funding support, oversaw the project and also constructed a number of mutant TLRs.

Acknowledgements

We would like to thank Drs.E.Galyov (Compton Laboratory, Berkshire (UK)), Drs. R.M. Macnab (Yale University, New Haven, Conn), S. Mizel (Wake Forest University, Winston-Salem, NC), and M. Kagnoff (UCSD, La Jolla, CA) for bacterial strains. We would also like to thank S. Akira and O Takeuchi (Osaka University, Osaka, JA) for the gift of MyD88 and TLR 2/4 double knockout cell lines. We also would like to thank S. Falkow (Stanford University, Stanford, CA), M. Karin (UCSD, La Jolla, CA), R. Medzhitov (Yale University, New Haven, Conn) and R. Ulevitch (TSRI, La Jolla, CA) and V. Dixit (then at Univ. of Michigan, Ann Arbor, MI) for gifts of plasmids. We would also like to thank B. Williams (CCF, Cleveland, OH) for thoughtful discussions and support on this project. This work was supported in part by grants from the National Institutes of Health, CA84406 (to J.A.D.) and the U.S. Army, DAMD 17-01-C-0065 (to B. Williams)

References

1. Kagnoff MF, Eckmann L: **Epithelial cells as sensors for microbial infection.** *J Clin Invest* 1997, **100**:6-10.

46. Lien E, Sellati TJ, Yoshimura A, Flo TH, Rawadi G, Finberg RW, Carroll JD, Espevik T, Ingalls RR, Radolf JD, Golenbock DT: **Toll-like receptor 2 functions as a pattern recognition receptor for diverse bacterial products.** *J Biol Chem* 1999, **274**:33419-33425.
47. Lien E, Means TK, Heine H, Yoshimura A, Kusumoto S, Fukase K, Fenton , Oikawa M, Qureshi N, Monks B, Finberg RW, Ingalls RR, Golenbock DT: **Toll-like receptor 4 imparts ligand-specific recognition of bacterial lipopolysaccharide.** *J Clin Invest* 2000, **105**:497 504.
48. Alexopoulou L, Holt AC, Medzhitov R, Flavell RA: **Recognition of double-stranded RNA and activation of NF-kappaB by Toll-like receptor 3.** *Nature* 2001, **413**:732-738.
49. Chuang TH, Ulevitch RJ: **Cloning and characterization of a subfamily of human toll-like receptors: hTLR7, hTLR8 and hTLR9.** *Eur Cytokine Netw* 2000, **11**:372-378.
50. Devary Y, Rosette C, DiDonato JA, Karin M: **NF-kappa B activation by ultraviolet light not dependent on a nuclear signal.** *Science* 1993, **261**:1442-1445
51. Heguy A, Baldari CT, Macchia G, Telford JL, Melli M: **Amino acids conserved in interleukin-1 receptors (IL-1Rs) and the Drosophila toll protein are essential for IL-1R signal transduction.** *J Biol Chem* 1992, **267**:2605-2609.
52. Croston GE, Cao Z, Goeddel DV: **NF-kappa B activation by interleukin-1 (IL-1) requires an IL-1 receptor-associated protein kinase activity.** *J Biol Chem* 1995, **270**:16514-16517.
53. Akashi S, Nagai Y, Ogata H, Oikawa M, Fukase K, Kusumoto S, Kawasaki K, Nishijima M, Hayashi S, Kimoto M, Miyake K: **Human MD-2 confers on mouse Toll-like receptor 4 species-specific lipopolysaccharide recognition.** *Int Immunol* 2001, **13**:1595-1599.
54. Schromm AB, Lien E, Henneke P, Chow JC, Yoshimura A, Heine H, Latz E, Monks BG, Schwartz JA, Miyake K, Golenbock DT: **Molecular genetic analysis of an endotoxin nonresponder mutant cell line: a point mutation in a conserved region of MD-2 abolishes endotoxin-induced signaling.** *J Exp Med* 2001, **194**:79-88.
55. Lillehoj EP, Kim H, Chun EY, Kim KC: **Pseudomonas aeruginosa Stimulates Phosphorylation of the Epithelial Membrane Glycoprotein Muc1 and Activates MAP Kinase.** *Am J Physiol Lung Cell Mol Physiol* 2004.
56. Lillehoj EP, Kim BT, Kim KC: **Identification of Pseudomonas aeruginosa flagellin as an adhesin for Muc1 mucin.** *Am J Physiol Lung Cell Mol Physiol* 2002, **282**:L751-L756.
57. Karin M, Takahashi T, Kapahi P, Delhase M, Chen Y, Makris C, Rothwarf D, Baud V, Natoli G, Guido F, Li N: **Oxidative stress and gene expression: the AP-1 and NF-kappaB connections.** *Biofactors* 2001, **15**:87-89
58. Jobin C, Sartor RB: **The I kappa B/NF-kappa B system: a key determinant of mucosalinflammation and protection.** *Am J Physiol Cell Physiol* 2000, **278**:C451-C462.
59. Wood MW, Jones MA, Watson PR, Siber AM, McCormick BA, Hedges S, Rosquist R, Wallis TE, Galyov EE: **The secreted effector protein of Salmonella dublin, SopA, is translocated into eukaryotic cells and influences the induction of enteritis.** *Cell Microbiol* 2000, **2**:293-303.
60. McCormick BA: **The use of transepithelial models to examine host-pathogen interactions.** *Curr Opin Microbiol* 2003, **6**:77-81.
61. Sakaguchi T, Kohler H, Gu X, McCormick BA, Reinecker HC: **Shigella flexneri regulates tight junction-associated proteins in human intestinal epithelial cells.** *Cell Microbiol* 2002, **4**:367-381
62. Kaiser P, Rothwell L, Galyov EE, Barrow PA, Burnside J, Wigley P: **Differential cytokine expression in avian cells in response to invasion by Salmonella typhimurium, Salmonella enteritidis and Salmonella gallinarum.** *Microbiology* 2000, **146(Pt 12)**:3217-3226.
63. Mizel SB, Snipes JA: **Gram-negative flagellin-induced self-tolerance is associated with a block in interleukin-1 receptor-associated kinase release from toll-like receptor 5.** *J Biol Chem* 2002, **277**:22414-22420.
64. Fitzgerald KA, Palsson-McDermott EM, Bowie AG, Jefferies CA, Mansell AS, Brady G, Brint E, Dunne A, Gray P, harte MT, McMurray D, Smith DE, Sims JE, Bird TA, O'Neill LA: **Mal (MyD88-adapter-like) is required for Toll-like receptor-4 signal transduction.** *Nature* 2001, **413**:78-83.
65. Horng T, Barton GM, Medzhitov R: **TIRAP: an adapter molecule in the Toll signaling pathway.** *Nat Immunol* 2001, **2**:835-841.
66. Mizel SB, West AP, Hantgan RR: **Identification of a sequence in human toll-like receptor 5 required for the binding of Gram-negative flagellin.** *J Biol Chem* 2003, **278**:23624-23629
67. Murthy KG, Deb A, Goonesekera S, Szabo C, Salzman AL: **Identification of conserved domains in Salmonella muenchen flagellin that are essential for its ability to activate TLR5 and to induce an inflammatory response in vitro.** *J Biol Chem* 2003.
68. Smith KD, Andersen-Nissen E, Hayashi F, Strobe K, Bergman MA, Barrett SL, Cookson BT, Aderem A: **Toll-like receptor 5 recognizes a conserved site on flagellin required for protofilament formation and bacterial motility.** *Nat Immunol* 2003, **4**:1247-1253.
69. Yamaguchi S, Fujita H, Sugata K, Taira T, Iino T: **Genetic analysis of H2, the structural gene for phase-2 flagellin in Salmonella.** *J Gen Microbiol* 1984, **130(Pt 2)**:255-265.
70. Williams AW, Yamaguchi S, Togashi F, Aizawa SI, Kawagishi I, Macnab RM: **Mutations in fliK and flhB affecting flagellar hook and filament assembly in Salmonella typhimurium.** *J Bacteriol* 1996, **178**:2960-2970.
71. Rock FL, Hardiman G, Timans JC, Kastelein RA, Bazan JF: **A family of human receptors structurally related to Drosophila Toll.** *Proc Natl Acad Sci U S A* 1998, **95**:588-593.

Am J Physiol Lung Cell Mol Physiol 287: L374–L381, 2004
First published April 23, 2004; 10.1152/ajplung.00039.2004.

Impaired nitric oxide synthase-2 signaling pathway in cystic fibrosis airway epithelium

Shuo Zheng,[1] Weiling Xu,[1] Santanu Bose,[2] Amiya K. Banerjee,[2] S. Jaharul Haque,[1] and Serpil C. Erzurum[1,2]

Departments of [1]Pulmonary and Critical Care Medicine, Cancer Biology, and [2]Virology, Cleveland Clinic Foundation, Lerner Research Institute, Cleveland, Ohio 44195

Submitted 9 February 2004; accepted in final form 21 April 2004

Zheng, Shuo, Weiling Xu, Santanu Bose, Amiya K. Banerjee, S. Jaharul Haque, and Serpil C. Erzurum. Impaired nitric oxide synthase-2 signaling pathway in cystic fibrosis airway epithelium. *Am J Physiol Lung Cell Mol Physiol* 287: L374–L381, 2004. First published April 23, 2004; 10.1152/ajplung.00039.2004.—Cystic fibrosis (CF) airway epithelial cells are more susceptible to viral infection due to impairment of the innate host defense pathway of nitric oxide (NO). NO synthase-2 (NOS2) expression is absent, and signal transducer and activator of transcription (STAT) 1 activation is reduced in CF. We hypothesized that the IFN-γ signaling pathway, which leads to NOS2 gene induction in CF airway epithelial cells, is defective. In contrast to a lack of NOS2 induction, the major histocompatibility complex class 2, an IFN-γ-regulated delayed-responsive gene, is similarly induced in CF and non-CF airway epithelial (NL) cells, suggesting an NOS2-specific defect in the IFN-γ signaling pathway. STAT1 and activator protein-1, both required for NOS2 gene expression, interact normally in CF cells. Protein inhibitor of activated STAT1 is not increased in CF cells. IFN-γ induces NOS2 expression in airway epithelial cells through an autocrine mechanism involving synthesis and secretion of IFN-γ-inducible mediator(s), which activates STAT1. Here, CF cells secrete IFN-γ-inducible factor(s), which stimulate NOS2 expression in NL cells, but not in CF cells. In contrast, IFN-γ-inducible factor(s) similarly inhibit virus in CF and NL cells. Thus autocrine activation of NOS2 is defective in CF cells, but IFN-γ induction of antiviral host defense is intact.

IFN-γ-inducible factor; antiviral host defense; signal transducer and activator of transcription 1

LUNG DISEASE IS THE LEADING CAUSE of morbidity and mortality in cystic fibrosis (CF) patients. Compared with other lung diseases, CF lung disease is striking in its relatively restricted bacteria flora, particularly with *Pseudomonas aeruginosa*. Once bacterial colonization is established, it cannot be eradicated. Airway obstruction, chronic bacterial infection, and excessive inflammation progressively destroy the lung and eventually lead to death. Successful therapies include early intervention to prevent bacterial colonization, delay disease progression, and improve the life expectancy of CF patients. As the largest epithelial surface area exposed to microorganisms and particles in the environment, human lungs have an elaborate array of pulmonary defense mechanisms to keep the lung free of infections (10). Increased mucus secretion and airway obstruction cannot solely account for the increased susceptibility to bacterial infection or the selection of the particular flora associated with CF. Furthermore, there does not appear to be a systemic immune defect in CF, rather susceptibility seems to reside within the respiratory tract itself (28). Our previous study showed that CF lung epithelial cells are more susceptible to viral infection, which may predispose CF airways to subsequent bacterial colonization. Loss of nitric oxide (NO) synthase (NOS)-2 expression was identified as one defect in the innate host defense of CF airway epithelial cells (44). High-level production of NO in human airways through the continuous expression of NOS2 is an important component of host defense of the respiratory epithelium (15, 34). Exhaled NO and airway NOS2 are elevated in individuals with inflammatory lung diseases, such as asthma and bronchiolitis compared with healthy controls (4, 18, 25). Despite the inflammatory nature of CF lung disease, NO levels in exhaled breath from CF patients are lower than those from healthy controls and individuals with other inflammatory lung diseases (2, 30). Infants with CF before the onset of respiratory symptoms have mean levels of exhaled NO threefold lower than healthy control infants, suggesting that lower NO in CF is not the result but, rather, a precursor of pulmonary disease (12). Significant reduction of NOS2 immunostaining in CF epithelium, but not in inflammatory cells (33), suggests that NOS2 gene is normal but the signaling pathway regulating its expression is abnormal in CF lung epithelium.

We have previously shown that IFN-γ and virus do not induce NOS2 expression at both the RNA and protein level in CF airway epithelial cells (44). Thus we hypothesize that the absence of NOS2 in CF epithelial cells is due to decreased gene expression as a result of an impaired signaling pathway. Here, we study the IFN-γ-stimulated signaling pathway that regulates NOS2 expression, as well as other IFN-stimulated genes (ISG), using primary human airway epithelial cells (HAEC) derived from CF and non-CF lungs.

MATERIALS AND METHODS

Extraction of HAEC and cell culture. Segments of bronchus were obtained at surgery. Fat and connective tissue were removed as much as possible, and bronchus segments were washed with HBSS (GIBCO Laboratories, Grand Island, NY) several times to remove all blood and connective tissue followed by incubation in 0.1% protease-DMEM (GIBCO) solution with 1% penicillin-streptomycin-fungizone, 20 μg/ml ciprofloxacin, and 200 μg/ml tobramycin at 4°C overnight. Protease was neutralized with 1 ml of heat-inactivated FCS. Tracheal segments were then incubated in HBSS containing 10 mM EDTA, 1% penicillin-streptomycin-fungizone, 20 μg/ml ciprofloxacin, and 200 μg/ml tobramycin at 37°C for 15 min. The epithelial side of the trachea was scraped with a sterile glass slide to remove remaining

Address for reprint requests and other correspondence: S. C. Erzurum, Lung Biology Program, Cleveland Clinic Foundation, Lerner Research Inst., 9500 Euclid Ave/NB40, Cleveland, OH 44195 (E-mail: erzurus@ccf.org).

The costs of publication of this article were defrayed in part by the payment of page charges. The article must therefore be hereby marked "*advertisement*" in accordance with 18 U.S.C. Section 1734 solely to indicate this fact.

adherent cells. Cells were also collected from all previous supernatants and seeded on tissue culture plates precoated with coating medium containing 29 μg/ml collagen (vitrogen; Collagen, Palo Alto, CA), 10 μg/ml BSA (Biofluids), and 10 μg/ml fibronectin (Calbiochem, La Jolla, CA), in serum-free bronchial epithelial basal medium (Clonetics, San Diego, CA) with 1% penicillin-streptomycin-fungizone, 20 μg/ml ciprofloxacin, and 200 μg/ml tobramycin. Some HAEC were also obtained through bronchoscopy with a flexible fiber optic bronchoscope (Olympus BS-IT10; Olympus Optical, Tokyo, Japan) from normal volunteers with no history of lung disease and on no medications. Informed consent was obtained under a protocol approved by the Institutional Review Board at the Cleveland Clinic Foundation. All cells were genotyped for CF mutations by Genzyme Genetics (Boston, MA). In addition, an aliquot of cultured cells was immunostained to confirm epithelial phenotype. In total, seven samples were collected from CF lungs and confirmed to have ΔF508/ΔF508 mutations; these cells are referred to as CF cells. All five samples collected from non-CF explanted lungs and four samples collected from bronchoscopic brushing of healthy volunteers were confirmed to have no known CFTR mutation; these cells are referred to as non-CF airway epithelial (NL) cells. All experiments were performed in CF and NL cells, replicated a minimum of two times, using a minimum of cells from two different donors each for NL and CF cells.

A549 cells, an epithelial cell line derived from lung adenocarcinoma [American Type Culture Collection (ATCC), Rockville, MD], were cultured in MEM (GIBCO) with 10% heat-inactivated FCS. Human IFN-γ was a gift from InterMune (Brisbane, CA). CV-1 cells (CCL 70, ATCC) were maintained in DMEM (GIBCO-BRL) supplemented with 10% fetal bovine serum, penicillin, streptomycin, and glutamine. Recombinant human IL-1β and TNF-α were from Genzyme. Human parainfluenza virus (HPIV) 3 was a gift from Dr. Bishnu De.

RNA extraction and Northern analysis. Total RNA was extracted by GTC-CsCl gradient method and evaluated by Northern analysis using a ^{32}P-labeled major histocompatibility complex class II (MHCII) (DRα) (pCCF52) probe (ATCC) (36) or, as a control, GAPDH cDNA probe (6), and then subjected to autoradiography. Expression of MHCII mRNA relative to GAPDH mRNA was accomplished with a PhosphorImager (Molecular Dynamics) to quantitate relative units.

NOS2 promoter luciferase reporter constructs, transient transfection, and luciferase assay. Full-length human NOS2 promoter luciferase reporter construct, a kind gift from Dr. Joel Moss (5), was transiently transfected into cells at 90% confluence with LipofectAMINE PLUS reagent (Invitrogen, Carlsbad, CA). Twenty-four hours after transfection, cells were treated with cytokines, and cell lysate was collected to evaluate luciferase activity with the Dual-Luciferase Reporter Assay (Promega, Madison, WI). Cotransfection with Renilla luciferase (Promega) was used to normalize transfection efficiency of the luciferase reporter construct.

Western analysis. Adherent cells were scraped off culture plates in lysis buffer [3 mM dithiothreitol (DTT), 5 μg/ml aprotinin, 1 μg/ml leupeptin, 1 μg/ml pepstatin A, 0.1 mM PMSF, 1% Nonidet P-40 (NP-40), and 40 mM HEPES, pH 7.5]. Cell lysate was prepared by three cycles of freeze-thaw and centrifugation at 14,000 *g* for 20 min at 4°C. The supernatant protein concentration was measured by Coomassie Plus protein assay (Pierce, Rockford, IL). Whole cell lysate protein was denatured and reduced in buffer containing 0.05 M Tris, pH 6.8, 1% sodium dodecyl sulfate (SDS), 10% glycerol, 0.00125% bromphenol blue, and 0.5% 2-mercaptoethanol for 2 min at 95°C. Total protein (50 μg/lane) was separated by electrophoresis on 8% or 10% SDS-polyacrylamide gel and then eletrophoretically transferred onto nitrocellulose membrane (Osmonics, Minnetonka, MN) for 1.5 h at 4°C. The membrane was blocked with 5% nonfat milk in 10 mM Tris, 150 mM NaCl, and 0.1% Tween 20, pH 7.0 at room temperature for 1 h with shaking and then with primary antibody overnight at 4°C. After washing, a peroxidase-conjugated secondary antibody was incubated with membrane for 1 h at room temperature followed by washing again. The primary antibodies used for protein detection included a rabbit polyclonal antibody against NOS2 protein (NO53; Merck, Rahway, NJ), a goat polyclonal antibody against protein inhibitor of activated STAT1 (PIAS1; Santa Cruz Biotechnology, Santa Cruz, CA), and a rabbit polyclonal antibody against N protein of HPIV3. The secondary antibodies used were peroxidase-linked donkey anti-rabbit antibody (Amersham, Arlington Heights, IL) or anti-goat antibody (Santa Cruz Biotechnology). As a control of equal protein loading, Western analysis for β-actin was performed with a primary monoclonal anti-β-actin antibody (A-5316; Sigma, St. Louis, MO) followed by a sheep secondary anti-mouse immunoglobulin antibody (Sigma). Enhanced chemiluminescent system (Amersham Laboratories) was used to detect signals and expose films. The image was scanned and relative intensity to β-actin quantitated by ImageQuant 1.2 (Molecular Dynamics).

Nuclear extract and EMSA. Adherent cells (90–100% confluent), treated with reagents as indicated, were washed twice with ice-cold PBS and harvested with a cell lifter. The cell suspensions were centrifuged and resuspended in 0.4 ml of ice-cold buffer [10 mM HEPES (pH 7.9), 10 mM KCl, 0.1 mM EDTA, 0.1 mM EGTA, 0.5 mM PMSF, and 1 mM DTT] by gentle pipetting in a yellow tip, and then cells were allowed to swell on ice for 15 min. Subsequently, 25 μl of 10% solution of NP-40 were added, vigorously vortexed for 10 s, and then spun for 30 s in a microfuge. The nuclear pellet was resuspended in 50 μl of ice-cold buffer [20 mM HEPES (pH 7.9), 25% glycerol, 0.4 M NaCl, 1 mM EDTA, 1 mM EGTA, 1 mM PMSF, and 1 mM DTT].

The duplex oligonucleotide corresponding to IFN-γ activation site [γ-activation sequence (GAS)] in NOS2 promoter region (5′-CGGGCGTTTCCAGTAAAAATC-3′) was synthesized by Operon (Alameda, CA) and then end-labeled with [γ-^{32}P]ATP by polynucleotide kinase. For binding reactions, nuclear extract (NE) containing 4 μg of protein was incubated in 20 μl of total reaction volume containing 20 mM HEPES (pH 7.9), 5% glycerol, 50 mM NaCl, 5 mM DTT, 0.1 mM EDTA, 100 μg/ml BSA, and 2 μg poly(dI-dC) for 15 min at room temperature. The ^{32}P-labeled oligonucleotide (2×10^5 counts/min) was added to the reaction mixture and incubated for 20 min at room temperature. The reaction mixture was analyzed by electrophoresis on a 4% polyacrylamide gel in 0.25× TBE (12.5 mM Tris, 12.5 mM borate, and 0.5 mM EDTA). The gels were dried and analyzed by autoradiography. To demonstrate specificity of binding, we performed competition by adding unlabeled wild-type and mutated oligonucleotide at a 100-fold molar excess of ^{32}P-labeled oligonucleotide probe in the binding reaction. To specifically identify activator protein (AP)-1, STAT1 proteins in binding complexes, 4 μg of rabbit anti-c-fos, c-jun, STAT1 antibody (Santa Cruz Biotechnology), or nonimmune rabbit IgG (Biodesign, Saco, ME) were added to the binding reaction mixture and incubated for 30 min at room temperature before the ^{32}P-labeled oligonucleotide was added.

Whole cell extract and EMSA. The cell suspensions were centrifuged at 1,000 *g* for 5 min at 4°C. The cell pellet was washed in ice-cold PBS and resuspended in 1 ml of ice-cold buffer [10 mM HEPES (pH 7.9), 1.5 mM $MgCl_2$, 10 mM KCl, 20 μM Na-orthovanadate, 0.5 mM DTT, and 0.5 mM PMSF], incubated on ice for 5–10 min, and centrifuged. The cell pellet was resuspended in equal volume of buffer [20 mM HEPES, pH 7.9, 25% glycerol, 0.42 M NaCl, 1.5 mM $MgCl_2$, 0.2 mM EDTA, 0.2 mM Na-orthovanadate, 0.5 mM DTT, 0.5 mM PMSF, 5 μg/ml leupeptin, 200 μg/ml aprotinin, and 10 μg/ml pepstatin A] and incubated on ice for 30 min. Extract was centrifuged at 14,000 *g* for 20 min at 4°C, and the supernatant was used for EMSA. Protein concentration was measured by the Coomassie Plus protein assay (Pierce).

The IFN-γ activation site (GAS) (5′-TCGAGCCTGATTTCCCCGAAATGACG GC-3′), corresponding to the inverted repeat element of human interferon regulatory factor (IRF)-1 gene with a

SalI linker at the 5′-end and the complementary strand, were synthesized by BRL Laboratories (Grand Island, NY). The annealed duplex oligonucleotides were end-labeled with [γ-^{32}P]ATP by polynucleotide kinase. Whole cell extract (WCE) containing 5 μg of protein was incubated at room temperature with total volume of 19 μl of binding reaction buffer [20 mM HEPES (pH 7.9), 10% glycerol, 80 mM NaCl, 1 mM DTT, 0.6 mM EDTA, pH 8.0, 4 mM Tris·HCl, pH 7.9, 5 mM $MgCl_2$, and 3 μg poly(dI-dC)] and 200 μg of end-labeled GAS duplex probe for 20 min. The protein-DNA complex was analyzed by electrophoresis on a 6% polyacrylamide (acrylamide/bis, 75.2) gel with 0.5× TBE (44.5 mM boric acid, 2 mM EDTA, pH 8.0) at room temperature for 1.5–2.0 h. Gels were dried and exposed to X-ray film at −70°C. To specifically identify STAT1 protein in the protein-DNA complex, we added STAT1 antibody (Santa Cruz Biotechnology) to the binding reaction mixture and incubated it for 30 min at room temperature before adding the ^{32}P-labeled oligonucleotide.

Conditioned medium transfer. Cells were stimulated with IFN-γ (1,000 U/ml) for 1 h and washed vigorously with HEPES-buffered saline to remove residual IFN-γ. Fresh culture media were added to the cells and incubated for 72 h. The overlying media [γ-conditioned medium (γCM)] were then transferred to unstimulated fresh cells as indicated. Cell lysates were collected 24 h later for Western analysis. WCE was collected 30 min after conditioned media transfer for EMSA.

Plaque assay. Culture supernatants overlying cells that underwent virus infection were collected, and the yield of infectious HPIV3 in the supernatants was measured by plaque assay as previously described (8). Briefly, samples to be tested were diluted from 1:10^2 to 1:10^7 in opti-MEM (GIBCO-BRL) and placed on CV-1 cells (CCL 70, ATCC). After 1 h at 37°C, the supernatants were removed, and cells were overlaid with freshly made MEM-agar that contains 1% agar, 10% FCS, penicillin, streptomycin, and glutamine. Cells were cultured for 24 h, and the plaques were counted visually under a microscope.

RESULTS

Lack of NOS2 expression and decreased NOS2 promoter activity in CF cells. To confirm that CF cells do not express NOS2 protein, we exposed CF and NL cells to IFN-γ, and cell lysates were collected at 8, 24, and 48 h. NL cells had NOS2 expression at 24 h, and the protein level increased further at 48 h, whereas CF cells did not have detectable NOS2 even at 48 h (Fig. 1*A*). To evaluate NOS2 gene transcription, we cotransfected a 8,296-bp human NOS2 promoter luciferase reporter construct and Renilla luciferase construct (RL-TK) into NL and CF cells at 90% confluence. Twenty-four hours after transfection, the cells were treated with 10^4 U/ml IFN-γ or cytokine mix (CK; 10^4 U/ml IFN-γ, 0.5 ng/ml IL-1β, and 10 ng/ml TNF-α) or left untreated. Cell lysates were collected for luciferase assay, and the NOS2 promoter luciferase activity was normalized to Renilla luciferase activity as a control for transfection efficiency. CF cells had significantly decreased NOS2 promoter activity upon IFN-γ or CK stimulation compared with NL cells ($P < 0.05$) (Fig. 1*B*), indicating a defect in NOS2 expression in CF cells at the transcriptional level.

IFN-γ-induced MHCII expression is not altered in CF cells. NOS2 and MHCII expression are induced as a delayed response to IFN-γ, requiring new protein synthesis. To evaluate whether MHCII expression is impaired in CF cells, we exposed CF and NL cells to 10^4 U/ml IFN-γ and extracted RNA at 2, 8, 24, and 48 h after treatment. Northern analysis revealed MHCII induction at 24 and 48 h after IFN-γ in NL and CF cells (Fig. 2*A*). CF cells were also exposed to different concentrations of IFN-γ (10^2-10^4 U/ml), and RNA was extracted 24 h later. Northern analysis showed a dose-dependent induction of MHCII in CF cells by IFN-γ (Fig. 2*B*). These results indicate that CF cells have a defect in NOS2 expression, whereas other delayed IFN-γ-responsive ISGs are not affected.

Normal STAT1/c-Fos interaction in CF cells following treatment with IFN-γ. Physical interaction between c-fos, a component of AP-1, and STAT1 plays a role in transcriptional activation of NOS2 gene (43). To investigate the interaction between c-fos and STAT1 in CF cells, we exposed CF and NL cells to IFN-γ for 1 h or unstimulated. The NE were analyzed by EMSA with a ^{32}P-labeled duplex oligonucleotide probe corresponding to the IFN-γ activation site (GAS) sequence present in the NOS2 promoter region (Fig. 3*A*). The EMSA revealed that GAS-STAT1 interaction was less in CF than in

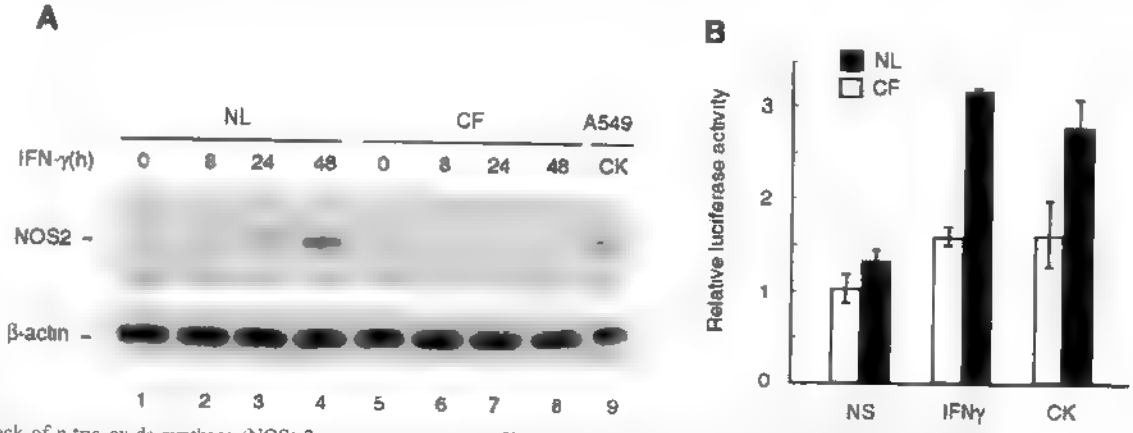

Fig. 1. *A*: lack of nitric oxide synthase (NOS)-2 expression in cystic fibrosis (CF) cells. Cell lysate (50 μg protein/lane) from non-CF airway epithelial (NL) and CF cells stimulated with IFN-γ for 8, 24, and 48 h were evaluated for NOS2 expression by Western blot. Lysate from A549 cells stimulated with cytokine mixture (CK, 10^4 U/ml IFN-γ, 0.5 ng/ml IL-1β, 10 ng/ml TNF-α) for 24 h was used only as positive control (*lane 9*). Similar results were obtained from 2 separate experiments using cells from different donors. *B*: decreased NOS2 promoter activity in CF cells. Cells were cotransfected with human NOS2 promoter luciferase reporter construct (1 ng/ml) and Renilla reporter construct (0.1 ng/ml RL-TK), and then treated with IFN-γ (10^4 U/ml) or CK. CF cells have less NOS2 promoter activity compared with NL ($P < 0.05$). NOS2 promoter activity means ± SD are from 6 separate experiments using cells from different donors. NS, nonstimulated.

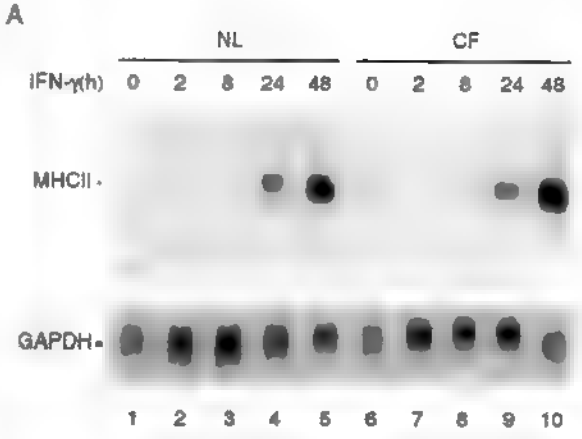

Fig. 2 Major histocompatibility complex class II (MHCII) expression in CF and NL cells. *A*: Northern analysis of total RNA from primary human airway epithelial cells from NL (*lanes 1–5*, 10 μg/lane) or CF (*lanes 6–10*, 10 μg/lane) at indicated hours after IFN-γ stimulation was performed with a ^{32}P-labeled MHCII (DRα) cDNA probe. *B*: Northern analysis of total RNA from airway epithelial cells from CF (*lanes 1–4*, 10 μg/lane) 24 h after IFN-γ stimulation at indicated doses. Human ^{32}P-labeled GAPDH cDNA probe was used as control for RNA loading. Similar results were obtained from 2 separate experiments using cells from different donors.

NL cells. Supershift analysis revealed the presence of STAT-1 and c-fos, but not c-Jun, in DNA-protein complexes in CF and NL cells. These results suggest that c-fos interacts with STAT1 in binding to GAS in CF and NL cells. Thus c-fos is not involved in the impairment of STAT1-DNA binding in CF cells following treatment with IFN-γ.

STAT1 activation is also impaired in mice lacking CFTR expression (24). A previous report suggests that the level of PIAS1 protein, which binds to and inactivates STAT1, is higher in lung epithelium of CF mice (24). Thus we evaluated the expression of PIAS1 in CF and NL cells. CF cells had PIAS1 expression similar to NL at baseline and a lower PIAS1

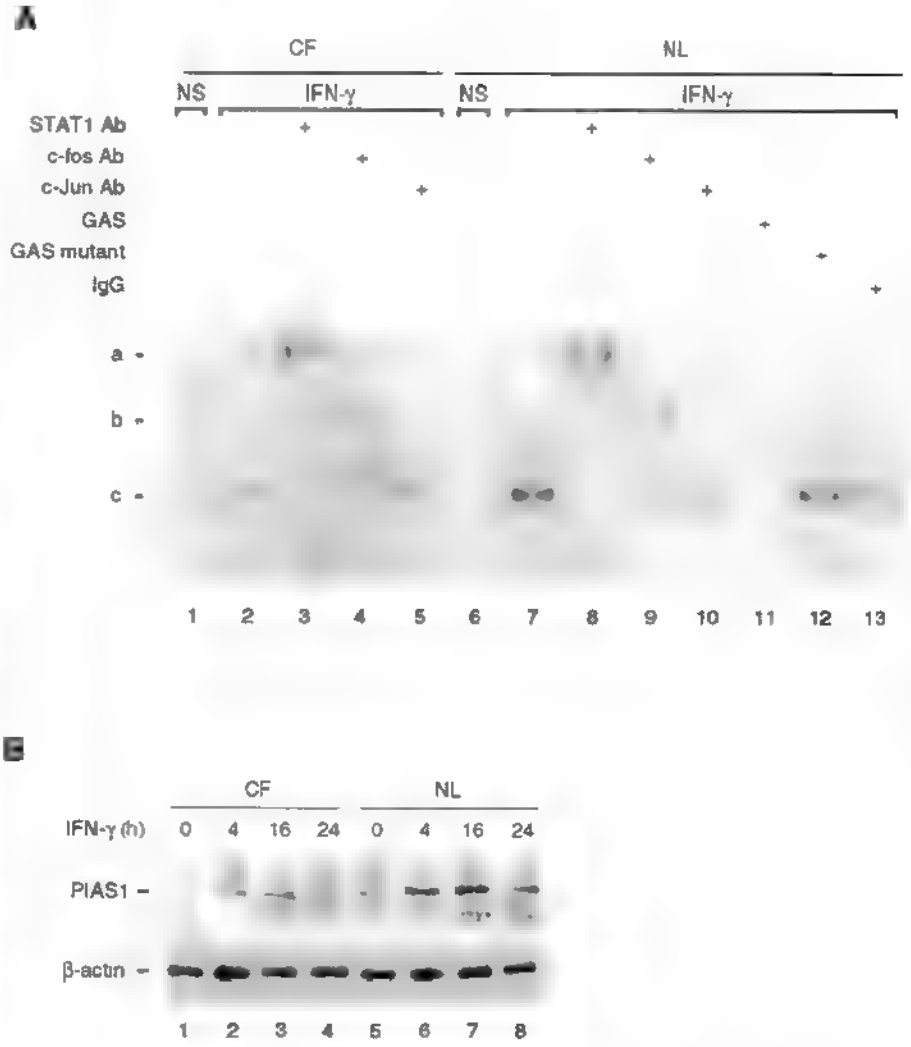

Fig. 3 Impaired STAT1 activation in CF airway epithelial cells. *A*: EMSA of nuclear extract from CF (*lanes 1–5*) or NL (*lanes 6–13*) was performed using [γ-^{32}P]ATP end-labeled NOS2 γ-activation sequence (GAS) oligonucleotide duplex probe. The binding complexes of both CF and NL cells were supershifted by STAT1 (p91) antibodies (Ab) (*lanes 3, 8*) and c-fos Ab (*lanes 4, 9*), but not by c-jun Ab (*lanes 5, 10*) or rabbit unimmune IgG (*lane 15*). Competition with unlabeled probe (*lane 11*) but not NOS2 GAS mutant probe (*lane 12*) confirmed the specificity of the binding complex. *B*: Western analysis of cell lysate (20 μg total protein/lane) from CF (*lanes 1–4*) or NL (*lanes 5–8*) with IFN-γ (10^4 U/ml) stimulation for indicated time was performed using protein inhibitor of activated STAT1 (PIAS1) Ab. β-Actin Ab was used as control of protein loading. Similar results were obtained from 2 separate experiments using cells from different donors.

level after IFN-γ treatment compared with NL cells (Fig. 3*B*). Thus unlike mouse lung epithelium, PIAS1 does not play a role in the decreased STAT-1 activation in CF airway epithelial cells in vitro.

CF cells do not respond to IFN-γ-induced soluble mediator(s). Our previous work identified an autocrine mechanism of induction and maintenance of NOS2 in HAEC through the synthesis and secretion of IFN-γ-stimulated soluble mediator(s) (39). To evaluate the ability of CF cells to produce and respond to these soluble mediator(s), we treated CF and NL cells with IFN-γ for 1 h and washed the cells five times with HEPES-buffered saline, then added fresh media, and cultured them for an additional 72 h. The IFN-γCM were collected and transferred to fresh CF and NL cells, and the cell lysates were collected 24 h later. Western blot analysis showed that, in contrast to the NL cells, CF cells fail to induce NOS2 expression following treatment with γCM derived from either CF or NL cells (Fig. 4*A*). The mechanism(s) of γCM-mediated induction of NOS2 expression is not completely understood but requires activation of STAT1 for NOS2 gene expression (39). To evaluate the STAT1-activating property of γCM derived from CF cells, WCE collected 30 min after γCM transfer to fresh CF and NL cells was subjected to EMSA with ^{32}P-labeled IRF-1 GAS probe, which binds activated STAT1. Both CF and NL cells activate STAT1 following treatment with γCM derived from CF or NL cells (Fig. 4*B*). Thus although STAT1 activation is required to induce NOS2 in cells, these results suggest that additional factors are necessary for NOS2 expression in airway epithelial cells. Furthermore, the ability of CF-γCM to induce NOS2 expression in NL cells lessens the likelihood of a NOS-inhibitory or blocking factor in CF.

Antiviral property of γCM in NL and CF cells. Although NOS2 is absent, IFN-γ pretreatment inhibits viral replication in CF cells, likely through induction of other host defense pathways including double-stranded RNA-dependent protein kinase (PKR) and 2′,5′-oligoadenylate synthetase (38). Because STAT1 activation is essential for antiviral defense and γCM from CF or NL cells led to similar levels of STAT1 activation, we evaluated whether or not the antiviral effect of γCM would be similar in CF and NL cells. γCM collected from CF or NL cells were transferred to other CF or NL cells. After overnight incubation, cells were exposed to HPIV3. Twenty-four hours later, cell lysates were collected and analyzed for viral N-protein synthesis by Western blot. γCM inhibited viral replication in both CF and NL cells, although γCM from CF cells was slightly less effective than γCM from NL (Fig. 5).

Definitive evidence of antiviral effect of conditioned media from NL cells was provided by quantitative viral titers. The active viral particles in the supernatant overlying HPIV3-infected NL cells pretreated with γCM or with the supernatant overlying NL HAEC not exposed to IFN-γ (mock-CM) were determined by viral plaque assay. Production of viral particles was inhibited by γCM compared with mock-CM [γCM, $(3 \pm 1) \times 10^4$ plaque-forming units (pfu)/ml; mock-CM, $(2 \pm 0.7) \times 10^6$ pfu/ml; $n = 3$]. Thus components in γCM from CF and NL HAEC provide antiviral effect. This suggests that CF cells have an inability to express NOS2 in response to IFN-γ or

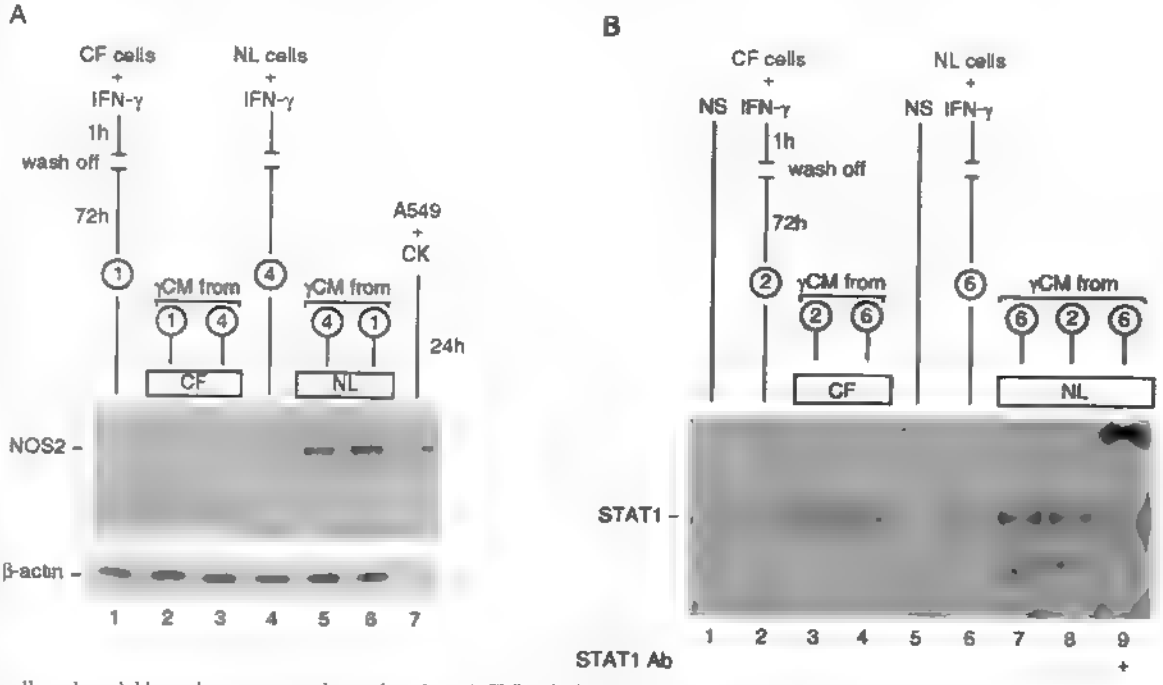

Fig. 4. CF cells make soluble mediator in γ-conditioned medium (γCM), which induces NOS2. *A*: γCM made from CF (*lane 1*) and NL (*lane 4*) cells were transferred to fresh cells. Cell lysates were collected 24 h later, and 20 μg of total protein were subject to Western analysis for NOS2. γCM from CF (*1*) and NL (*4*) both induced NOS2 expression in NL cells (*lanes 5, 6*), but not in CF cells (*lanes 2, 3*). A549 stimulated with CK (IFN-γ, IL-1β, TNF-α) served as positive control for NOS2 expression (*lane 7*). *B*: whole cell extracts were collected 30 min after γCM transfer to cells. Five micrograms of total protein were used in EMSA using ^{32}P-labeled interferon regulatory factor-1 GAS. γCM from both CF (*2*) and NL (*6*) cells activated similar level of STAT1 in CF (*lanes 3, 4*) and NL (*lanes 7–10*) cells. Supershift with STAT1 Ab confirmed the specificity of the binding complex (*lane 9*). Similar results were obtained from 2 separate experiments using cells from different donors.

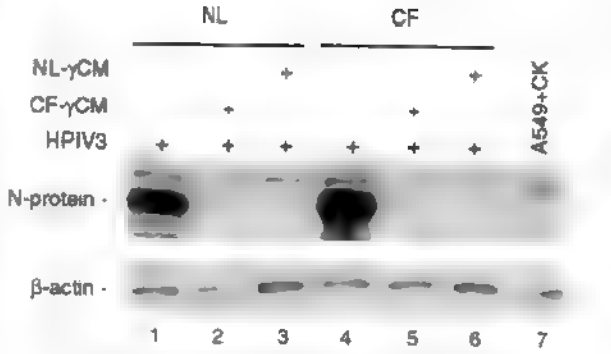

Fig. 5. γCM inhibits viral replication. Western analyses of viral N protein in lysates (20 μg/lane) of NL and CF cells infected with human parainfluenza virus (HPIV) 3. γCM derived from NL (NL-γCM) or CF cells (CF-γCM) inhibit viral N-protein production and, hence, virus replication in cells (*lanes 2, 3, 5, and 6*). CF-γCM may not be as completely effective in antiviral effect as NL-γCM. Similar results were obtained from 3 separate experiments using cells from different donors.

γCM but have other effective inducible antiviral systems that respond appropriately to IFN or γCM.

DISCUSSION

NO produced by NOS2, following its induction by inflammatory cytokines, acts as a major effector in host defense against virus and bacteria. The expression of NOS2 in healthy airway epithelial cells has been demonstrated at both the protein and mRNA levels in vivo (15, 16, 26). CF airway epithelial cells are more susceptible to viral and bacterial infection because of defective innate host defense mechanisms of NOS2 expression and STAT1 activation (23, 29, 44). Here, the mechanism for lack of NOS2 expression in CF is identified at the transcriptional level with decreased NOS2 promoter activity in CF cells in response to IFN-γ.

When bound to its specific receptor on the cell membrane, IFN-γ initiates a signaling cascade, which leads to immediate and/or delayed expression of ISGs (19, 42). NOS2, along with MHCII, is one of the genes induced by IFN-γ as a delayed response, whereas STAT1 and IRF-1 are immediate-response genes (1, 15–17, 41, 42). MHCII and IRF-1 are similarly induced by IFN-γ in both CF and NL cells (44). However, we previously showed that STAT1 induction and activation are impaired in CF (44). This suggests that the delayed and immediate IFN-γ-signaling pathways are intact but that component(s) involved in the regulation of NOS2 expression may be specifically affected in CF cells.

Studies of the human NOS2 promoter have identified important regulatory components in the promoter, including AP-1 sites, nuclear factor-κB sites, GAS, and IRF-1 sites (5, 31, 35). Only impairment of STAT1 has been identified in CF; other signal transduction molecules are similarly activated in CF and NL cells (44). Interaction between c-fos, a component of AP-1, and STAT1 is required for NOS2 induction by IFN-γ in airway epithelial cells (43). Here, CF cells exposed to IFN-γ have c-fos and STAT1 interaction and binding to GAS, indicating that AP-1 is not involved in the decreased STAT1-GAS binding. In contrast to previous studies using CF mouse models, PIAS1 is not overexpressed by human CF cells, and IFN-γ does not induce PIAS1 in CF or NL cells. Thus PIAS1 is not the cause of decreased STAT1 activation or lack of NOS2 expression in CF cells.

Induction of NOS2 by IFN-γ in airway epithelial cells occurs through an autocrine mechanism by which IFN-γ induces synthesis and secretion of soluble mediator(s) that activate STAT1 and induce NOS2 expression (15, 17, 39). Here, CF cells also synthesize and secrete soluble mediator(s) that induce NOS2 expression in NL cells. However, γCM derived from NL or CF cells does not induce NOS2 expression in CF cells, although CF cells respond to γCM through activation of STAT1. A similar level of STAT-1 activation in NL and CF cells by γCM suggests that the STAT1 activation in CF is not uniformly impaired for all inducing factors.

Consistent with the central role of STAT1 for antiviral effects, the γCM has potent antiviral activity, although the CF γCM is not as complete in antiviral protection as NL γCM. The fact that γCM fails to induce NOS2 expression in CF cells but still protects CF cells from viral infection indicates that NO does not mediate the antiviral effects of conditioned media and points out the redundancy in antiviral defenses.

Currently, we have little information about the identity of the IFN-γ-induced soluble mediator(s) that induces NOS2 and/or the antiviral factor(s) (17, 39). There are likely many proteins and mediators present in the γCM. Researchers have identified >300 ISGs from pooled data sets of HT1080 fibrosarcoma cells stimulated with IFN-α/β/γ. The ISGs are classified into functional categories, including 51 genes involved in host defense, 8 genes involved in antiviral mechanisms, 12 hormones, 15 growth factors, and 6 chemokines (9). Some of the cytokines and growth factors stimulate STAT1 activation, such as prolactin, colony-stimulating factor-1, and epidermal growth factor (7, 21, 32). Prolactin, a pituitary hormone, also acts as a cytokine at various extrapituitary sites including immune cells (40). Interestingly, prolactin may induce NOS2 expression in granulocytes and in peripheral blood mononuclear cells through at least two different signaling pathways, the STAT and the MAP kinase pathways (11). There are also several specific airway epithelial secreted factors that have antimicrobial activities, including β-defensin, lysozyme, surfactant, secretory phospholipase A_2, secretory leukocyte protease inhibitor, and the regulated on activation, normal T cells expressed and secreted factor (3, 14, 20, 27). Further investigation is required to understand in detail the precise mechanism(s) that regulates NOS2 expression in human lung epithelial cells and the role of NOS2 in innate host defense. However, on the basis of prior studies and our data, we suggest a model for NOS2 induction in respiratory epithelial cells and the defect in CF. Upon binding to its specific receptor on the cell membrane, IFN-γ activates the JAK/STAT pathway and induces the expression of a set of ISGs including the soluble mediator(s). The soluble mediator(s) is secreted and stimulates the cells in an autocrine fashion to activate STAT1 and other factors that are required for NOS2 expression (39). STAT1 activation and its downstream targets, as well as other secreted host defense ISGs, provide antiviral protection to cells. The defect in human CF cells appears to be in the response to the secreted soluble mediator(s).

Extension of CF children's life expectancy occurred with the introduction of antibiotics, but also through vaccination against virus. For example, vaccination against measles was one of the earliest interventions that led to improved survival in the 1960s

(22). Before vaccination, CF children who contracted measles, a virus like HPIV3 in the paramyxovirus family, had progressive decline in their general condition, worsening of pulmonary infections, and early death (13, 37). These clinical observations, together with the identification of enhanced virus susceptibility of CF airway cells, suggest that therapies aimed at improving antiviral host defense may further delay the onset of bacterial colonization and extend the lives of CF individuals.

ACKNOWLEDGMENTS

Thanks to C. Bevins and B. De for helpful discussions, B. De for HPIV3 antibody, J. Moss for NOS2 promoter, J. Lang for artwork, J. Foertch for assistance with clinical samples, and InterMune for IFN-γ.

GRANTS

This work was supported in part by Department of Army Medical Research and Development Grant 17-01-C-0065 and National Institutes of Health Grants HL-60917, HL-04265, M01 RR-018390, and AI-70649.

REFERENCES

1. **Asano K, Chee CB, Gaston B, Lilly CM, Gerard C, Drazen JM, and Stamler JS.** Constitutive and inducible nitric oxide synthase gene expression, regulation, and activity in human lung epithelial cells. *Proc Natl Acad Sci USA* 91: 10089–10093, 1994.
2. **Balfour-Lynn IM, Laverty A, and Dinwiddie R.** Reduced upper airway nitric oxide in cystic fibrosis. *Arch Dis Child* 75: 319–322, 1996.
3. **Bals R, Weiner DJ, and Wilson JM.** The innate immune system in cystic fibrosis lung disease. *J Clin Invest* 103: 303–307, 1999.
4. **Belvisi M, Barnes PJ, Larkin S, Yacoub M, Tadjkarimi S, Williams TJ, and Mitchell JA.** Nitric oxide synthase activity is elevated in inflammatory lung disease in humans. *Eur J Pharmacol* 283: 255–258, 1995.
5. **Chu SC, Marks-Konczalik J, Wu HP, Banks TC, and Moss J.** Analysis of the cytokine-stimulated human inducible nitric oxide synthase (iNOS) gene: characterization of differences between human and mouse iNOS promoters. *Biochem Biophys Res Commun* 248: 871–878, 1998.
6. **Comhair SA, Thomassen MJ, and Erzurum SC.** Differential induction of extracellular glutathione peroxidase and nitric oxide synthase 2 in airways of healthy individuals exposed to 100% O(2) or cigarette smoke. *Am J Respir Cell Mol Biol* 23: 350–354, 2000.
7. **Darnell JE Jr, Kerr IM, and Stark GR.** Jak-STAT pathways and transcriptional activation in response to IFNs and other extracellular signaling proteins. *Science* 264: 1415–1421, 1994.
8. **De BP, Gupta S, and Banerjee AK.** Cellular protein kinase C isoform zeta regulates human parainfluenza virus type 3 replication. *Proc Natl Acad Sci USA* 92: 5204–5208, 1995.
9. **De Veer MJ, Holko M, Frevel M, Walker E, Der S, Paranjape JM, Silverman RH, and Williams BR.** Functional classification of interferon-stimulated genes identified using microarrays. *J Leukoc Biol* 69: 912–920, 2001.
10. **DeLong PA and Kotloff RM.** An overview of pulmonary host defense. *Semin Roentgenol* 35: 118–123, 2000.
11. **Dogusan Z, Hooghe R, Verdood P, and Hooghe-Peters EL.** Cytokine-like effects of prolactin in human mononuclear and polymorphonuclear leukocytes. *J Neuroimmunol* 120: 58–66, 2001.
12. **Elphick HE, Demoncheaux EA, Ritson S, Higenbottam TW, and Everard ML.** Exhaled nitric oxide is reduced in infants with cystic fibrosis. *Thorax* 56: 151–152, 2001.
13. **Enders JF, McCarthy CK, Mitus A, and Cheatham WJ.** Isolation of measles virus at autopsy in cases of giant-cell pneumonia without rash. *N Engl J Med* 261: 875–881, 1959.
14. **Ganz T.** Antimicrobial polypeptides in host defense of the respiratory tract. *J Clin Invest* 109: 693–697, 2002.
15. **Guo FH, De Raeve HR, Rice TW, Stuehr DJ, Thunnissen FB, and Erzurum SC.** Continuous nitric oxide synthesis by inducible nitric oxide synthase in normal human airway epithelium in vivo. *Proc Natl Acad Sci USA* 92: 7809–7813, 1995.
16. **Guo FH and Erzurum SC.** Characterization of inducible nitric oxide synthase expression in human airway epithelium. *Environ Health Perspect* 106, *Suppl* 5: 1119–1124, 1998.
17. **Guo FH, Uetani K, Haque SJ, Williams BR, Dweik RA, Thunnissen FB, Calhoun W, and Erzurum SC.** Interferon gamma and interleukin 4 stimulate prolonged expression of inducible nitric oxide synthase in human airway epithelium through synthesis of soluble mediators. *J Clin Invest* 100: 829–838, 1997.
18. **Hamid Q, Springall DR, Riveros-Moreno V, Chanez P, Howarth P, Redington A, Bousquet J, Godard P, Holgate S, and Polak JM.** Induction of nitric oxide synthase in asthma. *Lancet* 342: 1510–1513, 1993.
19. **Haque SJ and Williams BR.** Signal transduction in the interferon system. *Semin Oncol* 25: 14–22, 1998.
20. **Hartshorn KL, Holmskov U, Hansen S, Zhang P, Meschi J, Mogues T, White MR, and Crouch EC.** Distinctive anti-influenza properties of recombinant collectin 43. *Biochem J* 366: 87–96, 2002.
21. **Hill CS and Treisman R.** Transcriptional regulation by extracellular signals: mechanisms and specificity. *Cell* 80: 199–211, 1995.
22. **Huang NN, Macri CN, Girone J, and Sproul A.** Survival of patients with cystic fibrosis. *Am J Dis Child* 120: 289–295, 1970.
23. **Kelley TJ and Drumm ML.** Inducible nitric oxide synthase expression is reduced in cystic fibrosis murine and human airway epithelial cells. *J Clin Invest* 102: 1200–1207, 1998.
24. **Kelley TJ and Elmer HL.** In vivo alterations of IFN regulatory factor-1 and PIAS1 protein levels in cystic fibrosis epithelium. *J Clin Invest* 106: 403–410, 2000.
25. **Kharitonov SA, Yates D, Robbins RA, Logan-Sinclair R, Shinebourne EA, and Barnes PJ.** Increased nitric oxide in exhaled air of asthmatic patients. *Lancet* 343: 133–135, 1994.
26. **Kobzik L, Bredt DS, Lowenstein CJ, Drazen J, Gaston B, Sugarbaker D, and Stamler JS.** Nitric oxide synthase in human and rat lung: immunocytochemical and histochemical localization. *Am J Respir Cell Mol Biol* 9: 371–377, 1993.
27. **Konno S, Grindle KA, Lee WM, Schroth MK, Mosser AG, Brockman-Schneider RA, Busse WW, and Gern JE.** Interferon-gamma enhances rhinovirus induced RANTES secretion by airway epithelial cells. *Am J Respir Cell Mol Biol* 26: 594–601, 2002.
28. **Konstan MW and Melvin B.** Infection and inflammation of the lung in cystic fibrosis. In: *Cystic Fibrosis*, edited by Davis PB. New York: Dekker, 1993, vol. 64, p. 223–233. (Lung Biol. Health Dis. Ser.)
29. **Kreiselmeier NE, Kraynack NC, Corey DA, and Kelley TJ.** Statin-mediated correction of STAT1 signaling and inducible nitric oxide synthase expression in cystic fibrosis epithelial cells. *Am J Physiol Lung Cell Mol Physiol* 285: L1286–L1295, 2003.
30. **Lundberg JO, Nordvall SL, Weitzberg E, Kollberg H, and Alving K.** Exhaled nitric oxide in paediatric asthma and cystic fibrosis. *Arch Dis Child* 75: 323–326, 1996.
31. **Marks-Konczalik J, Chu SC, and Moss J.** Cytokine-mediated transcriptional induction of the human inducible nitric oxide synthase gene requires both activator protein 1 and nuclear factor kappaB-binding sites. *J Biol Chem* 273: 22201–22208, 1998.
32. **Marshall CJ.** Specificity of receptor tyrosine kinase signaling: transient versus sustained extracellular signal-regulated kinase activation. *Cell* 80: 179–185, 1995.
33. **Meng QH, Springall DR, Bishop AE, Morgan K, Evans TJ, Habib S, Gruenert DC, Gyi KM, Hodson ME, Yacoub MH, and Polak JM.** Lack of inducible nitric oxide synthase in bronchial epithelium: a possible mechanism of susceptibility to infection in cystic fibrosis. *J Pathol* 184: 323–331, 1998.
34. **Sanders SP, Siekierski ES, Porter JD, Richards SM, and Proud D.** Nitric oxide inhibits rhinovirus-induced cytokine production and viral replication in a human respiratory epithelial cell line. *J Virol* 72: 934–942, 1998.
35. **Saura M, Zaragoza C, Bao C, McMillan A, and Lowenstein CJ.** Interaction of interferon regulatory factor-1 and nuclear factor kappaB during activation of inducible nitric oxide synthase transcription. *J Mol Biol* 289: 459–471, 1999.
36. **Sekaly RP, Tonnelle C, Strubin M, Mach B, and Long EO.** Cell surface expression of class II histocompatibility antigens occurs in the absence of the invariant chain. *J Exp Med* 164: 1490–1504, 1986.

37. **Shwachman H, Katz S, and Kulczycki LL.** Attenuated measles vaccine in cystic fibrosis. *Am J Dis Child* 103: 405–409, 1962.
38. **Stark GR, Kerr IM, Williams BR, Silverman RH, and Schreiber RD.** How cells respond to interferons. *Annu Rev Biochem* 67: 227–264, 1998.
39. **Uetani K, Thomassen MJ, and Erzurum SC.** Nitric oxide synthase 2 through an autocrine loop via respiratory epithelial cell-derived mediator. *Am J Physiol Lung Cell Mol Physiol* 280: L1179–L1188, 2001.
40. **Vera-Lastra O, Jara LJ, and Espinoza LR.** Prolactin and autoimmunity. *Autoimmun Rev* 1: 360–364, 2002.
41. **Warner RL, Paine R III, Christensen PJ, Marletta MA, Richards MK, Wilcoxen SE, and Ward PA.** Lung sources and cytokine requirements for in vivo expression of inducible nitric oxide synthase. *Am J Respir Cell Mol Biol* 12: 649–661, 1995.
42. **Williams BR.** Transcriptional regulation of interferon-stimulated genes. *Eur J Biochem* 200: 1–11, 1991.
43. **Xu W, Comhair SA, Zheng S, Chu SC, Marks-Konczalik J, Moss J, Haque SJ, and Erzurum SC.** STAT-1 and c-Fos interaction in nitric oxide synthase-2 gene activation. *Am J Physiol Lung Cell Mol Physiol* 285: L137–L148, 2003.
44. **Zheng S, De BP, Choudhary S, Comhair SA, Goggans T, Slee R, Williams BR, Pilewski J, Haque SJ, and Erzurum SC.** Impaired innate host defense causes susceptibility to respiratory virus infections in cystic fibrosis. *Immunity* 18: 619–630, 2003.

Analysis of genes induced by Sendai virus infection of mutant cell lines reveals essential roles of IRF-3, NFκB, and interferon, but not TLR3

Christopher P. Elco[1,3], Jeanna M. Guenther[2], Bryan R.G. Williams[2,3], Ganes C. Sen[1,3]*

Departments of Molecular Biology[1] and Cancer Biology[2], Lerner Research Institute, The Cleveland Clinic Foundation, Cleveland, OH 44195; and Graduate Program in Molecular Virology[3], Case Western Reserve University, Cleveland, OH 44106

Running Title: Gene induction by Sendai virus

*Corresponding author: Ganes C. Sen, Dept. of Molecular Biology/NC20, Lerner Research Inst., The Cleveland Clinic Foundation, 9500 Euclid Ave., Cleveland, OH 44195. Phone: 216-444-0636. Fax: 216-444-0513. Email: seng@ccf.org.

Word Count

Abstract: 213

Text: 5142

Abstract

Sendai virus (SeV) infection causes the transcriptional induction of many cellular genes that are also induced by interferon (IFN) or double-stranded (ds) RNA. We took advantage of various mutant cell lines to investigate the putative roles of the components of the IFN-and dsRNA-signaling pathways in the induction of those genes by SeV. Profiling the patterns of gene expression in SeV-infected cells demonstrated that Toll-Like Receptor 3, although essential for gene induction by dsRNA, was dispensable for gene induction by SeV. In contrast, Jak1, which mediates IFN signaling, was required for the induction of a small subset of genes by SeV. NFκB and IRF-3, the two major transcription factors activated by virus infection, were essential for the induction of two sets of genes by SeV. As expected, some of the IRF-3-dependent genes, such as ISG56, were more strongly induced by SeV in IRF-3-overexpressing cells. Surprisingly, in those cells, a number of NFκB-dependent genes, such as A20, were induced poorly. Using a series of cell lines expressing increasing levels of IRF-3, we demonstrated that the degree of induction of A20 mRNA, upon SeV infection, was inversely proportional to the cellular level of IRF-3, whereas that of ISG56 mRNA was directly proportional. Thus, IRF-3 can suppress the expression of NFκB dependent genes in SeV-infected cells.

Introduction

Many cellular genes, encoding proteins of diverse functions, are transcriptionally induced during viral infections (6, 15, 32, 40, 47). Because host-virus co-evolution has tolerated this host response to virus infection, it is thought to be conducive to maintaining proper homeostasis between viral proliferation and host survival. A large number of virally induced proteins have direct or indirect anti-viral effects. They may inhibit protein synthesis in the infected cells (17), impair viral assembly (7), initiate the innate immune response, or prime the adaptive immune response (29). Diverse components of the infecting viruses or viral intermediates, produced during its replication, can be the responsible agents that trigger the signaling pathways leading to cellular gene induction. Depending on the specific virus, viral envelope proteins (5), viral ribonucleoproteins (41), or viral single-stranded (ss) (28) or double-stranded (ds) RNAs (1, 11, 46) have been shown to be the critical agent. Among these, dsRNA has been viewed as the most important agent because it is produced in many virus-infected cells, moreover synthetic dsRNA, when added to cells, can induce transcription of some of the same cellular genes that are induced by virus infection (14). A major transducer of signaling, generated by exogenously added dsRNA or intracellular viral dsRNA, is a member of the Toll-like receptor (TLR) family, TLR3 (1).

One set of common genes induced by many viruses and dsRNA encode type I interferons (IFNs) (29). These secreted cytokines have strong anti-viral effects. Surprisingly, many dsRNA-induced and virally induced cellular genes are also induced by IFNs (37), thus creating a positive feedback loop that reinforces induction of the same genes in infected cells.

To better understand the repertoires of genes induced by Sendai virus (SeV) infection of cells in culture, we have classified them into groups that are induced by IFNs, dsRNA, or other viral products. For identifying SeV-induced genes, we used cDNA microarrays customized for this purpose, and based on genes we previously identified whose transcription is induced by IFNs (9, 10) or dsRNA (14). In addition to many virally induced genes, dsRNA- and IFN-inducible genes were represented in the microarray used here. We had previously used mutant cell lines, which could not respond to IFN or dsRNA to delineate the signaling pathways activated by the different inducers (3, 24, 43). To assess the relative contributions of the IFN- and the dsRNA-signaling pathways in gene induction by SeV, we again took advantage of some of those mutant cell lines. Other mutant cell lines were used to investigate the relative contributions of NFκB and IRF-3, the major transcription factors activated by SeV infection, to cellular gene induction (21, 36).

Our study revealed that among the genes that are induced immediately after SeV infection, only a few were dependent on IFN signaling and none were dependent on dsRNA signaling through TLR3. As expected, one class of genes required NFκB, whereas another class required IRF-3 for induction in SeV-infected cells. Surprisingly, viral induction of a subset of NFκB-dependent genes was negatively regulated by IRF-3, thus revealing a new aspect of cross-talk between the two transcription factors.

Materials and Methods

Cell culture. The cell lines used in this paper and their principal characteristics are listed in Table 1. All cell lines were cultured in DMEM with 10% FBS, 2mM L-Glutamine, 50 units/ml penicillin, and 50μg/ml streptomycin. 293/TLR3 cells were derived from 293 cells transfected with a TLR3 expression vector as described previously and cultured in 400 μg/ml G418(38). Wt 2fTGH cells, Jak1 deficient U4C cells, and IRF-3 deficient P2.1 cells have been discussed previously(24). The generation of U4C.2 cells, a U4C-derived line overexpressing IRF-3, along with 2F-SR cells, which express the dominant negative IκBα super repressor was described by Peters, et al (36). These cells were cultured respectively in the presence of either puromycin or G418. 1080.10 cells are a clonal line derived from HT1080 cells co-transfected with the IRF-3 expression vector, pCDNA3/hIRF-3 and the selection vector pBABE/Puro. Following selection with puromycin, 1080.10 and other clones were picked from the stably transfected cells and screened by Western blotting for increased IRF-3 expression.

Treatment methods. Treatment of cells with dsRNA was carried out as described previously(36). Briefly, poly(I)•poly(C) (Amersham) was added directly to the culture media to a final concentration of 100 μg/ml for six hours. Sendai virus infection was carried out as previously described by Heylbroeck, et al (20). Culture media was removed from cells and replaced with serum-free DMEM. Sendai virus (Charles River, SPAFAS, Cantell strain) was added directly to the media to a final concentration of 1HAU/4.0x10^3 cells (~10-15 pfu/cell) and incubated for 1 hour with gentle shaking every

10 minutes. Following viral adsorption, the media was removed and replaced with DMEM containing 10% FBS for the remainder of the experiment.

RNA Isolation. For both Microarray and RPA experiments, total cellular RNA was isolated from cells using the RNA-Bee kit (Tel-Test, Friendswood, TX). Following isolation, RNA was washed twice in 70% EtOH and dissolved in water.

Array construction. The array used in this study comprised a subset of sequence verified cDNA clones from the Research Genetics 40K set. The clones included 950 genes containing adenylate/uridylate rich elements and 18 genes potentially involved in AU-directed mRNA decay as previously described (13), 855 interferon stimulated genes representing an expansion of a previously described clone set (9), 288 genes responsive to the viral analog poly (I).poly(C), representing an expansion of the clone set described by Geiss et.al.(14) and 85 housekeeping genes. DNA preparation and slide printing were as previously described (13) except for the use of 50% DMSO as printing solution.

RNA labeling and array hybridization. Cy3 or Cy5 labeled cDNA was prepared by direct incorporation. 100 µg of total RNA, 2 µg dT_{12-18} primer (Invitrogen), and 1 µl anti-RNAse (Ambion) were combined in a reaction volume of 30 µl and incubated for 10 min at 70°C. Reverse transcription was for 2hr at 42°C in a 50 µl reaction containing annealed RNA template, 1X 1st strand buffer (Invitrogen), 500 µM each dATP, dCTP, dGTP, 300µM dTTP, 250 µM dUTP (Sigma), 3nmol Cy3-dUTP or Cy5-dUTP, 10mM DTT, and 6U/µl Superscript II. For template hydrolysis, 10 µl 0.1M NaOH was added to the

reverse transcription reaction and the mixture was incubated for 10 mins at 70°C, allowed to cool at room temperature for 5 min and neutralized by addition of 10 µl 0.1M HCl. The cDNA was purified with GFX columns following the manufacturer's instructions (Amersham Pharmacia Biotech), dried down, and resuspended in hybridization buffer containing 2X SSC, 0.1% SDS, 4 µg of poly(dA)40-60, and 4 µg of yeast tRNA. The Cy3 and Cy5-labeled cDNAs were pooled and after 2 min denaturation at 90°C the hybridization mixture was applied to the microarray slide under a coverslip. Hybridization proceeded overnight in a sealed moist chamber in a 55°C waterbath. Post-hybridization, slides were washed successively for 5 min each in 2 X SSC plus 0.1% SDS at 55°C, 2 X SSC at 55°C, and 0.2 X SSC at room temperature, spun dry, and scanned on a GenePix 4000A scanner (Axon).

Data acquisition and normalization. Data were acquired with a GenePix 4000A laser scanner and GenePix Pro 5.0 software as previously described(13). Raw data were imported into Genespring 6.0 software (Silicon Genetics) and normalized based on the distribution of all values with locally weighted linear regression (LOWESS) before further analysis.

To assure reproducibility, three microarrays experiments, using different biological repeats and one dye swap, were performed for every cell line infected with SeV. For assessing the effects of dsRNA, two microarray experiments, using different biological samples were conducted in both the 293 and 293/TLR3 cell lines. Spots representing genes with fluorescent intensities of less than 200 units in the SeV- or dsRNA-treated samples were excluded when surveying for changes in expression. A

gene was considered to be induced by SeV or dsRNA in a particular cell type if its expression in treated cells was at least two-fold greater than its expression in uninfected cells in at least two microarray experiments.

Ribonuclease Protection Assay (RPA) and Northern Blotting.

RPAs were performed using the RPA III kit (Ambion, Austin, TX). The actin and 561 RPA probes were described previously by Peters *et al.* (36). The A20, Follistatin and NOXA RPA probes were made from their respective cDNA microarray constructs and correspond to the final 220, 164, or 158 nucleotides of each mRNA. Northern blotting was performed as described previously(14). The full length cDNA was used as a probe for OAS p69. Gene induction was measured using a Storm Imager and quantified with Image Quant 5.2 (Molecular Dynamics).

Results

Role of TLR3 in gene induction by Sendai virus.

To determine the importance of the TLR3-mediated dsRNA- signaling pathway for gene induction by SeV we used HEK293-derived cell lines. The parental cell line does not express any TLR3 whereas a derived line, 293/TLR3, does. In the absence of TLR3, 293 cells do not respond to exogenously added dsRNA, however upon the expression of TLR3, the cells are able to respond robustly (1). Thus, a comparison of the genes induced by SeV in this pair of cell lines enabled us to assess the importance of TLR3-mediated viral dsRNA-signaling. To focus on the primary cellular response to virus in the absence of paracrine or autocrine signaling, cells were infected with SeV at a high m.o.i. and gene induction was measured six hours after infection. From our previous experience, six hours was the optimum time to observe the strong direct induction of genes by SeV, with minimal secondary induction (18).

For transcript profiling, a cDNA microarray of 2196 genes including 288 previously identified dsRNA-regulated genes(14) and 855 interferon induced genes(9) was used. Because dsRNA and IFN induce many of the same genes as viral infection does, this array was well suited to study differential gene induction. Total RNA from infected cells and their uninfected counterparts was used to make fluorescently-labeled cDNA and compared to each other by microarray analysis. Individual gene induction or repression by SeV infection was determined from the ratio of relative fluorescent intensities between the infected and uninfected samples.

SeV infection was able to alter the expression of multiple genes in 293 cells; expression of 36 genes was elevated whereas that of many others was reduced in virus-

infected cells (Fig. 1A). In 293/TLR3 cells, the patterns were not markedly different (Fig. 1B), indicating that TLR3 plays an insignificant role in gene induction by SeV. In contrast, TLR3 was required for the responsiveness of the cells to dsRNA treatment (Fig. 1C, 1D).

We next examined induction of specific genes to verify the apparent lack of importance of TLR3 in global gene regulation by SeV. All of the genes induced over 2-fold in at least two of three microarray experiments by SeV in 293/TLR3 cells were also induced in 293 cells. Interferon stimulated genes (ISGs) 15, 54 and 56, along with A20 (TNFAIP3) and interleukin 8 genes, were all strongly induced by SeV- infection and dsRNA-treatment; induction of all five genes by dsRNA required TLR3, but SeV was able to induce them all without TLR3 (Fig. 1E). To confirm the microarray data, we used RNase-protection assays to quantitate the levels of ISG56mRNA (Fig. 1F). As expected, SeV induction of ISG56 was TLR3-independent, while its induction by dsRNA was TLR3-dependent. Moreover, the levels of ISG56 mRNA in SeV-infected 293 and 293/TLR3 cells were similar (Fig. 1F, lanes 3 and 6), indicating that even for the maximal induction of this mRNA, the viral signaling pathway did not require TLR3.

Although there was a differential need of TLR3, because both agents induced many common genes, we wondered whether the profiles of genes induced by dsRNA and SeV were completely overlapping. This was not the case. Of the 36 genes were induced by SeV in 293 cells, and the 35 genes induced by dsRNA in 293/TLR3 cells, only nine were common. In addition to the five genes shown in Fig 1E, FUT2, syndecan4, IκBα, and NOXA also belonged to this class. A few examples of differentially induced genes

are given in Fig. 2. These results suggest that the signaling pathways used by the two agents are different, although some of them may be shared.

Involvement of IFN-signaling in gene induction by SeV

SeV-infection is known to induce IFN synthesis and many of the genes induced by SeV are also induced by IFNs. Thus, it is possible that some genes are induced in SeV-infected cells by the autocrine action of newly synthesized IFN. To test this possibility, we compared gene induction in SeV-infected U4C and 2fTGH cells (Fig. 3). U4C cells, unlike their parental line 2fTGH, lack functional Jak1, which is required for both type I and type II IFN signaling. Consequently, IFNs cannot induce any genes in U4C cells (31). As in 293 cells, many genes were strongly induced in 2fTGH cells after 6h of SeV-infection (Fig. 3A). Using the criterion of 2-fold induction as the cut-off, we observed that 49 genes were induced in 2fTGH cells. Only, a small subset of genes, 14 of the 49 were not induced over 2-fold by SeV in U4C cells as well. Hence the majority of genes induced in 2fTGH cells were also induced in U4C cells indicating that Jak1, and hence IFN-signaling, were not involved in their induction. A20 and OAS p69 were selected as representatives of IFN-independent and dependent genes and induction of the corresponding mRNAs was monitored by RPA and Northern blotting respectively. Those quantitative assays supported the conclusions drawn from the microarray analyses: A20 mRNA was induced by SeV-infection of either cell line but OAS mRNA was not induced in U4C cells (Fig. 3B). Surprisingly, another small subset of six genes was induced in U4C cells but not in 2fTGH cells, suggesting a suppressive function of Jak1 (Fig. 3A).

Role of NFκB in SeV signaling

One of the major transcription factors activated by viral infections is NFκB. To assess its role in gene induction by SeV, we took advantage of another mutant cell line 2F-SR. This line was derived from the 2fTGH line by expressing a non-phosphorylatable mutant of IκB, which acts as a super-repressor of NFκB. Cytokines, dsRNA or SeV cannot activate NFκB in the 2F-SR cells (2, 36, 45). Of the 49 genes induced by SeV infection in 2fTGH cells, 28 of these were not induced in 2F-SR cells. Thus, almost 60% of the induced genes were NFκB-dependent while just over 40% were not. Examples of both classes of genes are given in Fig. 4A. Quantitative assays again confirmed our conclusions: NOXA and ISG56 mRNAs were induced equally well in both cell lines whereas A20 and mannose binding lectin 2 mRNAs were not induced in 2F-SR cells (Fig. 4B). These results confirm the notion that NFκB is a major transcription factor used by SeV to induce cellular genes.

Role of IRF-3 in gene induction by SeV

In addition to NFκB, another major transcription factor activated by SeV is IRF-3. To identify genes requiring IRF-3 for induction by SeV, we used P2.1 cells(24). These cells were derived from U4C cells and hence lack Jak1. In addition, their IRF-3 level is very low and consequently, the IRF-3 signaling pathway is defective in these cells(36). As expected, we observed that one set genes, 30 of the 42 genes induced by SeV in U4C cells, were induced well in P2.1 cells and another set, the remaining 12 genes, was not.

Examples of the two sets of genes are given in Fig. 5. These results demonstrated that induction of some genes by SeV-infection required IRF-3.

To further characterize this requirement, we used U4C.2 cells in which IRF-3 was overexpressed. The only difference between U4C cells and U4C.2 cells was in the level of IRF-3 expressed in the two cell lines. Forty-five genes were induced in U4C.2 cells, including a group of 19 genes that were induced much better than in U4C cells (Fig. 6A). An extreme example of this group is follistatin; quantitative assays confirmed that its mRNA was barely induced in U4C cells but strongly induced in U4C.2 cells (Fig. 6C). Induction of another group of mRNAs was hardly affected by the IRF-3 level (Fig. 6B and 6D) These results indicate that among the IRF-3-dependent genes, some, but not all, can be induced efficiently only when the cellular IRF-3 level is high.

Role of IRF-3 in suppressing gene induction by SeV-infection

In addition to the results discussed above, the array analysis shown in Fig. 6 produced an unexpected result. We observed that at least eight genes, or about 20% of those strongly induced in U4C, were poorly induced in U4C.2 cells, indicating that IRF-3 was negatively affecting their expression (Fig. 6B). RPA for A20 mRNA confirmed the conclusions from the microarray analysis (Fig. 6E).

To test further the possibility that IRF-3 was acting as a negative regulator of SeV-induced gene expression, five cell lines, all derived from the U4C line, expressing increasing levels of IRF-3 protein were used (Fig. 7A). The cell lines were infected with SeV and the levels of the ISG56 and A20 mRNAs measured by RPA before and after virus infection. Actin mRNA levels were used for normalization of the data. Neither

mRNA was detectable in any uninfected cell line. ISG56 mRNA was barely induced in P2.1 cells, which expressed the lowest level of IRF-3, and its induction levels increased with increasing levels of IRF-3 expression. Conversely, A20 mRNA was most strongly induced in P2.1 cells and very poorly induced in cells expressing high levels of IRF-3 (Fig. 7B).

Although the above analysis validated our original observation, we were concerned that the phenomenon might be restricted to the U4C cells from which all the above lines were derived. Because the U4C cells lacked Jak1 and were obtained by extensive mutagenesis of 2fTGH cells, it remained possible that the observed suppressing function of IRF-3 required either the absence of Jak1 or the presence of an unknown mutation in U4C cells. If that were the case, our observation would have restricted significance. To test the generality of the observation, a new cell line was derived from the Wt HT1080 cells. This line, 1080.10, expressed a much higher level of IRF-3 as compared to the parental cells (Fig. 8A). Confirming the results seen with the U4C derivative lines, A20 mRNA was induced strongly upon SeV infection in HT1080 cells, but only weakly in 1080.10 cells (Fig. 8B). The above series of experiments allowed us to conclude that the cellular abundance of IRF-3 can both positively and negatively influence the extent of induction of specific cellular genes in response to infection by SeV.

Discussion

In this study, we focused our attention on identifying the signaling pathways responsible for inducing specific sets of cellular genes early after SeV infection. The cDNA microarray screening used was convenient for profiling the expression of a large number of genes simultaneously, but to ensure reliability we had to perform multiple repeats of the same screen and accept an arbitrary cut-off of at least two-fold change as significant. Consequently, our calculations of the number of genes induced in different cell lines are likely underestimates. The overall gene induction patterns in different SeV-infected cell lines are summarized in Table 2. This Table includes only the genes whose expression was induced by at least 2-fold in wt 2fTGH cells. Following classification of different induced genes into distinct groups, representative members were selected for further analysis using more Northern blotting or RNase-protection assays. The choice of these sentinel genes was dictated by their degree of inducibility and their abundance, because we could make much more reliable conclusions for genes that were highly induced and the corresponding mRNA levels were easily measurable.

Other groups have previously sought to profile some of the genes induced by SeV. Strahle et al. employed SeV mutants to profile the effects of viral proteins on the induction of cellular genes in virus infected cells (40), and Matikainen et al. looked at chemokine induction by SeV (30). In the current study we see induction by SeV of many of the same genes previously identified, including IL-8, IP-10 and class I MHC genes. Further, we have been able to characterize the signaling pathways involved in the induction of not only these genes, but numerous other genes not formerly known to be induced by SeV.

Given the parameters of our experiment, there did not appear to be a role for TLR3 in gene induction by SeV. The paramyxovirus replication cycle takes upwards of 10 hours, so it remains possible that at later times after virus infection TLR3-signaling is used by viral dsRNA for induction of the dsRNA-inducible genes that were not induced by SeV at 6h (Fig. 2) (23). Since some genes induced by dsRNA and SeV were common, it is also possible that the virus used intracellular viral dsRNA to induce them, and TLR3 was required for exogenous dsRNA, but not for SeV, because it mediates efficient uptake of dsRNA. Although our data showed that TLR3 was not required for gene induction early after SeV infection, viral dsRNA could have used other cellular sensors of dsRNA. PKR and RIG-I are two such intracellular dsRNA-receptors that have recently been shown to mediate dsRNA-signaling(11, 46). The apparent irrelevance of TLR3 in gene induction by SeV is supported by the fact that TLR3 -/- mice are not deficient in clearing infections with other ssRNA viruses in vivo (12). Further, vesicular stomatitis virus (VSV), another single-stranded RNA virus has also been shown to activate downstream signaling factors independent of TLR3 in TLR3-deficent MEFs (42). It is highly unlikely that viral single-stranded RNA was the gene inducer in our experiments because 293 cells do not respond to ssRNA without expression of exogenous TLR7 or TLR8, the human TLRs that sense ssRNA (19, 26).

Our investigation of the role of IFN and the corresponding signaling pathway in gene induction by SeV produced both anticipated and unanticipated results. In U4C cells, lacking functional Jak1, we observed that some genes were not induced, as compared to Wt cells. This result was expected because some genes might be induced by the autocrine action of IFN induced by SeV-infection. Many genes of this class, such as

OAS2 and MHC class I genes, are known IFN-stimulated genes (Fig. 3). Further, our findings with SeV correspond with those observed in Newcastle Disease virus infected cells, where type I IFN signaling was required for OAS induction (33). However, other genes of the same family, such as ISG56 and ISG54, were induced even in U4C cells confirming previous observations by us and others that these genes are directly induced upon infection with many viruses (18, 34). The fact that these genes were induced in infected cells independent of autocrine IFN signaling, is not unexpected, because IRF-3, which is activated in the infected cells, can induce these genes directly. The surprising observation was that a cohort of genes was induced only in U4C cells, indicating that Jak1 or IFN-signaling somehow negatively regulates the expression of these genes in Wt cells. The implications and the mechanism of this regulation need to be further explored in the future. To distinguish between the needs for IFN-signaling and other putative functions of Jak1, we also analyzed the gene induction profiles in SeV-infected U2A cells and U3A cells (data not shown), which are also defective in IFN signaling because they lack functional IRF-9 and STAT1, respectively. The MHC class I, which were not induced by SeV in U4C cells were not induced in U2A and U3A cells either, indicating that IFN-signaling was needed for their induction. In contrast, the Jak1-repressed genes (Fig. 3), although induced in U4C cells, were not induced in U2A and U3A cells (data not shown) suggesting that it is the absence of Jak1 or another mutation specific to the cell line, and not the loss of IFN signaling that lead to SeV-mediated induction of this class of genes in U4C cells. These results indicate that autocrine IFN signaling and Jak1 per se can influence the pattern of cellular gene-induction by SeV-infection.

For assessing the relative contributions of NFκB and IRF-3, two major transcription factors activated by SeV-infection we took advantage of other mutant lines generated by us and our colleagues. The 2F-SR line was derived from 2fTGH cells by overexpressing a dominant negative inactivatable mutant of IκB. NFκB cannot be activated by IL-1, TNF-α, dsRNA, or SeV infection in these cells, as judged by electrophoretic mobility shift assays (36). Consequently, these cells are functionally NFκB-null cells. As expected, we observed that many genes could not be induced by SeV in the absence of NFκB signaling (Fig. 4). Some of these genes, such as IKKα, NFκB p105, and A20, encode proteins that are involved in the NFκB signaling pathway itself. Similarly, another set of genes was completely dependent on IRF-3 (Fig. 5). For identifying them, we used p2.1 cells, derived for U4C, which express little IRF-3 (36). Many of these genes fall in the category of viral-stress inducible genes, or VSIGs (37) because they can be independently induced by IFN, dsRNA, or virus infection. Although the same cis-element, ISRE, present in their promoter is responsible for their induction by the three agents, different trans-acting factors mediate the process. Infection of these genes by IFNs is mediated by ISGF3, a trimeric complex of IRF-9, STAT1, and STAT2. Induction by dsRNA and viruses, on the other hand, is mediated by activated IRF-3, which also binds to ISRE. However, the signaling pathways, triggered by dsRNA and viruses, that lead to IRF-3 activation overlap only partially (39). Thus it appears that VSIGs can be induced by multiple inducers using multiple signaling pathways. There were also genes, that were induced when either the NFκB pathway or the IRF-3 pathway were inoperative (Figs. 4 and 5). These genes probably get induced through other transcription factors activated by virus infection.

One such NFκB and IRF-3-independent gene is NOXA. NOXA, also known as PMAIP1, originally discovered as a mediator of p53-induced apoptosis (35), has been shown to be induced by a constitutively active IRF-3 mutant (IRF-3 5D) (16, 21). However in the context of induction by SeV, IRF-3 does not appear to play an important role in NOXA induction (Fig. 5 and 6 B, D). In the absence of STAT1, NOXA induction through the p53 response element in its promoter is impaired (44); likewise SeV fails to induce NOXA in STAT1$^{-/-}$ U3A cells (data not shown) This finding suggests that SeV may induce a subset of genes through the IRF-3-, NFκB-, and IFN-independent activation of STAT1 or p53. It also raises the possibility that the constitutively active IRF-3 5D mutant and virally activated IRF-3 do not induce equivalent sets of genes. Active SeV infection causes additional phosphorylation of IRF-3 beyond that required for the IRF-3 mediated induction of ISG56 (8). These additional modifications to IRF-3 might very well impair its ability to mediate the induction of other genes, such as NOXA.

Further explorations of the role of IRF-3 in gene induction by SeV produced interesting results. Using two related cell lines that expressed different levels of IRF-3, we could demonstrate that although some genes were induced equally well in both, others were induced better in U4C.2 cells which expressed a higher level of IRF-3 (Fig. 6A). Thus, it seems that at least in the 2fTGH cell lineage, IRF-3 expression is the limiting factor and the degree of gene induction can be modulated easily by changing the cellular concentration of IRF-3. The above conclusion was confirmed by a more quantitative assay using a series of cell lines expressing increasing amounts of IRF-3 (Fig. 7). Similar results were obtained with the same cell lines when the inducer was dsRNA, not SeV (36). Among the genes induced by SeV in U4C.2 cells were the MHC genes which were

not induced in U4C cells, but induced in 2fTGH cells (Figs. 3 and 6). Thus, a high level of IRF-3 could mediate SeV-induction of genes which otherwise required IFN-signaling. Other genes, such as Follistatin, were induced by SeV very strongly in U4C.2 cells, whereas the induction was minimal in U4C or 2fTGH cells (Fig. 6A, 6C).

The most surprising observation was that a higher level of IRF-3 expression negatively affected the degree of induction of some genes (Fig. 6B, 6E). Using the A20 gene as the sentinel for this group of genes, we could demonstrate that unlike induction of the ISG56 gene, induction of A20 mRNA was inversely related to the level of IRF-3 (Fig. 7). This phenomenon was not restricted to the U4C cells and its derivatives; the same trend was also observed in Wt HT1080 cells by overexpressing IRF-3 (Fig. 8). It is not clear how IRF-3 affects A20 gene induction by SeV. The promoter of this gene contains κB sites (22), but no consensus ISRE and, as expected, its induction required NFκB (Fig. 4) but not IRF-3 (Fig. 5). Thus, the observed negative effect of IRF-3 is probably not exerted through its direct interaction with the A20 promoter. Further investigation should reveal the nature of the cross-talk between the two major virus-activated signaling pathways.

What are the possible physiological implications of the above phenomenon? SeV and other viruses cause active and rapid degradation of IRF-3 in infected cells (27). Consequently, the degree of induction of genes, such as A20, can be temporally regulated in the infected cells. Moreover, the level of IRF-3 expression varies greatly among different cell types and different tissues (data not shown). From the observations reported here one can predict that the profiles of gene induction, and hence the outcome of virus infection, will also vary greatly among different host cells. A20 is required for

attenuation of NFκB activity induced both through TNFα (25) and Toll-like receptors (4). Consequently, cells expressing high levels of IRF-3 would have to sustained NFκB and IRF-3 responses due to their inability to make A20. To further speculate about the possible cellular functions of the genes that are negatively regulated by IRF-3, it is interesting to note that several, such as A20, CIAP1 and CIAP2, have anti-apoptotic functions. The encoded proteins may protect the infected cells from the actions of the pro-apoptotic proteins that are also induced with virus-infection. It has been reported that apoptosis of SeV-infected cells is mediated by IRF-3 (20). Our results suggest that this function of IRF-3 may be mediated not only by inducing pro-apoptotic genes, but also by suppressing the induction of anti-apoptotic genes.

Acknowledgements

Our appreciation is extended to George Stark and Kristi Peters for use of various cell lines. We would like to especially thank Roger Slee and Mat Frevel for their help and advice in conducting the microarray experiments. We are also grateful to Mat Frevel as well as Ge Guo for their contribution to the development of the customized cDNA microarray.

This work was supported in part by National Institutes of Health Grants CA62220, CA68782, Medical Scientists Training Grant GM07250, and in part by Merck.

References

1. **Alexopoulou, L., A. C. Holt, R. Medzhitov, and R. A. Flavell.** 2001 Recognition of double-stranded RNA and activation of NF-kappaB by Toll-like receptor 3. Nature **413:**732-738.

2. **Algarte, M., H. Nguyen, C. Heylbroeck, R. Lin, and J. Hiscott.** 1999. IkappaB-mediated inhibition of virus-induced beta interferon transcription. J. Virol. **73:**2694-2702.

3. **Bandyopadhyay, S. K., G. T. Leonard, Jr., T. Bandyopadhyay, G. R. Stark, and G. C. Sen.** 1995. Transcriptional induction by double-stranded RNA is mediated by interferon-stimulated response elements without activation of interferon-stimulated gene factor 3. J. Biol. Chem. **270:**19624-19629.

4. **Boone, D. L., E. E. Turer, E. G. Lee, R. C. Ahmad, M. T. Wheeler, C. Tsui, P. Hurley, M. Chien, S. Chai, O. Hitotsumatsu, E. McNally, C. Pickart, and A. Ma.** 2004. The ubiquitin-modifying enzyme A20 is required for termination of Toll-like receptor responses. Nat. Immunol. **5:**1052-1060.

5. **Boyle, K. A., R. L. Pietropaolo, and T. Compton.** 1999. Engagement of the cellular receptor for glycoprotein B of human cytomegalovirus activates the interferon-responsive pathway. Mol. Cell. Biol. **19:**3607-3613.

6. **Chang, Y. E., and L. A. Laimins.** 2000. Microarray analysis identifies interferon-inducible genes and Stat-1 as major transcriptional targets of human papillomavirus type 31. J. Virol. **74:**4174-4182.

7. **Chin, K. C., and P. Cresswell.** 2001. Viperin (cig5), an IFN-inducible antiviral protein directly induced by human cytomegalovirus. Proc. Natl. Acad. Sci. USA **98:**15125-15130.

8. **Collins, S. E., R. S. Noyce, and K. L. Mossman.** 2004. Innate cellular response to virus particle entry requires IRF3 but not virus replication. J. Virol. **78:**1706-1717.

9. **de Veer, M. J., M. Holko, M. Frevel, E. Walker, S. Der, J. M. Paranjape, R. H. Silverman, and B. R. Williams.** 2001. Functional classification of interferon-stimulated genes identified using microarrays. J. Leukoc. Biol. **69:**912-920.

10. **Der, S. D., A. Zhou, B. R. Williams, and R. H. Silverman.** 1998. Identification of genes differentially regulated by interferon alpha, beta, or gamma using oligonucleotide arrays. Proc. Natl. Acad. Sci. USA **95:**15623-15628.

11. **Diebold, S. S., M. Montoya, H. Unger, L. Alexopoulou, P. Roy, L. E. Haswell, A. Al-Shamkhani, R. Flavell, P. Borrow, and C. Reis e Sousa.** 2003. Viral infection switches non-plasmacytoid dendritic cells into high interferon producers. Nature **424:**324-328.

12. **Edelmann, K. H., S. Richardson-Burns, L. Alexopoulou, K. L. Tyler, R. A. Flavell, and M. B. Oldstone.** 2004. Does Toll-like receptor 3 play a biological role in virus infections? Virology **322:**231-238.

13. **Frevel, M. A., T. Bakheet, A. M. Silva, J. G. Hissong, K. S. Khabar, and B. R. Williams.** 2003. p38 Mitogen-activated protein kinase-dependent and -independent signaling of mRNA stability of AU-rich element-containing transcripts. Mol. Cell. Biol. **23:**425-436.

14. **Geiss, G., G. Jin, J. Guo, R. Bumgarner, M. G. Katze, and G. C. Sen.** 2001. A comprehensive view of regulation of gene expression by double-stranded RNA-mediated cell signaling. J. Biol. Chem. **276:**30178-30182.

15. **Geiss, G. K., M. Salvatore, T. M. Tumpey, V. S. Carter, X. Wang, C. F. Basler, J. K. Taubenberger, R. E. Bumgarner, P. Palese, M. G. Katze, and A. Garcia-Sastre.** 2002. Cellular transcriptional profiling in influenza A virus-infected lung epithelial cells: the role of the nonstructural NS1 protein in the evasion of the host innate defense and its potential contribution to pandemic influenza. Proc. Natl. Acad. Sci. USA **99:**10736-10741.

16. **Grandvaux, N., M. J. Servant, B. tenOever, G. C. Sen, S. Balachandran, G. N. Barber, R. Lin, and J. Hiscott.** 2002 Transcriptional profiling of interferon regulatory factor 3 target genes: direct involvement in the regulation of interferon-stimulated genes. J. Virol. **76:**5532-5539.

17. **Guo, J., D. J. Hui, W. C. Merrick, and G. C. Sen.** 2000. A new pathway of translational regulation mediated by eukaryotic initiation factor 3. Embo J. **19:**6891-6899.

18. **Guo, J., K. L. Peters, and G. C. Sen.** 2000. Induction of the human protein P56 by interferon, double-stranded RNA, or virus infection. Virology **267:**209-219.

19. **Heil, F., H. Hemmi, H. Hochrein, F. Ampenberger, C. Kirschning, S. Akira, G. Lipford, H. Wagner, and S. Bauer.** 2004. Species-specific recognition of single-stranded RNA via toll-like receptor 7 and 8. Science **303:**1526-1529.

20. **Heylbroeck, C., S. Balachandran, M. J. Servant, C. DeLuca, G. N. Barber, R. Lin, and J. Hiscott.** 2000. The IRF-3 transcription factor mediates Sendai virus-induced apoptosis. J. Virol. **74:**3781-3792.

21. **Hiscott, J., N. Grandvaux, S. Sharma, B. R. Tenoever, M. J. Servant, and R. Lin.** 2003. Convergence of the NF-kappaB and interferon signaling pathways in the regulation of antiviral defense and apoptosis. Ann. N.Y. Acad. Sci. **1010:**237-248.

22. **Laherty, C. D., N. D. Perkins, and V. M. Dixit.** 1993. Human T cell leukemia virus type I Tax and phorbol 12-myristate 13-acetate induce expression of the A20 zinc finger protein by distinct mechanisms involving nuclear factor kappa B. J. Biol. Chem. **268:**5032-5039.

23. **Lamb, R. A., and D. Kolakofsky.** 2001. Paramyxoviridae: The Viruses and Their Replication, p.1305-1339. *In* D. M. Knipe, P. M. Howley (ed.), Field's virology, 4th ed. Lippincott Williams & Wilkins, Philadelphia, PA.

24. **Leaman, D. W., A. Salvekar, R. Patel, G. C. Sen, and G. R. Stark.** 1998. A mutant cell line defective in response to double-stranded RNA and in regulating basal expression of interferon-stimulated genes. Proc. Natl. Acad. Sci. USA **95:**9442-9447.

25. **Lee, E. G., D. L. Boone, S. Chai, S. L. Libby, M. Chien, J. P. Lodolce, and A. Ma.** 2000. Failure to regulate TNF-induced NF-kappaB and cell death responses in A20-deficient mice. Science **289:**2350-2354.

26. **Lee, J., T. H. Chuang, V. Redecke, L. She, P. M. Pitha, D. A. Carson, E. Raz, and H. B. Cottam.** 2003. Molecular basis for the immunostimulatory activity of

guanine nucleoside analogs: activation of Toll-like receptor 7. Proc. Natl. Acad. Sci. USA **100:**6646-6651.

27. **Lin, R., C. Heylbroeck, P. M. Pitha, and J. Hiscott.** 1998. Virus-dependent phosphorylation of the IRF-3 transcription factor regulates nuclear translocation, transactivation potential, and proteasome-mediated degradation. Mol. Cell. Biol. **18:**2986-2996.

28. **Lund, J. M., L. Alexopoulou, A. Sato, M. Karow, N. C. Adams, N. W. Gale, A. Iwasaki, and R. A. Flavell.** 2004. Recognition of single-stranded RNA viruses by Toll-like receptor 7. Proc. Natl. Acad. Sci. USA **101:**5598-5603.

29. **Malmgaard, L.** 2004. Induction and Regulation of IFNs During Viral Infections. J. Interferon Cytokine Res. **24:**439-454.

30. **Matikainen, S., J. Pirhonen, M. Miettinen, A. Lehtonen, C. Govenius-Vintola, T. Sareneva, and I. Julkunen.** 2000. Influenza A and sendai viruses induce differential chemokine gene expression and transcription factor activation in human macrophages. Virology **276:**138-147.

31. **McKendry, R., J. John, D. Flavell, M. Muller, I. M. Kerr, and G. R. Stark.** 1991. High-frequency mutagenesis of human cells and characterization of a mutant unresponsive to both alpha and gamma interferons. Proc. Natl. Acad. Sci. USA **88:**11455-11459.

32. **Mossman, K. L., P. F. Macgregor, J. J. Rozmus, A. B. Goryachev, A. M. Edwards, and J. R. Smiley.** 2001. Herpes simplex virus triggers and then disarms a host antiviral response. J. Virol. **75:**750-758.

33. **Nakaya, T., M. Sato, N. Hata, M. Asagiri, H. Suemori, S. Noguchi, N. Tanaka, and T. Taniguchi.** 2001. Gene induction pathways mediated by distinct IRFs during viral infection. Biochem. Biophys. Res. Commun. **283:**1150-1156.

34. **Navarro, L., K. Mowen, S. Rodems, B. Weaver, N. Reich, D. Spector, and M. David.** 1998. Cytomegalovirus activates interferon immediate-early response gene expression and an interferon regulatory factor 3-containing interferon-stimulated response element-binding complex. Mol. Cell. Biol. **18:**3796-3802.

35. **Oda, E., R. Ohki, H. Murasawa, J. Nemoto, T. Shibue, T. Yamashita, T. Tokino, T. Taniguchi, and N. Tanaka.** 2000. Noxa, a BH3-only member of the Bcl-2 family and candidate mediator of p53-induced apoptosis. Science **288:**1053-1058.

36. **Peters, K. L., H. L. Smith, G. R. Stark, and G. C. Sen.** 2002. IRF-3-dependent, NFkappa B- and JNK-independent activation of the 561 and IFN-beta genes in response to double-stranded RNA. Proc. Natl. Acad. Sci. USA **99:**6322-6327.

37. **Sarkar, S. N., and G. C. Sen.** Novel functions of proteins encoded by Viral Stress-Inducible Genes. Pharmacol. Ther. **103:**245-259.

38. **Sarkar, S. N., H. L. Smith, T. M. Rowe, and G. C. Sen.** 2003. Double-stranded RNA signaling by Toll-like receptor 3 requires specific tyrosine residues in its cytoplasmic domain. J. Biol. Chem. **278:**4393-4396.

39. **Servant, M. J., N. Grandvaux, and J. Hiscott.** 2002. Multiple signaling pathways leading to the activation of interferon regulatory factor 3. Biochem. Pharmacol. **64:**985-992.

40. **Strahle, L., D. Garcin, P. Le Mercier, J. F. Schlaak, and D. Kolakofsky.** 2003. Sendai virus targets inflammatory responses, as well as the interferon-induced antiviral state, in a multifaceted manner. J. Virol. **77:**7903-7913.

41. **tenOever, B. R., M. J. Servant, N. Grandvaux, R. Lin, and J. Hiscott.** 2002. Recognition of the measles virus nucleocapsid as a mechanism of IRF-3 activation. J. Virol. **76:**3659-3669.

42. **tenOever, B. R., S. Sharma, W. Zou, Q. Sun, N. Grandvaux, I. Julkunen, H. Hemmi, M. Yamamoto, S. Akira, W. C. Yeh, R. Lin, and J. Hiscott.** 2004. Activation of TBK1 and IKKvarepsilon kinases by vesicular stomatitis virus infection and the role of viral ribonucleoprotein in the development of interferon antiviral immunity. J. Virol. **78:**10636-10649.

43. **Tiwari, R. K., J. Kusari, and G. C. Sen.** 1987. Functional equivalents of interferon-mediated signals needed for induction of an mRNA can be generated by double-stranded RNA and growth factors. Embo J. **6:**3373-3378.

44. **Townsend, P. A., T. M. Scarabelli, S. M. Davidson, R. A. Knight, D. S. Latchman, and A. Stephanou.** 2004. STAT-1 interacts with p53 to enhance DNA damage-induced apoptosis. J. Biol. Chem. **279:**5811-5820.

45. **Van Antwerp, D. J., S. J. Martin, T. Kafri, D. R. Green, and I. M. Verma.** 1996. Suppression of TNF-alpha-induced apoptosis by NF-kappaB. Science **274:**787-789.

46. **Yoneyama, M., M. Kikuchi, T. Natsukawa, N. Shinobu, T. Imaizumi, M. Miyagishi, K. Taira, S. Akira, and T. Fujita.** 2004. The RNA helicase RIG-I

has an essential function in double-stranded RNA-induced innate antiviral responses. Nat. Immunol. **5:**730-737.

47. **Zhu, H., J. P. Cong, G. Mamtora, T. Gingeras, and T. Shenk.** 1998. Cellular gene expression altered by human cytomegalovirus: global monitoring with oligonucleotide arrays. Proc. Natl. Acad. Sci. USA **95:**14470-14475.

Figure legends

Fig. 1. Effect of TLR3 on the regulation of cellular genes by SeV and dsRNA. Global changes in mRNA levels in 293 cells (A, C) or 293 cells expressing TLR3 (B, D) six hours after SeV infection at 1HAU/4.0x10^3 cells (A, B) or dsRNA treatment at 100μg/ml (C, D) as determined by cDNA microarray experiment. Each point on the scatter plots represents the expression of an individual mRNA message, as determined by units of fluorescent intensity, in untreated cells (x-axis) plotted against its expression six hours after SeV infection or dsRNA treatment (y-axis). The central diagonal line (black) represents equal expression in treated and untreated samples, while two-fold differences in expression are indicated by the two flanking blue lines. (E) Regulation of specific genes by dsRNA and SeV in 293(-) and 293/TLR3 (+) cells. The tiles show the fold-increase in mRNA expression for specific genes in SeV- or dsRNA-treated cells relative to untreated cells as a function of color. Green, expression was unchanged. Yellow→Red, expression was induced to increasing degrees. (F) RNase protection assay (RPA) of ISG56 induction in untreated (1, 4), dsRNA treated (2, 5), or SeV-infected (3, 6) 293 cells (lanes 1-3) or 293/TLR3 cells (lanes 4-6).

Fig. 2. Differential induction of genes by SeV and dsRNA. Select genes differentially regulated by SeV and dsRNA in 293 cells expressing (+) or not expressing (-) TLR3. Colors represent fold-induction by SeV (left column) or dsRNA (right column) as described in Fig. 1.

Fig. 3. IFN dependent regulation of SeV-induced genes. Select SeV-regulated genes displaying differential induction patterns in Wt (2fTGH) and Jak1^{--} (U4C) cells. (A) Microarray data showing average fold-increase in mRNA expression six hours after SeV infection in 2fTGH and U4C cells. Genes are grouped based on their independence, dependence, or impairment by Jak1 for induction. (B) RPA (A20) and Northern (OAS, p69) analysis of mRNA expression in 2fTGH and U4C cells, before or six hours after SeV infection.

Fig. 4. Requirement of NFκB for gene induction by SeV. Genes regulated by SeV in Wt (2fTGH) and NFκB null (2F-SR) cells. (A) Average fold-induction of SeV-regulated genes, grouped by dependence on NFκB, as determined by microarray. (B) Quantitative analysis of NOXA, ISG56 and A20 mRNA induction by RPA.

Fig. 5. IRF-3 dependent gene induction. Examples of genes regulated by SeV in U4C cells and p2.1 cells in which IRF-3 expression is impaired. Genes are grouped by their dependence on IRF-3 for induction.

Fig. 6. Regulation of SeV-induced genes by IRF-3. Altered expression of SeV-regulated genes in U4C cells and U4C.2 cells, which expressing high levels of IRF-3. (A, B) Microarray data for the fold-induction of select SeV-regulated genes in U4C and U4C.2 cells. Genes are grouped as follows: IRF-3 enhanced, genes with augmented expression in IRF-3 overexpressing cells (induced more strongly in U4C.2); IRF-3 neutral, genes unaffected by cellular IRF-3 levels (induced at equivalent levels in both

cell lines); IRF-3 repressed, SeV-induced genes negatively regulated by IRF-3 (induced in U4C, but not U4C.2 cells). Quantitative RPA analysis of (C) Follistatin, (D) NOXA, and (E) A20 mRNA induction in U4C and U4C.2 cells before or after SeV infection.

Fig. 7. Modulation of A20 mRNA and ISG56 mRNA expression by cellular levels of IRF-3. Cell lines, derived from U4C and p2.1 cells, expressing different levels of IRF-3 protein were infected with SeV and analyzed for their expression of A20 mRNA and ISG56 mRNA. (A) Western blot showing the relative levels of IRF-3 expression in the different cell lines relative to actin. (B) Percent maximum fold-induction of A20 mRNA (white) and ISG56 mRNA (black) in cells six hours after infection, normalized to actin mRNA expression as determined by RPA.

Fig. 8. Negative regulation of SeV-induced A20 mRNA expression by IRF-3 not in Wt cells. (A) Western analysis of IRF-3 expression in HT1080 and 1080.10 cells. (B) RPA comparing A20 mRNA induction in untreated (-) or SeV-infected (+) HT1080 and 1080.10 cells.

TABLE 1. Mutant cell lines used

Cell Line	Lineage	Relevant altered protein	Affected pathway(s)
HEK293	——	None	TLR3 non-responsive
293/TLR3	HEK293	TLR3	TLR3 responsive
2fTGH	HT1080	None	None
2F-SR	2fTGH	IkB	NFκB signaling
1080.10	HT1080	Increased IRF-3	IRF-3 signaling
U4C	2fTGH	Jak1	IFN signaling
U4C.2	U4C	Increased IRF-3	IRF-3, IFN signaling
P2.1	U4C	Decreased IRF-3	IRF-3, IFN signaling
P2.1.6	P2.1	Increased IRF-3	IRF-3, IFN signaling
P2.1.17	P2.1	Increased IRF-3	IRF-3, IFN signaling

TABLE 2. Genes induced or repressed by SeV infection in various cell lines[a]

Encoded Proteins	Unigene ID	Symbol	2fTGH	U4C	2F-SR	p2.1	U4C.2
2'-5'-oligoadenylate synthetase 2 (69-71 kD)	Hs.414332	OAS2	I	U	U	R	U
Activating transcription factor 3	Hs.460	ATF3	I	I	U	I	I
Apoptosis Inhibitor 1	Hs.75263	cIAP1	I	I	U	I	U
Apoptosis Inhibitor 2	Hs.127799	cIAP2	I	I	U	U	U
Bcl-2 binding component 3	Hs.87246	BBC3 (PUMA)	I	I	U	U	I
Chemokine (C-X-C motif) ligand 10	Hs.2248	IP10 (CXCL10)	I	I	U	I	I
Colony stimulating factor 1 (macrophage)	Hs.173894	CSF1	I	I	U	I	I
Fibroblast growth factor 2 (basic)	Hs.284244	FGF2	I	U	I	U	U
Fucosyltransferase 2	Hs.292999	FUT2	I	I	I	I	I
General transcription factor IIF, polypeptide 1	Hs.68257	GTF2F1	I	U	U	U	U
GTP cyclohydrolase 1 (dopa-responsive dystonia)	Hs.86724	GCH1	I	U	U	U	U
IFN-induced protein with tetratricopeptide repeats 1	Hs.20315	ISG56	I	I	I	U	I
IFN-induced protein with tetratricopeptide repeats 2	Hs.293797	ISG54	I	I	I	U	I
IFN-induced protein with tetratricopeptide repeats 4	Hs.181874	ISG60	I	U	U	U	U
Inhibin, beta A (activin A, activin AB alpha polypeptide)	Hs.727	INHBA	I	I	U	U	U
Inhibitor of kappa B, alpha	Hs.81328	IκBα	I	I	U	I	I
Interferon regulatory factor 1	Hs.80645	IRF-1	I	I	U	U	U
Interferon regulatory factor 2	Hs.83795	IRF-2	I	U	U	U	U
Interferon, alpha-inducible protein (clone IFI-15K)	Hs.833	ISG15	I	I	I	U	I
Interleukin 6	Hs.93913	IL-6	I	I	U	U	I
Interleukin 8	Hs.624	IL-8	I	I	U	I	I
Jun B proto-oncogene	Hs.515157	JUNB	I	I	U	I	U
Macrophage Inflammatory Protein 1, alpha	Hs.73817	MIP1α (CCL3)	I	I	U	I	I
Mannose-binding lectin (protein C) 2	Hs.2314	MBL2	I	I	R	I	I
MHC, class I, A	Hs.181244	HLA-A	I	U	I	U	I
MHC, class I, C	Hs.277477	HLA-C	I	U	U	I	I
MHC, class I, F	Hs.110309	HLA-F	I	U	U	U	I
MHC, class I, G	Hs.73885	HLA-G	I	U	U	U	I
Monocyte Chemotactic Protein 1	Hs.303649	MCP1 (CCL2)	I	U	U	U	U
Natural killer cell transcript 4	Hs.943	NK4	I	U	U	U	I
Nexin, plasminogen activator inhibitor type 1	Hs.82085	PAI1 (SERPINE1)	I	I	I	I	I
NFκB p105	Hs.83428	NFκB1	I	I	U	I	I
Nuclear factor (erythroid-derived 2)-like 3	Hs.22900	NFE2L3 (NRF3)	I	I	U	I	U
Nucleoside phosphorylase	Hs.75514	NP	I	U	I	U	I
Phorbol-12-Myristate-13-Acetate-Induced Protein 1	Hs.96	NOXA (PMAIP1)	I	I	I	I	I
Protein tyrosine phosphatase, non-receptor type 11	Hs.83572	PTPN11 (SHP2)	I	I	U	U	I
Protein tyrosine phosphatase, receptor type, Kappa	Hs.79005	PTPRK	I	U	U	U	U
Short stature homeobox	Hs.105932	SHOX	I	U	U	U	I
Similar to S. cerevisiae SSM4	Hs.380875	TEB4	I	I	I	I	U
Stanniocalcin	Hs.25590	STC1	I	I	I	U	U
Syndecan 4 (amphiglycan, ryudocan)	Hs.252189	SDC4	I	I	U	I	I
Tight junction protein 2 (zona occludens 2)	Hs.75608	TJP2	I	I	I	I	I
TNF receptor-associated factor 1	Hs.2134	TRAF1	I	I	R	U	U
Transcription factor AP-2 gamma	Hs.61796	ERF1 (TFAP2C)	I	U	U	I	U
Tumor necrosis factor, alpha-induced protein 3	Hs.211600	TNFAIP3 (A20)	I	I	U	I	I
UDP-N-acetyl-alpha-D-galactosamine-polypeptide N-acetylgalactosaminyltransferase 2	Hs.130181	GALNT2	I	U	I	U	U
Vascular endothelial growth factor C	Hs.79141	VEGFC	I	I	I	U	U
Viperin	Hs.17518	CIG5	I	U	I	U	I
Zinc finger CCCH type, antiviral 1	Hs.35254	ZC3HAV1	I	I	I	U	U

[a] 'I' denotes induced, 'U' denotes unchanged, 'R' denotes repressed.

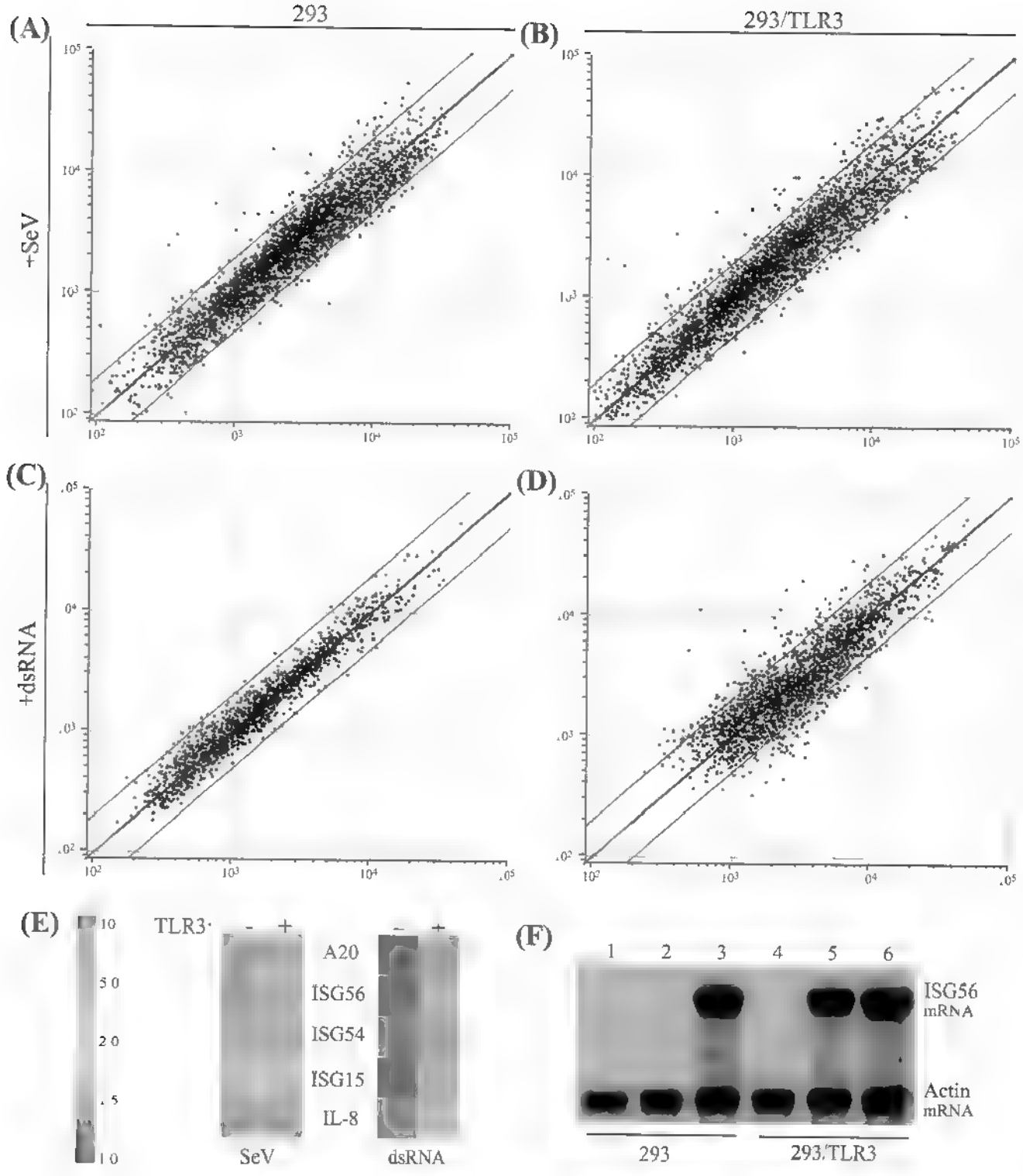
(A)
293
+SeV
(B)
293/TLR3
(C)
+dsRNA
(D)
(E)
TLR3
-
+
-
+
A20
ISG56
ISG54
ISG15
IL-8
SeV
dsRNA
(F)
1
2
3
4
5
6
ISG56
mRNA
Actin
mRNA
293
293/TLR3

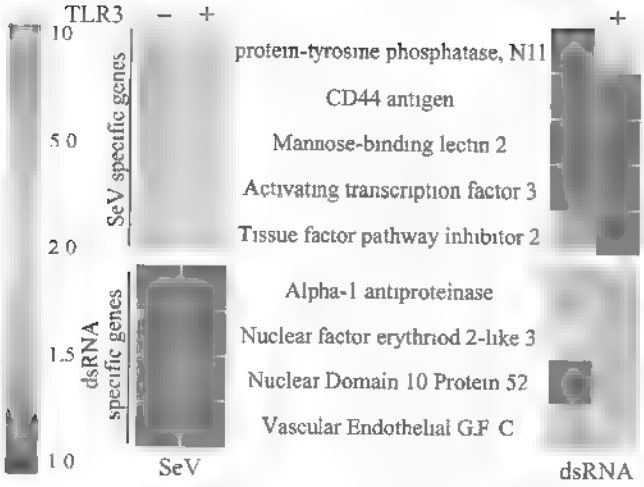
TLR3
–
+
+
10
5.0
2.0
1.5
1.0
SeV specific genes
dsRNA specific genes
protein-tyrosine phosphatase, N11
CD44 antigen
Mannose-binding lectin 2
Activating transcription factor 3
Tissue factor pathway inhibitor 2
Alpha-1 antiproteinase
Nuclear factor erythroid 2-like 3
Nuclear Domain 10 Protein 52
Vascular Endothelial G.F. C
SeV
dsRNA

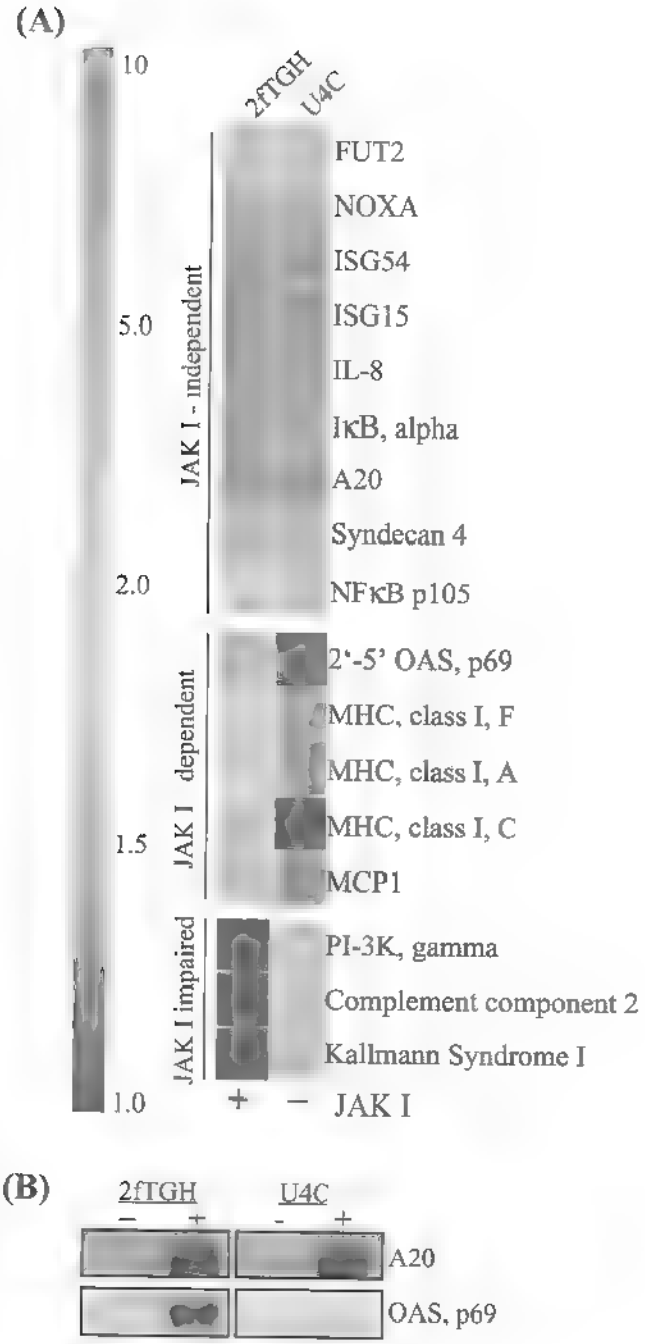
(A)
10
5.0
2.0
1.5
1.0
2fTGH
U4C
JAK I - independent
JAK I dependent
JAK I impaired
FUT2
NOXA
ISG54
ISG15
IL-8
IκB, alpha
A20
Syndecan 4
NFκB p105
2'-5' OAS, p69
MHC, class I, F
MHC, class I, A
MHC, class I, C
MCP1
PI-3K, gamma
Complement component 2
Kallmann Syndrome I
+
−
JAK I
(B)
2fTGH
U4C
−
+
-
+
A20
OAS, p69

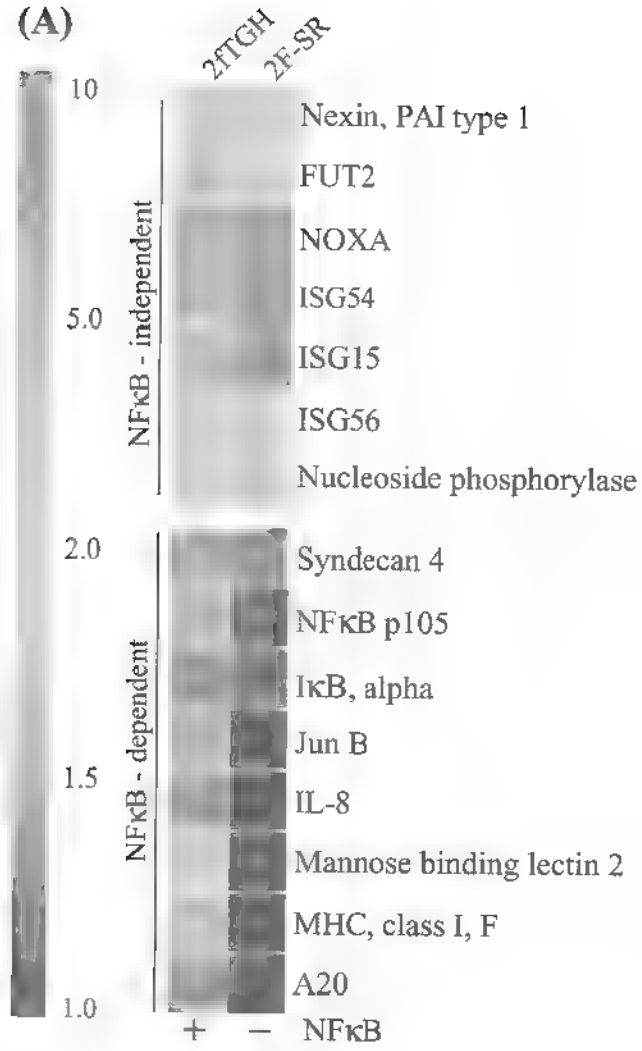
(A)
2fTGH
2F-SR
10
5.0
NFκB - independent
Nexin, PAI type 1
FUT2
NOXA
ISG54
ISG15
ISG56
Nucleoside phosphorylase
2.0
1.5
1.0
NFκB - dependent
Syndecan 4
NFκB p105
IκB, alpha
Jun B
IL-8
Mannose binding lectin 2
MHC, class I, F
A20
+ − NFκB
(B)
2fTGH
2F-SR
− + − +
NOXA
ISG56
A20
mRNA

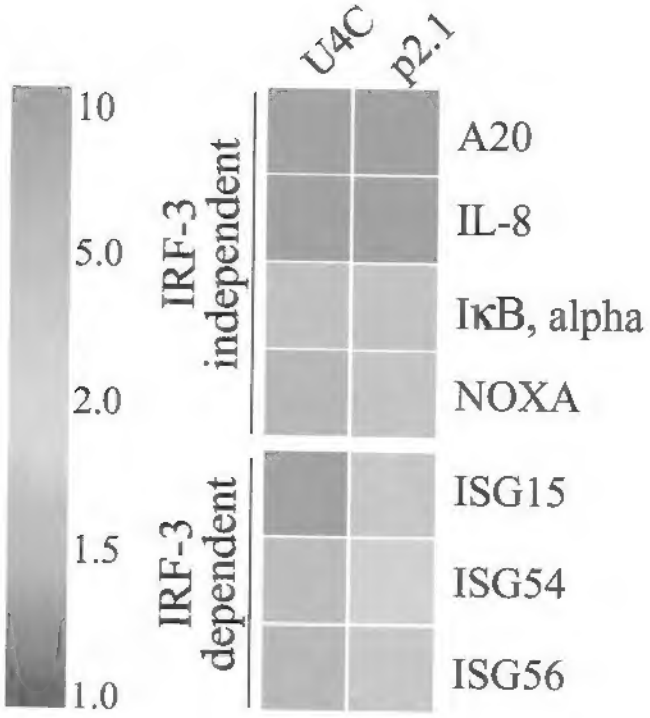
U4C
p2.1
10
5.0
2.0
1.5
1.0
IRF-3 independent
IRF-3 dependent
A20
IL-8
IκB, alpha
NOXA
ISG15
ISG54
ISG56

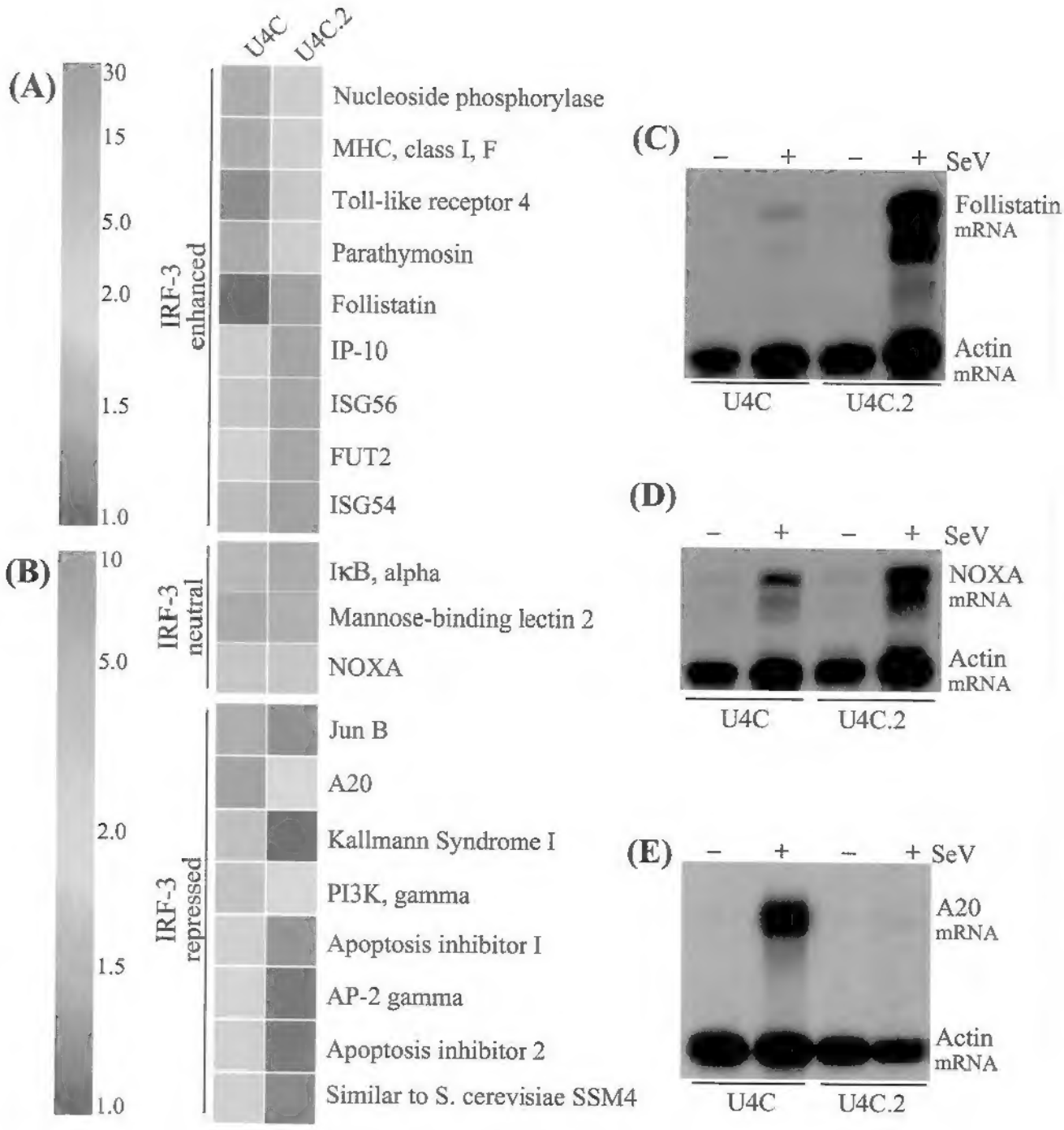
(A)
30
15
5.0
2.0
1.5
1.0
U4C
U4C.2
IRF-3 enhanced
Nucleoside phosphorylase
MHC, class I, F
Toll-like receptor 4
Parathymosin
Follistatin
IP-10
ISG56
FUT2
ISG54
(B)
10
5.0
2.0
1.5
1.0
IRF-3 neutral
IκB, alpha
Mannose-binding lectin 2
NOXA
IRF-3 repressed
Jun B
A20
Kallmann Syndrome I
PI3K, gamma
Apoptosis inhibitor I
AP-2 gamma
Apoptosis inhibitor 2
Similar to S. cerevisiae SSM4
(C)
– + – + SeV
Follistatin mRNA
Actin mRNA
U4C
U4C.2
(D)
– + – + SeV
NOXA mRNA
Actin mRNA
U4C
U4C.2
(E)
– + – + SeV
A20 mRNA
Actin mRNA
U4C
U4C.2

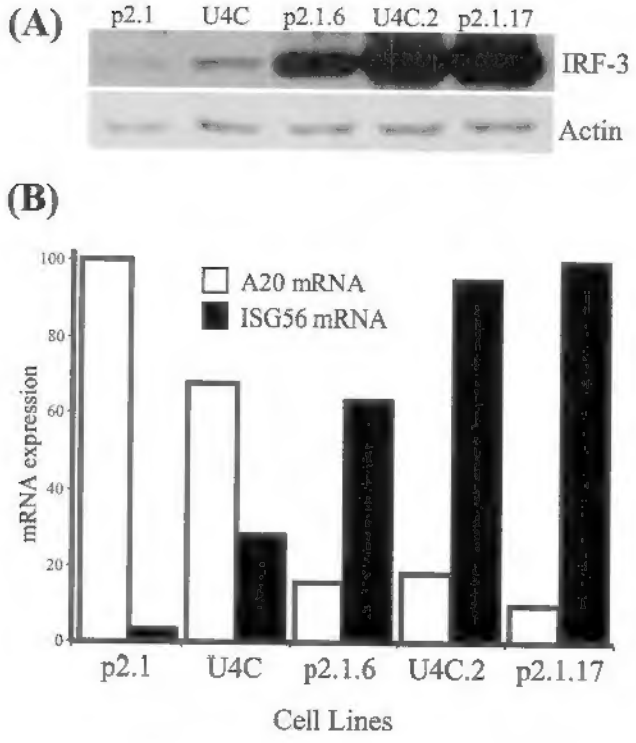
(A)
p2.1
U4C
p2.1.6
U4C.2
p2.1.17
IRF-3
Actin
(B)
A20 mRNA
ISG56 mRNA
mRNA expression
100
80
60
40
20
0
p2.1
U4C
p2.1.6
U4C.2
p2.1.17
Cell Lines

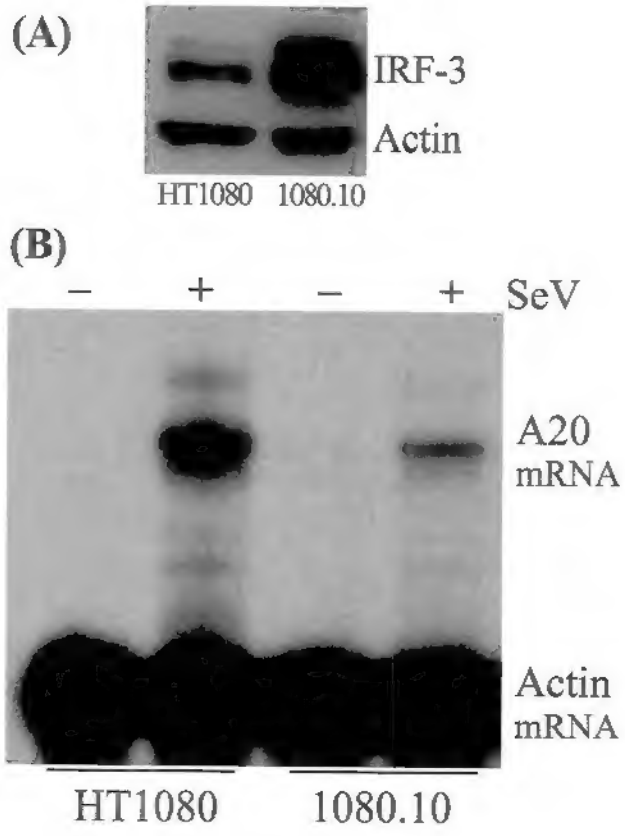
(A)
IRF-3
Actin
HT1080
1080.10
(B)
–
+
–
+
SeV
A20
mRNA
Actin
mRNA
HT1080
1080.10